MINISTRY OF HIGHER EDUCATION
AND SCIENTIFIC RESEARCH
UNIVERSITY OF BABYLON
COLLEGE OF ENGINEERING
DEPARTMEMT OF CIVIL ENGINEERING

SIMULATION OF FLOW OF GROUNDWATER IN KARBALA CITY

A THESIS
SUBMITTED TO THE COLLEGE OF ENGINEERING
OF THE UNIVERSITY OF BABYLON IN PARTIAL
FULFILLMENT OF THE REQUIREMENTS
FOR THE DEGREE OF MASTER
OF SCEINCE IN CIVIL
ENGINEERING

BY
NABEEL M. HUSSAIN
(H. Dip. Sc.)

July
2008

Supervisors
Dr. Salah Tawfeek
Dr. Abdul-Hassan K.Shukur


بسم الله الرحمن الرحيم

﴿ قَالُواْ سُبْحَنَكَ لَا عِلْمَ لَنَآ إِلَّا مَا عَلَّمْتَنَآ إِنَّكَ أَنتَ الْعَلِيمُ الْحَكِيمُ ﴾ البقرة – صدق الله العظيم


We certify that the preparation of this thesis was carried out under our supervision at University of Babylon in partial fulfillment of the requirement for the degree of Master of Science in Civil Engineering.

Signature : Salah Tawfeek
Name : Asst. Prof. Dr.
Salah Tawfeek
(supervisor)
Date : 3 / 8 /2008

Signature : A-H-K. Al-Shukur
Name : Asst. Prof. Dr.
Abdul-Hassan K.Shukur
(supervisor)
Date : 27 / 7 /2008

Certification

We certify as an examining committee that we have read this thesis entitled (***Simulation of Flow of Groundwater in Karbala City***) and examined the student (***Nabeel Mohammed Hussain Hussain***), in its content and what related to it, and found it meets the standard of a thesis for the degree of Master of Science in Civil Engineering (Water Resources Engineering).

Signature :
Name: Asst. Prof. Dr. Jawad K.AL-Rifai
(Member)
Date : 29 / 7 /2008

Signature : K.N. Al-Taee
Name : Asst. Prof. Kadhim N.AL-Taee
(Member)
Date : 27 / 7 /2008

Signature : Salah Tawfeek
Name : Asst. Prof. Dr.
Salah Tawfeek
(supervisor)
Date : 3 / 8 /2008

Signature : A.H.K. Al-Shukur 27.7.2008
Name : Asst. Prof. Dr.
Abdul-Hassan K.Shukur
(supervisor)
Date : / /2008

Signature : K. R. Al-Murshidi
Name: Asst. Prof. Dr. Kareem Radhi Al-Murshidi
(Chairman)
Date : 29 / 7 /2008

Approval of Civil Engineering Department

Signature :
Name : Asst. Prof. Dr. Ammar Y. Ali
Head of Civil Engineering Department .
Date : 3 / 8 /2008

Approval of Deanery of the College of Engineering .

Signature : Salah Tawfeek
Name : Asst. Prof. Dr. Salah Tawfeek
Deane of the College of Engineering.
Date : 3 / 8 /2008

Acknowledgement

Cordial thanks and deepest gratitude with full respect are to my supervisor Asst. Prof. Dr. Salah Tawfeek for his valuable guidance and his forceful encouragement throughout the preparation of this work.

I would like to express my gratitude to my supervisor Asst. Prof. Dr. Abdul-Hassan K.Shukur for his assistance and kindness throughout this work.

I also record my thanks to University of Babylon, College of Engineering and Civil Engineering Department staff for all the facilities they introduced to me .

I record my sincere gratitude to my family for their encouragement and support during the study.

Nabeel

Abstract

Karbala city is one of the most important islamic cities in the world. Its importance comes from the two holy shrines of Imam AL- Hussain and his brother AL-Abbas.

Karbala city suffers from shallow groundwater level problem especially in the area near the two holy shrines where the highest groundwater levels were recorded. Previous studies prove that the main sources of groundwater recharge are the leakage of drinking pipes network, sewer pipes network, and septic tanks. Previous studies also show that the soil profile of the study area consists of three layers, upper layer which represents the unconfined aquifer with mean thickness of 5m, lower layer which represents a semi-confined aquifer with mean thickness of 30m, and intermediate layer (semi-pervious layer) with mean thickness of 2m.

Two numerical finite difference models are used in the present study to evaluate the various possible sources of groundwater recharge. The first one is the GMS model while the second is a mathematical model developed in this study and applied using the Quick Basic language. The two models are also used to examine some procedures of lowering groundwater levels in the study area. They prove that a 75% reduction of leakage will lead to a drawdown more than 2m in the area of the two holy shrines. They also prove that the vertical drainage of the lower layer by using four wells around each holy shrine can be adopted to reach to the same drawdown.

GMS model prove that the horizontal drainage of the upper layer by opening all the drains in the study area will lead to a considerable drawdown that extends over all the study area but not with a sufficient value under the two holy shrines where the drawdown is found not to exceed 1m. This study also shows that the second mathematical model simulates the flow better than the GMS model.

Table of Contents

Subject	Page
Acknowledgment	I
Abstract	II
Table of contents	III
Table of figures	V
Table of symbols	X
Table of tables	XI
Chapter One :Introduction	1
1.1 Description of the study area	1
1.2 Objective of the present study	6
Chapter Two :Literature Review	7
2.1 General	7
2.2 Previous studies on groundwater in Karbala City	10
Chapter Three :The GMS Model	48
3.1 Brief description of the GMS. program	48
3.2 The Karbala GMS model	50
3.3 Initial input data	58
3.4 Calibration of the GMS model	61
Chapter Four: Development of Different Mathematical Model	77
4.1 General	77
4.2 Two dimensional finite difference model	77
4-2-1 Considerations and assumptions of hydraulic conditions	77
4-2-2 Mathematical derivation and formulation	78
4-2-2-1 Model derivation for the phreatic (Upper) layer	81

Subject	Page
4-2-2-1-1 Average transmissivities (inter nodal transmissivities) for the upper layer	86
4-2-2-1-2 Nodal groundwater balance	90
4-2-2-2 Model derivation for the leaky (lower) layer	97
4-2-2-2-1 Average transmissivities (inter nodal transmissivities) for the lower layer	98
4-2-2-2-2 Nodal groundwater balance	99
4-2-3 Boundary conditions simulation	104
4-2-4 Brief description of the Quick Basic program	105
4-2-5 Calibration of the mathematical model	114
Chapter Five : Comparison, Conclusions, and Recommendations	125
5.1 Comparison between the results of the GMS model and the second mathematical model	125
5.2 Conclusions	128
5.3 Recommendations	129
References	130
Appendices	
Appendix (A)	A-I
Appendix (B)	B-I
Appendix (C)	C-I

Table of Figures

Fig. No.	Description	Page
1.1	Location of Karbala city in Iraq	2
1.2	Map of the study area	3
2.1	Locations of the drilled borehole around the holy shrine of AL-Abbas	12
2.2	Locations of the borehole and the piezometers around the holy shrine of AL-Hussain	12
2.3	Groundwater head observations by the NCCL during the period (15/12/1997 to 15/1/1998) for the piezometers (P1 to P8	13
2.4	Locations of the boreholes and the piezometers in the area surrounding the two holy shrines	15
2.5	Areal distribution of the monthly average groundwater head for the upper and the lower layer (ISSWR,1999) (mal)	22
2.6	Groundwater heads measured at the sallow piezometers (S7 and S6) and the deep piezometers (D4 and D5) respectively (ISSWR,1999)	25
2.7	Groundwater heads measured at the sallow piezometers (S4 and S3) and the deep piezometer (D4) and the well (W) respectively (ISSWR,1999)	26
2.8	Locations of the piezometers installed inside and nearby the study area boundary by the FCSDIP (1995) and Hassan AL-Khateeb (2001).	28
2.9	Areal distribution of the groundwater head for the upper l measured by the DSWK (2000) (mal).	29

Fig. No.	Description	Page
2.10	Longitudinal section of a typical shallow piezometer instilled by Hassan AL-Khateeb (2001)	31
2.11	Areal distribution of the upper layer permeability based on data from Hassan AL-Khateeb (2001)	33
2.12	Observed groundwater level, (After AL-Khateeb (2001))	36
2.13	Areal distribution of the groundwater head for the lower layer measured by Hassan AL-Khateeb (2001) (mal)	39
2.14	Groundwater heads measured at the piezometers (P2 to P8) by Hassan AL-Khateeb (2001)	40
2.15	Groundwater heads measured at the piezometers (S7,S8,S9,Ns10, and D4) by Hassan AL-Khateeb (2001)	41
2.16	Topography of the study area (mal)	43
2.17	Thickness of the upper layer contour map	44
2.18	Bottom elevation of the upper layer contour map (mal)	45
2.19	Thickness of the middle layer contour map	46
3.1	The register image dialog	50
3.2	Locations of the boreholes that are used in the model	54
3.3	Locations of the Nodes of Karbala GMS model	56
3.4	Grid design and boundary conditions of the study area	59

Fig. No.	Description	Page
3.5	Simulated and observed water table level for the upper layer by the GMS model (march2000)	63
3.6	Simulated and observed peizometric head for the lower layer by the GMS model (march2000)	64
3.7	Calibrated recharge to the upper layer by the GMS model (constant value for each coverage) (m3/day) per nodal cell	65
3.8	Water table level of the upper layer after reducing the local recharge about 50%	67
3.9	Water table drawdown of the upper layer after reducing the local recharge about 50%	68
3.10	Water table level of the upper layer after reducing the local recharge about 75%	69
3.11	Water table drawdown of the upper layer after reducing the local recharge about 75%	70
3.12	The locations of the lower layer wells	71
3.13	Water table level of the upper layer after operating four wells surrounding each holy shrine	72
3.14	Water table drawdown of the upper layer after operating four wells surrounding each holy shrine	73
3.15	Water table level of the upper layer after opening all clogged drains	75
3.16	Water table drawdown of the upper layer after opening all clogged Drains	76
4.1	Aquifer types discussed in (Kinzelbach,1986).	79

Fig. No.	Description	Page
4.2	Discretization of the Solution Region	80
4.3	Flow in A typical Nodal Cell.	82
4.4	Leakage from surface water body to the upper layer in his two cases.	84
4.5	Directional (Inter nodal) Transmissivities considered by the mathematical model	88
4.6	Flow chart of the quick basic program	108
4.7	Simulated and observed water table level for the upper layer by the mathematical model (march 2000)	115
4.8	Simulated and observed peizometric head for the lower layer by the mathematical model (march2000)	116
4.9	Calibrated (model) recharge (m3/day) per nodal cell	117
4.10	Simulation water table level of the upper layer by the mathematical model after reducing the local recharge about 50%	119
4.11	Simulation water table drawdown of the upper layer by the mathematical model after reducing the local recharge about 50%	120
4.12	Simulation water table level of the upper layer by the mathematical model after reducing the local recharge about 75%	121
4.13	Simulation water table drawdown of the upper layer by the mathematical model after reducing the local recharge about 75%	122

Fig. No.	Description	Page
4.14	Water table level of the upper layer after operating four wells surrounding each holy shrine	123
4.15	Water table drawdown of the upper layer after operating four wells surrounding each holy shrine	124

Table of Symbols

Symbol	Definition
BCF	Block centered flow
BL1	Bottom elevation of the upper layer
BLT	Bottom elevation of the middle layer
Beb	Bottom elevation of the Bed of Surface Water Body
DWSK	Directorate of water supply and sewerage of Karbala
FCSDIP	AL-Furate center for studies and designs of irrigation projects
GMS	Groundwater modeling system
GSL	Ground surface level
HO1	Head of the upper layer
HO3	Piezometeric head of the lower layer
IADI	Iterative alternating direction implicit procedure
ISSWR	Iraqi scientific society of water resources
LCM	Leakage coefficient for the middle layer
LCB	Leakage coefficient for the bed of surface water body
mal	Meter above see level
NCCL	National center for construction laboratories
Qleak	Amount of leakage between upper and lower layer
Qnet	Local recharge to the upper layer
QU	Amount of Leakage Between the cells in the Upper Layer
QL	Amount of Leakage Between the cells in the Lower Layer
Qswb	Amount of Leakage From Surface Water Bodies
Qqw	Discharge of Wells
RMSE	Root Mean Square Error
Teb	Top Elevation of the Surface Water Body
TIFF	Tags Image File Format

Symbol	Definition
thic	Thickness of the Middle Layer
thicr	Thickness of the Bed of Surface Water Body

Table of Tables

Table No.	Description	Page
1.1	Monthly and annual averages of meteorological elements at Karbala station for the period (1980-2006)	5
2.1	Results of the permeability tests at a different depths for the boreholes (B1 to B8)	17
2.2	Results of the pumping tests	18
2.3	Results of the recovering test after pumping was stopped	19
2.4	Monthly average observed data of groundwater levels	21
2.5	Results of the permeability tests for the upper layer for piezometers (H1 toH7)	32
2.6	Monthly average observed data of groundwater levels by Hassan AL-Khateeb	35
3.1	Dimensions of the Three Points of Registration	51
3.2	The information of the Boreholes That used in the Models	52
3.3	Information of the Nodes of Karbala GMS model	56
5.1	Comparison the results between the mathematical model and the GMS model	127

CHAPTER ONE

INTRODUCTION

1-1 Description of the Study Area

The area which is considered in this study is located in Karbala city. Karbala city lies between longitude (43° 59′ 12′′ — 44° 04′) E and latitude (32° 33′ 51′′ — 32° 38′ 27′′) N. It is about 100 km southwest of the capital Baghdad. The city has its importance from the shrines of Imam AL-Hussain and his brother AL-Abbas (peace be upon them). They were buried in this city with some of their companions after they were killed for freedom in one of the most historical famous battle named (AL-Taff). After that, the city has become one of the most visited places for the Muslims who come from different places in the world. In fact karbala city has been formed and extended because of the two holy shrines which are now surrounded by a considerable number of hotels, restaurants, and markets. Figure (1-1) illustrates the location of karbala city in Iraq and shows a satellite photograph to the study area. The river Euphrates lies to the east of the study area, and one of its branches named AL-Hussainyia river bonds it at its north side. AL-Hussainyia river branches into two irrigation canals whose names are Rushdiyah canal and Hindiyah canal, the last one is lined and passes through the study area while the first one lies to the north of the study area.

The study area is surrounded by agricultural lands with the exception of the southwest side, and it is about 3.2 Km^2 in area. Open Western Drain locates at the west boundary while covered drains are located at the other boundaries, they are Karbala Covered Drain and Eastern Covered Drain, Figure (1-2). There is a third covered drain in the study area which is the Western Covered Drain which is parallel to the Hussainiya river. The covered drains were constructed instead of the open drains at the same place because of the extension of the city. Covered western Drain was constructed in 1974 while the other covered drains were constructed in 1966.

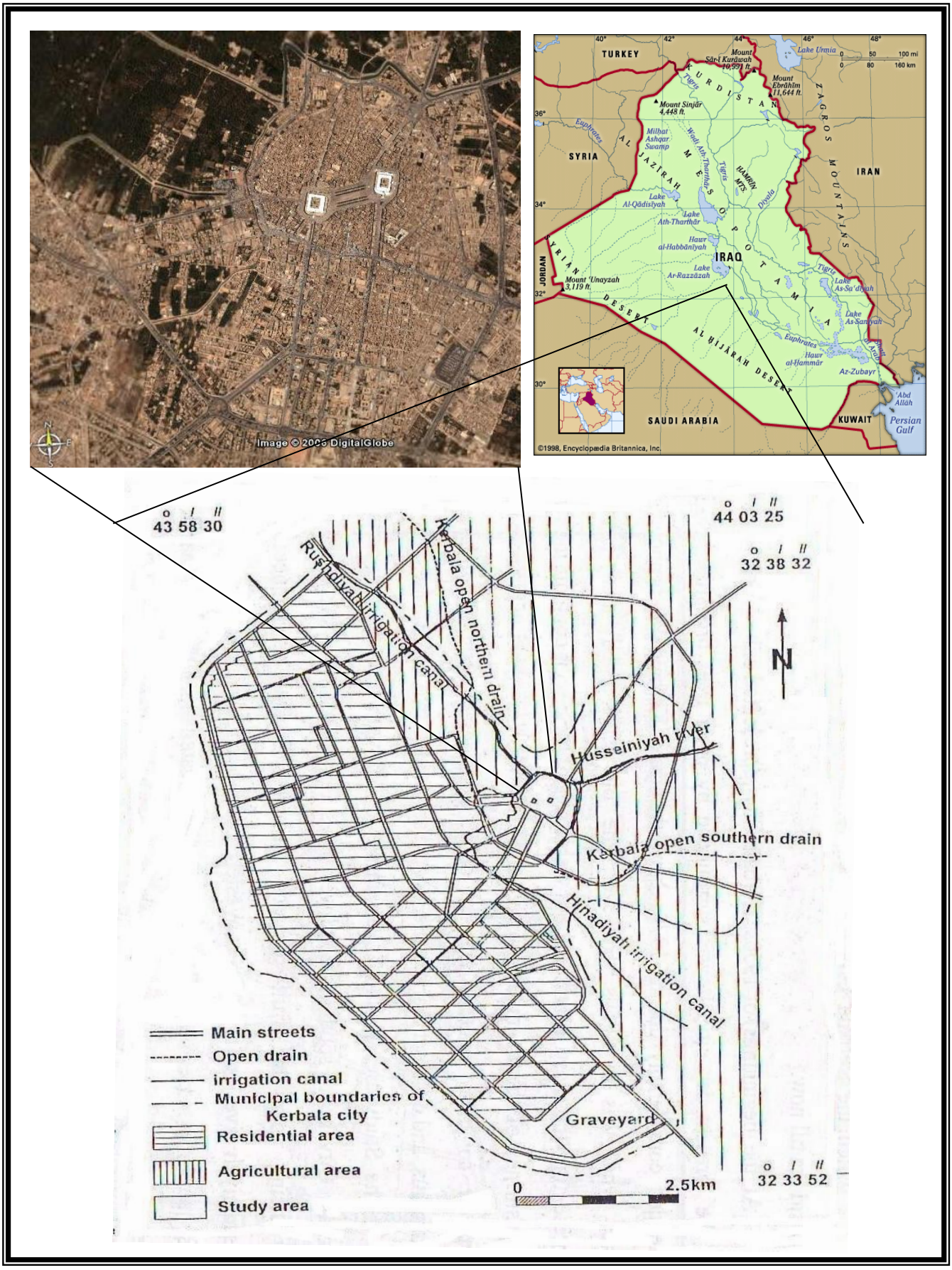

Figure(1-1) Location of Karbala city in Iraq (Google Earth)

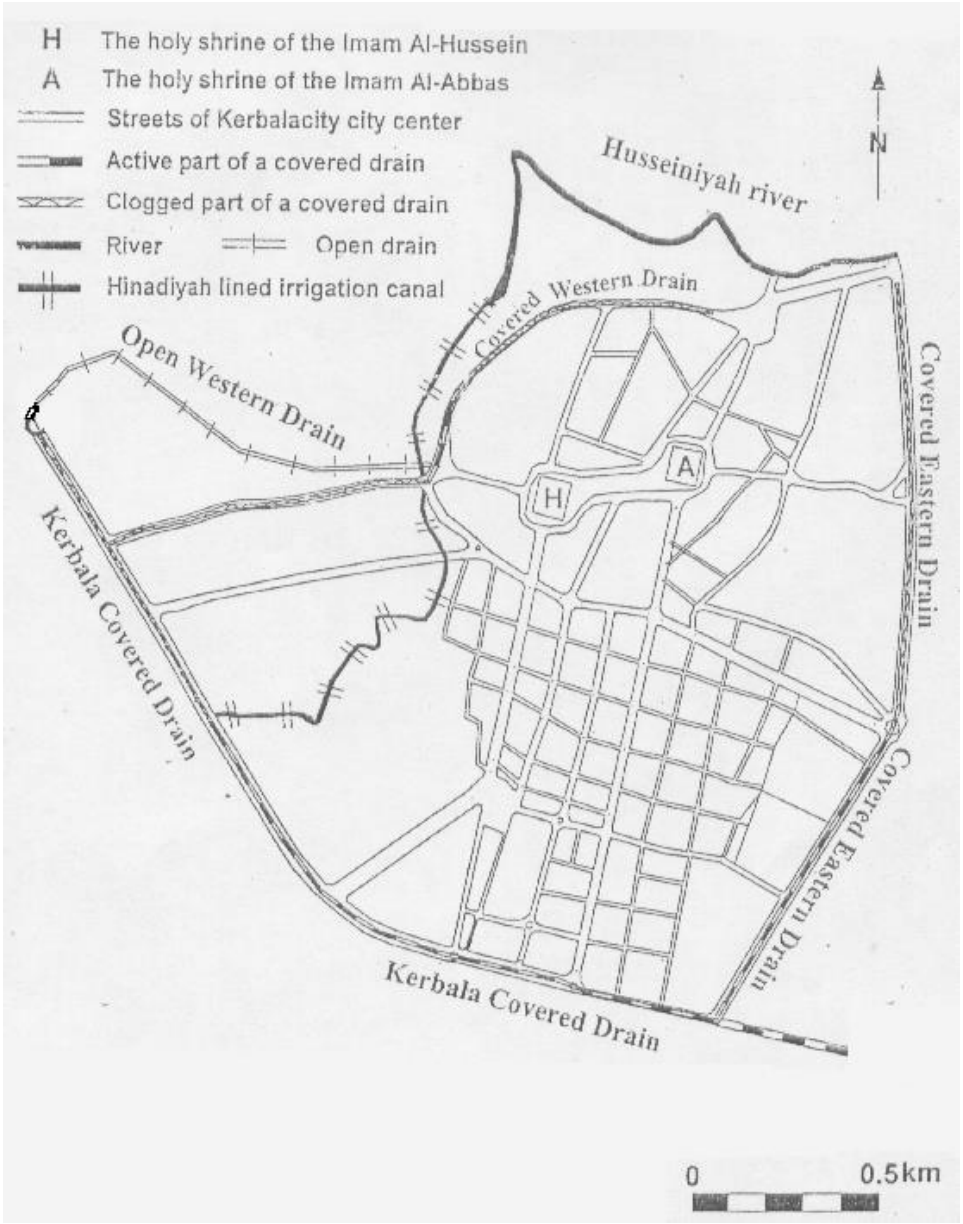

Figure (1-2) Map of the study area (Hassan AL-Khateeb, 2001)

The covered drains consist of pieces of reinforced concrete pipe with a diameter (1.2)m for Karbala Covered Drain and (0.8)m for the other two covered drains. The pieces are connected to each other by joints surrounded by filters of gravel layers. The length of the Karbala Covered Drain is about (3)km while the lengths of Eastern and Western covered drains are about (2.2)km.

After few years of construction the Covered Western Drain was clogged, and because of difficulty of cleaning, an open drain called Open Western Drain was constructed in 1999 instead of it, but not in the same place, Figure (1-2). Also due to the absence of the periodical maintenance, the remaining two covered drains were clogged too. In 1998 a work of cleaning some parts of these two drains was carried out, but also the absence of periodical maintenance caused clogging most of their parts in the years after that.

There are three water treatment plants in the city for drinking water. They are Old Drinking Water Project instilled in 1961 with a capacity of 27000 m3/day, Hai AL-Hussain Project instilled in 1973 with a capacity of 59000 m3/day, and Project No.7 instilled in 1985 with a capacity of 120900 m3/day. The three plants take the water from AL-Hussainyia river.

Sewers and septic tanks are the two methods by which the sewage is disposed. Sewer system covers only about 75% of the study area while some clogged and leaking cases were observed during the last fifteen years.

The climate of the study area can be classified into two seasons, hot-dry season in summer and cold-wet season in winter. Recorded meteorological data of Karbala meteorological station can be used to evaluate the climate characteristics of the study area. Table (1.1) shows the monthly average meteorological data of temperature, sunshine, relative humidity, wind speed, rainfall and evaporation at Karbala station through the period (1980-2006).

At the beginning of 1970, shallow groundwater levels were observed in the basements of buildings in the study area especially in the two holy shrine basements were the rising water level was first observed at the holy shrine of AL-Abbas.

Table (1.1) Monthly and annual averages of meteorological elements at Karbala station for the period (1980-2006) (Iraqi Meteorology Organization).

Month	Temperature. °C	Sunshine Duration hr/day	Relative Humidity %	Wind Speed m/sec	Rainfall mm	Evaporation mm
January	**10.39**	**6.14**	**74.96**	**2.208**	**17.67**	**64.45**
February	**12.68**	**7.27**	**61.79**	**2.67**	**16.07**	**97.98**
March	**17.4**	**8.02**	**53.42**	**3.065**	**16.81**	**177.88**
April	**24.15**	**8.53**	**43.2**	**3.18**	**15.11**	**264.8**
May	**29.76**	**9.42**	**33.77**	**3.307**	**4.47**	**364.81**
June	**34.16**	**11.66**	**28.81**	**4.15**	**0**	**455.22**
July	**36.5**	**11.57**	**29.92**	**4.35**	**0**	**495.67**
August	**35.91**	**11.13**	**32.0**	**3.6**	**0**	**445.88**
September	**32.12**	**10.27**	**35.96**	**2.49**	**0.46**	**333.34**
October	**25.6**	**8.43**	**45.81**	**2.1**	**4.535**	**222.23**
November	**17.43**	**7.18**	**61.92**	**1.95**	**12.43**	**111.38**
December	**11.84**	**6.21**	**74.46**	**1.97**	**17.72**	**66.64**
Annual	**23.995**	**8.82**	**48.00**	**2.92**	**8.77**	**258.36**

1-2 Objective of the Present Study

Until now there is no any adopted solution to the problem of rising groundwater level which still exists in the basements of the two holy shrines in Karbala city. Since the problem becomes one of the most important problems that endanger the safety of the two holy shrines and the city as a whole, it is important to find measures to lower the water table. The objectives of this study are:

1- Simulating the groundwater flow in the study area using the GMS model
2- Establishing the main sources of the groundwater recharge in the area using the same model .
3- Examining different possible measures of lowering groundwater table.
4- Using a numerical model other than the GMS one for the same above mentioned purposes.
5- Comparing the results of the GMS model with those obtained from the new model.

CHAPTER TWO
LITERATURE REVIEW

2-1 General

Groundwater problems are represented by models. A model is perhaps most simply defined as a representation of a real system or process (Jacques W. Delleur,1999). The construction and operation of such model is called simulation (Mercer & Faust,1981). Groundwater models vary in complexity. The complexity of the model used to analyze a specific site should be determined by the type of problem being analyzed. While more complex models increase the range of situations that can be described, a higher level and range of skill of the modelers are required.(Water science and technology board, 1990). In general groundwater model can be as simple as a construction of saturated sand packed in a glass container or as complex as a three-dimensional mathematical representation requiring solution of hundreds of thousands of equations by a large computer.(U.S. Army Corps of Engineers ,1999).

Prickett (1975) and Wang(1982) divide the groundwater models into three types, sand tank models, analog models, and mathematical models. The mathematical models are a set of equations that depend on two concepts, mass balance and Darcy's law. The mathematical models express quantitatively the hypothesis for how a real system or process operates. This hypothesis is called the conceptual model (Jacques W. Delleur,1999). The conceptual model is defined by (P Hulme, M Grout, K Seymour, K Rushton, L Brown, and R Low, 2002) as a description of how a hydrogeological system is believed to behave.

The equations of the mathematical model are usually partial differential equations. Numerical solution is often used in the solution of these equations because the analytical solution is applied only to a simplified subset of equations. Therefore, mathematical models are divided into numerical models and analytical models. A numerical model needs high speed digital computers because of the large number of

equations. Several programs were developed to represent this type of models such as MODFLOW.

MODFLOW is a modular three-dimensional finite-difference groundwater model published by the U. S. Geological Survey. The first public version of MODFLOW was released in 1988 and is referred to as MODFLOW-88 (McDonald, MG and Harbaugh, AW,1988). It was originally designed to simulate saturated three-dimensional groundwater flow through porous media. The applications of MODFLOW-88 to describe and predict the behavior of groundwater flow systems have increased significantly over the last years partially due to a wide range of add-on codes, such as parameter estimation programs and solute transport models, and partially due to the availability of various easy-to-use graphical user interfaces,(Wen- Hsing Chiang.2005). One of the most famous groundwater models programs that used the MODFLOW as a code is the (GMS) program.

The Groundwater Modeling System (GMS) is a modeling environment used for groundwater simulations. It contains a graphical interface and a number of different analysis codes, including MODFLOW and MODPATH. GMS provides tools that allow the user to characterize the study area, conceptualize the model and generate the inputs for the various models in the system. It also performs the calculations and interpolations needed to visualize the result (Victoria Ljungberg & Sarah Qvist, 2004).

Engineering Computer Graphics Laboratory (ECGL) of Brigham Young University constructed a groundwater model using the GMS program for a site located in East Texas. It was assumed that what was required was the evaluating the suitability of a proposed landfill site with respect to potential groundwater contamination. The model simulated the groundwater flow in the valley sediments bounded by the hills to the north and the two converging rivers to the south. The site is underlain by limestone bedrock which outcrops to the hills at the north end of the site. (GMS v2.0, Tutorials, 1996).

Victoria Ljungberg & Sarah Qvist (2004) made a groundwater flow model using the GMS program for Sulur watershed which lays in the Coimbatore District in Tamil

Nadu in southern India. The situation is on a plateau surrounded by mountains forming a rain shadow area that results in a dry climate, which affects the water availability and also most inhabitants are dependent on agriculture, and as the surface water is limited, groundwater becomes the main source of water. To meet the demand for irrigation, water is diverted from the River Noyil to the Sulur Big and Small Tank. Due to the discharge of untreated sewage water into the Small Tank the water has become unsuitable for irrigation. The contaminated water will also infiltrate to the groundwater and affect the water quality in the surrounding wells. The Sulur watershed hence faces a problem of both quantity and quality of water. They found that water level can be increased by the introduction of percolation ponds and As a result of the small amount of available water, the influence of the Small Tank is restricted to its direct vicinity.

The most commonly used three-dimensional (3D) computer software packages, Groundwater Modeling System (GMS) and Visual MODFLOW, plus the two-dimensional (2D) software package, BIOPLUME III were selected by You-Kuan Zhang, Byong-min Seo, Nanh Lovanh, Pedro J.J. Alvarez, and Richard Heathcote (2001) to be evaluated for the purpose of assessment the contaminated sites in Iowa. They found from the comparison of the three software packages, that GMS is superior to Visual MODFLOW and BIOPLUME III because (1) GMS does everything Visual MODFLOW and BIOPLUME III do and more, and (2) GMS is better documented and more to users friendly.

Ibtisam R. Karim (2005) made a groundwater flow model using the groundwater modeling system (GMS) for the Ancient Babylon city which suffers from high groundwater level, that interferes with and hampers the process of archeological investigations and surveys, therefore the purpose of construction the (GMS) model was to study the lowering of the water table level below the oldest archeological zone, which was expected to be at a depth (14-16m) below ground surface. The lowering processes assumed in that study was a ringed well system surrounding the study area with (45) wells distributed in area about 5.5km^2. Each well was assumed to penetrate a depth of (45m), and discharged at a rate of (17L/s). The model shows

that the lowering of the water table level to the required depth may be after 250 days of pumping.

Two-dimensional finite-difference model of the deep confined aquifer of Powder River Basin of northeastern Wyoming and southeastern Montana that contains a large coal reserves was developed by Konikow (1976) to improve the conceptual model of groundwater flow in the aquifer system.

Two dimensional groundwater model was developed by McWhorter & Sunada (1977) to analyze the groundwater heads in confined and unconfined aquifers using the Gauss elimination procedure. Rushton & Redshaw (1979) used the digital computer to solve the problems of two and three dimensional models with steady and transient states.

A two dimensional model applied on unconfined, semi confined, and confined aquifers with regular and irregular grids was developed by Boonstra & de Ridder (1981). The solution of the finite difference equations in this model was made by Gauss Seidal method.

2-2 Previous Studies on Groundwater in Karbala City

Previous studies on groundwater in Karbala city were conducted by the following workers:

1- National Center for Construction Laboratories (NCCL).

2-Iraqi Scientific Society of Water Resources(ISSWR).

3- AL-Furate Center for Studies and Designs of Irrigation Projects (FCSDIP).

4- Directorate of Water Supply and Sewerage of Karbala (DWSK).

5- AL-Kutubi Engineering Laboratory.

6- Hassan Mahdi AL-Khateeb.

Several borehole, piezometer, and sinks observations were made by these workers. The logs are as shown in appendix (B).

The NCCL Study

Groundwater levels were recorded by NCCL using boreholes and piezometers as described below:-

a. In 1981 five boreholes were drilled around the holy shrine of AL-Abbas, their names are 1,2,3,4, and 5, and their locations are shown in Figure (2-1). Boreholes 1,2, and,3 have a depth of 20m while boreholes 4 and 5 have a depth of 20.5m.
b. In 1992 four boreholes were drilled around the inside building of AL-Abbas holy shrine, Figure (2-1). Their depths are 12m.
c. In 1998 four boreholes were drilled around the holy shrine of AL-Hussain, one borehole at each corner, Figure (2-2). The depths of these boreholes are about 15m.
d. Also in 1998 four shallow piezometers and four deep piezometers were made around the holy shrine of AL-Hussain. The depths of the shallow piezometers ranges between (3.75-7.05)m and their names are P1,P5,P7, and P8 while the depths of the deep piezometers ranges between (9.9-11.15)m and their names are P2,P3,P4, and P6, Figure (2-2). The logs of these piezometers are not available.

The observation of groundwater level was during one month from 15/12/1997 to 15/1/1998 using the eight piezometers surrounding the holy shrine of AL-Hussain (P1 to P8), Figure (2-3) shows a graphical representation of the observation data. From this figure the deep piezometers (P2,P3,P4, and P6) shows a different behavior from the shallow piezometers (P1,P5,P7, and P8).

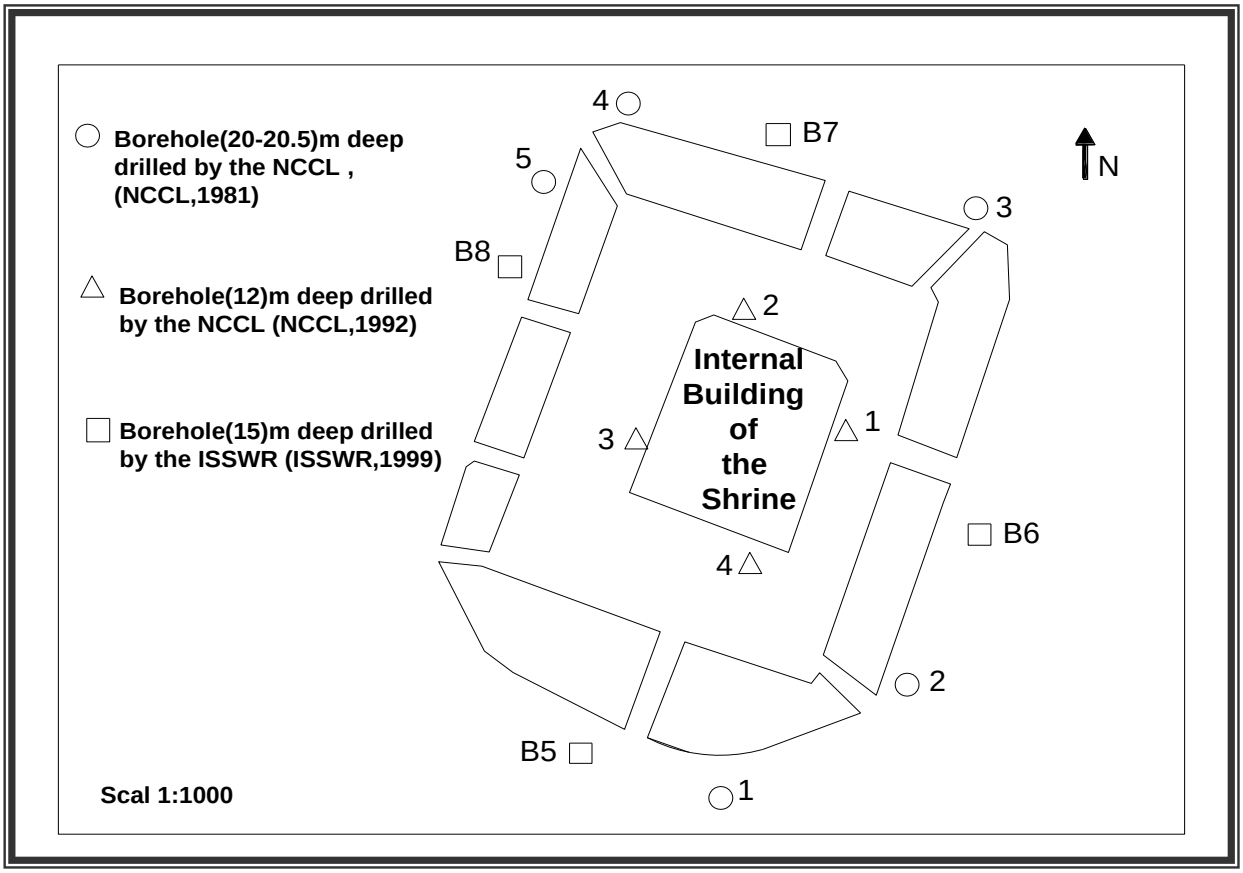

Figure (2-1) Locations of the drilled borehole around the holy shrine of AL-Abbas

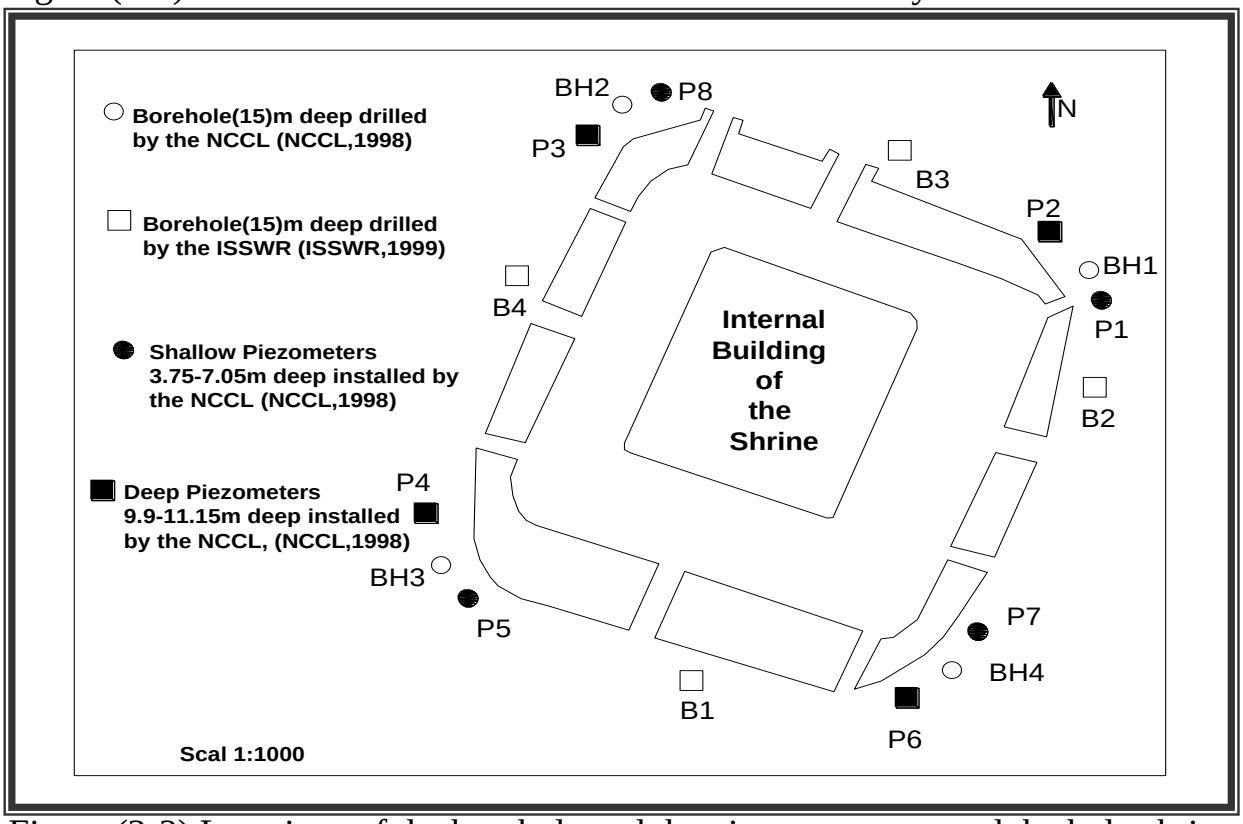

Figure (2-2) Locations of the borehole and the piezometers around the holy shrine of AL-Hussain

they record a big rising in groundwater head during one month (about 6m). It was concluded that the deep piezometers did not represent the hydraulic head of the lower layer during that time, but the figure is useful to show that, in total, the groundwater head in the lower layer is less than the groundwater head in the upper layer. The figure also shows a considerable fluctuation in the shallow piezometers, that was assigned to a local recharge water sources of unsteady nature, from that it was concluded that these sources might be a leakage from pipe networks or sewer systems. Also it was found from these observations that the groundwater flow in the upper layer have a general trend from northeast to southwest.

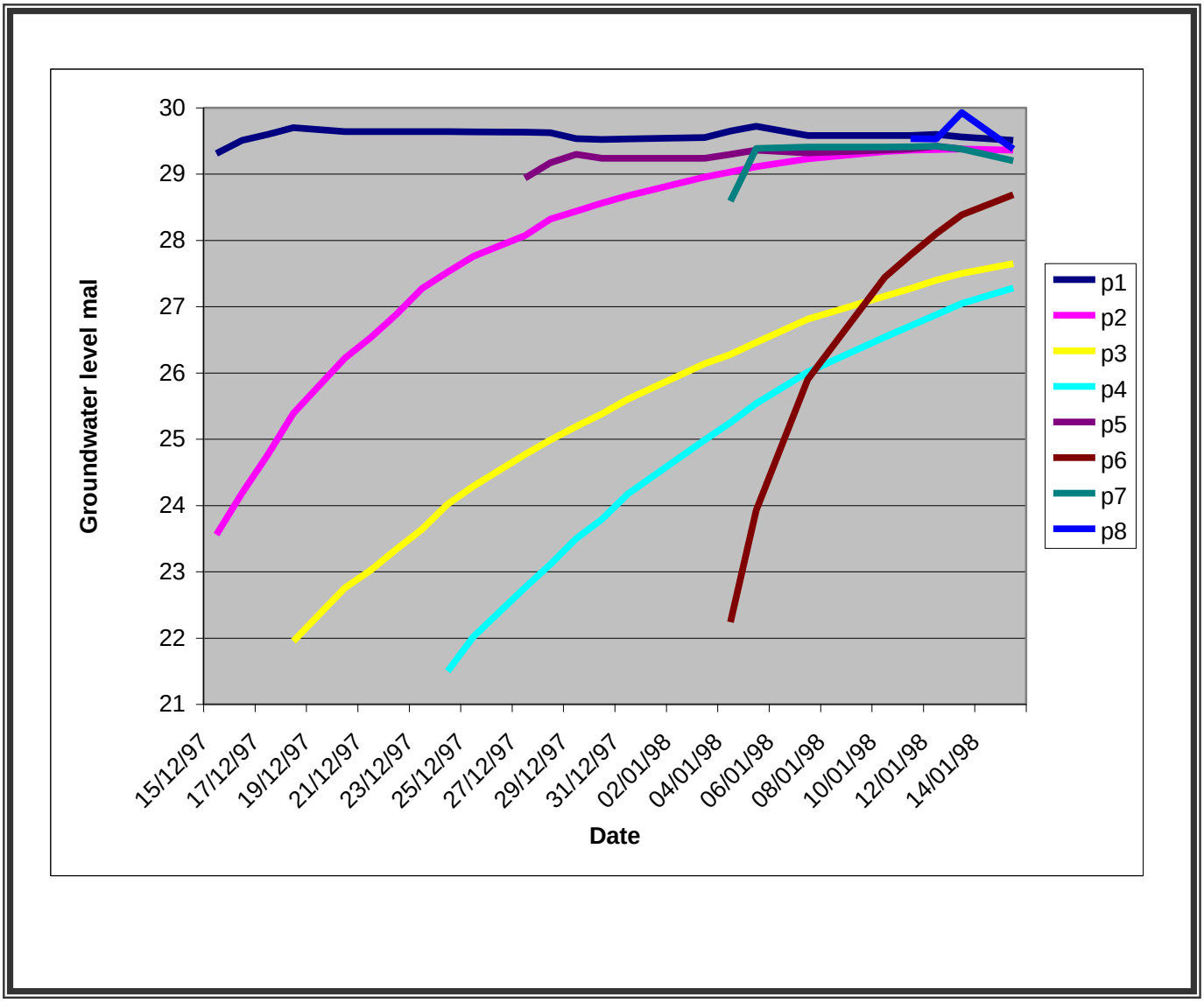

Figure (2-3) Groundwater head observations by the NCCL during the period (15/12/1997 to 15/1/1998) for the piezometers (P1 to P8)

The ISSWR Study

The works were made by the ISSWR in 1999 :

a. Eight boreholes were drilled around the two holy shrines, four around each one, their depths are 15m and their names are (B1 to B8), the first four around the holy shrine of AL-Hussain while the remaining are around the holy shrine of AL-Abbas. Figures (2-1) and (2-2).
b. Nine shallow piezometers with a depths of (6)m and with a names of (S1 to S9) were installed around the two holy shrines in addition to five deep piezometers with a depths of (15)m and with a names of (D1 to D5), Figure (2-4).
c. Three sinks were constructed in the area surrounding the two holy shrines, their names are (SK1,SK2, and SK3) and their locations are shown in figure (2-4). The purpose of installing these sinks was to discharge the water from the upper layer to the lower layer considering the idea that say, the hydraulic head of the upper layer is higher than the hydraulic head of the lower layer.
d. One well was constructed between the two holy shrines, Figure (2-4), its name (W) and its depth and diameter are (30)m and (0.25)m respectively.

A field permeability tests were carried out by the (ISSWR) in 1999 using the boreholes (B1 to B8) that surround the two holy shrines at a different depths. Constant head permeability test was used, the results are shown in Table (2-1). The table shows that the permeability of the upper layer ranges between (0.118-84.672) m/day and the permeability of the lower layer ranges between (0.055-6.376) m/day, while the permeability of the middle layer ranges between (0-2.272) m/day.

Also a pumping test was carried out in the study area by the (ISSWR) in 1999 using the well (W) for pumping and the piezometers (S4) and (D1) for observation. These piezometers are at a distance (17.7)m and (12)m from the well (W) respectively. The test was to find the storage coefficient and the transmissivity of the lower layer, as well as, to deduct the hydraulic relationship between the upper layer and the lower

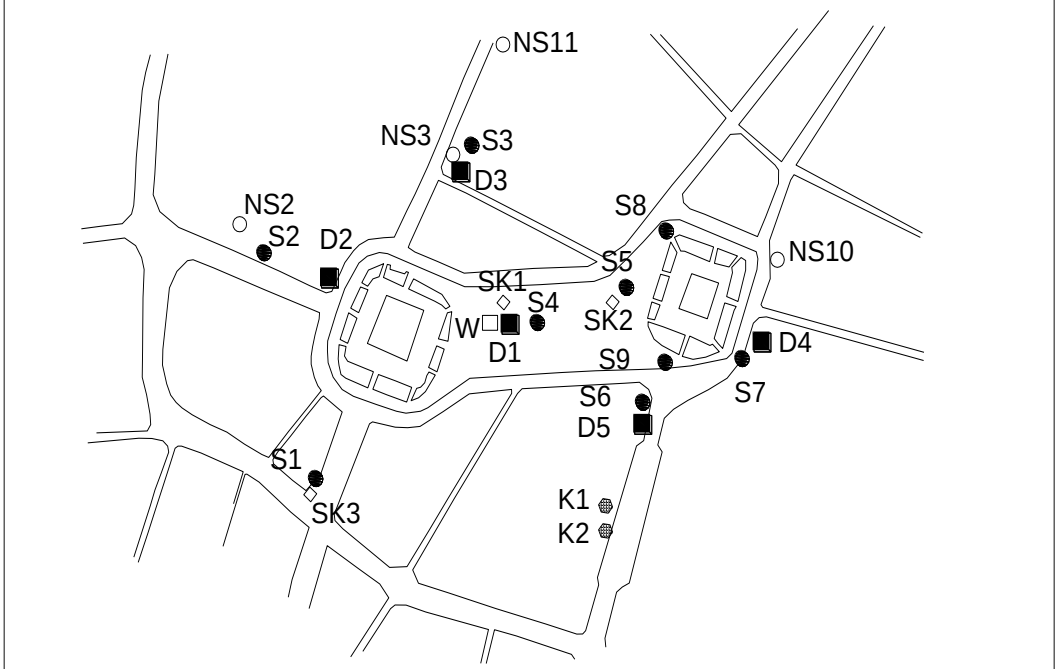

● S Shallow piezmeters (6m deep) installed by the ISSWR(ISSWR,1999)

○ NS Shallow piezmeters (6m deep) installed by the DSWK(Auwayid,2000)

■ D Deep piezmeters (15m deep) installed by the ISSWR(ISSWR,1999)

◇ SK Sinks connecting the upper and the lower layers(15m deep) installed by the ISSWR(ISSWR,1999)

□ W Well(30m deep) installed by the ISSWR(ISSWR,1999)

◍ K Boreholes (7.5-9.2m deep) drilled by AL-Kutubi Engineering lab. (AL-Kutubi Engineering lab,1999)

Scal 1:10000

Figure (2-4) Locations of the boreholes and the piezometers in the area surrounding the two holy shrines

layer. The pumping was at rate 4L/sec, and the results are given in Table (2-2). From this table the following points were recorded:-

1- There was a simultaneous drawdown in the water level in the deep piezometer (D1), while the drawdown in the water level in the shallow piezometer (S4) began after 20 minutes of pumping.
2- Water level in the deep piezometer (D1) reached a stable level after 30 minutes of continues pumping, while the water level in the shallow piezometers continued lowering.
3- In total, the deep piezometer (D1) had the biggest drawdown, its drawdown (0.63)m began after 75 minutes of continuous pumping, while, the drawdown in the shallow piezometer (S4) is only (0.03)m.

From that it was certified that the two piezometers were related to two different hydraulic system, the lower layer was a leaky aquifer, and the middle layer acted as a semi pervious layer. the results in Table (2-2) were used to calculate the hydraulic characteristics of the leaky aquifer (ISSWR, 1999). The standard Walton curves (Walton,1962; Kruseman and Deridder,1979) were applied and the following results were obtained:-

1- Transmissivity (T)= 206 m2/day
2- Storage coefficient (S)= 0.0087
3- Vertical permeability of the middle layer (K)= 0.028 m/day

Table (2-3) shows the recovery data of the piezometers (D1) and (S4) after pumping was stopped. The data shows that the water rises in the deep pieazometer (D1) faster than the shallow piezometer (S4), it raised (0.3)m in piezometer (D1) during 42 minutes while it raised only (0.02)m in piezometer (S4), this insures the conclusion of the pumping data that the two piezometers are related to two different hydraulic system. The recovery data was again applied and the transmissivity 197 m2/day was obtained, this value is near to the pervious calculated value 206 m2/day. A value of 200 m2/day was adopted by ISSWR (1999).

Table (2-1) Results of the permeability tests at a different depths for the boreholes (B1 to B8) (ISSWR,1999)

Borehole name	Depth range (m)	Permeability m/day
B1	5.2-6.2	1.028
	6.2-7.2	0
	11.0-12.0	6.376
B2	3.5-5.25	0.118
	10.0	0.755
B3	4.15-6.25	7.569
	6.5-7.5	0.024
	10.0-12.5	0.068
B4	6.4-7.4	0.038
	9.0-10.0	0.041
	13.0-14.0	0.71
B5	2.5-4.5	8.64
	6.8-7.5	0.046
	11.5-13.5	0.555
B6	4.0-6.0	84.672
	7.0-8.0	0.219
	8.0-11.0	0.638
	12.0-14.0	0.055
B7	1.0-4.0	0.795
	7.0-8.0	0.000
	8.2-9.2	2.748
B8	1.9-3.1	8.64
	5.0-6.0	7.327
	7.5-8.5	0.013
	8.8-10.8	2.272
	13.0-14.0	2.687

Table (2-2) Results of the pumping tests (ISSWR,1999)

Time (min)	Water depth (m)		
	W	S4	D1
0	3.1	2.89	2.98
1	-	2.89	3.1
2	-	2.89	3.21
3	-	2.89	3.26
4	-	2.89	3.3
5	-	2.89	3.34
6	-	2.89	3.37
7	-	2.89	3.39
10	-	2.89	3.43
15	6.29	2.89	3.45
20	6.13	2.89	3.46
30	6.98	2.9	3.61
45	6.51	2.915	3.61
60	6.32	2.915	3.61
75	6.2	2.92	3.61

Table (2-3)Results of the recovering test after pumping was stopped (ISSWR,1999)

Time after pumping was stopped (min)	Water depth (m)	
	S4	D1
3	2.92	3.4
4	2.92	3.37
5	2.92	3.34
6	2.92	3.332
7	2.92	3.3
8	2.92	3.29
9	2.92	3.29
10	2.915	3.275
15	2.91	3.2
20	2.91	3.17
25	2.91	3.14
30	2.9	3.13
45	2.9	3.1

The observations of groundwater were made during six months from 14/12/1998 to 10/6/1999 using the nine shallow piezometers (S1 to S9), the five deep piezometers (D1 to D5), the three sinks (SK1 to SK3), and the only well (W). The data are listed in appendix (C-1) and the monthly average data are listed in Table (2-4). Figure (2-5) shows the areal distribution of the monthly average of water table of the upper layer and the monthly average of piezometeric head of the lower layer for the months (December, March, and June). The figure shows that the highest levels of the two layers are near the holy shrine of AL-Abbas, and the levels of the upper layer are higher than the levels of the lower layer. The figure also shows that there is a difference in the magnitude of heads between the months which indicates that the heads are effected by a local recharge conditions. Since the maximum level of the shoulders of AL-Hussainya river is about (28.5)mal which is less than the maximum groundwater level in the area of the two holy shrines (30.7)mal, it was concluded that this local recharge may be due to leakage from drinking pipe networks, sewers, and septic tanks.

To find the relationship between the upper and the lower layers groundwater heads, the fluctuations of the heads are drawn in the figures (2-6) and (2-7) for some shallow and deep piezometers which are very near to each other. From these figures it is very easy to conclude that the groundwater level of the upper layer is higher than the piezometric head of the lower layer, which means that the lower layer is recharged from the upper layer through the middle layer.

Table (2-4) Monthly average observed data of groundwater levels (ISSWR,1999)(mal)

Piezometer name	Month name						
	December 1998	January 1999	February 1999	March 1999	April 1999	May 1999	June 1999
S1	28.95	——	28.57	28.61	28.62	28.61	28.64
S2	29.08	28.99	29.0	29.07	29.19	29.18	29.16
S3	30.36	30.5	30.49	30.41	30.54	——	——
S4	30.04	30.02	30.01	30.14	30.05	30.1	30.13
S5	30.66	30.28	30.32	30.43	30.18	30.64	30.61
S6	30.44	30.74	30.76	30.7	30.68	——	——
S7	30.14	30.13	30.17	30.2	30.19	30.22	30.25
S8	30.43	30.5	30.57	30.8	30.78	30.81	30.79
S9	30.27	30.23	30.28	30.34	30.3	30.4	30.5
D1	30.25	30.06	29.96	29.8	29.78	29.89	29.94
D2	29.43	29.46	29.47	29.49	29.45	29.66	29.66
D3	29.83	30.16	30.15	30.11	30.17	30.2	30.25
D4	29.96	30.0	30.07	30.05	30.07	30.09	30.12
D5	29.4	29.97	30.0	30.05	30.04	30.14	30.18
SK1	——	30.06	30.04	30.05	30.06	30.12	30.27
SK2	30.61	30.34	30.31	30.47	30.5	30.59	30.59
SK3	28.47	28.56	28.58	28.94	28.69	28.64	28.66
W	29.87	29.92	29.91	29.93	29.95	29.85	29.88

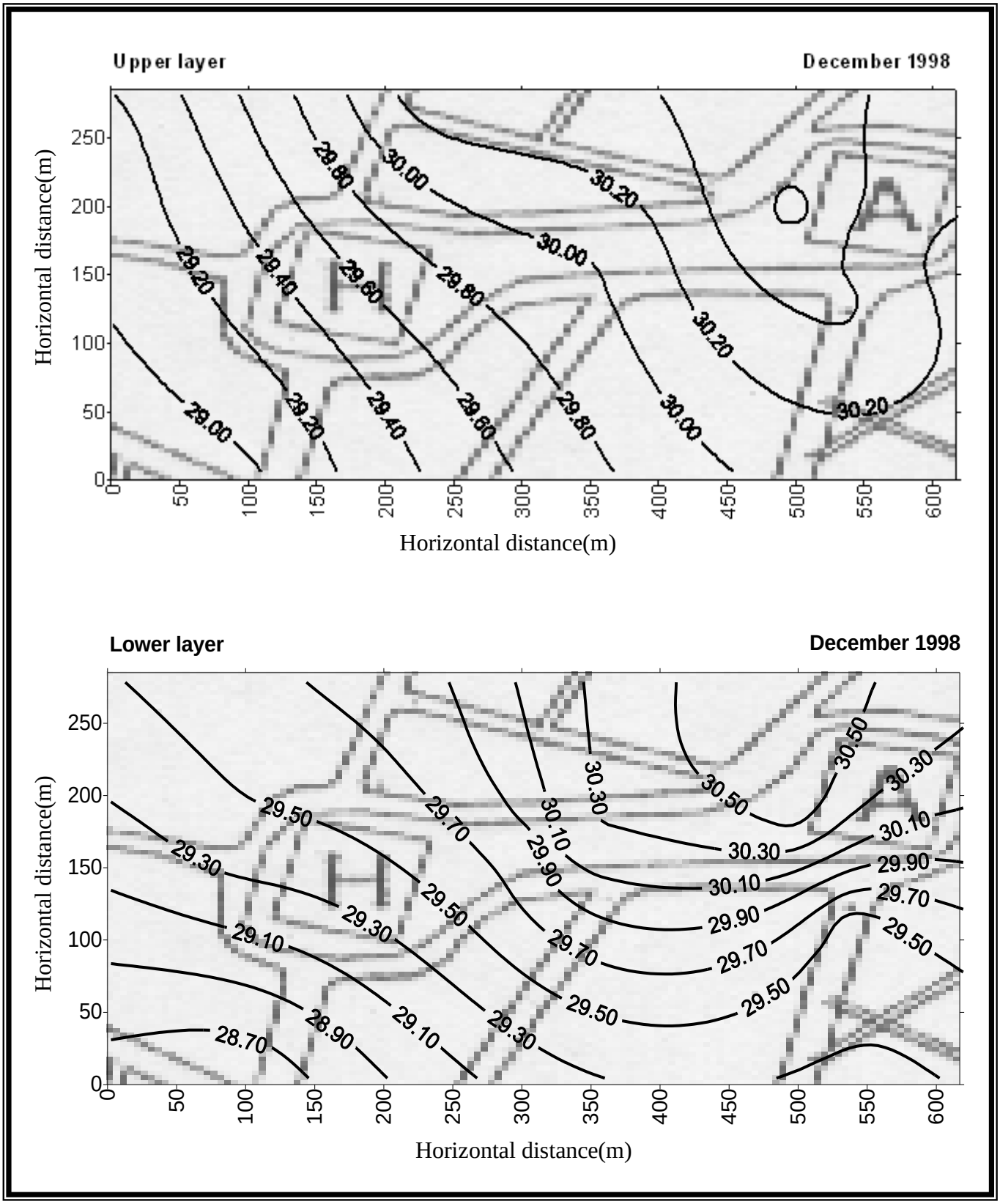

Figure (2-5) Areal distribution of the monthly average groundwater head for the upper and the lower layer (ISSWR,1999) (mal)

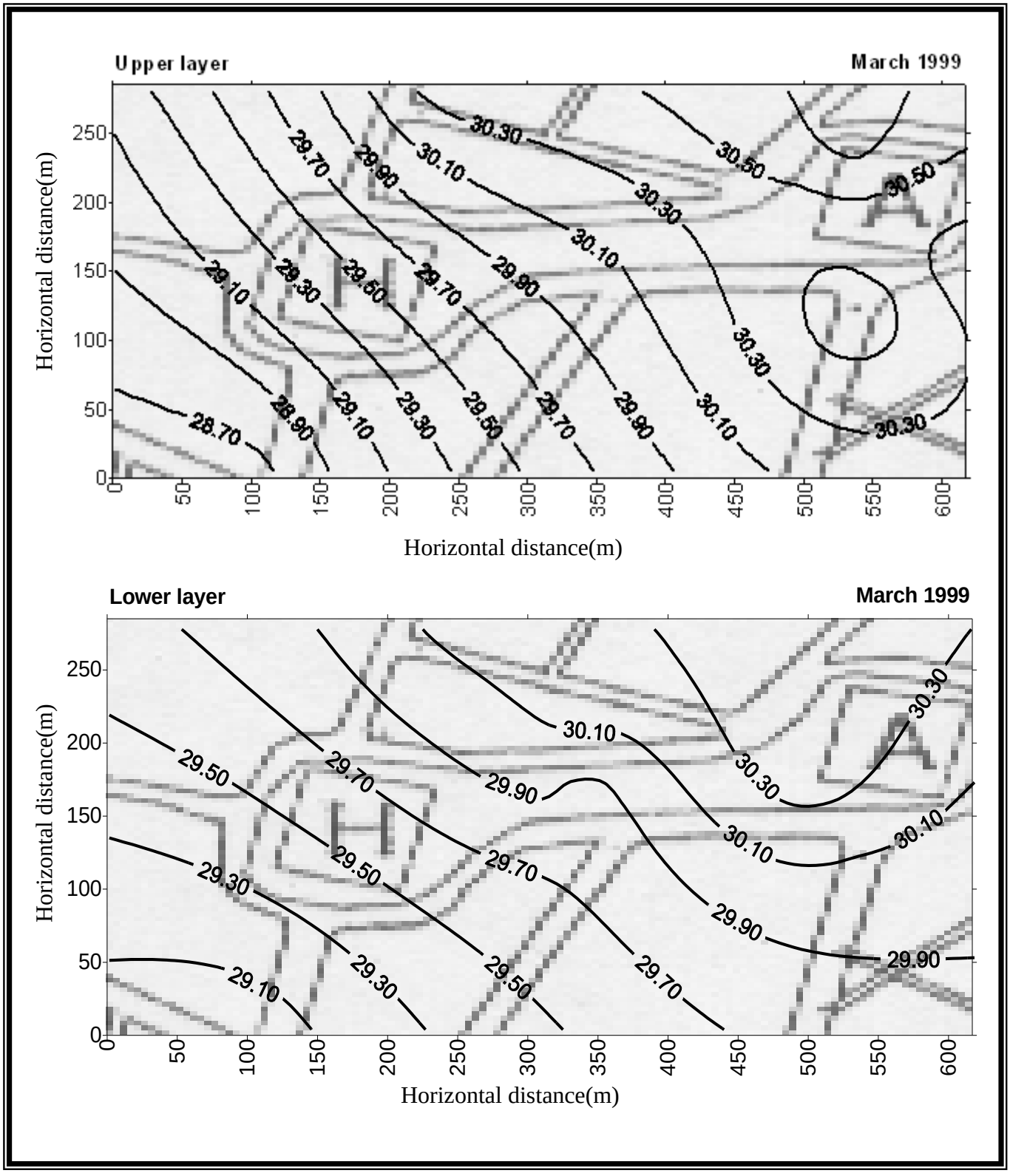

Figure (2-5) continue

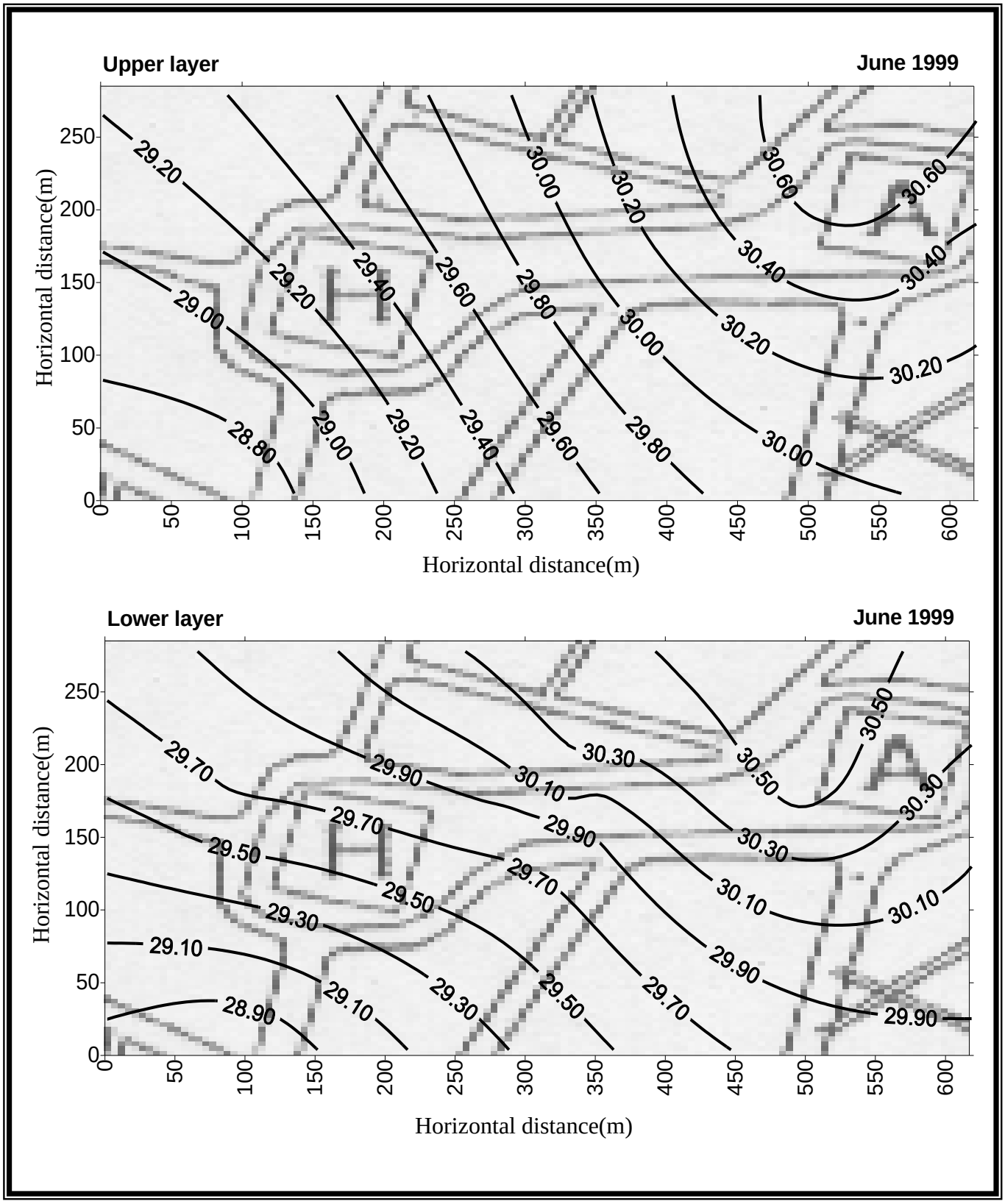

Figure (2-5) continue

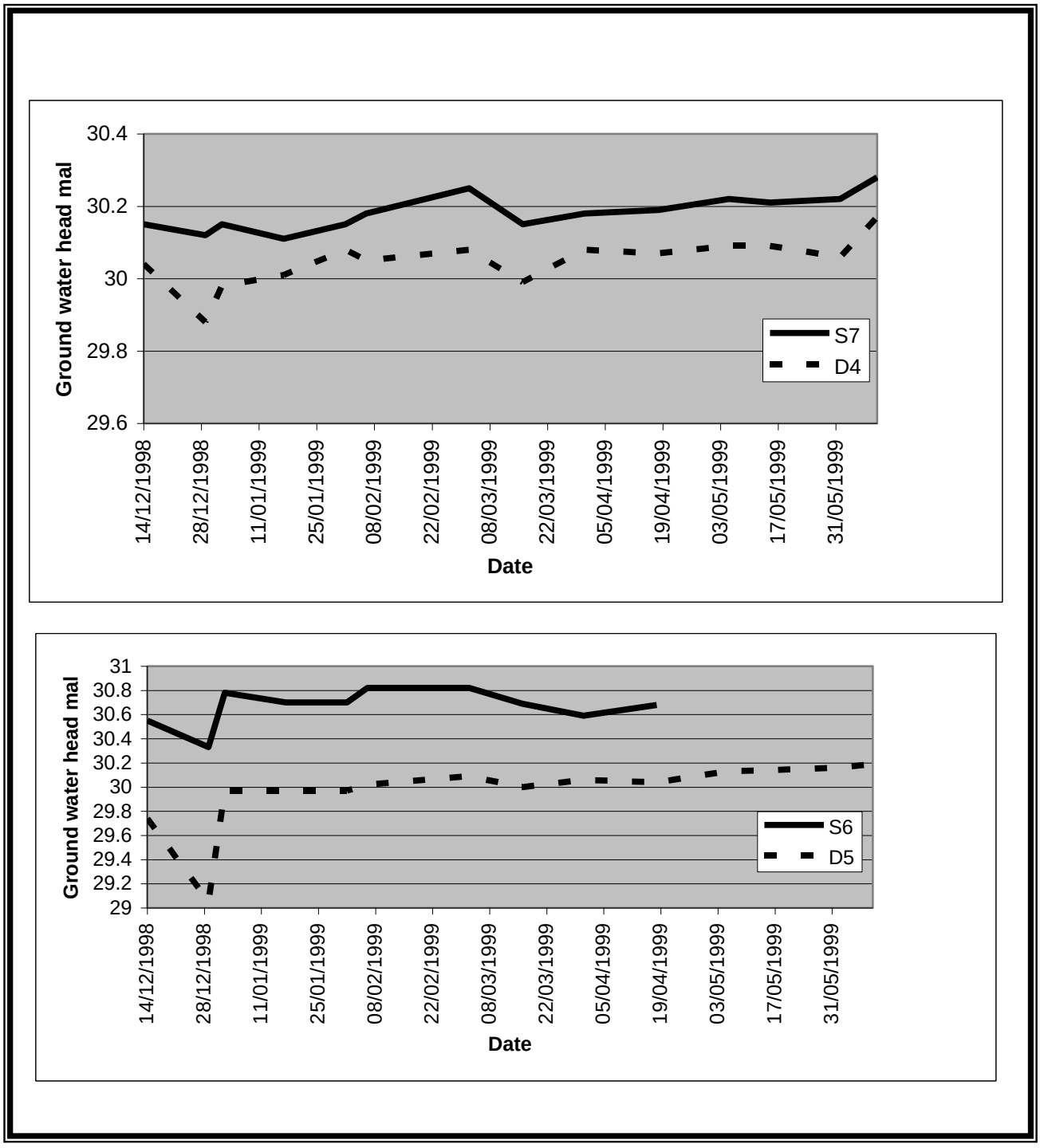

Figure (2-6) Groundwater heads measured at the sallow piezometers (S7 and S6) and the deep piezometers (D4 and D5) respectively, (ISSWR,1999)

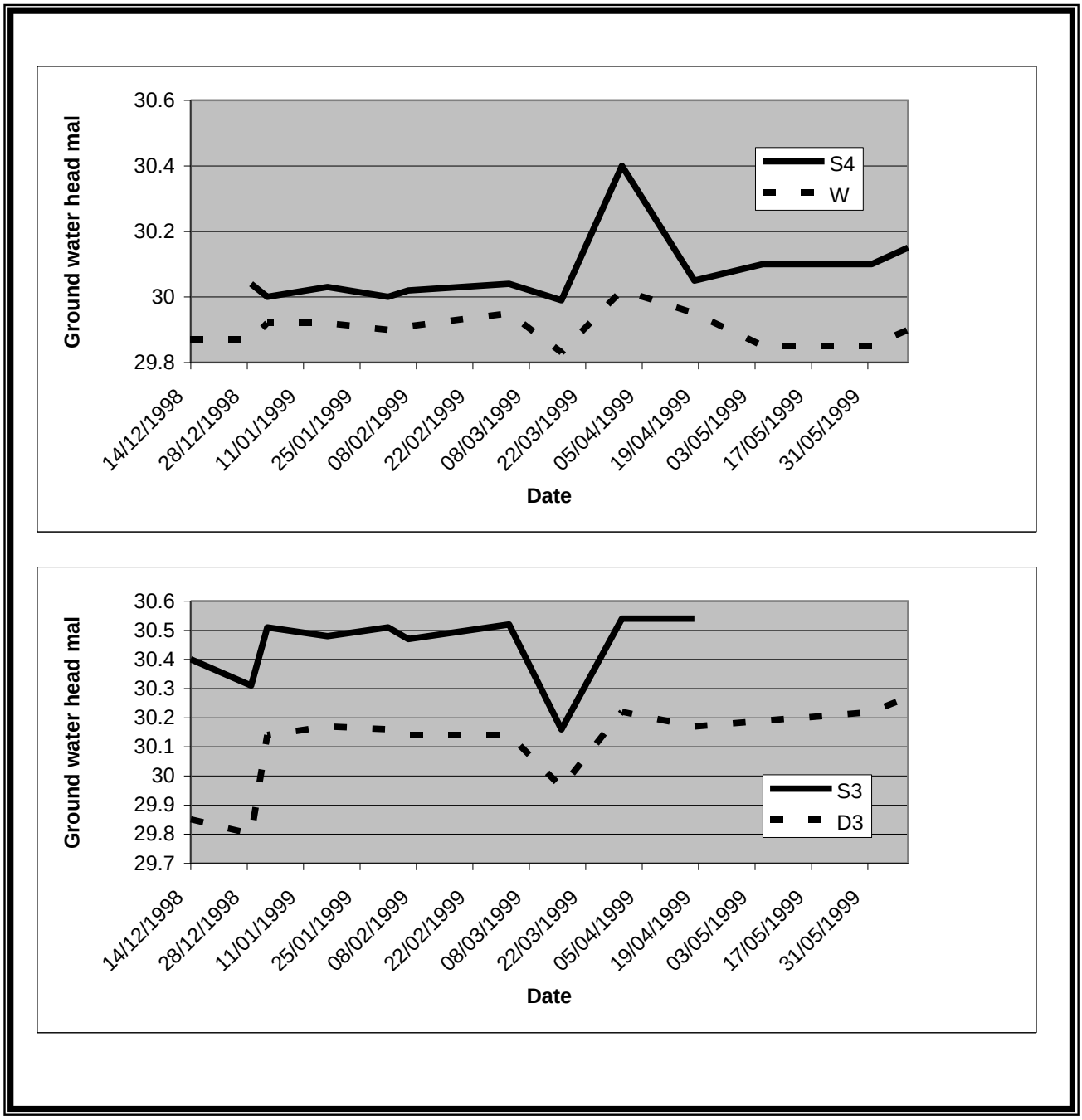

Figure (2-7) Groundwater heads measured at the sallow piezometers (S4 and S3) and the deep piezometer (D4) and the well (W) respectively (ISSWR,1999)

The FCSDIP Study

Twenty four piezometers were installed by the FCSDIP (1995), twelve were shallow with a depth of (5)m and the other twelve were deep with a depth between (15-30)m. They were distributed to cover the area between the study area (center of karbala) and the Razzaza lake. One of the shallow piezometers was installed inside the study area its name is (A8), and three of the shallow piezometers (A3,A7,and A9) were installed nearby the study area boundary, Figure (2-8). At the year 2000 these four Shallow piezometers were found to be damaged by Hassan AL-Khateeb but their logs are still available.

The DWSK Study

Four shallow piezometers with a depth of (6)m were installed by DWSK (2000), their names are (NS2,NS3,NS10, and NS11), Figure (2-4) shows their locations.

The observations of groundwater were made during four months from 16/11/1999 to 19/3/2000, the observations were made by the engineer (M.Auwayid) using the shallow piezometers (NS2 to NS11, S7 to S9, P5,P7, and P8) and the deep piezometers (P2,P3,P4, and P6). The available data are drawn in Figure (2-9), the figure shows that the highest level was recorded at the piezometer S8 while the lowest was recorded at the piezometer NS2, this agrees with the data recorded by the ISSWR, Figure (2-6). Also same conclusion was adopted here in, local leakage from the drinking pipe networks, sewers, and septic tanks recharge the upper layer and the recharge seems to be higher near the piezometer S8.

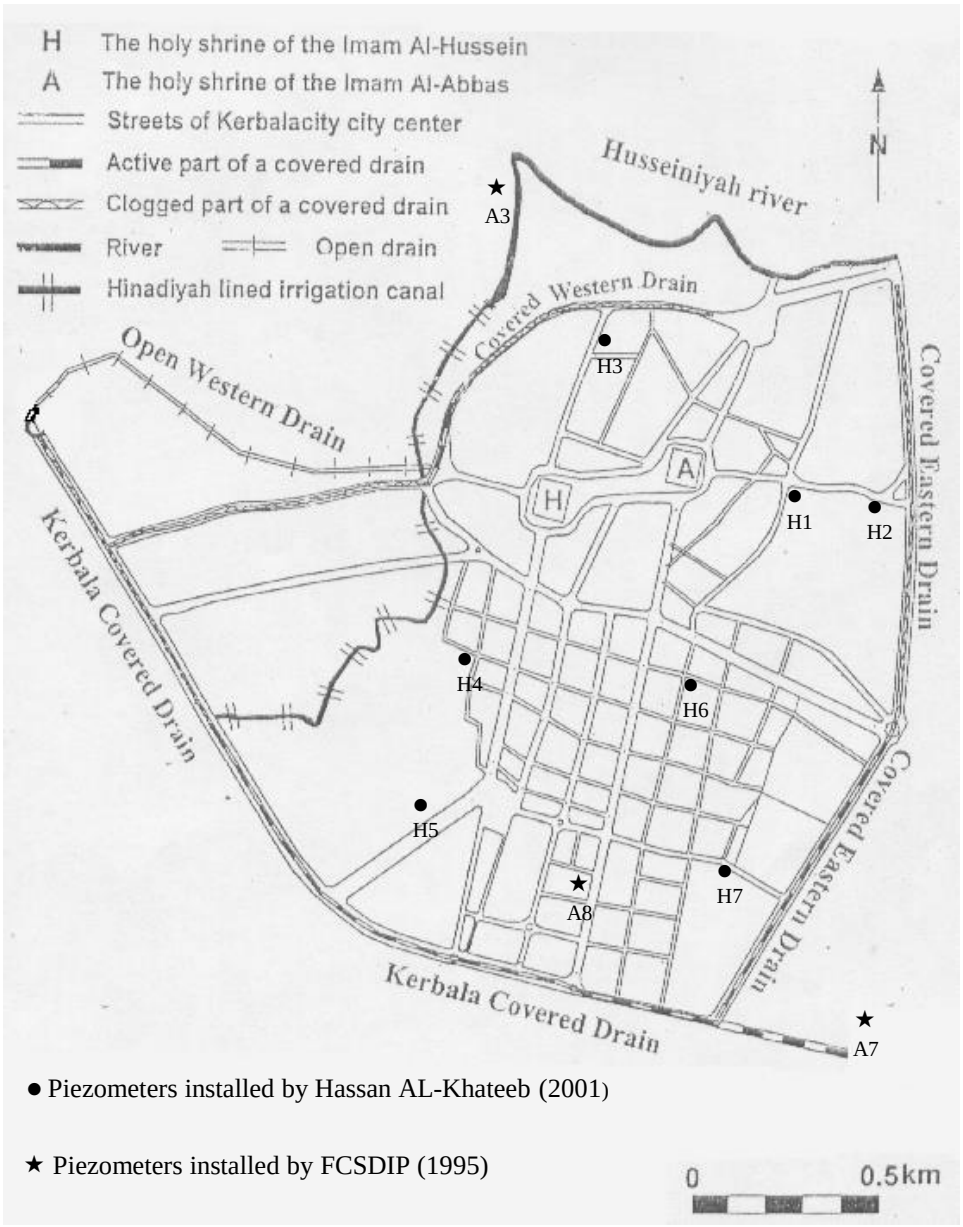

Figure (2-8) Locations of the piezometers installed inside and nearby the study area boundary by the FCSDIP (1995) and Hassan AL-Khateeb (2001).

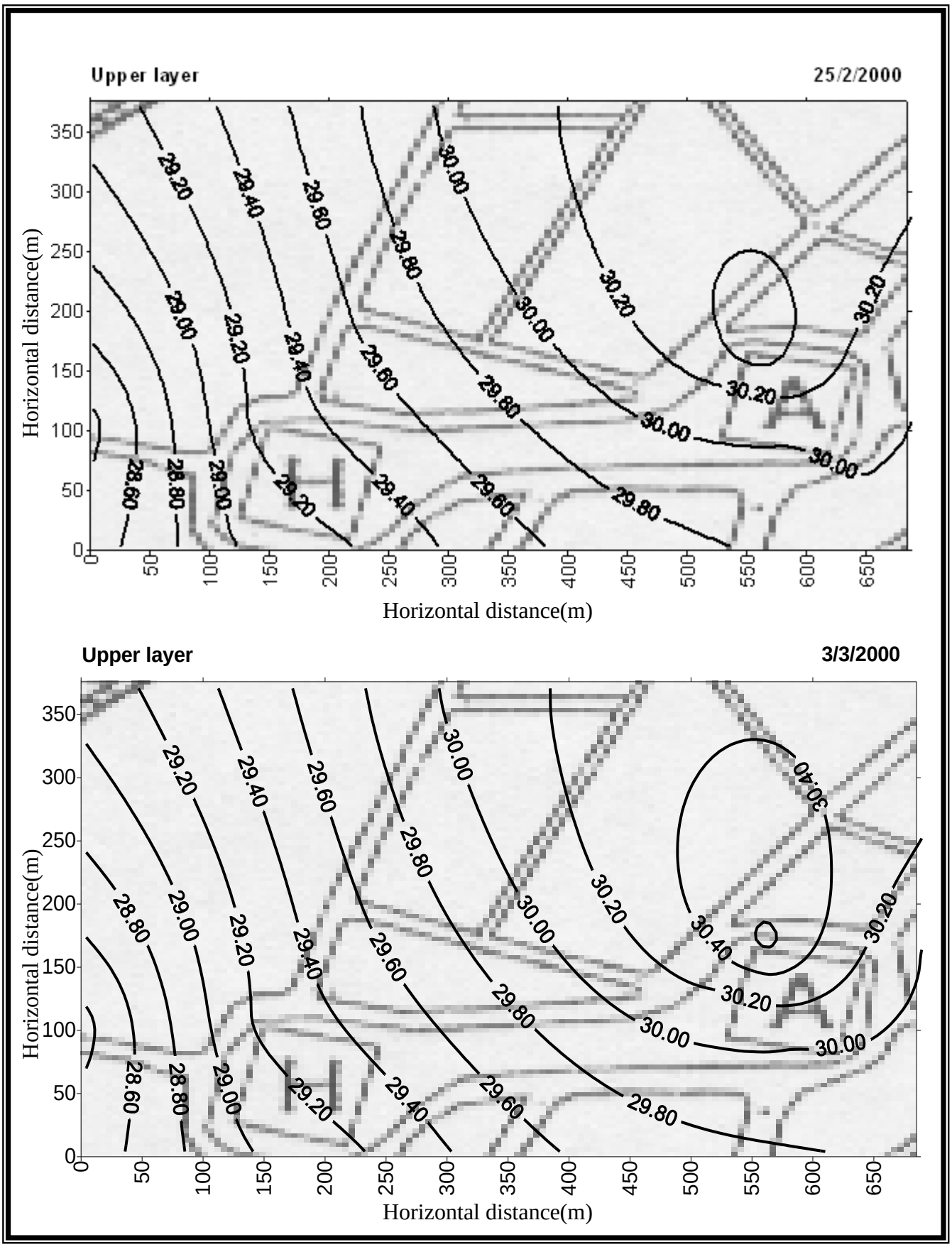

Figure (2-9)Areal distribution of the groundwater head for the upper layer measured by the DSWK (2000) (mal)

AL-Kutubi Engineering Laboratory study

Two boreholes (K1 and K2) were drilled by AL-Kutubi Engineering Laboratory (1999) to make a soil investigation for a building under construction, their locations are shown in Figure (2-4).

Hassan Mahdi AL-Khateeb study

Because all the working piezometers in the study area were concentrated at the two holy shrines and the small area surrounding them, seven shallow piezometers (H1 to H7) were installed by Hassan AL-Khateeb (2001), to cover the area between the two holy shrines and the boundary of the study area, their locations are shown in the Figure (2-8). They are of (0.12)m in diameter and (5)m in depth, Figure (2-10) shows a longitudinal section of a typical one of the seven shallow piezometers that installed by him.

Another field permeability test was made by him using the shallow piezometers (H1 to H7), of course before installing them, the tests were at a different depths for the upper layer only, and they were by the Auger Hole Method. The results are shown in Table (2-5), this table shows that permeability of the upper layer ranges between (0.54-0.923) m/day, also Figure (2-11) shows the areal distribution of the upper layer permeability based on this data .

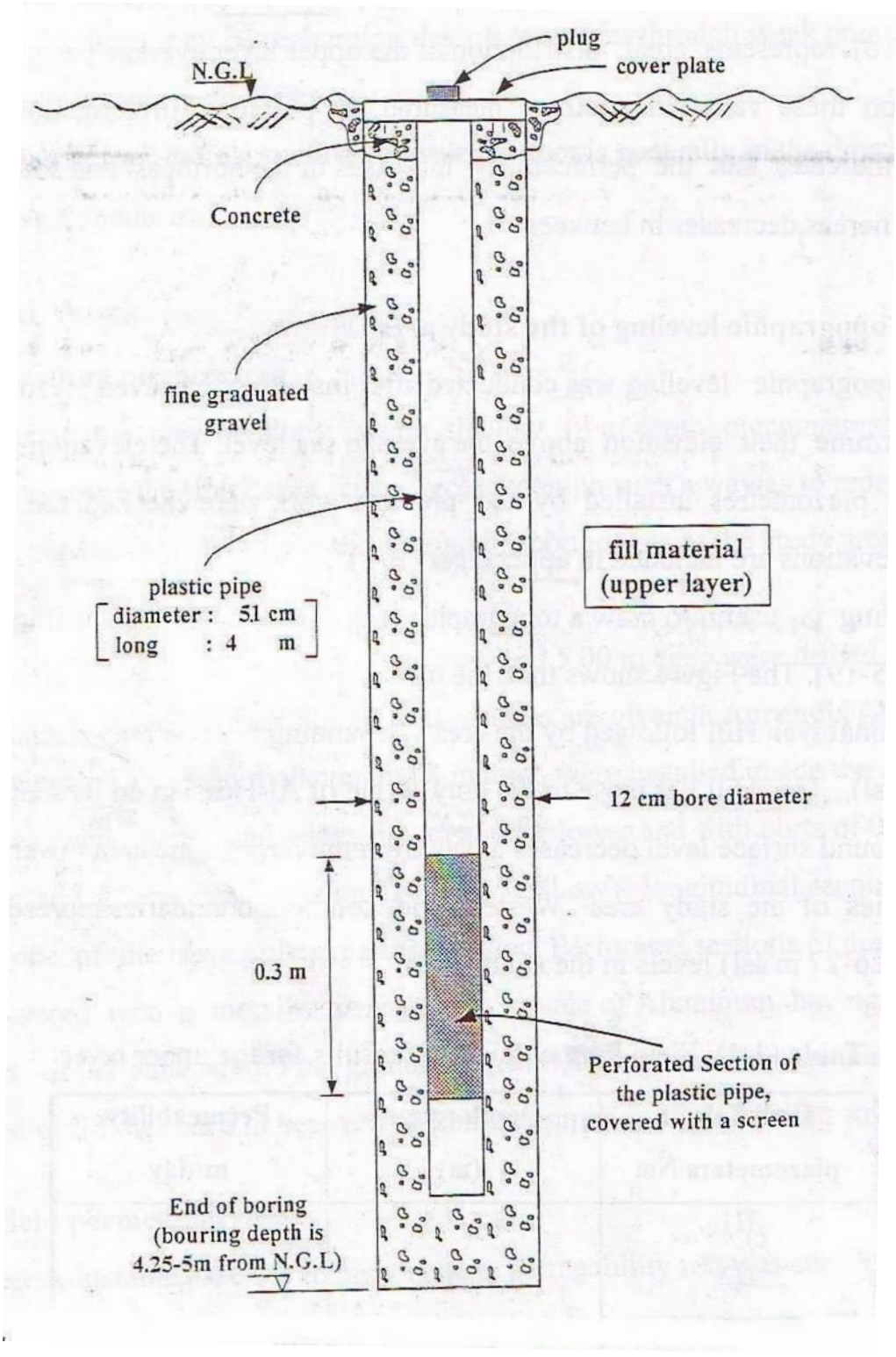

Figure (2-10) Longitudinal section of a typical shallow piezometer installed by Hassan AL-Khateeb (2001)

Table (2-5) Results of the permeability tests for the upper layer for piezometers (H1 toH7) by Hassn AL-Khateeb (2001)

Drilled borehole of the piezometer	Depth range (m)	Permeability m/day
H1	1.5-3.5	0.659
H2	1.36-3.00	0.923
H3	0.85-3.00	0.782
H4	0.4-2.8	0.55
H5	0.69-2.5	0.821
H6	1.01-3.5	0.612
H7	0.87-3.5	0.54

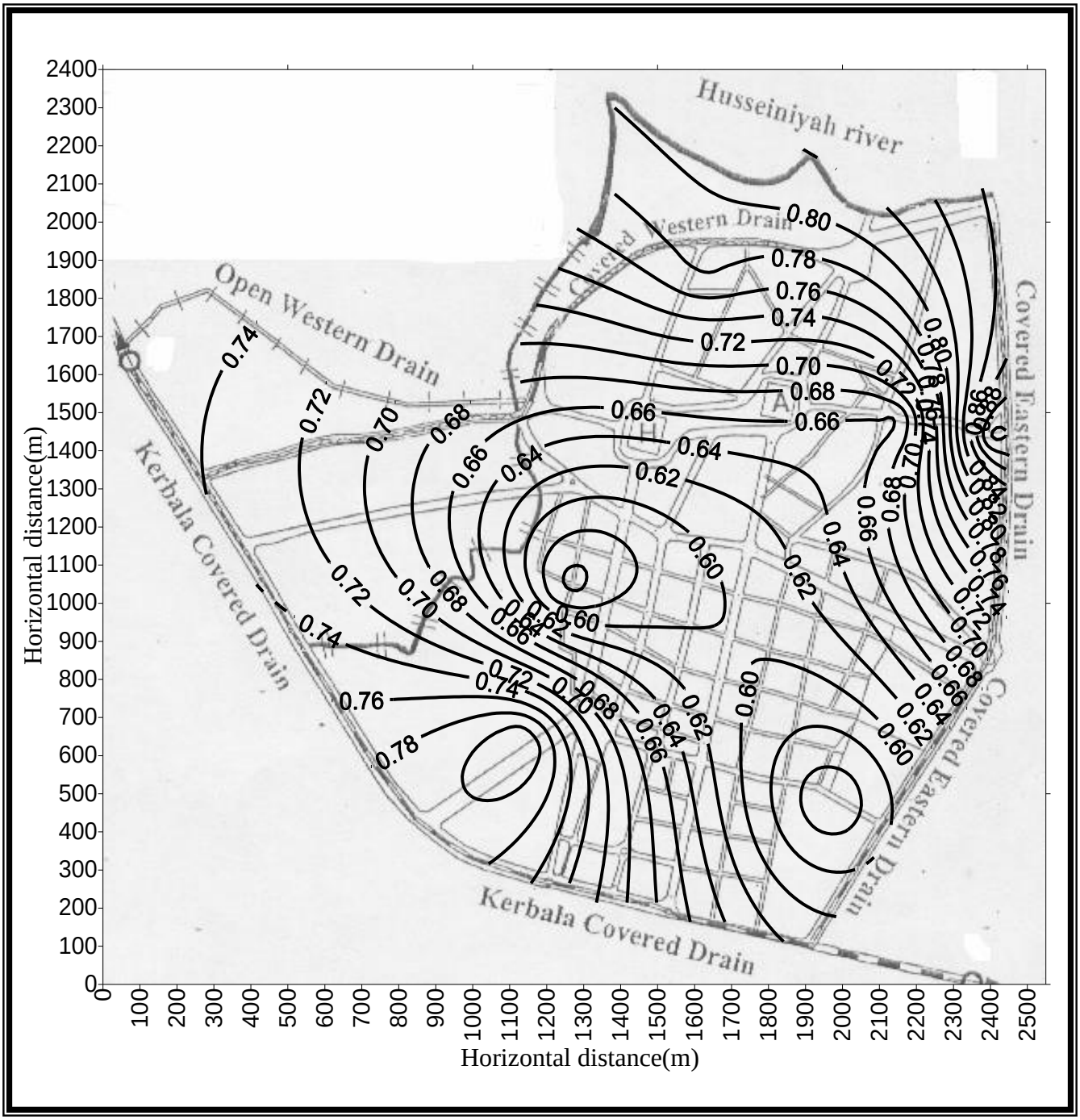

Figure (2-11) Areal distribution of the upper layer permeability based on data from Hassan AL-Khateeb (2001)

The observations of groundwater was made during four months from 1/3/2000 to 13/7/2000 using seventeen shallow piezometers (H1 to H7, P5, P7, P8, NS2, NS3, NS10, NS11, S7, S8, and S9), and six deep piezometers (P2, P3, P4, P6, D1, and D5). The data are listed in Appendix (C-2) and the monthly average data are listed in table (2-6). Figure (2-12) shows the areal distribution of the monthly average of water table of the upper layer while figure (2-13) shows the monthly average piezometeric head of the lower layer for an area surrounding the two holy shrines, both figures for the three months (March, May, and July). The figures show the same distribution pattern for the three months for both upper and lower layers, the highest level (30.68)m is recorded at the shallow piezometer S8 in the area of the two holy shrines.

Groundwater level fluctuation for the piezometers (P2 to P8) that surround the holy shrine of AL-Hussain and for piezometers that surround the holy shrine of AL-Abbas are drawn in the figures (2-14) and (2-15) respectively. During April and May there was a periodical intermittence of potable water at an average of 6 hr/day, as well as, there was an accidental intermission extend for two days (4^{th} and 5^{th} of May) (Hassan AL-Khateeb,2001). These figures show clear decrease in the groundwater heads in all pizometers at this period which supports the pervious conclusion that say that the upper layer is recharged by the leakage from drinking pipe networks, sewers, and septic tanks.

Table (2-6) Monthly average observed data of groundwater levels by Hassan AL-Khateeb (2001)(mal)

Piezometer name	Month name				
	March 2000	April 2000	May 2000	June 2000	July 2000
P5	28.99	28.83	28.74	28.79	28.87
P7	29.19	29.02	28.92	29.07	29.15
P8	29.31	29.23	29.13	29.19	29.27
NS2	28.24	28.34	28.02	28.09	28.26
NS3	29.45	29.44	29.26	29.39	29.39
S7	30.03	30.04	29.99	30.02	———
S8	30.68	30.63	30.51	30.63	30.72
S9	29.91	29.94	29.79	29.81	29.85
NS10	29.86	29.91	29.75	29.78	29.82
NS11	30.12	30.13	30.16	30.17	30.19
H1	28.65	28.65	28.56	28.56	28.58
H2	28.58	28.61	28.52	28.52	28.5
H3	28.92	28.92	28.9	28.97	29.03
H4	27.36	27.33	27.24	27.26	27.31
H5	26.54	26.51	26.44	26.44	26.47
H6	27.97	28.00	27.9	27.92	27.88
H7	26.3	26.29	26.17	26.17	26.23
P2	29.28	29.06	28.97	29.09	29.23
P3	29.04	29.00	28.85	28.96	29.06
P4	29.01	28.81	28.72	28.77	28.85
P6	29.15	29.00	28.88	29.05	29.13
D1	29.6	29.59	29.52	29.53	29.55
D4	29.78	29.77	29.75	29.76	———

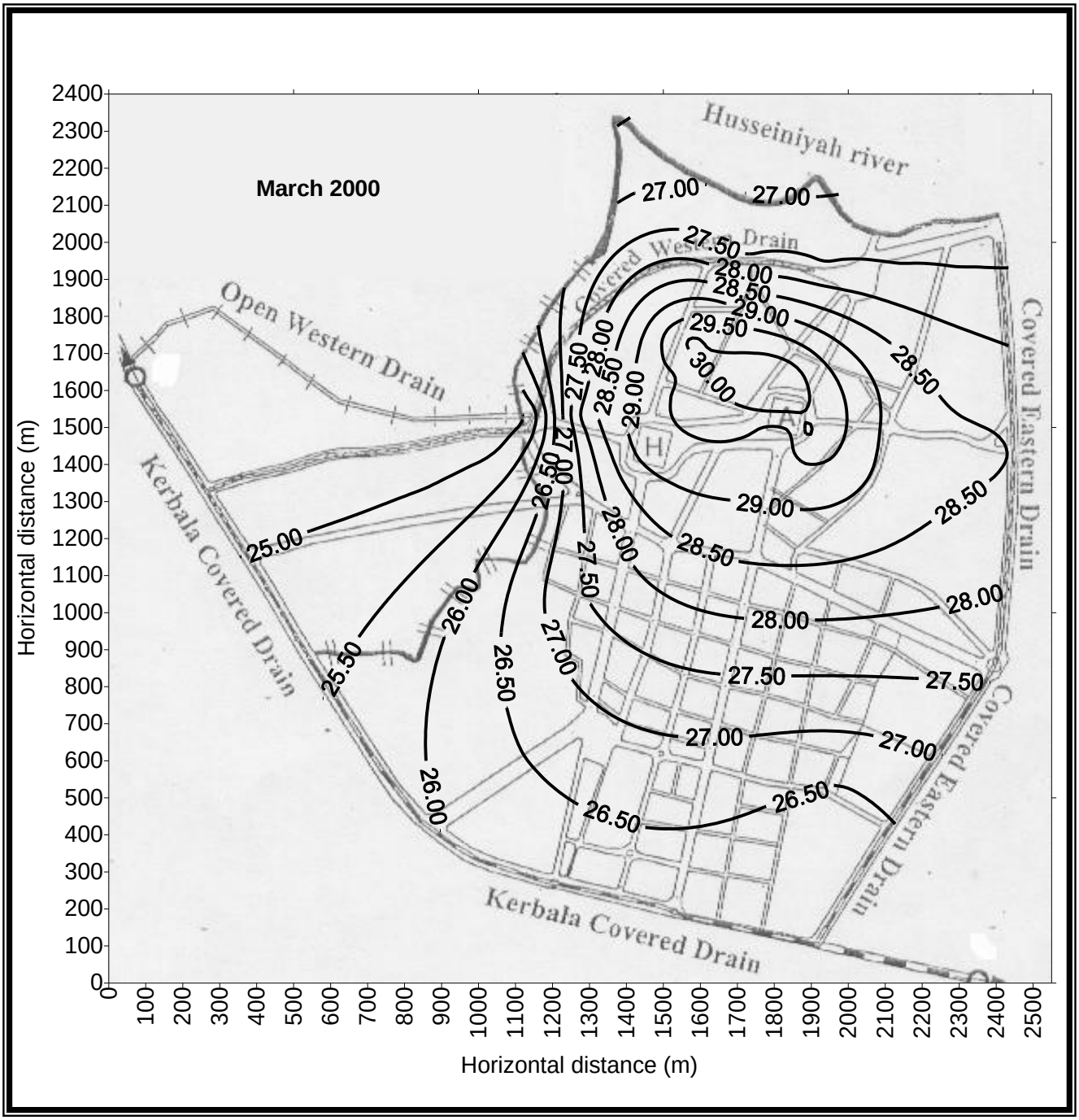

Figure 2-12A: Observed Groundwater Level, March 2000 (After AL-Khateeb (2001)).

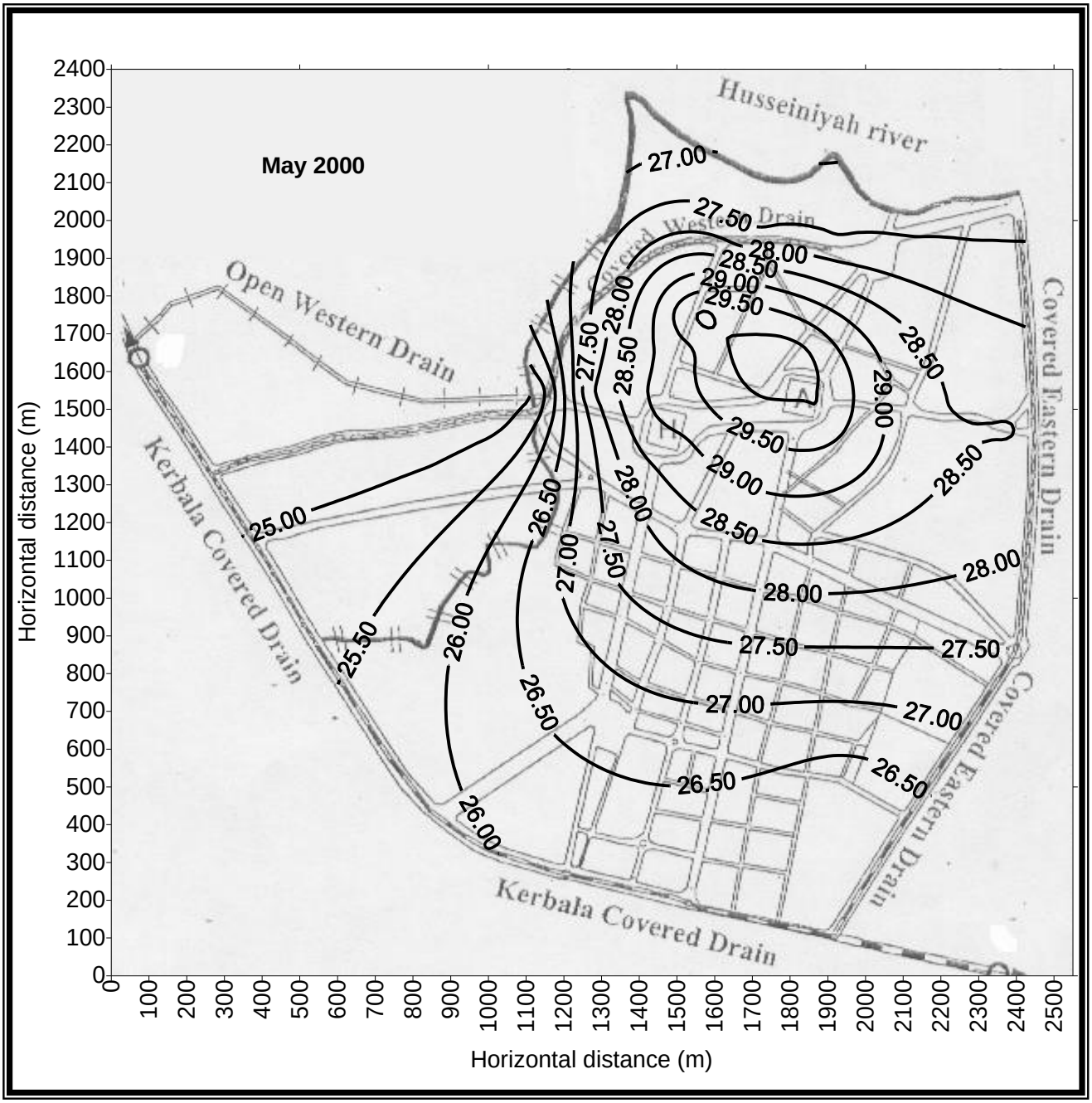

Figure 2-12B: Observed Groundwater Level, May 2000 (After AL-Khateeb (2001)).

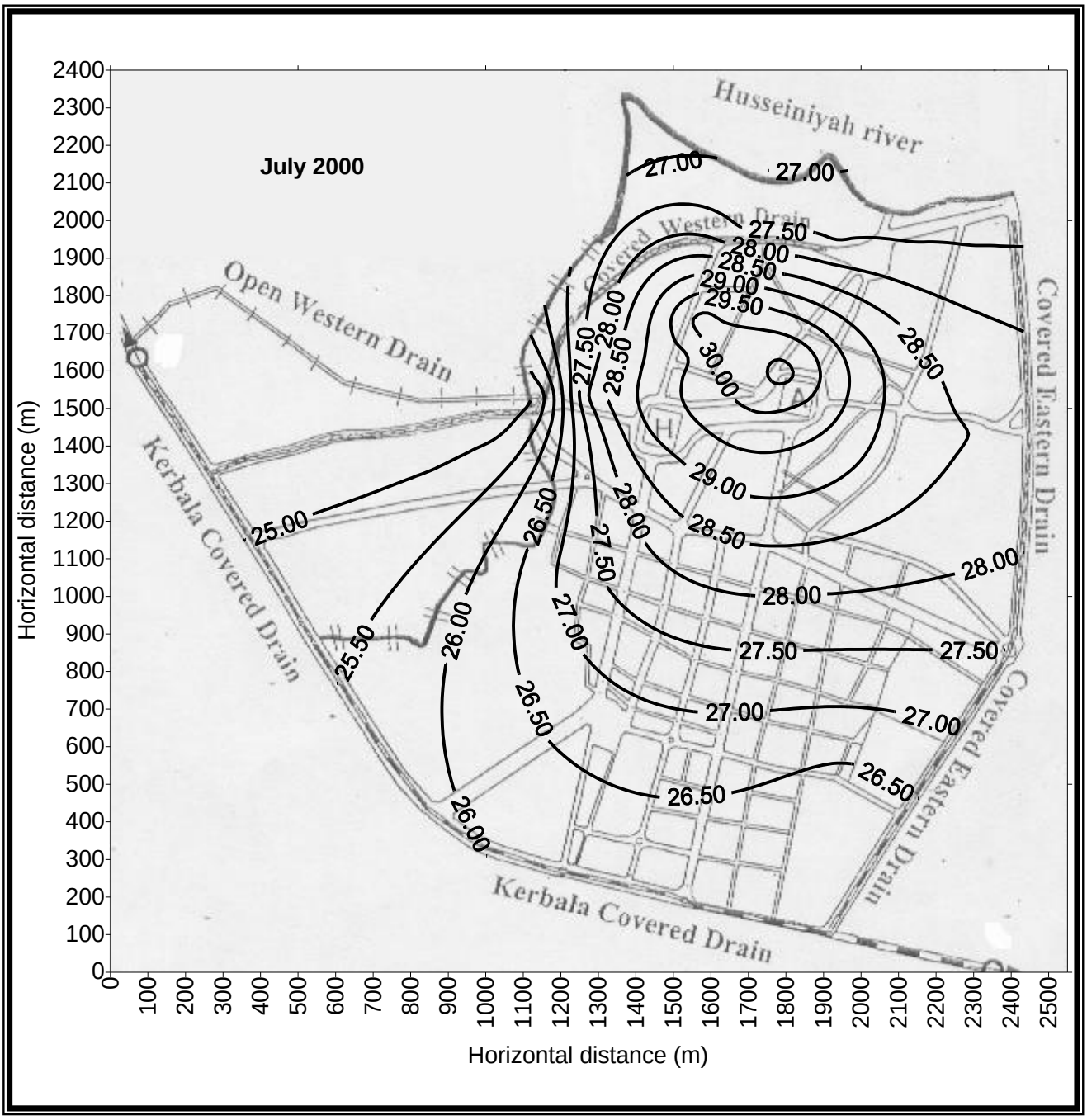

Figure 2-12C: Observed Groundwater Level, July 2000 (After AL-Khateeb (2001)).

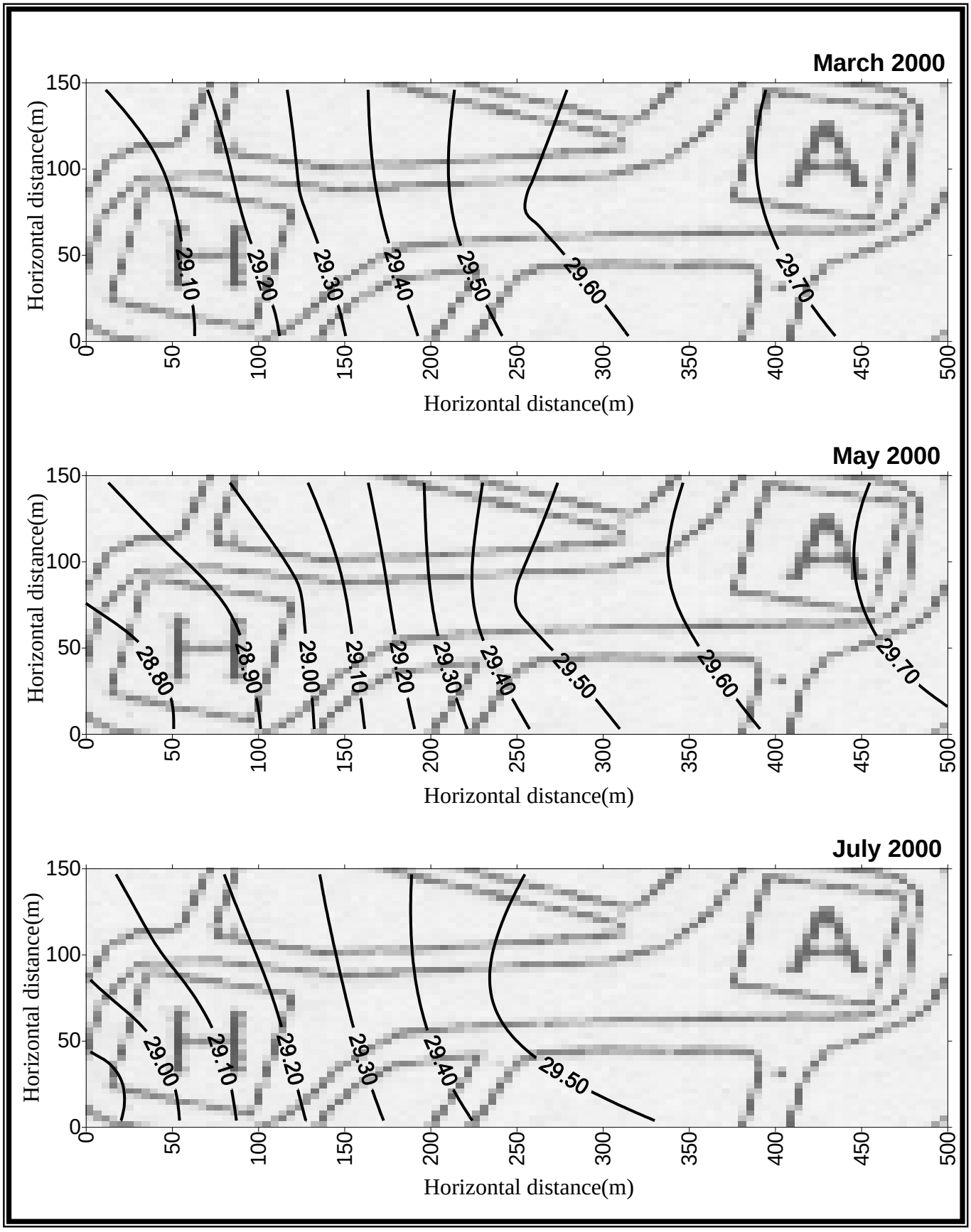

Figure 2-13: Piezometric Level for the lower layer (After AL-Khateeb (2001)).

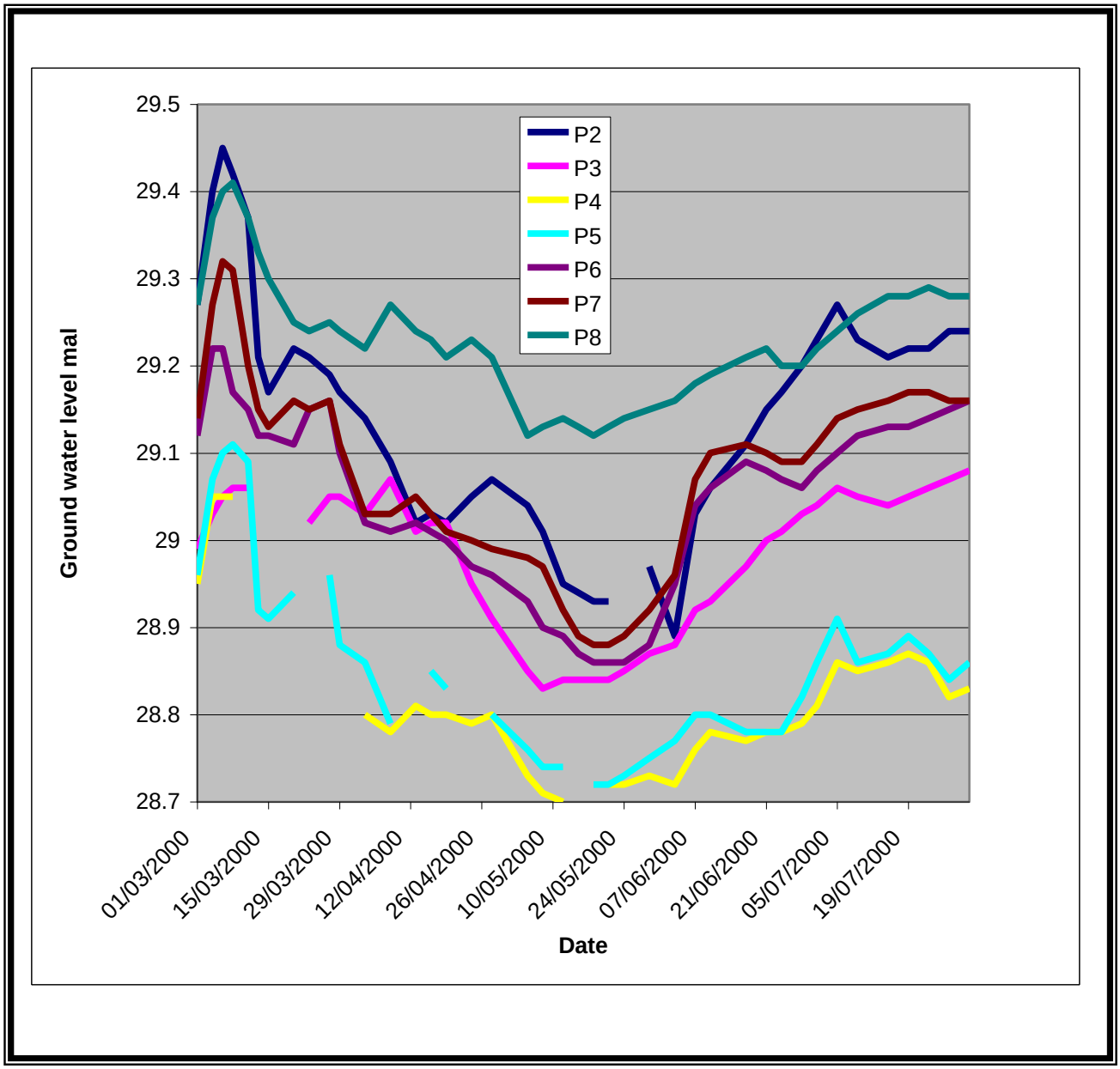

Figure (2-14) Groundwater heads measured at the piezometers (P2 to P8) by Hassan AL-Khateeb (2001)

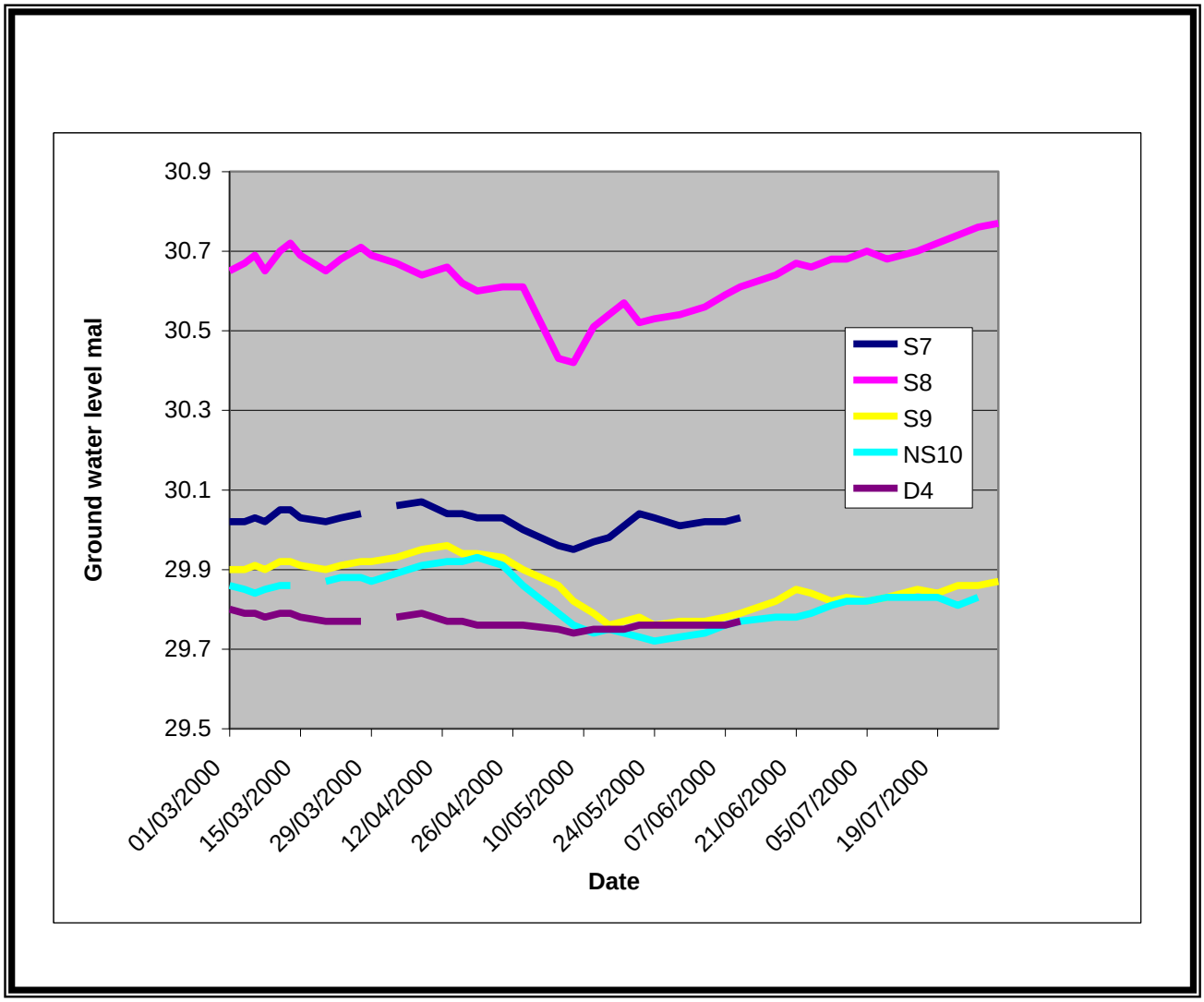

Figure (2-15) Groundwater heads measured at the piezometers (S7,S8,S9,Ns10, and D4) by Hassan AL-Khateeb (2001)

Hassan AL-Khateeb not only installed seven shallow piezometers (H1 to H7) and make an observations for groundwater heads for some piezometers, but also performed two additional important works:-

First he made a groundwater quality analysis to locate the recharging sources. Hydrochemical parameters such as the concentration of calcium ion (Ca^{+2}), magnesium ion (Mg^{+2}), sodium ion (Na^{+1}), potassium ion (K^{+1}), bicarbonate ion (HCO_3^{-1}), sulfate ion (SO_4^{-1}), chloride ion (Cl^{-1}), and nitrateion (NO_3^{-1}) in groundwater as well as pH, total dissolved solids (TDS), and coilform bacteria were used as indictors to identify types and locations of such sources. Groundwater samples were collected from piezometers P5, NS2, NS3, S7, S8, S9, NS10, NS11, D1, D4, and H1 to H7 in 4/5/2000 and 7/6/2000. He concluded from that analysis that the upper layer is recharged by leakage from drinking pipe network, sewers, and septic tanks.

Second he constructed three mathematical models to simulate the hydraulic conditions and the dewatering of the two holy shrines. The dewatering was based on assuming a rectangular cut-off wall (diaphragm) around each of the two holy shrines, this diaphragm rests on the middle semi pervious layer.

Boreholes and piezometers were also used to find the types and the properties of the soil, the available logs of the these boreholes and piezometers show that there were three layers, the upper layer was of fill material with a thickness ranges between (5-8)m, the fill material consists of silt and sand mixed with fine gravel and brick fragment, in addition to some cavities were recorded in this layer, (Hassan AL-Khateeb, 2001). The middle layer is of cohesive silty clay with a thickness which ranges between (1.5-5.8)m, this layer contains some thin packets of fine sand or silty sand with a thickness rangers between (0.1-0.2)m, (ISSWR, 1999).The lower layer is a cohesionless layer with a dense to very dense sand, the thickness of this layer is about (30)m, (FCSDIP, 1995).

The three layers form a hydraulic system of two aquifers. The first aquifer is unconfined aquifer represented by the upper layer while the lower layer represents the second aquifer which is either confined or semi confined aquifer depending on the middle layer whether it is pervious or semi pervious layer.

Figures (2-16), (2-17), (2-18) and (2-19) represent the contour maps of the topographic leveling, thickness of the upper layer, bottom elevation of the upper layer, and thickness of the middle layer respectively after interpolating the data of the boreholes and piezometers in Appendix B all over the study area.

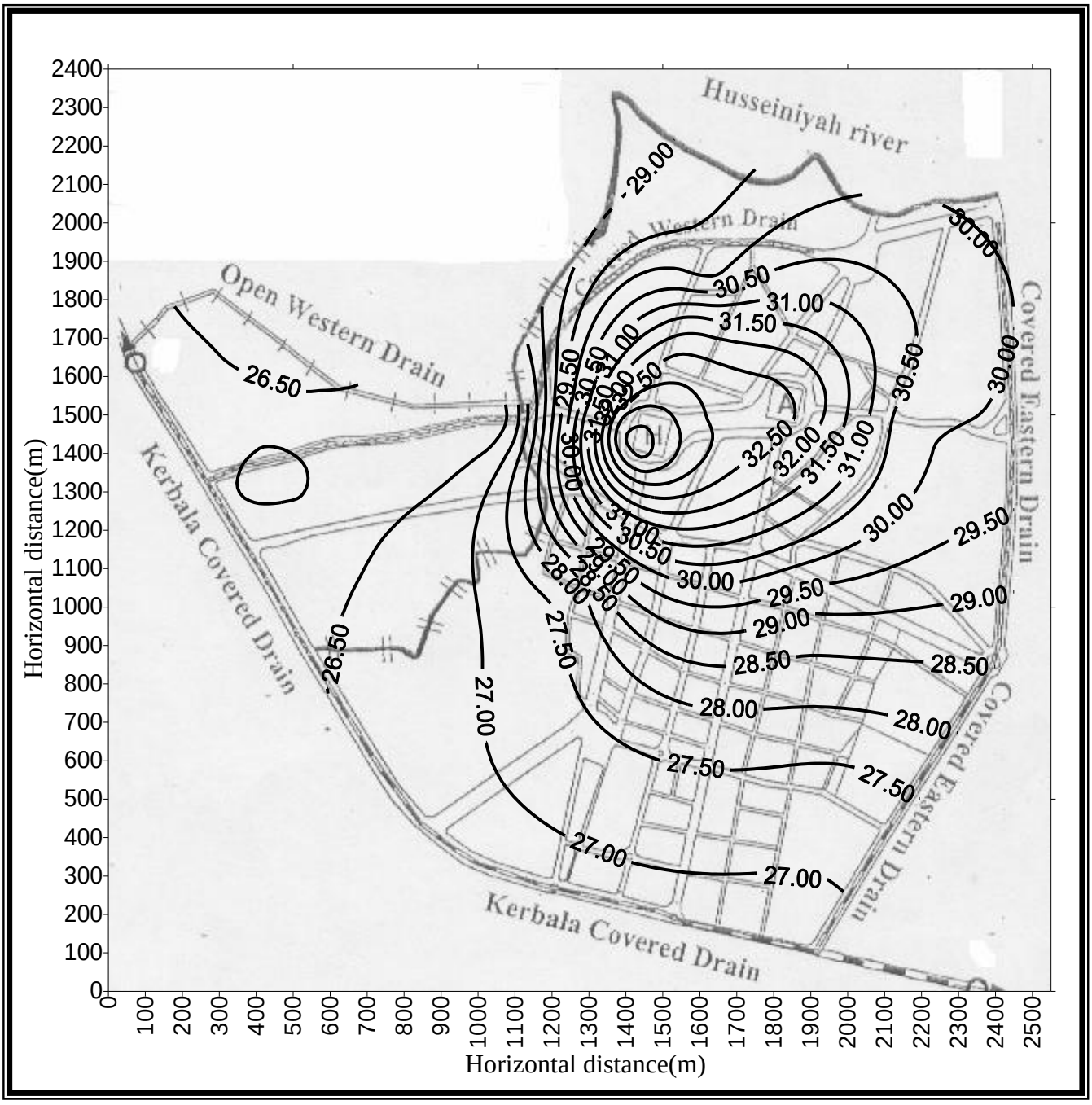

Figure (2-16) Topography of the study area (mal)

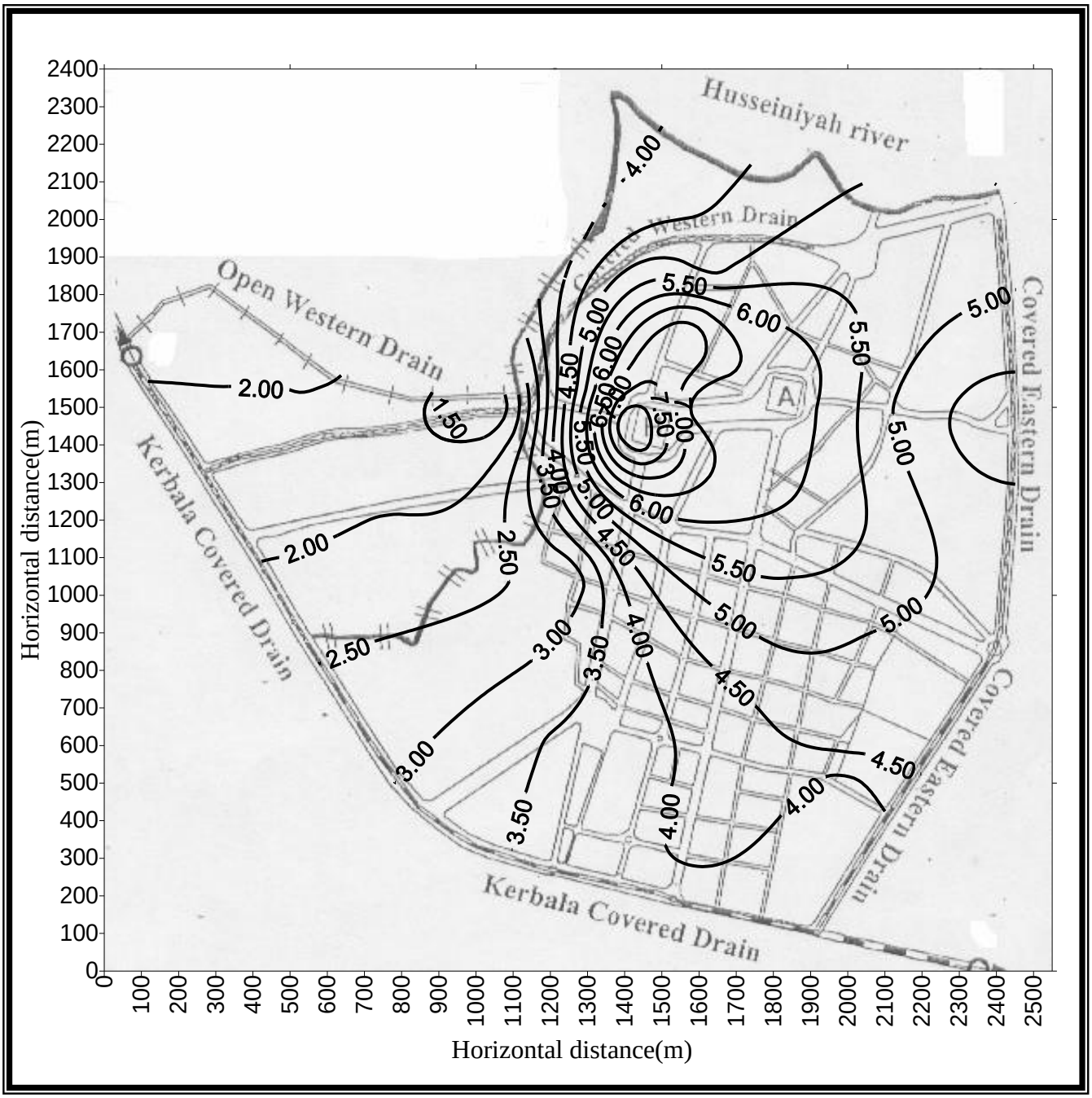

Figure (2-17) Thickness of the upper layer contour map

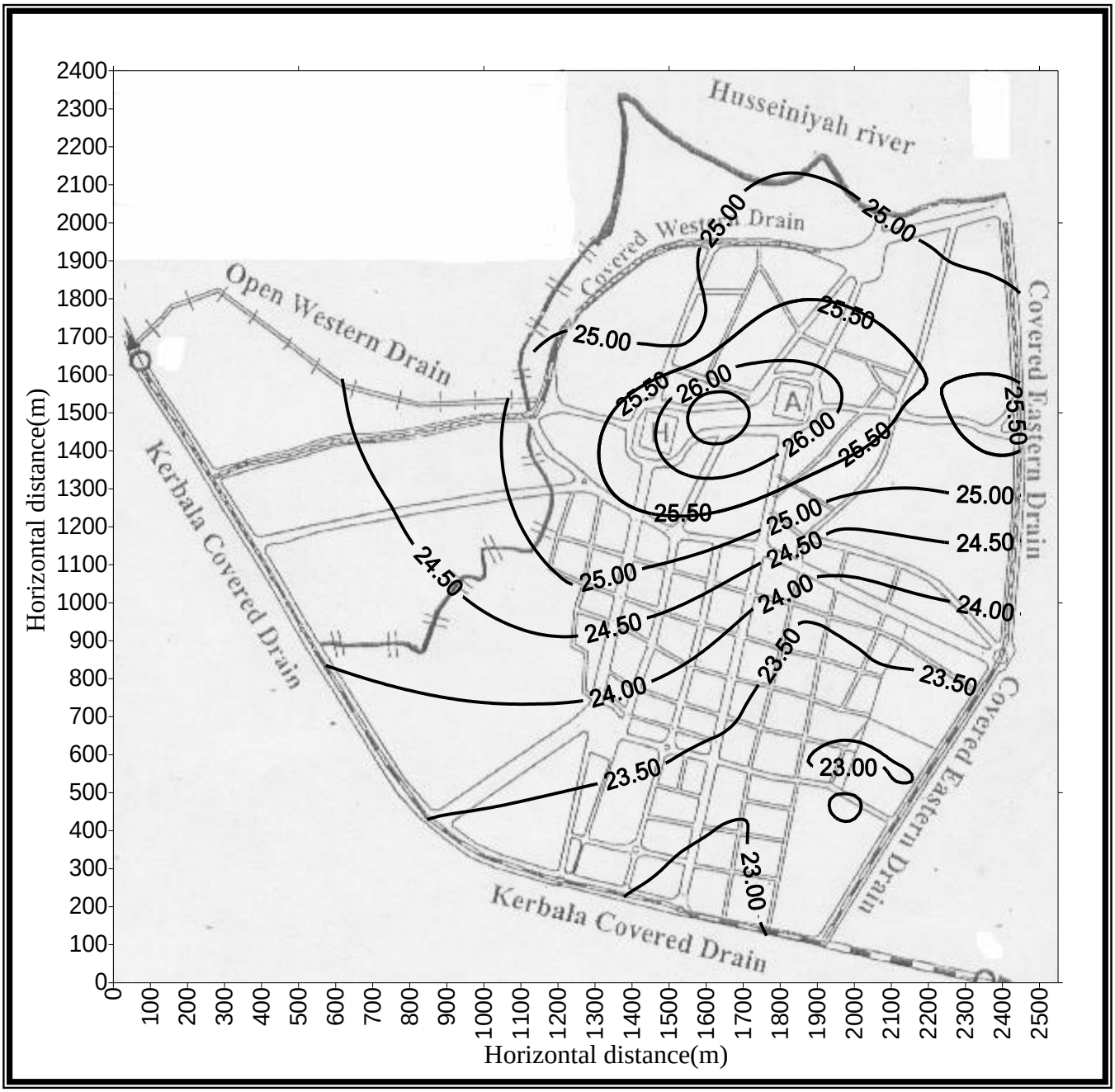

Figure (2-18) Bottom elevation of the upper layer contour map (mal)

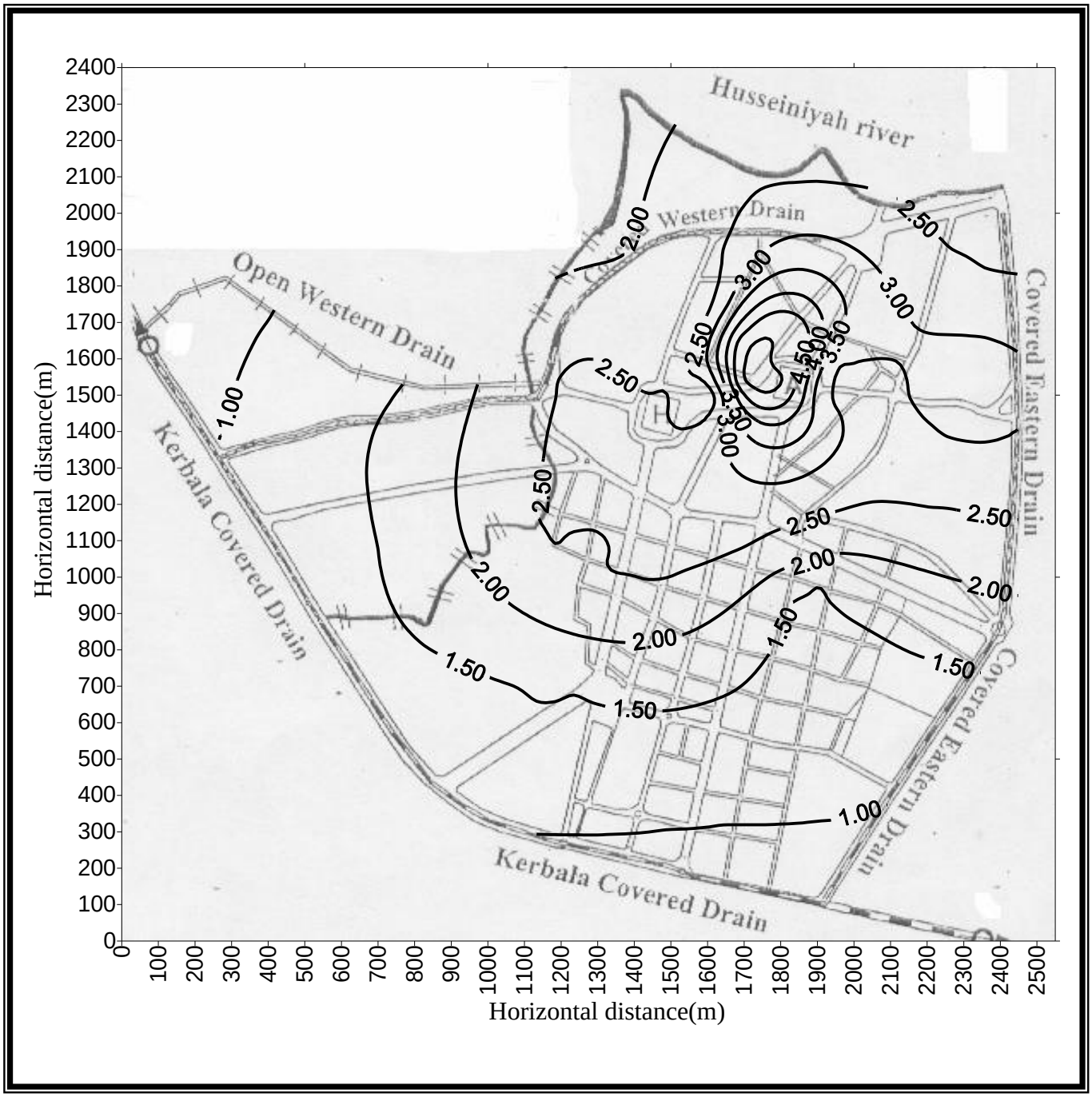

Figure (2-19) Thickness of the middle layer contour map

From the previous discussion, the following points are concluded:-

1- The soil profile of the model area is of three layers, the upper layer is unconfined aquifer, the lower layer is a semi confined aquifer, and in between the middle layer is a semi pervious layer.
2- The upper layer is recharged by leakage from drinking pipe networks, sewers, and septic tanks.
3- The lower layer is recharged by the leakage from the upper layer through the middle layer.
4- The month march records the higher observation data of the groundwater heads for both layers.

CHAPTER THREE

THE GMS MODEL

3-1 Brief Description of the GMS. Program

Ground Water Modeling System (GMS) is a comprehensive graphical user environment for performing ground water simulations. The development of this program was by the Engineering Computer Graphics Laboratory of Brigham Young University in partnership with the U.S Army Engineer Waterways Experiment Station.

The interface for GMS is divided into ten Separate modules(GMS v2.0 Reference, 1996). A model is provided for each of the basic data types supported by GMS. Switching from one module to another can be done instantaneously to facilitate the simultaneous use of several data types when necessary. Only five of the ten modules were used in the construction of karbala groundwater model which are:

1- Triangulated Irregular Network (TIN) Module

The TIN Module is used for surface modeling .TINs are formed by connecting a set of XYZ points (scattered or gridded) with edges to form a network of triangles. The surface is assumed to vary in a linear fashion across each triangle.

2- Borehole Module

The Borehole Module is used to display borehole data. Borehole data can be entered via a spreadsheet- like dialog. Once the boreholes are in memory they can be displayed in a three dimensional oblique view with depth perspective and colors to represent the different zones encountered by the borehole. Contacts or origins on the boreholes can be selected interactively and used in the construction of TINs.

3- Two Dimensional (2D) Scatter Points Module

The 2D Scatter Points Module is used to interpolate from groups of 2D Scatter data to any of the other data types. For example hydraulic conductivity or porosity can be interpolated from the sampling locations to the cells in a layer of a three dimensional grid for use in a MODFLOW simulation, MODFLOW can be defined as a modular three dimensional finite difference groundwater model published by the U.S. Geological Survey.

4- Three Dimensional (3D) Grid Module

The 3D Grid Module is used to create 3D Cartesian grids. These grids can be used for 3D interpolation, isometric surface rendering, cross sections and finite difference modeling.

5- Map Module

The Map Module is used to manipulate four types of objects, DXF objects, image objects, drawing objects and feature objects. The first three objects, DXF objects, image objects, and drawing objects are primarily used as graphical tools to enhance the development and presentation of a model. DXF objects consist of drawings imported from standard CAD packages such as AUTOCAD. Drawing objects are a simple set of tools that are used to draw text, lines, poly lines, arrows, rectangles, etc., to add annotation to the graphical representation of a model. Image Objects are digital images representing aerial photos or scanned maps in the form of TIFF file. The fourth type of object, feature objects, are used to construct conceptual models. Once a conceptual model is constructed it can automatically be converted to a numerical model.

3-2 The Karbala GMS Model

When constructing a model within GMS, it is often convenient to work with a graphical aerial image or map of the site in the background of the Graphics Window. The first step in using a new digital image is to import the image. This is accomplished by selecting the import command in the images menu, this brings up the file Browser which is used to select the TIFF file. After selecting the TIFF file Browser, the register Image dialog all ways appear because the image must be registered before using it. Figure (3-1)

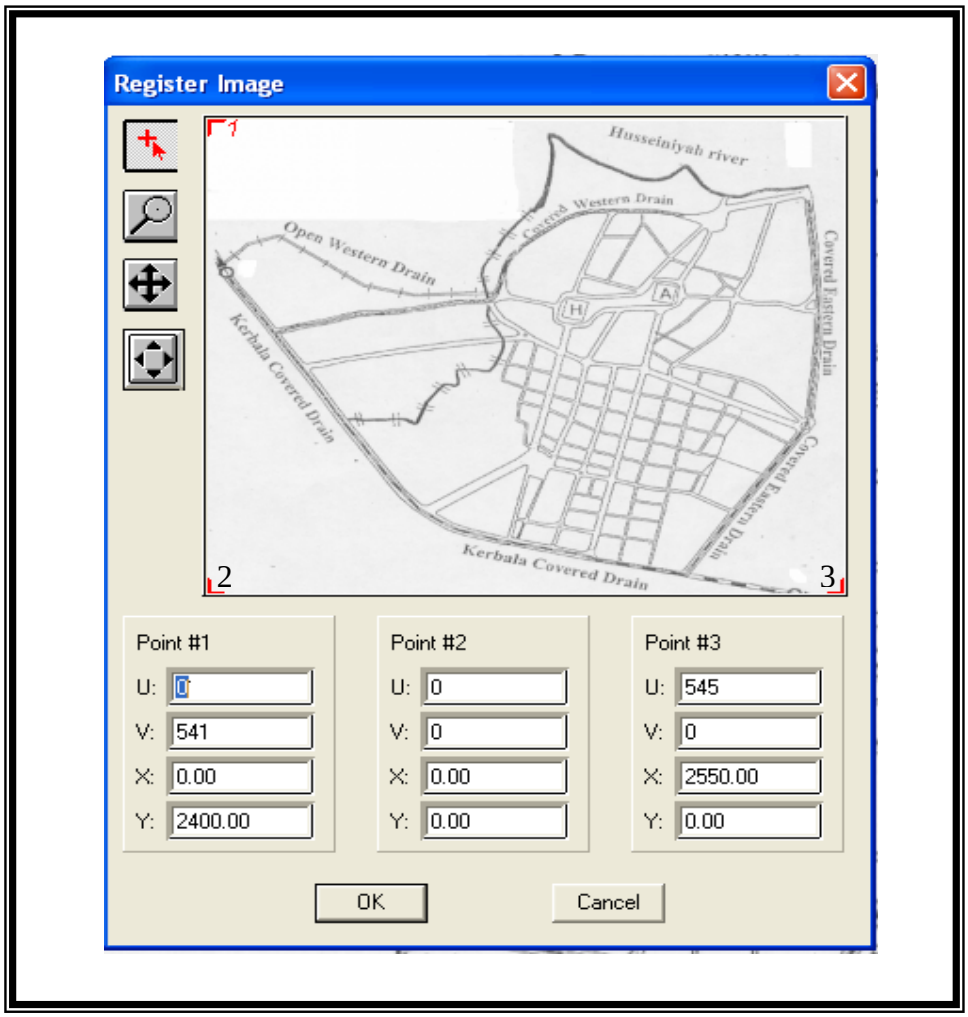

Figure (3-1) The Register Image Dialog

Hence, a map of the center of karbala city that represents the site of the problem is shown in Figure (1-2). The coordinates of the three points of registration are shown in Table 3-1, U and V represent the horizontal and vertical coordinates of the point on the digital image respectively while X and Y represent the horizontal and vertical coordinates of the point on the ground respectively

Table 3-1 Dimensions of the Three Points of Registration

Point	**(U)**	**(V)**	**(X) m**	**(Y) m**
1	0	541	0	2400
2	0	0	0	0
3	545	0	2550	0

Borehole module is also used to enter the borehole data of the site before the inception in construction of model. Table 3-2 with the help of Figure 3-2 shows the information of the boreholes used in the model.

Table3-2 The information of the Boreholes That used in the Model (Hassan AL-Khateeb, 2001)

Piezometer Name	X Coordinate (m)	Y Coordinate (m)	Z Coordinate (m)	Mat. Number	Thickness of the Upper Layer (m)	Permeability m/day
D1	1589.5	1483.47	32.98	1	6	———
	1589.5	1483.47	26.98	5		
	1589.5	1483.47	24.98	6		
	1589.5	1483.47	17.98	6		
D4	1894.65	1501.32	32.19	1	6	———
	1894.65	1501.32	27.19	3		
	1894.65	1501.32	26.19	5		
	1894.65	1501.32	23.19	6		
	1894.65	1501.32	17.19	6		
H1	2138.18	1461.38	30.12	1	4.72	0.659
	2138.18	1461.38	26.12	3		
	2138.18	1461.38	25.4	4		
	2138.18	1461.38	25.12	4		
H2	2372.77	1430.35	29.93	1	4.12	0.923
	2372.77	1430.35	27.13	2		
	2372.77	1430.35	26.73	3		
	2372.77	1430.35	25.81	4		
	2372.77	1430.35	24.93	4		
H3	1606.92	1842.17	29.84	1	4.75	0.782
	1606.92	1842.17	26.34	3		
	1606.92	1842.17	25.09	5		
	1606.92	1842.17	24.84	5		
H4	1248.22	1040.63	27.77	1	2.7	0.55
	1248.22	1040.63	26.97	3		
	1248.22	1040.63	25.07	4		
	1248.22	1040.63	24.65	5		
	1248.22	1040.63	23.4	4		
	1248.22	1040.63	22.77	4		
H5	1137.72	642.4	27.24	1	3.44	0.821
	1137.72	642.4	25.19	3		
	1137.72	642.4	24.69	2		
	1137.72	642.4	24.24	3		
	1137.72	642.4	23.8	5		
	1137.72	642.4	22.49	4		
	1137.72	642.4	22.24	4		

Table3-2 continue ……..

Borehole Name	X Coordinate (m)	Y Coordinate (m)	Z Coordinate (m)	Mat. Number	Thickness of the Upper Layer (m)	Permeability m/day
H6	1837.28	974.325	28.94	1	———	0.612
	1837.28	974.325	25.04	3		
	1837.28	974.325	23.94	3		
H7	1947.78	487.275	27.15	1	3.4	0.54
	1947.78	487.275	26.2	2		
	1947.78	487.275	25.84	3		
	1947.78	487.275	23.75	4		
	1947.78	487.275	23.2	5		
	1947.78	487.275	22.15	5		
Ns10	1908.25	1585.47	31.94	1	———	———
	1908.25	1585.47	26.94	3		
	1908.25	1585.47	25.94	3		
Ns11	1553.8	1718.07	32.79	1	3	———
	1553.8	1718.07	29.79	4		
	1553.8	1718.07	26.54	4		
Ns2	1288.18	1527.67	30.92	1	3	———
	1288.18	1527.67	27.92	4		
	1288.18	1527.67	25.92	4		
	1288.18	1527.67	25.56	4		
	1288.18	1527.67	24.92	4		
Ns3	1522.78	1633.92	32.57	1	———	———
	1522.78	1633.92	28.21	3		
	1522.78	1633.92	26.57	3		
S7	1868.3	1465.63	32.21	1	———	———
	1868.3	1465.63	27.21	3		
	1868.3	1465.63	26.21	3		
S8	1793.07	1589.72	32.42	1	5.41	———
	1793.07	1589.72	27.01	4		
	1793.07	1589.72	26.42	4		
S9	1806.25	1474.55	32.65	1	———	———
	1806.25	1474.55	26.65	1		
P2	1529.79	1493.85	32.84	———	———	———
P3	1440.51	1490.87	32.44	———	———	———
P4	1422.66	1413.5	32.25	———	———	———
P5	1430.59	1401.59	32.25	———	———	———
P6	1505.98	1383.74	32.36	———	———	———
P7	1520.85	1397.63	32.44	———	———	———
P8	1451.42	1504.76	32.44	———	———	———

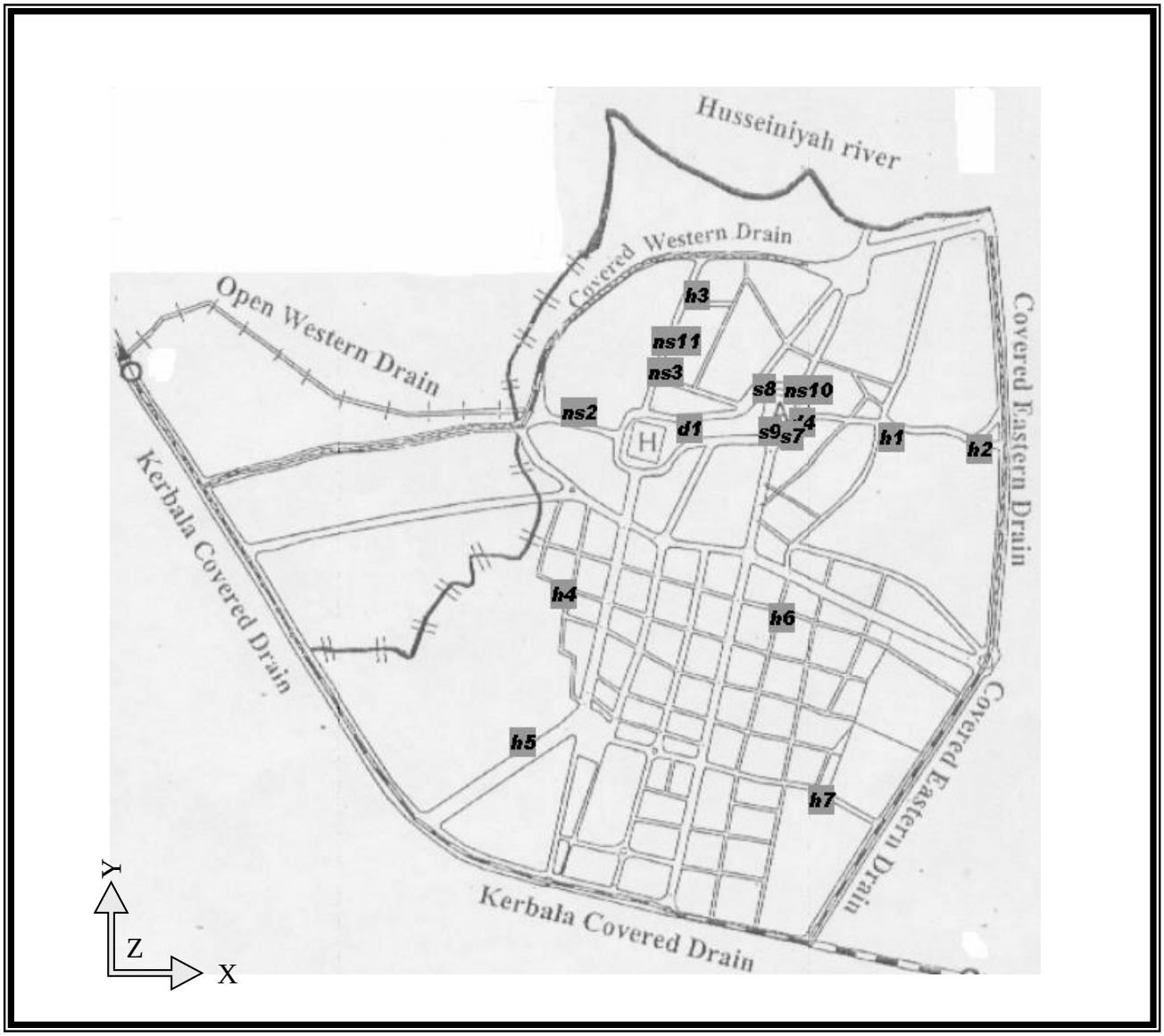

Figure 3-2 Locations of the Boreholes that are used in the model

The first step in the building of the model is the specifications of the model boundaries. Table (3-3) indicates the specified head, the elevation of the drain, and the stages of the river at the nodes 1,2,3,4 and 5 are shown in Figure 3-3.

The GMS model uses Darcy's law:

$$Q = k * i * A \quad \text{..... (3.1)}$$

where Q is the flow rate (L^3/T), k is the hydraulic conductivity (L/T), i represents the hydraulic gradient (unit less), and A represents the cross-sectional area of flow (L^2). Darcy's law can also be expressed as:

$$Q = k * \frac{\Delta H}{L} * A \quad \text{..... (3.2)}$$

where ΔH represents the head loss and L represents the length of flow. Since the unknown on the right side is the head, it is convenient to group all of the other terms together and call them conductance:

$$Q = C * \Delta H \quad \text{..... (3.3)}$$

This results in the following general definition for conductance:

$$C = \frac{k * A}{L} \quad \text{..... (3.4)}$$

This may be represented more specifically in the following form.

$$C = \frac{k}{t} * l * w \quad \text{..... (3.5)}$$

Where t represents the thickness of the material in the direction of flow, and $l * w$ represents the cross-sectional area perpendicular to the flow direction.

Table (3-3) Information of the Nodes of Karbala GMS model

Node	Specified Head	Bed elevation of the Drain	Elevation of the bed of the river	Stage
1	27.25	——	25.0	27.25
2	27.15	——	24.9	27.15
3	25	24.9	——	——
4	24.5	24.4	——	——
5	26.25	——	——	——

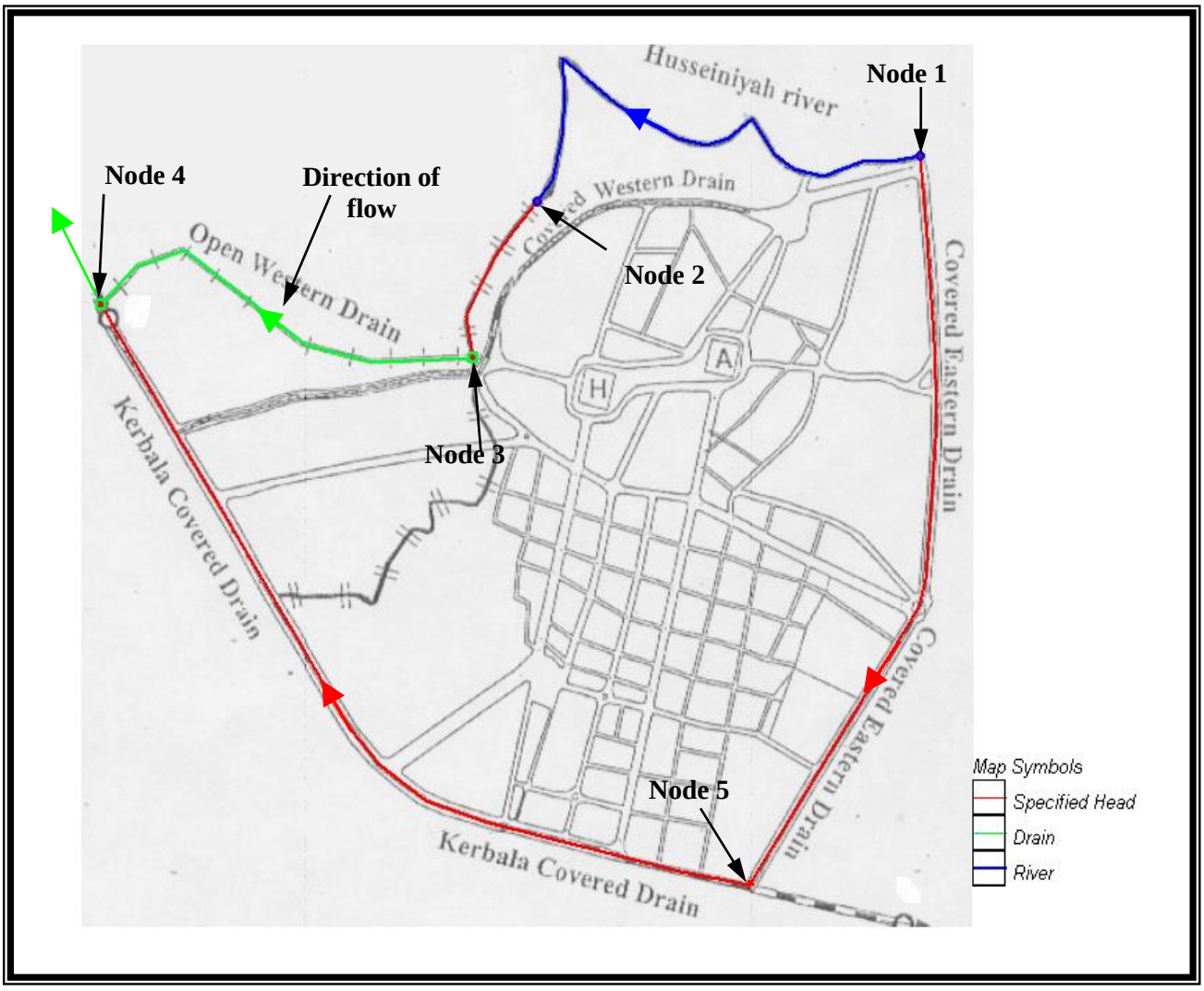

Figure (3-3) Locations of the Nodes of Karbala GMS model

Converting the bottom elevation and the permeability of the upper layer (unconfined aquifer) and the transmissivity of the lower layer (semi confined aquifer) to the three dimensional grid is the next step. The converting can be done by switching the 2D scatter points module and using the open command from the file menu to locate and open the files that construct using the Borehole model by using, … to 3D Grid command from interpolation menu. The interpolated values of permeability can be entered to the array of the hydraulic conductivity by selecting the hydraulic conductivity button in the BCF package dialog from the MODFLOW menu and selecting the button data set -> Grid, this will overwrite the current grid data. The same procedure can be used to interpolate the bottom elevation of the upper layer to the bottom elevation array.

Once a grid is generated and all of the analysis options and boundary conditions have been specified, the next step is to save the simulation to disk and run MODFLOW. However, before saving the simulation and running MODFLOW, the model should be checked with the MODFLOW Model Checker. The Model Checker analyzes the input data currently defined for a MODFLOW simulation and reports any obvious errors or potential problems. There should be no error and no warring.

Once a simulation has been created, checked, and saved, the MODFLOW executable program can be launched. MODFLOW can be executed in one of two ways, from the MODFLOW menu in GMS or from the DOS command line. In the present study the way of running MODFLOW from the MODFLOW menu by using Run MODFLOW command is used. The dialog shows the complete path name for the super file that was saved.

Head and drawdown files (or any data file) can be imported to GMS as data sets by selecting the Import button in the Data Browser. This button brings up a dialog which lists the type of files which can be imported as data sets.

The simulation can be designed as either steady state or transient. Transient simulation can be chosen (if the type of simulation is transient) in the BCF package dialog from the MODFLOW menu. The initial values of primary storage coefficient for the upper and lower layer can be entered to the array using the Constant-> Layer

button. The Starting Head button on the left side of the Basic Package dialog is used to enter the values of the starting head array.

3-3 Initial Input data

The study area is divided into uniform square grid containing 48 rows and 51 columns with a grid spacing of 50 meters, this division continues vertically through the three layers that makes each layer contain 2448 cell.

The boundary of the GMS model is so clear and so easily defined, the attribute command in the feature objects menu can be used for that, as explained above, Hussainiya river is defined as a river boundary, open Western drain is defined as drain boundary, and the other boundaries are defined as specified head boundary considering that Karbala covered drain and Eastern covered drain are completely clogged. All cells outside the boundaries are assigned as inactive cells, Figure (3-4).

Transmissivity is assigned as 200 m2/day for all cells in the lower layer inside and at the boundary of the model region. Storage coefficient is assigned as 0.0087 for all the cells in the lower layer inside the model region. Vertical permeability value for the middle layer is taken as 0.028 m/day, this value is divided on the thickness of the middle layer, Figure (2-19), at each cell to obtain the corresponding initial leakage coefficient. The values of leakage coefficient of the middle layer is multiplied by the initial difference in heads between upper and lower layers to obtain the leakage rate for each cell. Leakage rate is needed as input data in the GMS model. The values of transmissivity, storage coefficient, and vertical permeability of the middle layer are evaluated from pumping test analysis carried out by ISSWR (1999).

The permeability for the upper layer is taken as the average values of the field permeability tests for piezometers H1 to H7 made by Hassan AL-Khateeb (2001), Figure (2-11). Effective porosity of the upper layer is taken within the range (0.15-0.2) for all cells as a roughly estimation for loamy sand soils (Mc-Whorter and Sunada, 1977, Bouwer, 1978, and US department of the interior, 1985)

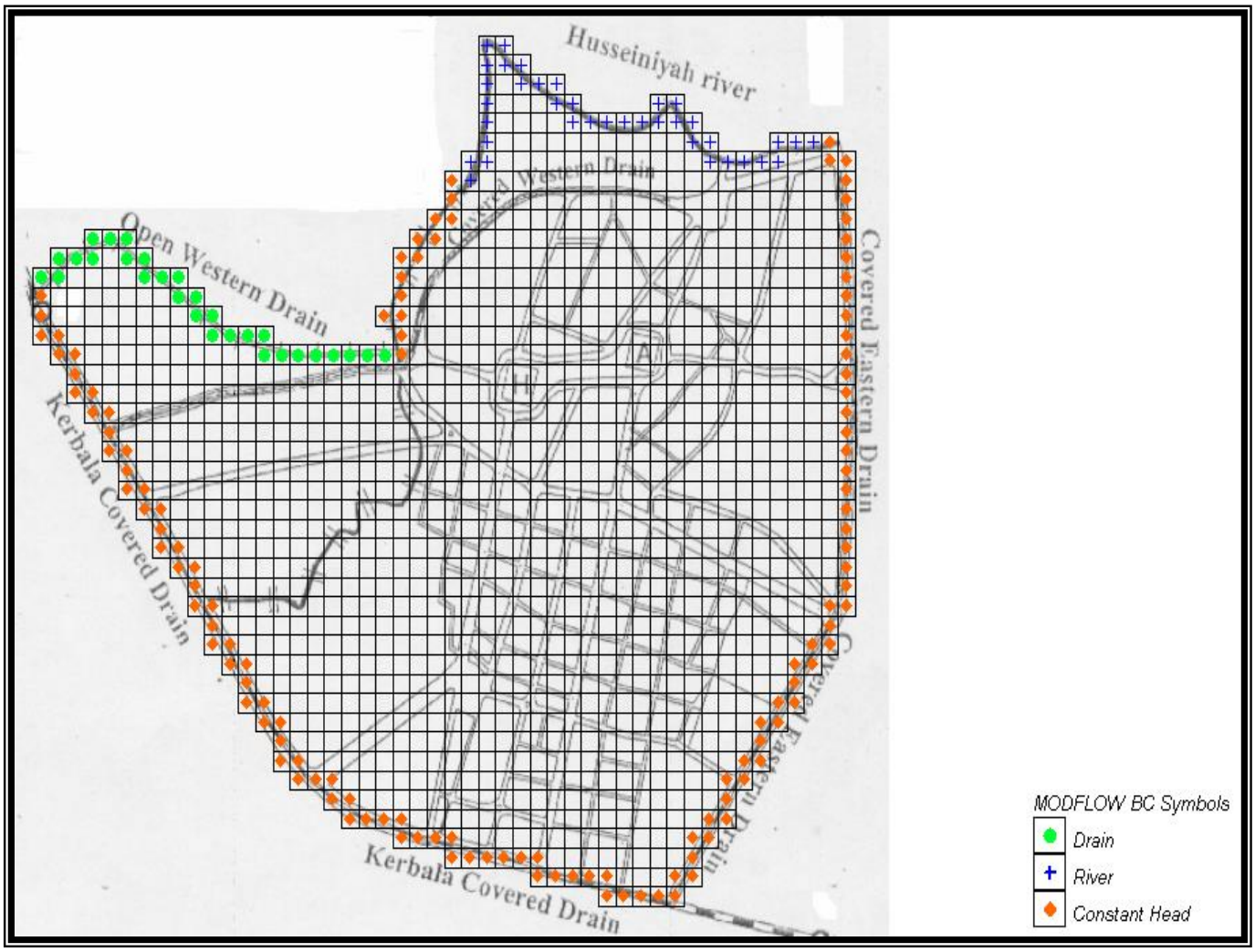

Figure (3-4) Grid design and boundary conditions of the study area

Based on the observed data made by the previous studies, bottom level of the upper layer is entered for each cell, Figure (2-18). Initial distribution of water table (starting head in GMS model) in the upper layer is taken as the average of data observed by Hassan AL-Khateed (2001) during March-2000, Figure (2-12). March is chosen herein from the months March to July because the highest water levels are observed during this month. The data observed by the ISSWR, 1999, show that the average piezometer head of the lower layer is less than the average water table in the upper layer by about 0.2m. Thus, the initial distribution of the piezometer head in the lower layer is estimated by 0.2m less than the corresponding ground water heads in the upper layer. The constant values 0.5m,and 1.6 1/day are considered for the bed thickness, and leakage coefficient for the Hussainya river respectively.

Initial estimation of local recharge to the study area is assumed using the available literature (Lerner, 1986; Lerner, 1989; AL-Rawi,2000; Hassan AL-Khateeb,2001) by this estimation the local recharge to the study area is assumed to be coming only from the leakage of sewers, septic tanks, and drinking water pipe network.

Drinking water is supplied to the study area from two projects named as project No.7 with a capacity of 120900 m3/day and the old project with a capacity of 27000 m3/day, a 34% and 95% of the two projects capacities respectively are assumed to reach to the study area :

0.34*120900+0.95*27000=66756 m3/day

25% of the water supplied to the study area is assumed to be leakage rate from pipe network :

0.25*66756=16689 m3/day

10% of water supplied to the consumers is assumed to be consumes by human activities :

0.9*0.75*66756=45060.3 m3/day

25% of the disposed water is assumed to be disposed to the septic tanks:

0.25*45060.3=11265.1 m3/day

20% of west water is assumed to leak from sewer pipes network :

0.2*0.75*45060.3=6759.1 m3/day

from this it can be said that the total recharge to the study area from leakage is:

16689+11265.1+6759.1=34713.15 m3/day

the local recharge for each cell can be considered as :

$$\frac{34713.15}{3.2*10^6}*2500 = 27.12 m^3/day$$

in the GMS model the local recharge is entered to the model as recharge rate in m/day, thus the initial recharge rate is assumed constant over all the study area as :

$$\frac{34713.15}{3.2*10^6} = 0.011 m/day$$

3-4 Calibration of the GMS Model

A trial and error method is used to find the calibrated local recharge of the model. The local recharge is adjusted after each run until a good match is obtained between the simulated and the observed contour lines for both upper and lower layers. A steady state simulation is adopted herein because it gives more reasonable results.

The area of the model is divided into thirteen coverages, the calibrated recharges are entered for each coverage separately and then adjusted after each run to obtain the best match between the observed and the simulated contour lines under steady state condition.

The best fit between simulated and observed contour lines is evaluated by calculating the Root Mean Square Error (RMSE) for the both layers, equation (3-6).

$$RMSE_{(k)} = \frac{\sqrt{\sum_{i=1}^{R*C} (HSk_{(i,j)} - HOk_{(i,j)})^2}}{R*C} \quad \text{.....(3-6)}$$

Where:

K : equal 1 for the upper layer and equal 3 for the lower layer.

R : number of rows.

C : number of columns.

HS : simulated head.

HO : observed head

Figures (3-5) and (3-6) show a comparison between the observed and simulated contour lines for both upper and lower layer respectively. The root-mean-square error (RMSE) must be less than one-tenth of the observed head range across the area of interest (Geo Trans, Inc., Roswell, GA, 2001). RMSE for the upper layer is found as 1.45 cm and for the lower layer is found as 1.96 cm , The RMSE for both layers is less than 10% of the total observed hydraulic head difference across the modeled area, which is about 55 cm. So, it can be said that the model successfully simulates steady state where close agreement was obtained between the observed and simulated heads.

The calibrated local recharges to the upper layer are shown in Figure (3-7), the recharge rate is entered separately as a constant value for each coverage of all the thirteen coverages, and then it is adjusted after each run until a good match is obtained. The calibrated recharge ranges between (0-20) m3/day per cell . Total recharge is found by the GMS model as 760.71 m3/day. All the other model parameters data are used as the initial input data except the transmissivity which is reduced to 100m2/day to give more compatible between the observed and simulated contour lines in the lower layer.

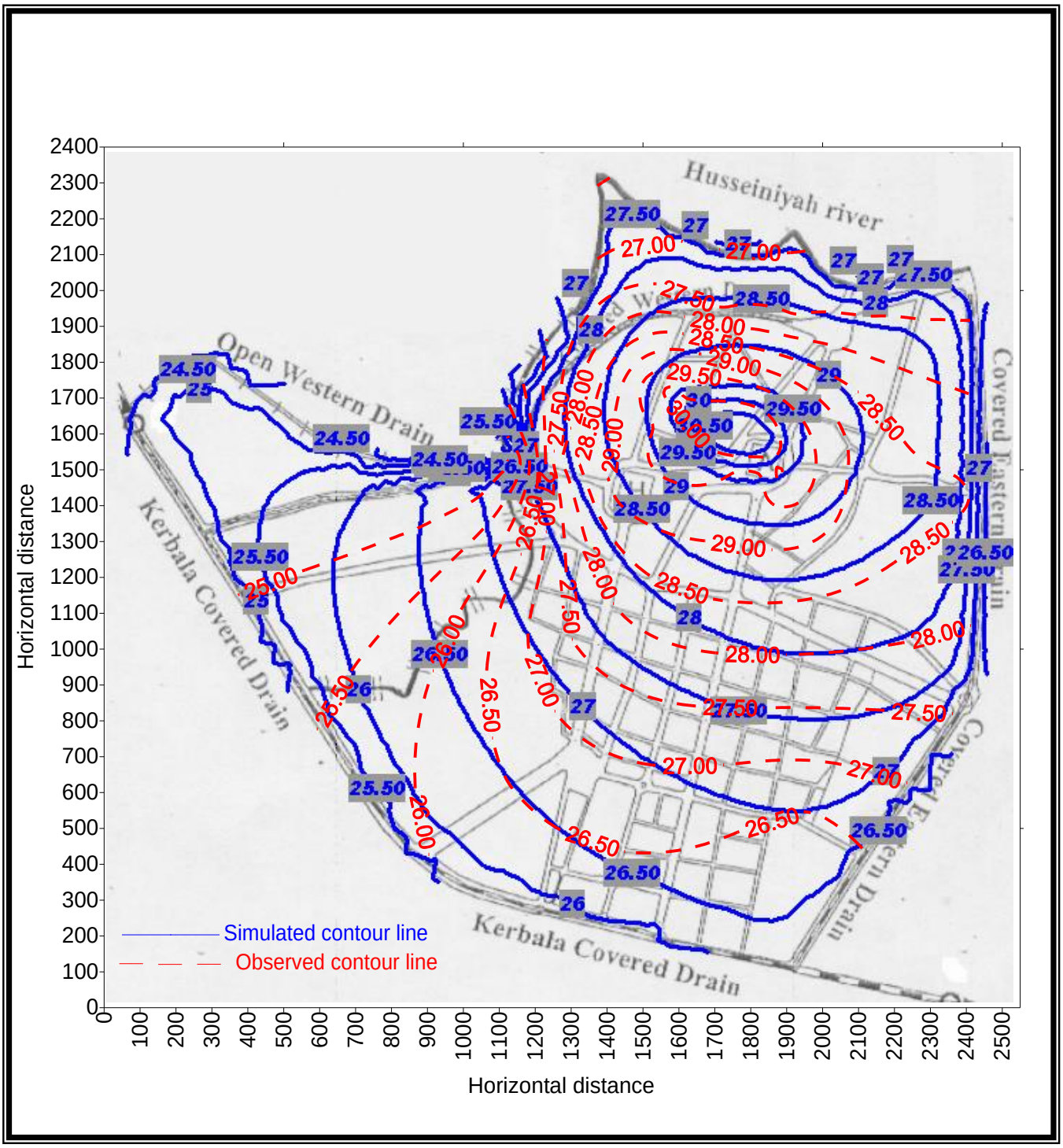

Figure (3-5) Simulated and observed water table level for the upper layer by the GMS model (march2000)

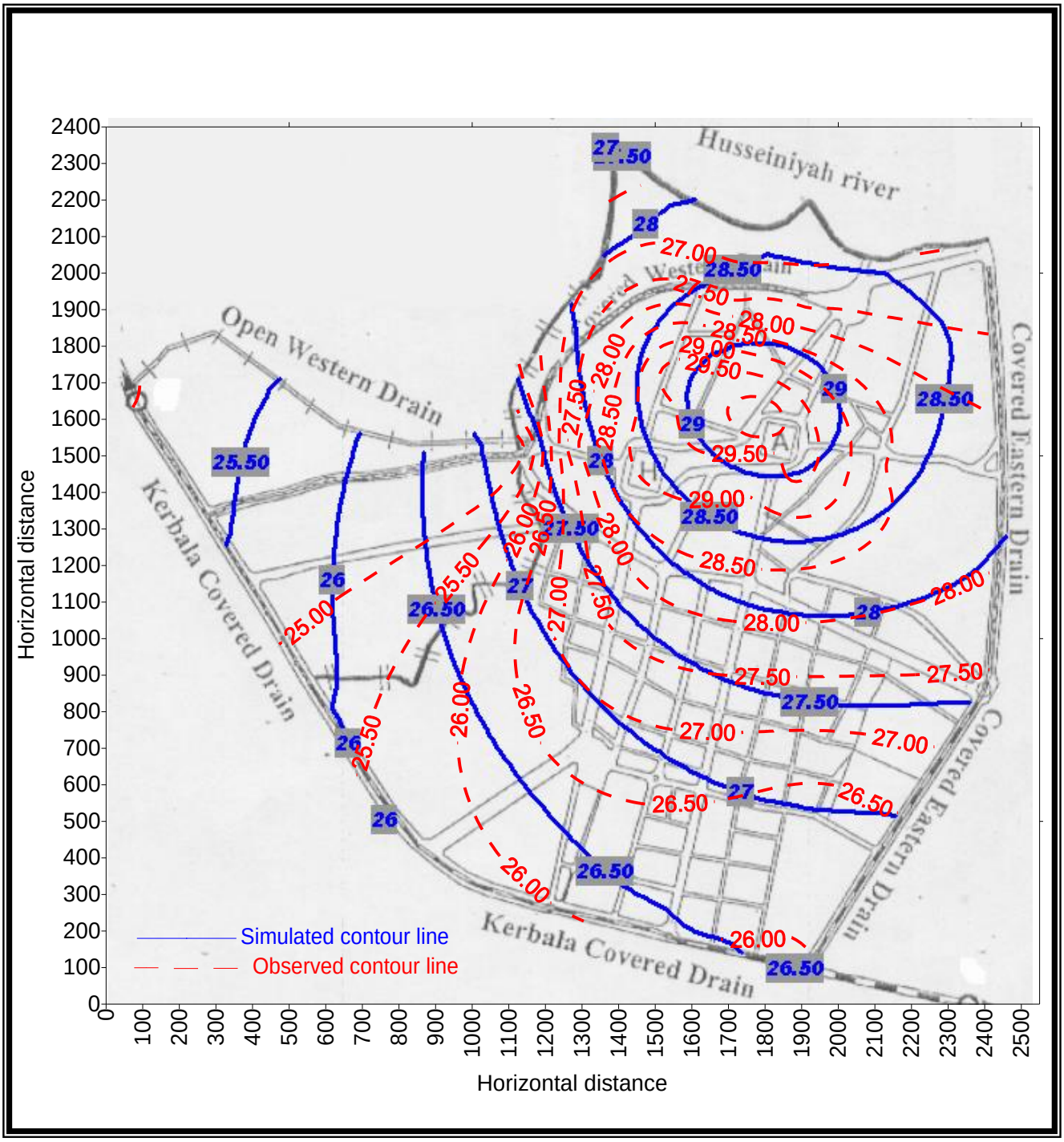

Figure (3-6) Simulated and observed peizometric head for the lower layer by the GMS model (march2000)

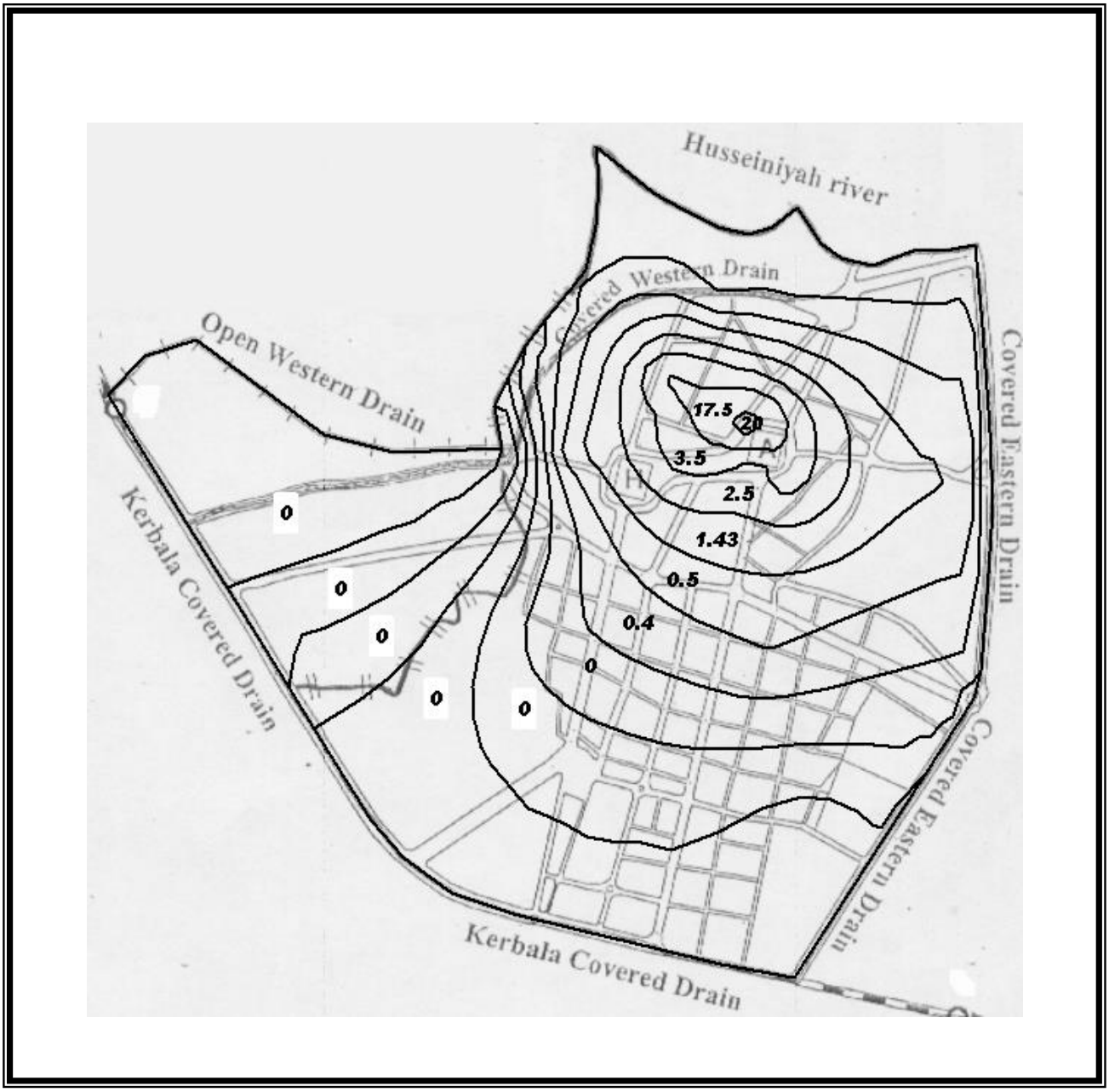

Figure (3- 7) Calibrated recharge to the upper layer by the GMS model (constant value for each coverage) (m3/day) per nodal cell

The GMS model can now be used to examine some procedures of lowering ground water levels of the upper layer in the area of the two holy shrines regarding the city as a hole. Three procedures have been adopted herein; First, examining the effect of reducing local recharge to the upper layer, second, examining the effect of vertical drainage of the lower layer, and third examining the effect of opening all the drains in the study area. The aim of the three procedures is to reduce the water level of the upper layer in the area of the two holy shrines to the basement level of AL-Abbas holy shrine which is about 28m above see level.

Since the initial estimation of the local recharge from the leakage of water supply networks is about 48% of the total initial estimation of the local recharge a reduction of 50 % of the local recharge has been examined first. Figures (3-8) and (3-9) illustrate the simulated results of the water table level and the water table drawdown of this case respectively. The figures show that the drawdown range is between (0-1.499)m, the maximum value is found in the area of the two holy shrines. The drawdown decreases towards the study area boundaries. This drawdown is insufficient therefore reduction in the recharge by about 50% will not be enough. The second examination assumes a reduction in the local recharge about 75%. Figures (3-10) and (3-11) illustrate the simulated results of the water table level and the water table drawdown of this case respectively. The figures show that the drawdown ranges between (0-2.33), the maximum value is observed in the area of the two holy shrines, and it is an acceptable value that agrees with the aim of the procedure therefore, it can be said that reducing the local recharge of the upper layer by about 75% or more can be adopted as a unique solution to solve the problem of rising ground water level in the area of the two holy shrines. That reduction can be achieved by replacing the septic tanks with an efficient sewer system, in addition to repairing and maintaining of the drinking water pipe network and the sewer system that exits within the area.

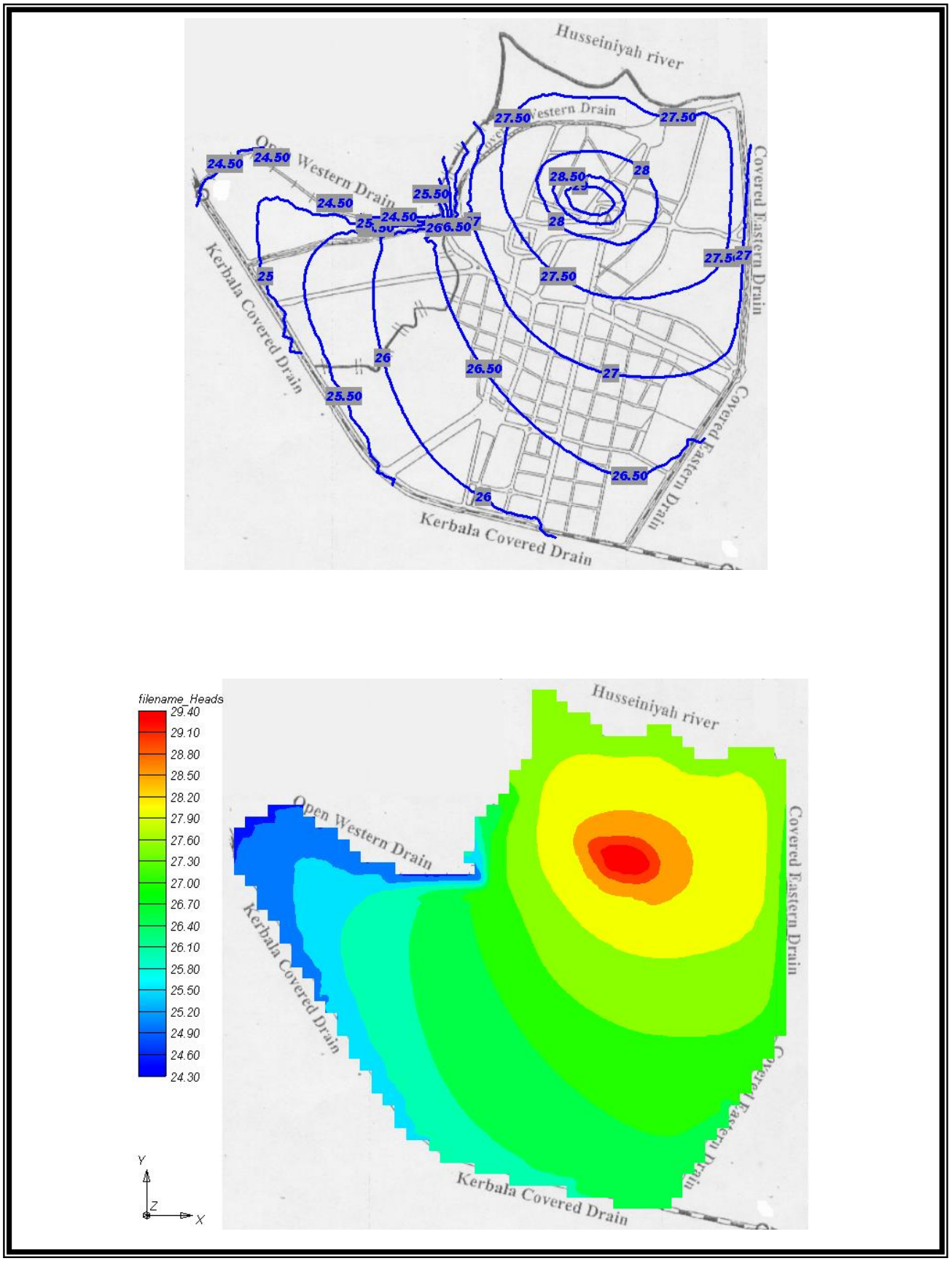

Figure (3-8) Water table level of the upper layer after reducing the local recharge about 50%

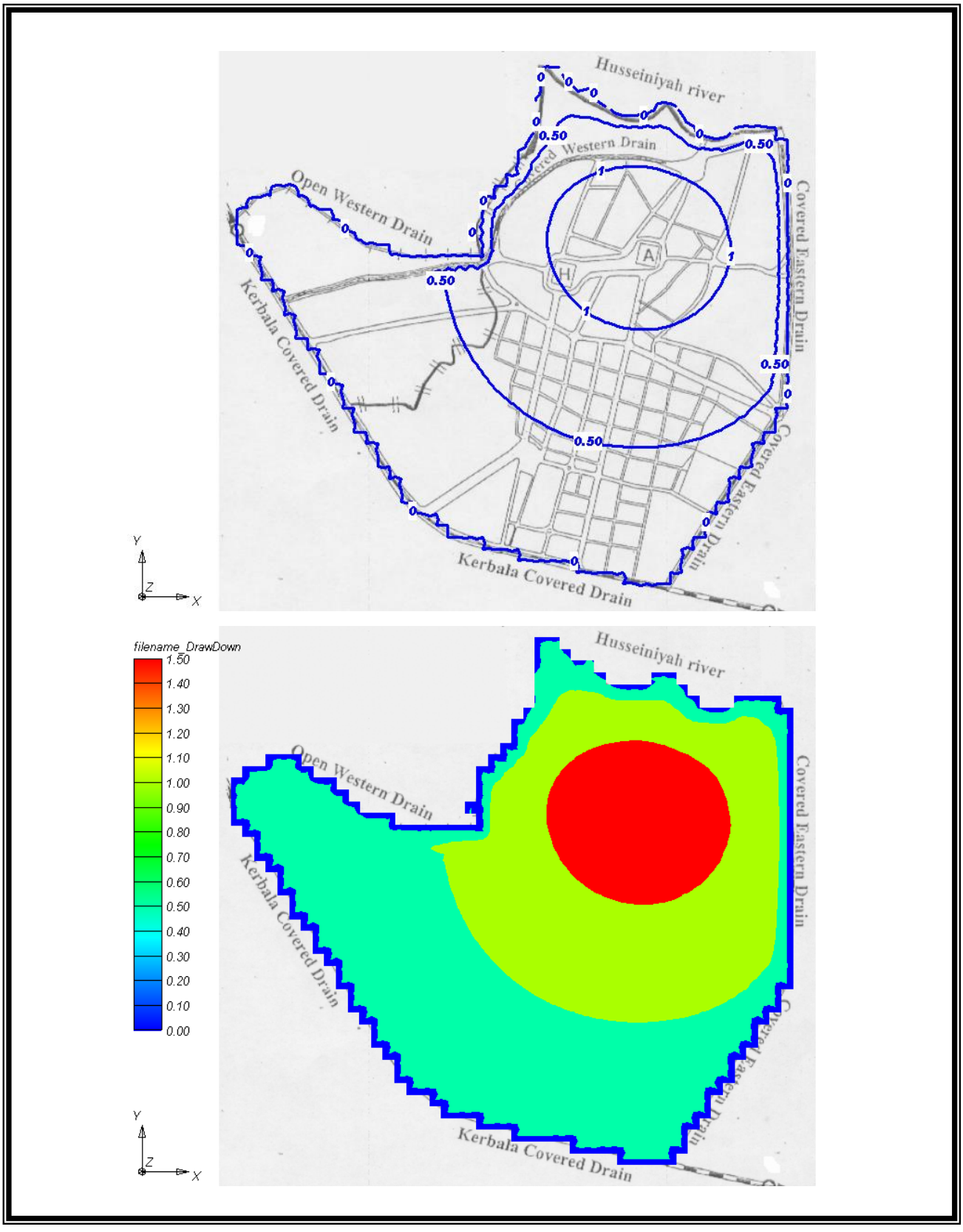

Figure (3-9) Water table draw down of the upper layer after reducing the local recharge about 50%

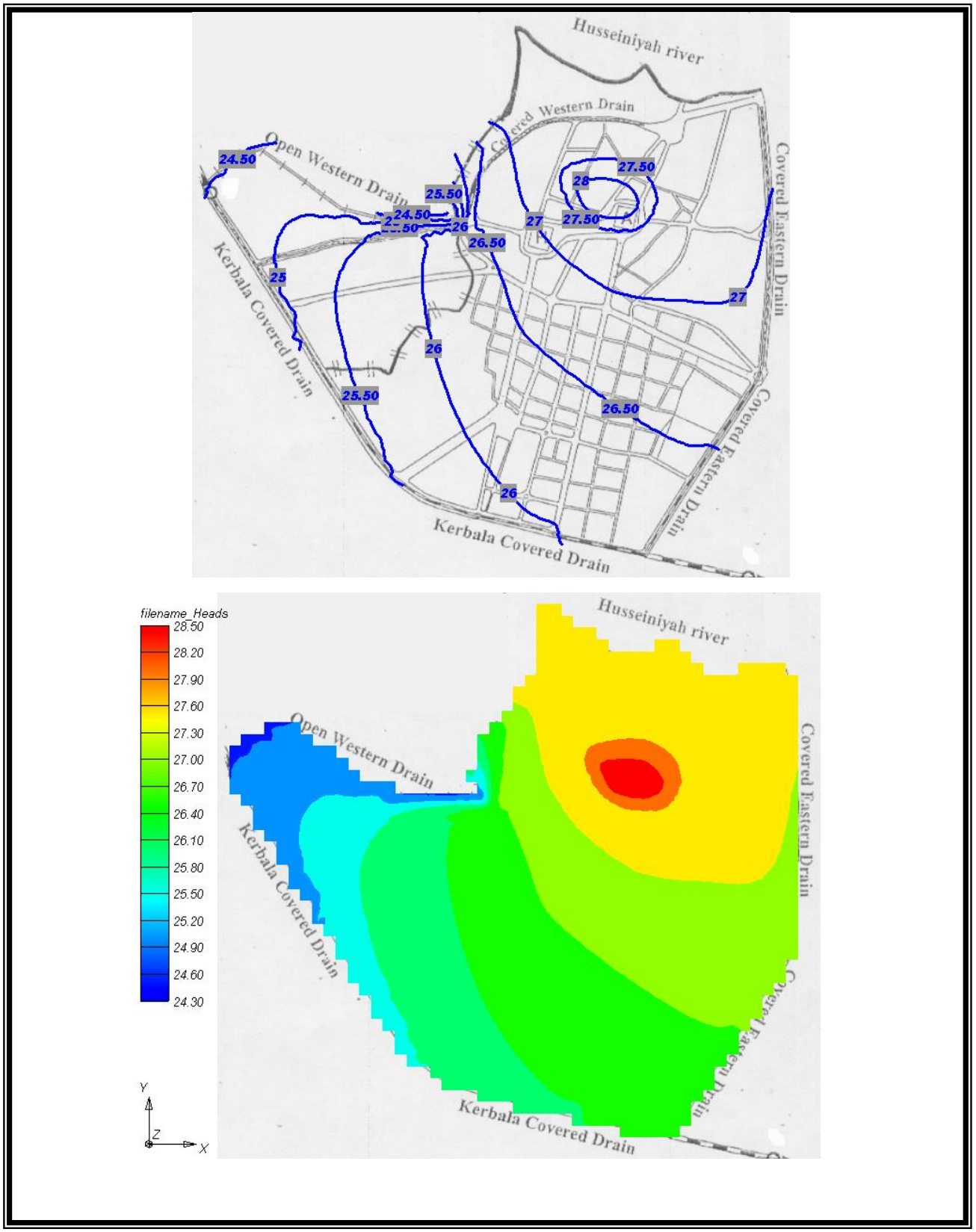

Figure (3-10) Water table level of the upper layer after reducing the local recharge about 75%

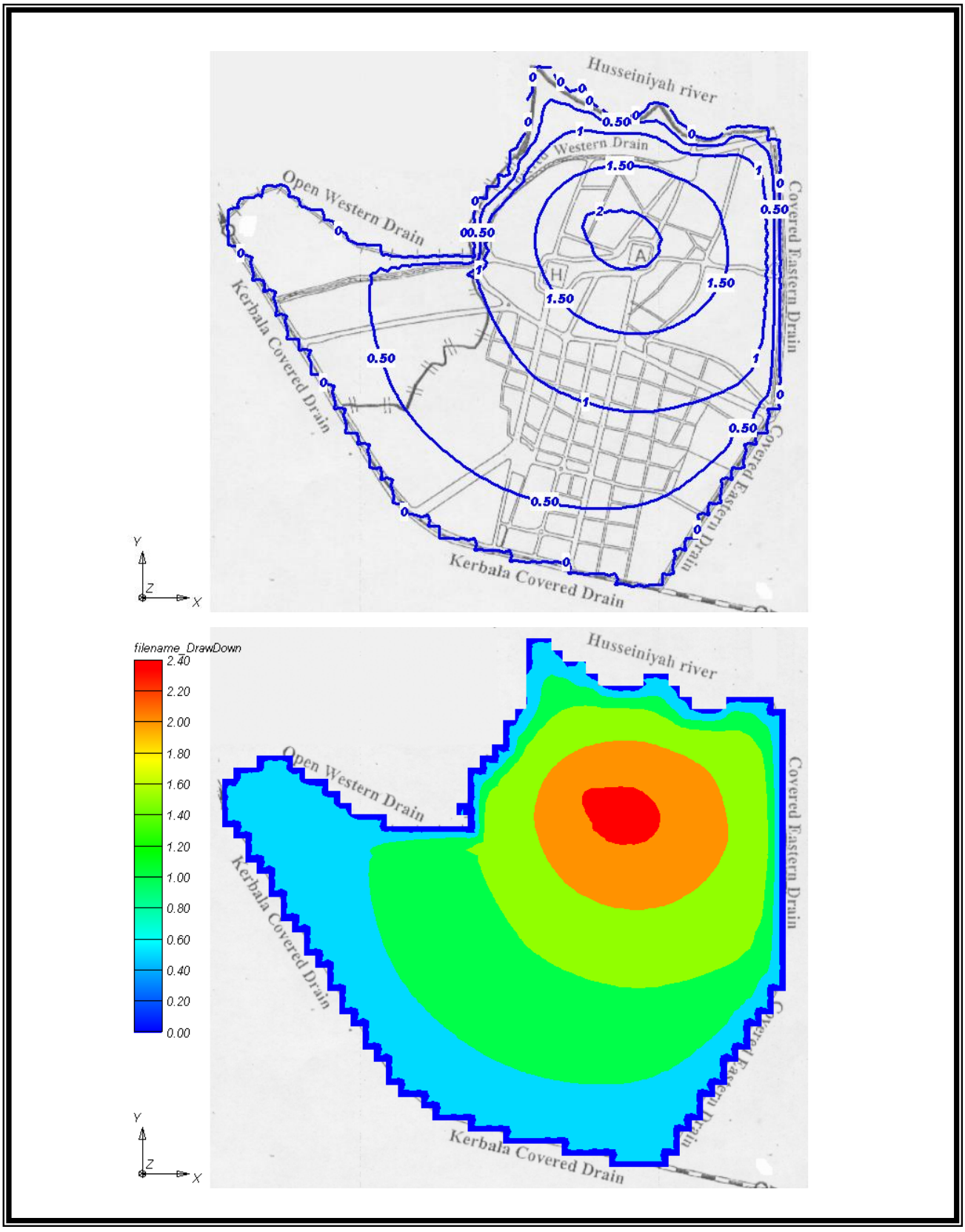

Figure (3-11) Water table drawdown of the upper layer after reducing the local recharge about 75%

Procedure of the vertical drainage of lower layer can be carried out by using eight wells outside each corner of the two holy shrines, Figure (3-12). Long term pumping schedules are used at a discharge of 70 m3/day for each well. Figures (3-13) and (3-14) illustrate the simulated results of the water table level and the water table drawdown of this case respectively. The figures show that the drawdown ranges between (0-2.44)m, the maximum value is observed at the holy shrine of AL-Abbas. Its clear from the figures that this procedure can be adopted also as a unique solution to solve the problem.

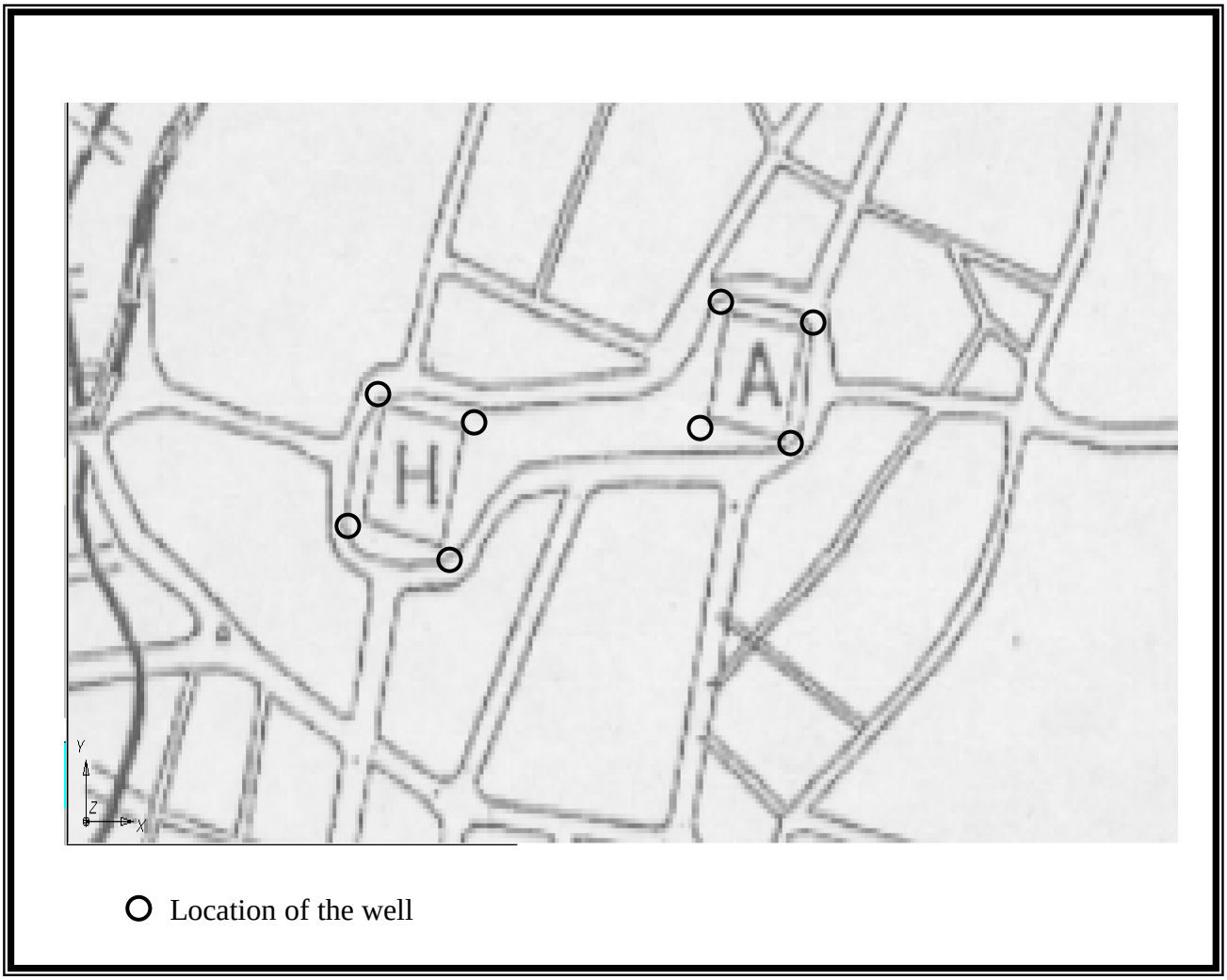

Figure (3-12) The locations of the lower layer wells

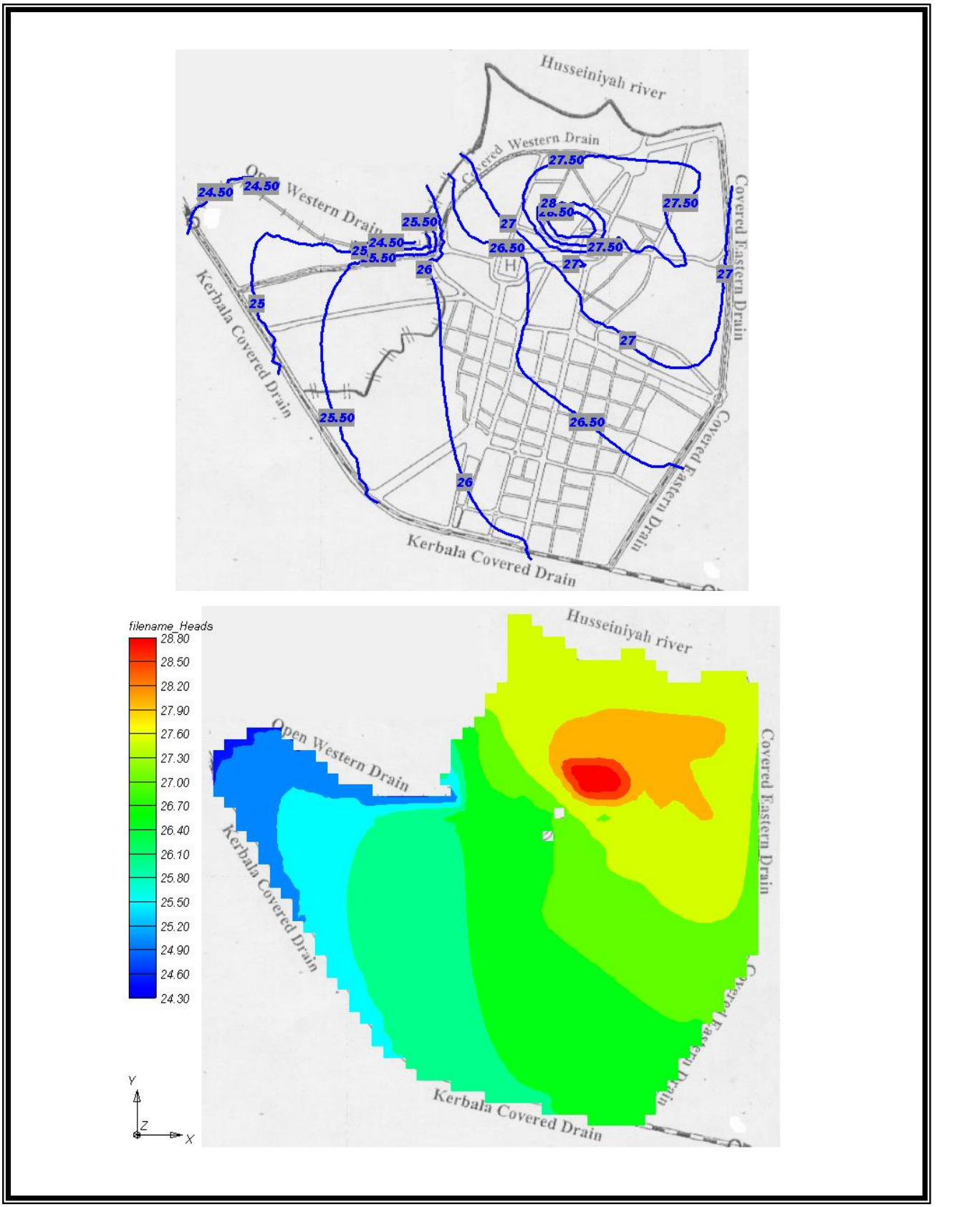

Figure (3-13) Water table level of the upper layer after operating four wells surrounding each holy shrine

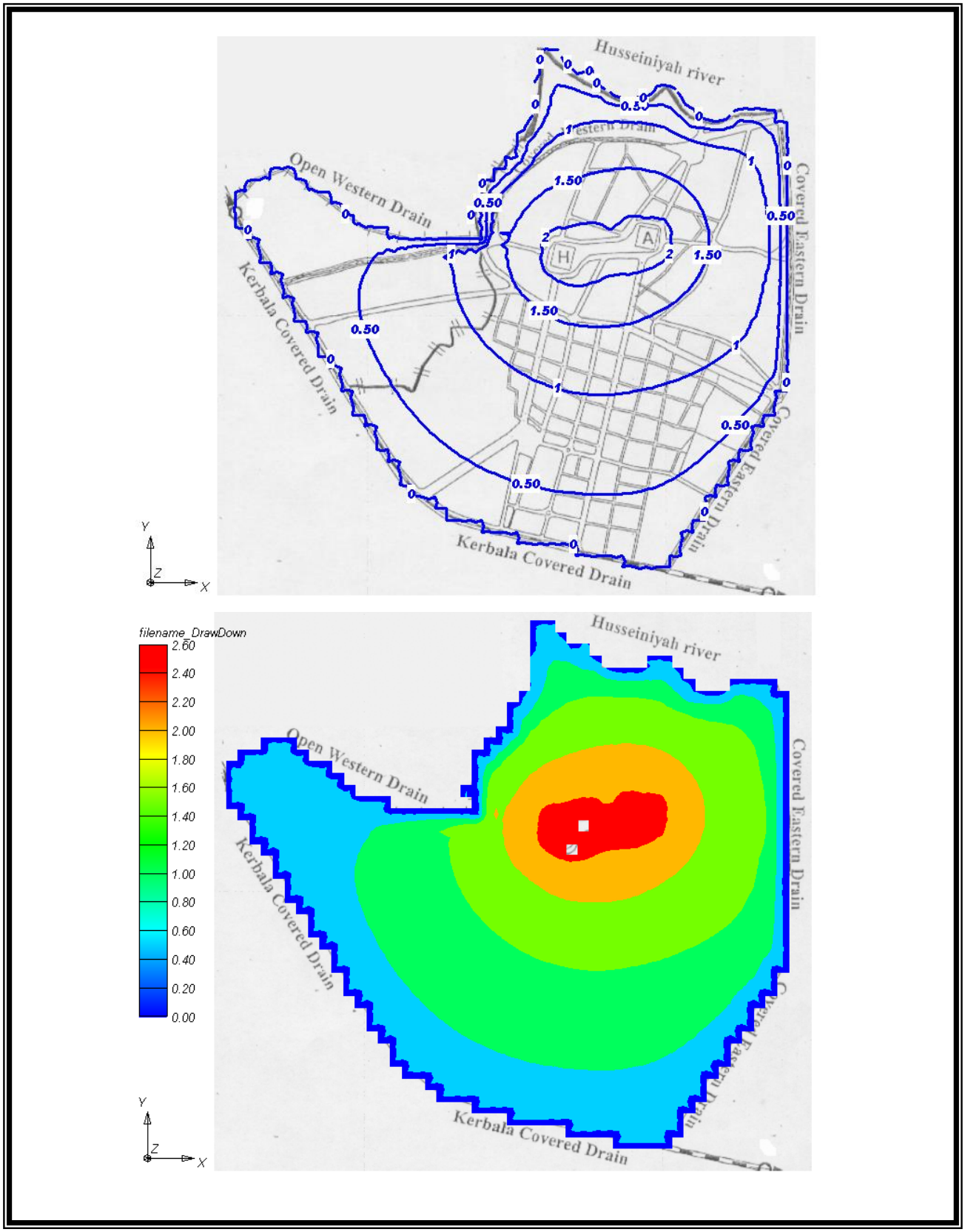

Figure (3-14) Water table drawdown of the upper layer after operating four wells surrounding each holy shrine

Procedure of operating of the Covered Eastern Drain ,Karbala Covered Drain, and the Covered Western Drain can be examined now. Several clogs were observed by the previous works in the first two drains while the third one which discharges water to the open western drain by gravity was completely clogged. The assumption that there are no clogs in the drains can be achieved by cleaning the drains or reconstructing their clogged parts and maintaining good operation of the two pumping stations located at the terminals of the karbala Covered Drain. For such condition all the drains are assumed in the upper layer. Figures (3-15) and (3-16) illustrate the water table level and the water table drawdown for the upper layer respectively. The figures show that the drawdown caused by the Eastern Covered Drain is greater than that caused by the Karbala Covered Drain, the figures also show that the drawdown ranges between (0- 2.85)m, the maximum value at the Western Covered Drain and it reduces gradually to wards Hussainyia River and the Open Western Drain where the drawdown is zero, however, at the area of the two holy shrines the drawdown ranges between (0.5-1)m which is not enough; therefore, it can be said that the opening of all drains can not be adopted as a unique solution because although it can reduce the water table level at the most area of the model region, the drawdown at the two holy shrines area is not sufficient.

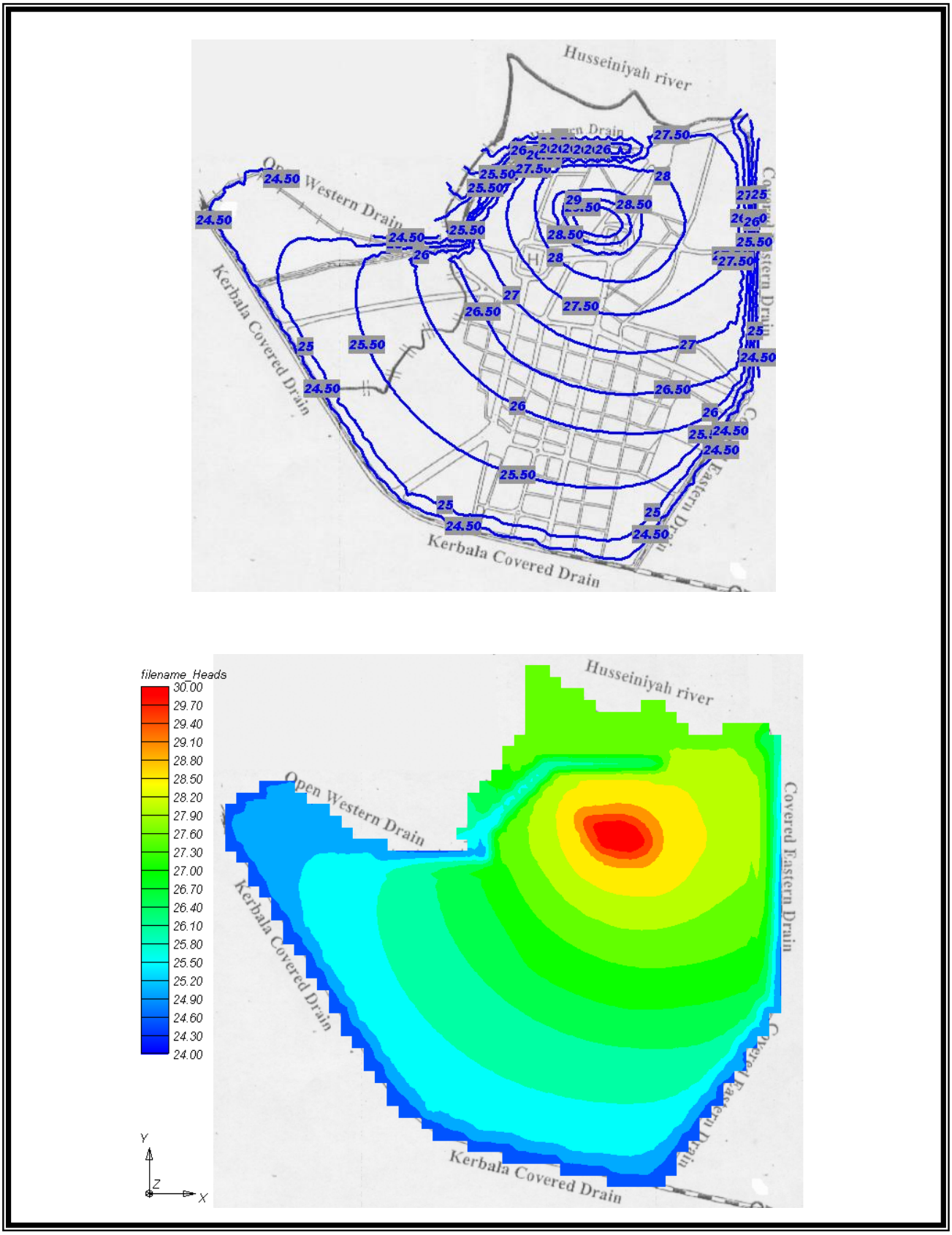

Figure (3-15) Water table level of the upper layer after opening all clogged drains

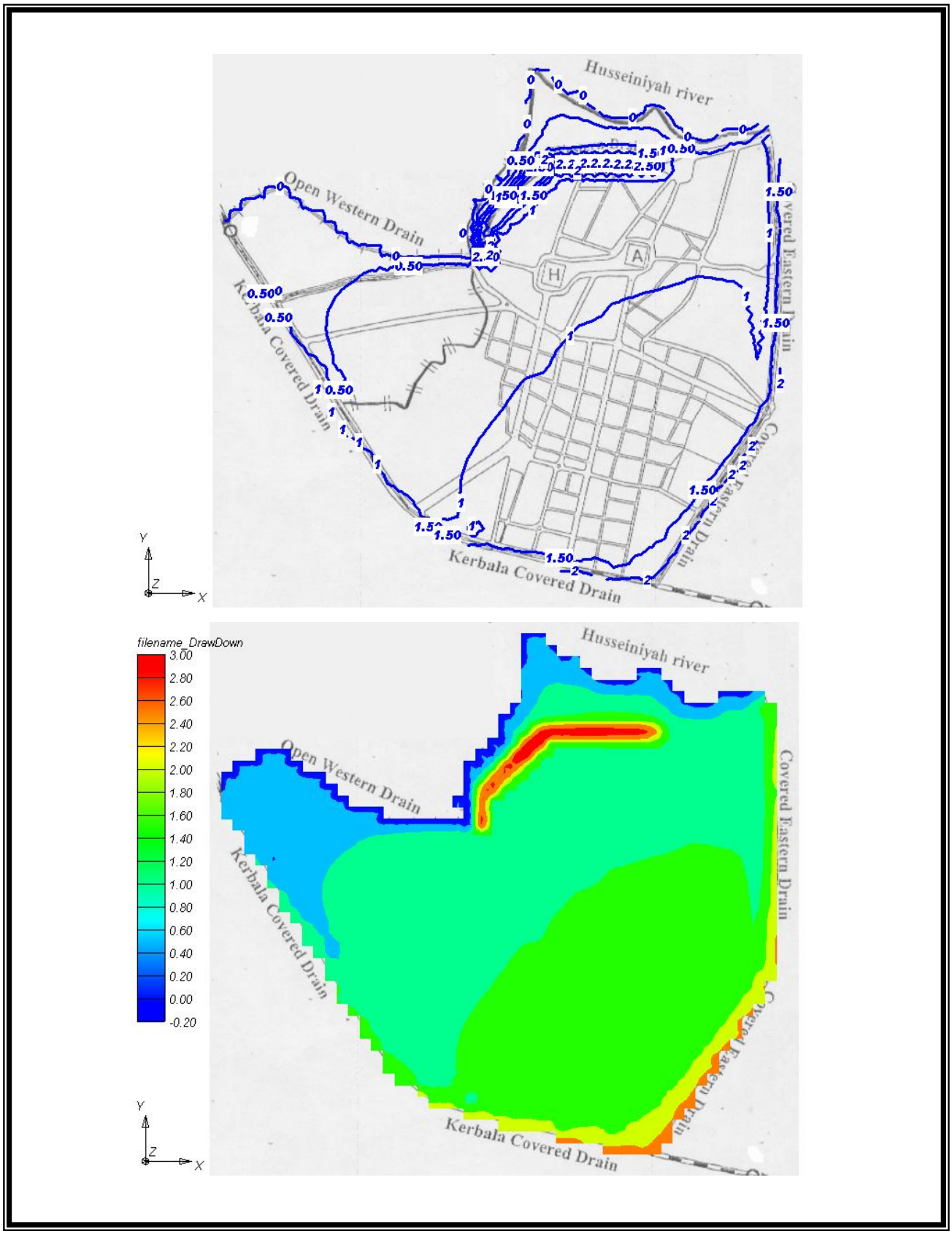

Figure (3-16) Water table drawdown of the upper layer after opening all clogged Drains

CHAPTER FOUR

DEVELOPMENT OF DIFFERENT MATHIMATICAL MODEL

4-1 General

This chapter deals with the construction of mathematical groundwater model other than the GMS model described in Chapter Three. This model is also a numerical one which simulates the hydraulic conditions described in Chapter Two. The finite difference technique is used in this model, so that the model is able to simulate , as closely as possible, the groundwater hydraulic conditions of karbala city including their spatial variables. The model is used to examine proposed solutions to the groundwater problem regarding the city as a whole.

4-2 Two Dimensional Finite Difference Model

4-2-1 Considerations and Assumptions of Hydraulic Conditions

Three types of aquifers are mentioned in Kinzelbach (1986), they are confined aquifer, phreatic aquifer, and semi confined or leaky aquifer which receives water from or loses water to overlying or underlying aquifers through a slightly pervious layer, Figure (4-1). According to the borehole data mentioned in Chapter Two from the pervious studies the aquifer of the study area is of the third type; therefore, the following points can be considered for this Two Dimensional Finite Difference Model.

1- The flow in the upper and lower aquifers is assumed horizontal in two dimensions, while the flow between the neighboring aquifers through the middle layer is proportional to their head difference according to Darcy's law.

2- Surface water bodies, like rivers and open drains, exist only in the upper layer (i.e., bed level of surface water bodies is higher than the bottom level of the upper layer).

3-Downward water infiltration from ground surface to the upper layer is considered such as water leaks from septic tanks and leakage of drinking water pipe networks and sewer systems,.

4- Variation in time and rate of pumping in the leaky aquifer is included.

5- The hydraulic characteristics, such as permeability and transmissivity, are assumed variables horizontal while they are constant in the vertical direction.

6- Surface water bodies are assumed to have constant bed thickness, and constant leakage coefficient.

4-2-2 Mathematical Derivation and Formulation

As explained before, the finite difference method replaces the partial differential equation of flow by a set of finite difference equations in discretized space (plane for two dimensional flow) and time. This discretization may be uniform or nonuniform, however, a uniform grid is adopted in the following derivation.

The system of the three layers is divided into a rectangular grid (i.e., into a number of rectangular nodal cells). The nodal distances in X and Y direction are ΔX and ΔY respectively. The grid extends in vertical direction over the entire depth of the system, Figure (4-2-a). Time is discretized into time levels t_0, t_1,t_2, …. separated by a constant time interval Δt.

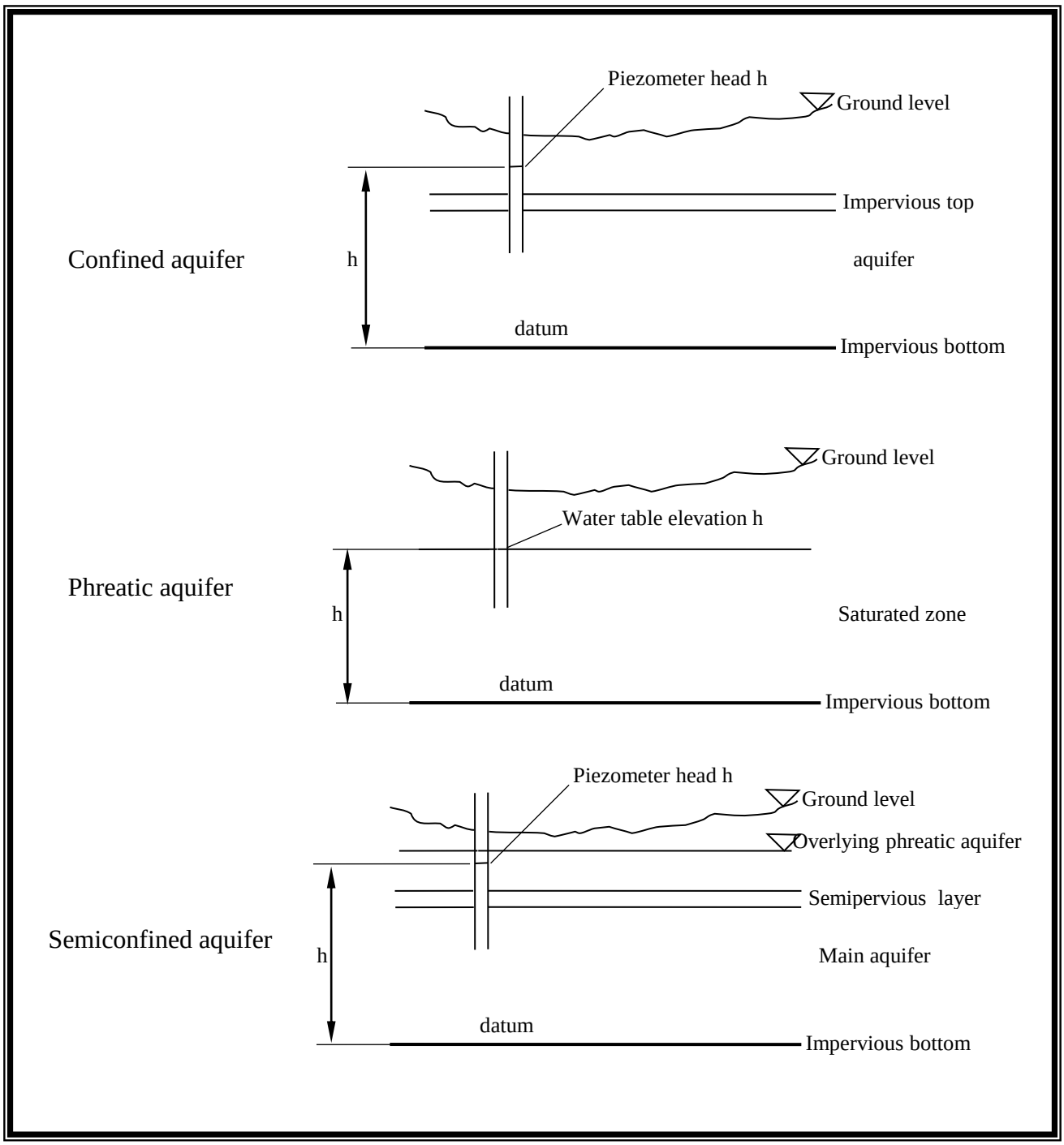

Figure (4-1) Aquifer types discussed in (Kinzelbach,1986).

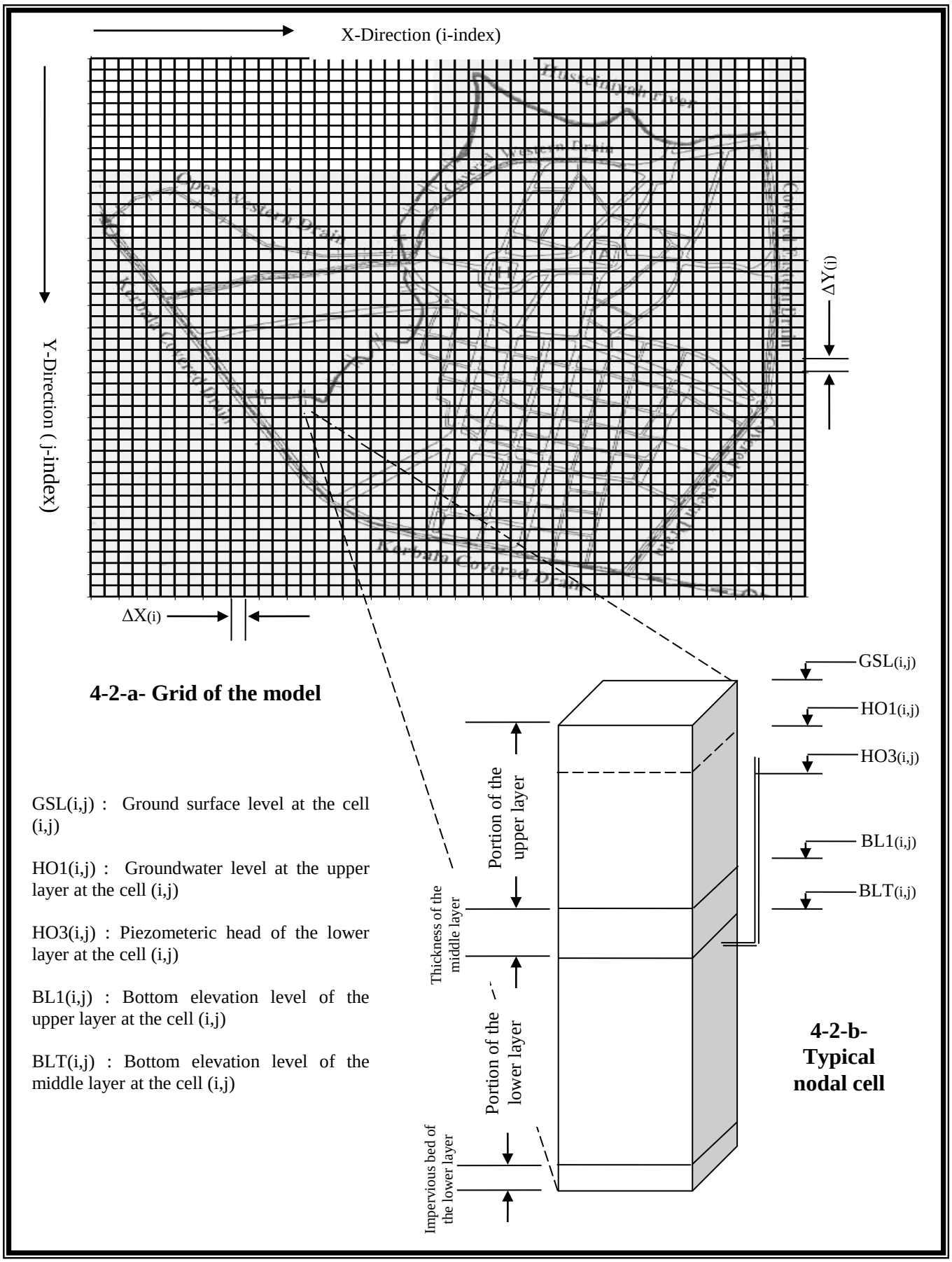

figure 4-2: Discretization of the Solution Region

Numerical solution of flow equations starts from an initial piezometric head distribution at time t_0 for the discrete nodes of the modeled region, then heads are computed at those nodes for later discrete time intervals t1, t2,….. To obtain the appropriate equations for this process, the continuity equation and the Darcy's law can be applied to every cell over a time interval of Δt, assuming that the flow will occur only between the cell and its four direct neighboring cells in horizontal extent (along X and Y axis) and the other layers within the same cell in vertical direction. The resulting system of equations allows the computation of piezometric heads at the nodes at the end of time interval ($t,t+\Delta t$), provided that the heads are known at the beginning of that time interval.

The grid cells are specified by two subscripts (i) and (j) with reference to Y and X directions respectively, Figure (4-2-a). Since the system consists of three layers, the derivation is made for each layer as a part of one typical cell. Middle layer behaves as a leaky layer for the others, therefore, it will be included by the upper and lower layers in the derivation of model.

4-2-2-1 Model Derivation for the Phreatic (Upper) Layer.

Figure (4-3) shows a phreatic layer portion of a typical cell. Water balance of the portion may be made over a short time interval that the in / outflow rates vary only little and can be expressed by averages of the heads over the time interval. There are four horizontal in / outflows ($QU1_{(i,j)}$, $QU2_{(i,j)}$, $QU3_{(i,j)}$, and $QU4_{(i,j)}$) from / to four upper portions of neighboring cells. In addition, there are three vertical flows ($Qswb_{(i,j)}$, $Qnet_{(i,j)}$, and $Qleak_{(i,j)}$) the first two are vertical to the upper face, while the third is vertical to the lower face. $Qleak_{(i,j)}$ represents leakage rate between the upper layer and the lower layer through the semi pervious (middle) layer. $Qswb_{(i,j)}$ is also leakage rate from / to surface water bodies through their beds. $Qnet_{(i,j)}$ is a summation of local upward loss flow rates (like evaporation or evapotranspiration) and downward recharge rates (like rain water percolation and local city services leakage from sewers or drinking water pipe networks). $Qnet_{(i,j)}$ may be upward or downward (discharge or

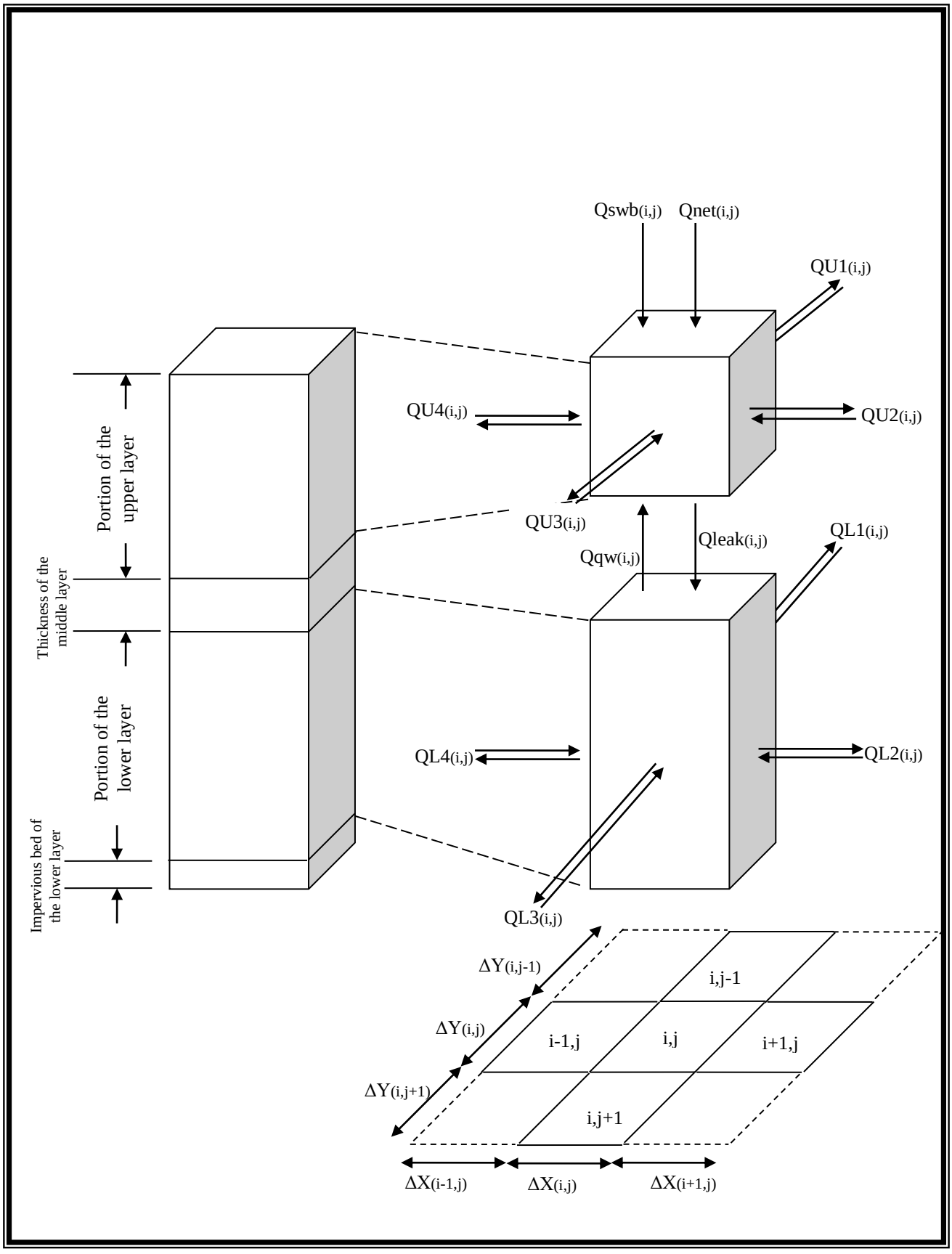

figure (4-3): Flow in A typical Nodal Cell.

recharge) depending on its sources. It is assumed that $Qnet_{(i,j)}$ is independent of the hydraulic heads in the upper and lower layers. In the urban areas, evaporation can be neglected due to the fact that the ground surface is covered with pavement and buildings. Rain water percolation can be neglected too, if it is small. With the exception of $Qnet_{(i,j)}$ the remaining vertical and horizontal flow components depend on hydraulic head and layer physical properties. Thus $Qnet_{(i,j)}$ can be estimated for each node separately as a fixed value.

Considering Figure (4-3), the amount of leakage between the phreatic layer and the leaky aquifer through the middle layer $Qleak_{(i,j)}$ can be expressed according to Darcy's law as :

$$Qleak_{(i,j)} = LCM_{(i,j)}(HO1_{(i,j)} - HO3_{(i,j)})\Delta X * \Delta Y \quad \text{.....(4-1)}$$

in which

$$LCM_{(i,j)} = \frac{K_{(i,j)}}{thic} \text{.....(4-1-a)}$$

Where

$LCM_{(i,j)}$: Leakage coefficient of the middle layer, L/T

$K_{(i,j)}$: Vertical permeability of the middle layer at a nodal cell (i,j), L/T

thic : Thickness of the middle layer at nodal cell (i,j), L

$HO1_{(i,j)}$: Groundwater level at the upper layer at the nodal cell (i,j), L

$HO3_{(i,j)}$: Piezometer head at the lower layer at the nodal cell (i,j), L

$\Delta X_{(i,j)}$ and $\Delta Y_{(i,j)}$: Dimension of the cell (i,j) (in horizontal plan) in X and Y directions respectively, L

With reference to figure 4-4, the leakage from /to surface water bodies through their beds ($Qswb_{(i,j)}$) may occur in two cases (Kinzelbach,1986). The first is when the hydraulic head of the upper layer ($HO1_{(i,j)}$) is higher than the bottom level of the surface water body bed, Figure 4-4-a. In this case ($Qswb_{(i,j)}$) is determined according to Darcy's law as:

$$Qswb_{(i,j)} = LCB_{(i,j)}(WL_{(i,j)} - HO1_{(i,j)}) * \Delta X * \Delta Y \text{.....(4-2)}$$

in which:

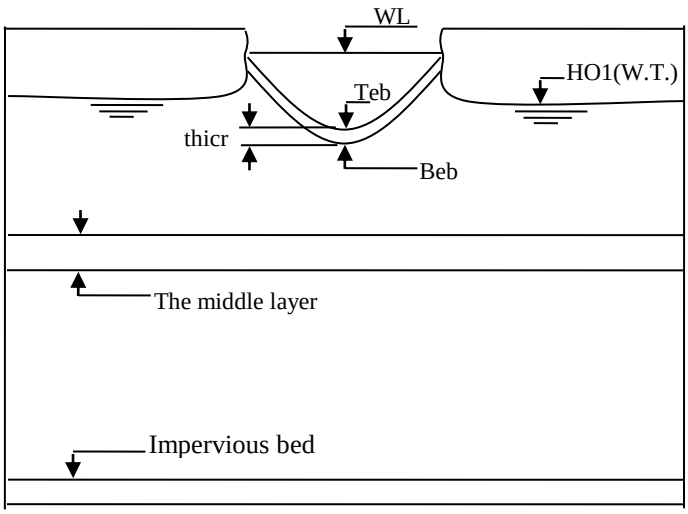

Case a

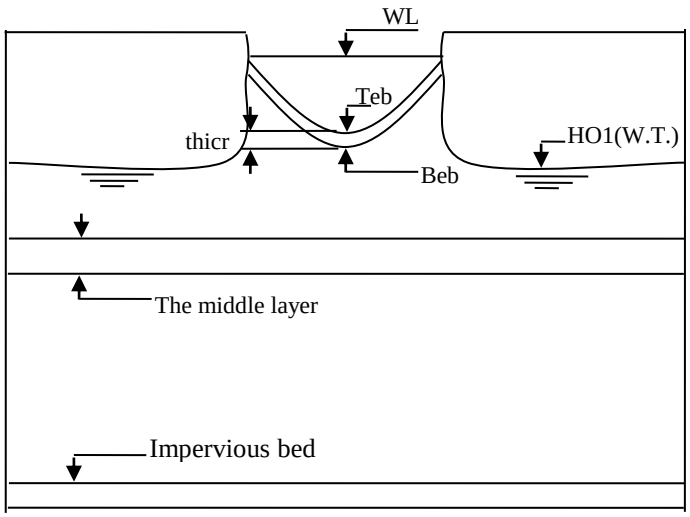

Case b

figure 4-4: Leakage from surface water body to the upper layer in his two cases.

$$LCB_{(i,j)} = \frac{Kr_{(i,j)}}{thicr_{(i,j)}} \quad \text{.....(4-2-a)}$$

where:

$LCB_{(i,j)}$: Leakage coefficient of surface water body bed at nodal cell (i,j) , 1/T

$Kr_{(i,j)}$: Vertical permeability of surface water body bed at a nodal cell (I,j), L/T

$thicr_{(i,j)}$: Thickness of surface water body bed at a nodal cell (i,j), L

$WL_{(i,j)}$: Water level of surface water body at a nodal cell (i,j), L

$HO1_{(i,j)}$: Ground water level at the upper layer at a nodal cell (i,j), L

$\Delta X_{(i,j)}$ and $\Delta Y_{(i,j)}$: Dimension of the cell (i,j) (in horizontal plan) in X and Y directions respectively, L

The second case, when the groundwater table ($HO1_{(i,j)}$) drops below the river bottom, Figure 4-4-b, the inflow becomes independent from the groundwater table. The governing head difference is then the head of the surface water body with respect to the river bottom. The application of Darcy's law can be as follows :

$$Qswb_{(i,j)} = LCB_{(i,j)}(WL_{(i,j)} - Teb_{(i,j)}) * \Delta X * \Delta Y \quad \text{.....(4-3)}$$

where :

$Teb_{(i,j)}$: Top elevation of the surface water body bed at a nodal cell (I,j), L

The four lateral flows ($QU1_{(i,j)}$, $QU2_{(i,j)}$, $QU3_{(i,j)}$, and $QU4_{(i,j)}$) can be obtained as follows :

$$QU1_{(i,j)} = TU1average \frac{HO1_{(i,j-1)} - HO1_{(i,j)}}{0.5(\Delta Y_{(i,j-1)} + \Delta Y_{(i,j)})} \Delta X_{(i,j)} \text{.....(4-4)}$$

$$QU2_{(i,j)} = TU2average \frac{HO1_{(i+1.j)} - HO1_{(i,j)}}{0.5(\Delta X_{(i+1,j)} + \Delta X_{(i,j)})} \Delta Y_{(i,j)} \text{.....(4-5)}$$

$$QU3_{(i,j)} = TU3average \frac{HO1_{(i,j+1)} - HO1_{(i,j)}}{0.5(\Delta Y_{(i,j+1)} + \Delta Y_{(i,j)})} \Delta X_{(i,j)} \text{.....(4-6)}$$

$$QU4_{(i,j)} = TU4average \frac{HO1_{(i-1.j)} - HO1_{(i,j)}}{0.5(\Delta X_{(i-1,j)} + \Delta X_{(i,j)})} \Delta Y_{(i,j)} \quad \text{.....(4-7)}$$

where:

TU1average, TU2average, TU3average, and TU4 average are the average values of upper layer local transmissivities between the node (i,j) and its four direct neighboring nodes (i,j-1), (i+1,j), (i,j+1), and (i-1,j) respectively. $HO1_{(i,j)}$ is the head at the upper layer at the nodal cell (i,j)

4-2-2-1-1 Average Transmissivities (inter nodal transmissivities) for the Upper layer

Using average transmissivities rather than local one became more efficient because in a realistic regional model grid size may be anything from some meters to some hundreds of meters (Boonstra and de Ridder, 1981). A correct description of flow between nodes must, thus, be interpolated. To obtain the neede averages (inter nodal transmissivities) between nodes, arithmetic mean may be applied as (for TU1average as example):

$$TU1average = \frac{T1_{(i,j-1)} + T1_{(i,j)}}{2} \quad \text{.....(4-8)}$$

where $T1_{(i,j-1)}$ and $T1_{(i,j)}$ are local transmissivities in the nodes (i,j-1) and (i,j) respectively, in the upper layer.

The harmonic average has the advantage of the allowing of incorporation of impervious boundaries and the inactive cells in a simple way with the equations of simulation. Therefore the local transmissivities can be add harmonically as :

$$TU1average = \frac{2*(T1_{(i,j-1)} * T1_{(i,j)})}{T1_{(i,j-1)} + T1_{(i,j)}} \quad \text{.....(4-9)}$$

Consequence to equation (4-9) the other three transmissivities can be formulated as :

$$TU2average = \frac{2*(T1_{(i+1,j)} * T1_{(i,j)})}{T1_{(i+1,j)} + T1_{(i,j)}} \quad \text{.....(4-10)}$$

$$TU3average = \frac{2*(T1_{(i,j+1)} * T1_{(i,j)})}{T1_{(i,j+1)} + T1_{(i,j)}} \quad \text{.....(4-11)}$$

$$TU4average = \frac{2*(T1_{(i-1,j)} * T1_{(i,j)})}{T1_{(i-1,j)} + T1_{(i,j)}} \quad \text{.....(4-12)}$$

For simplicity, each node of the grid is assigned two average transmissivity values ($TX1_{(i,j)}$) and ($TY1_{(i,j)}$) in X and Y directions, respectively. ($TX1_{(i,j)}$) is the transmissivity between the node (i,j) and its next neighbor node in the positive X direction (i+1,j). ($TY1_{(i,j)}$) is the transmissivity between the node (i,j) and its next neighbor node in the positive Y direction (i,j+1), Figure (4-5). The four transmussivities between node (i,j) and its four next neighbors are replaced by:

TU1average $\longrightarrow$ $TY1_{(i,j-1)}$

TU2average $\longrightarrow$ $TX1_{(i,j)}$

TU3average $\longrightarrow$ $TY1_{(i,j)}$

TU4average $\longrightarrow$ $TX1_{(i-1,j)}$

Average transmissivities according to this assignment system may be called (directional) or (inter nodal) transmissivities (Kinzelbach,1986).

In the phreatic layer, transmissivity depends on the ground water level. Referring to Figure 4-1, local transmissivity $T1_{(i,j)}$ may be defined as:

$$T1_{(i,j)} = perm_{(i,j)} * (HO1_{(i,j)} - BL1_{(i,j)}) \quad \text{.....(4-13)}$$

where:

$perm_{(i,j)}$: Local permeability of the upper layer at a nodal cell (i,j), L/T

$HO1_{(i,j)}$: Observed ground water level at the upper layer at a nodal cell (i,j), L

$BL1_{(i,j)}$: Bottom elevation of the upper layer at a nodal cell (i,j), L

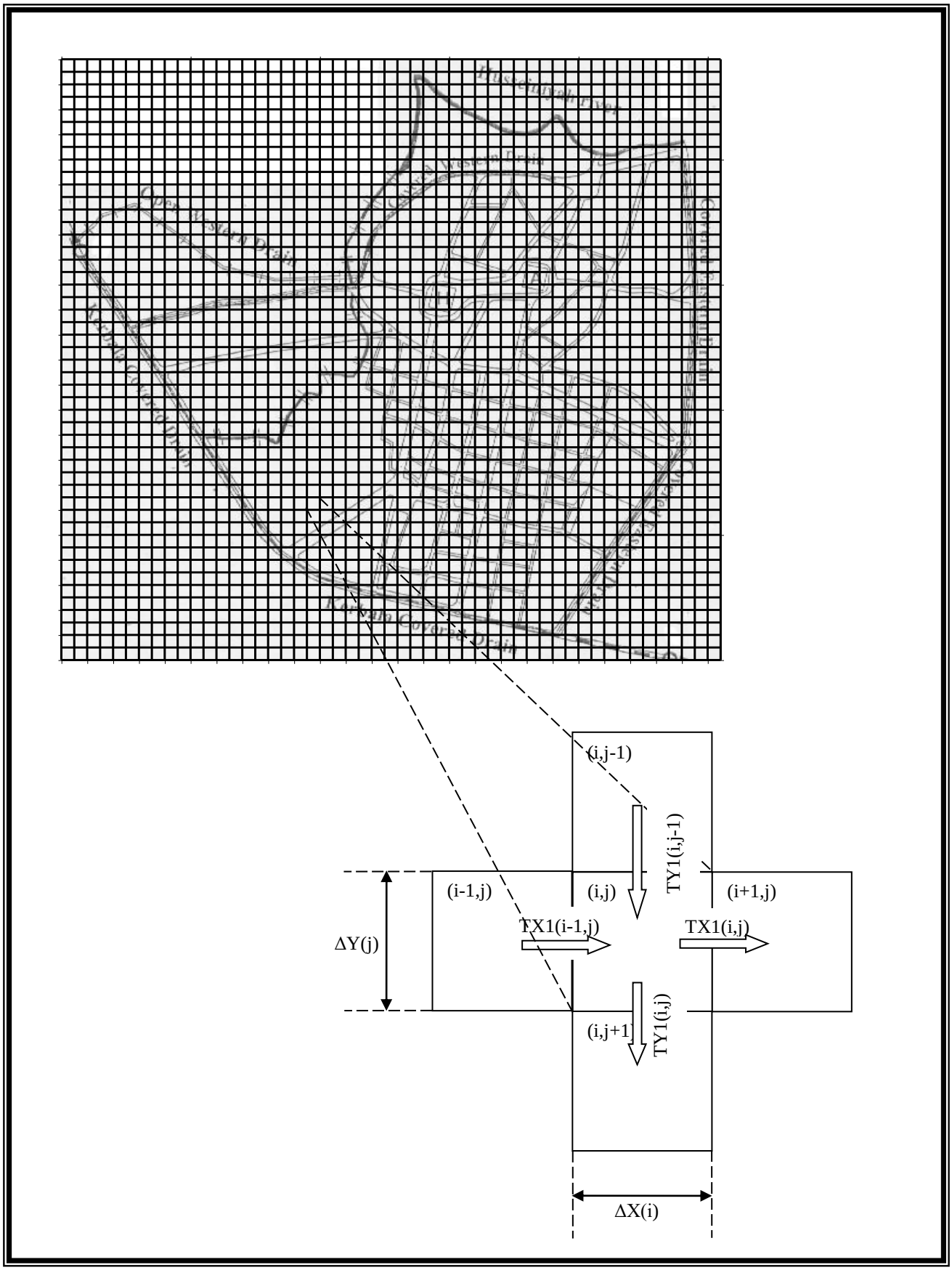

Figure 4-5: Directional (Inter nodal) Transmissivities considered by the mathematical model

According to (Butler,1957 ; Bear and Verruijt,1987) the formulation of ($TX1_{(i,j)}$) and ($TY1_{(i,j)}$) can be obtained by multiplying the harmonic averages of the permeability by the geometric averages of saturated thickness along the X and the Y directions respectively:

$$TX1_{(i,j)} = permx_{(i,j)}\sqrt{(HO1_{(i+1,j)} - BL1_{(i+1,j)})(HO1_{(i,j)} - BL1_{(i,j)})} \quad \text{.....(4-14)}$$

in which

$$permx_{(i,j)} = \frac{2*(perm_{(i,j)} * perm_{(i+1,j)})}{(perm_{(i,j)} + perm_{(i+1,j)})} \quad \text{.....(4-14-a)}$$

$$TY1_{(i,j)} = permy_{(i,j)}\sqrt{(HO1_{(i,j+1)} - BL1_{(i,j+1)})(HO1_{(i,j)} - BL1_{(i,j)})} \quad \text{.....(4-15)}$$

in which

$$permy_{(i,j)} = \frac{2*(perm_{(i,j)} * perm_{(i,j+1)})}{(perm_{(i,j)} + perm_{(i,j+1)})} \quad \text{.....(4-15-a)}$$

where:

$perm_{(i,j)}$, $perm_{(i,j+1)}$, $perm_{(i+1,j)}$ are local permeability of the upper layer at the cells (i,j), (i,j+1), and (i+1,j) respectively, L/T

$permx_{(i,j)}$ and $permy_{(i,j)}$ are harmonically averaged permeability between nodes (i,j) and (i,j+1), and (i+1,j) respectively, L/T

Equations (4-4) to (4-7) can be rewritten using the inter nodal transmissivity :

$$QU1_{(i,j)} = TY1_{(i,j-1)}\frac{HO1_{(i,j-1)} - HO1_{(i,j)}}{0.5(\Delta Y_{(i,j-1)} + \Delta Y_{(i,j)})}\Delta X_{(i,j)} \quad \text{.....(4-16)}$$

$$QU2_{(i,j)} = TX1_{(i,j)}\frac{HO1_{(i+1.j)} - HO1_{(i,j)}}{0.5(\Delta X_{(i+1,j)} + \Delta X_{(i,j)})}\Delta Y_{(i,j)} \quad \text{.....(4-17)}$$

$$QU3_{(i,j)} = TY1_{(i,j)}\frac{HO1_{(i,j+1)} - HO1_{(i,j)}}{0.5(\Delta Y_{(i,j+1)} + \Delta Y_{(i,j)})}\Delta X_{(i,j)} \quad \text{.....(4-18)}$$

$$QU4_{(i,j)} = TX1_{(i,j-1)} \frac{HO1_{(i-1.j)} - HO1_{(i,j)}}{0.5(\Delta X_{(i-1,j)} + \Delta X_{(i,j)})} \Delta Y_{(i,j)} \quad \text{.....(4-19)}$$

4-2-2-1-2 Nodal Ground Water Balance

According to principles of continuity, inflows minus outflows over the time interval (t,t+Δt) must equal the quantity of water stored in the cell over this time. For such balance it can be assumed that the signs of inflows are positive and the sign of out-flows are negative. For the upper layer portion, Figure 4-2, ($Qleak_{(i,j)}$) is assumed as outflow and the other flows are assumed as inflows, therefore the water balance of this cell portion can be expressed as :

$$\Delta t(QU1_{(i,j)(t+\Delta t)} + QU2_{(i,j)(t+\Delta t)} + QU3_{(i,j)(t+\Delta t)} + QU4_{(i,j)(t+\Delta t)} + Qnet_{(i,j)} + Qswb_{(i,j)(t+\Delta t)} - Qleak_{(i,j)(t+\Delta t)}) = (HO1_{(i,j)(t+\Delta t)} - HO1_{(i,j)(t)}) * effe_{(i,j)} * \Delta X_{(i,j)} * \Delta Y_{(i,j)} \quad \text{.....(4-20)}$$

Where:

$effe_{(i,j)}$: Effective porosity of the upper layer at anodal cell (i,j), dimensionless

The signs of the flows $QU1_{(i,j)}$, $QU2_{(i,j)}$, $QU3_{(i,j)}$,$Qu4_{(i,j)}$, $Qswb_{(i,j)}$,and $Qleak_{(i,j)}$ in equation (4-20) are automatically corrected through the model application depending on the hydraulic heads in and around the cell under consideration. $Qnet_{(i,j)}$ is time independent and its one of the input data to the model, its assumed and resigned for each cell separately, depending on the cell it self, for the drain cells $Qnet_{(i,j)}$ may be negative and positive for the recharging cells.

By substituting equations (4-1) to (4-3), equations (4-14) to (4-15-a), and equations (4-16) to (4-19) into equation (4-20),and divided the both sides on Δt two equations can be obtained depending on the heads of ground water in the upper layer in the cells of surface water body:

$$TY1_{(i,j-1)(t+\Delta t)}\frac{HO1_{(i,j-1)(t+\Delta t)}-HO1_{(i,j)(t+\Delta t)}}{0.5(\Delta Y_{(i,j-1)}+\Delta Y_{(i,j)})}\Delta X_{(i,j)}+TX1_{(i,j)(t+\Delta t)}\frac{HO1_{(i+1,j)(t+\Delta t)}-HO1_{(i,j)(t+\Delta t)}}{0.5(\Delta X_{(i+1,j)}+\Delta X_{(i,j)})}\Delta Y_{(i,j)}+$$

$$TY1_{(i,j)(t+\Delta t)}\frac{HO1_{(i,j+1)(t+\Delta t)}-HO1_{(i,j)(t+\Delta t)}}{0.5(\Delta Y_{(i,j+1)}+\Delta Y_{(i,j)})}\Delta X_{(i,j)}+TX1_{(i-1,j)(t+\Delta t)}\frac{HO1_{(i-1,j)(t+\Delta t)}-HO1_{(i,j)(t+\Delta t)}}{0.5(\Delta X_{(i-1,j)}+\Delta X_{(i,j)})}\Delta Y_{(i,j)}+$$

$$Qnet_{(i,j)}+LCB_{(i,j)}(WL_{(i,j)}-HO1_{(i,j)(t+\Delta t)})\Delta X_{(i,j)}\Delta Y_{(i,j)}-$$

$$LCM_{(i,j)}(HO1_{(i,j)(t+\Delta t)}-HO3_{(i,j)(t+\Delta t)})\Delta X_{(i,j)}\Delta Y_{(i,j)}=$$

$$\frac{HO1_{(i,j)(t+\Delta t)}-HO1_{(i,j)(t)}}{\Delta t}effe_{(i,j)}\Delta X_{(i,j)}\Delta Y_{(i,j)} \quad \text{.....(4-21)}$$

In equation (4-21) it is assumed that $HO1_{(i,j)}$ is greater than $Beb_{(i,j)}$.

$$TY1_{(i,j-1)(t+\Delta t)}\frac{HO1_{(i,j-1)(t+\Delta t)}-HO1_{(i,j)(t+\Delta t)}}{0.5(\Delta Y_{(i,j-1)}+\Delta Y_{(i,j)})}\Delta X_{(i,j)}+TX1_{(i,j)(t+\Delta t)}\frac{HO1_{(i+1,j)(t+\Delta t)}-HO1_{(i,j)(t+\Delta t)}}{0.5(\Delta X_{(i+1,j)}+\Delta X_{(i,j)})}\Delta Y_{(i,j)}+$$

$$TY1_{(i,j)(t+\Delta t)}\frac{HO1_{(i,j+1)(t+\Delta t)}-HO1_{(i,j)(t+\Delta t)}}{0.5(\Delta Y_{(i,j+1)}+\Delta Y_{(i,j)})}\Delta X_{(i,j)}+TX1_{(i-1,j)(t+\Delta t)}\frac{HO1_{(i-1,j)(t+\Delta t)}-HO1_{(i,j)(t+\Delta t)}}{0.5(\Delta X_{(i-1,j)}+\Delta X_{(i,j)})}\Delta Y_{(i,j)}+$$

$$Qnet_{(i,j)}+LCB_{(i,j)}(WL_{(i,j)}-Teb_{(i,j)})\Delta X_{(i,j)}\Delta Y_{(i,j)}-$$

$$LCM_{(i,j)}(HO1_{(i,j)(t+\Delta t)}-HO3_{(i,j)(t+\Delta t)})\Delta X_{(i,j)}\Delta Y_{(i,j)}=$$

$$\frac{HO1_{(i,j)(t+\Delta t)}-HO1_{(i,j)(t)}}{\Delta t}effe_{(i,j)}\Delta X_{(i,j)}\Delta Y_{(i,j)} \quad \text{.....(4-22)}$$

In equation (4-22) it is assumed that $HO1_{(i,j)}$ is less than or equal to $Beb_{(i,j)}$. By dividing both sides of each of equations (4-21) and (4-22) by $\Delta X_{(i,j)} * \Delta Y_{(i,j)}$ and rearranging :

$$\frac{TY1_{(i,j-1)(t+\Delta t)}}{0.5(\Delta Y_{(i,j-1)}+\Delta Y_{(i,j)})\Delta Y_{(i,j)}} * HO1_{(i,j-1)(t+\Delta t)} + \frac{TX1_{(i,j)(t+\Delta t)}}{0.5(\Delta X_{(i+1,j)}+\Delta X_{(i,j)})\Delta X_{(i,j)}} * HO1_{(i+1,j)(t+\Delta t)} +$$

$$\frac{TY1_{(i,j)(t+\Delta t)}}{0.5(\Delta Y_{(i,j+1)}+\Delta Y_{(i,j)})\Delta Y_{(i,j)}} * HO1_{(i,j+1)(t+\Delta t)} + \frac{TX1_{(i-1,j)(t+\Delta t)}}{0.5(\Delta X_{(i-1,j)}+\Delta X_{(i,j)})\Delta X_{(i,j)}} * HO1_{(i-1,j)(t+\Delta t)} +$$

$$HO1_{(i,j)(t+\Delta t)}[-\frac{TY1_{(i,j-1)(t+\Delta t)}}{0.5(\Delta Y_{(i,j-1)}+\Delta Y_{(i,j)})\Delta Y_{(i,j)}} - \frac{TX1_{(i,j)(t+\Delta t)}}{0.5(\Delta X_{(i+1,j)}+\Delta X_{(i,j)})\Delta X_{(i,j)}}$$

$$-\frac{TY1_{(i,j)(t+\Delta t)}}{0.5(\Delta Y_{(i,j+1)}+\Delta Y_{(i,j)})\Delta Y_{(i,j)}} - \frac{TX1_{(i-1,j)(t+\Delta t)}}{0.5(\Delta X_{(i-1,j)}+\Delta X_{(i,j)})\Delta X_{(i,j)}} - LCB_{(i,j)} - LCM_{(i,j)} - \frac{effe_{(i,j)}}{\Delta t}] =$$

$$-\frac{HO1_{(i,j)(t)} * effe_{(i,j)}}{\Delta t} - \frac{Qnet}{\Delta X_{(i,j)} * \Delta Y_{(i,j)}} - LCB_{(i,j)} * WL_{(i,j)} - LCM_{(i,j)} * HO3_{(i,j)(t+\Delta t)} \quad \ldots\ldots\ldots (4\text{-}23)$$

equation (4-23) is another form of equation (4-21) after rearranging terms, provided that $HO1_{(i,j)}$ is greater than $Beb_{(i,j)}$.

$$\frac{TY1_{(i,j-1)(t+\Delta t)}}{0.5(\Delta Y_{(i,j-1)}+\Delta Y_{(i,j)})\Delta Y_{(i,j)}} * HO1_{(i,j-1)(t+\Delta t)} + \frac{TX1_{(i,j)(t+\Delta t)}}{0.5(\Delta X_{(i+1,j)}+\Delta X_{(i,j)})\Delta X_{(i,j)}} * HO1_{(i+1,j)(t+\Delta t)} +$$

$$\frac{TY1_{(i,j)(t+\Delta t)}}{0.5(\Delta Y_{(i,j+1)}+\Delta Y_{(i,j)})\Delta Y_{(i,j)}} * HO1_{(i,j+1)(t+\Delta t)} + \frac{TX1_{(i-1,j)(t+\Delta t)}}{0.5(\Delta X_{(i-1,j)}+\Delta X_{(i,j)})\Delta X_{(i,j)}} * HO1_{(i-1,j)(t+\Delta t)} +$$

$$HO1_{(i,j)(t+\Delta t)}[-\frac{TY1_{(i,j-1)(t+\Delta t)}}{0.5(\Delta Y_{(i,j-1)}+\Delta Y_{(i,j)})\Delta Y_{(i,j)}}-\frac{TX1_{(i,j)(t+\Delta t)}}{0.5(\Delta X_{(i+1,j)}+\Delta X_{(i,j)})\Delta X_{(i,j)}}$$

$$-\frac{TY1_{(i,j)(t+\Delta t)}}{0.5(\Delta Y_{(i,j+1)}+\Delta Y_{(i,j)})\Delta Y_{(i,j)}}-\frac{TX1_{(i-1,j)(t+\Delta t)}}{0.5(\Delta X_{(i-1,j)}+\Delta X_{(i,j)})\Delta X_{(i,j)}}-LCM_{(i,j)}-\frac{effe_{(i,j)}}{\Delta t}]=$$

$$-\frac{HO1_{(i,j)(t)}*effe_{(i,j)}}{\Delta t}-\frac{Qnet}{\Delta X_{(i,j)}*\Delta Y_{(i,j)}}-LCB_{(i,j)}(WL_{(i,j)}-Teb_{(i,j)})-LCM_{(i,j)}*HO3_{(i,j)(t+\Delta t)}.(4\text{-}24)$$

Equation (4-24) is another form of equation (4-22) after rearranging, provided that $HO1_{(i,j)}$ is less than or equal to $Beb_{(i,j)}$. These equations are the finite difference equations for the upper layer and they need know to be solved, however, these two equations are solved iteratively in the present research. One popular method of solving the nodal equations iteratively is the IADI- Method (Iterative Alternating Direction Implicit procedure) (Kinzelbach, 1986) starting from an initial guess value for the W.T. elevation in Equations (4-23) and (4-24) after assuming that there is (R) rows and (C) columns(i.e. R*C finite difference equation) , in the first iteration the system of layers equations is solved column by column starting from left to the right for both layers and then by using the latest calculation results for head values, the system is solved raw by raw starting from down to top for both layers. In the second iteration the system of layers equations is solved column by column using the latest head values starting from right to the left for both layers and then raw by raw starting from top to down for both layers, and the solution continues in such away until it reaches to the good convergence. Therefore, the equations of finite difference for the upper and lower layers must be rearranged in a column system and a raw system. For the upper layer, the column system will be explained as example while the raw system will be explained as example for the lower layer, however, the system of column equations for the phreatic layer can be arranged as:

$$\frac{TY1_{(i,j-1)(t+\Delta t)}}{0.5(\Delta Y_{(i.j-1)}+\Delta Y_{(i,j)})\Delta Y_{(i,j)}} * HO1_{(i,j-1)(t+\Delta t)} + [-\frac{TY1_{(i,j-1)(t+\Delta t)}}{0.5(\Delta Y_{(i.j-1)}+\Delta Y_{(i,j)})\Delta Y_{(i,j)}} -$$

$$-\frac{TX1_{(i,j)(t+\Delta t)}}{0.5(\Delta X_{(i+1,j)}+\Delta X_{(i,j)})\Delta X_{(i,j)}} - \frac{TY1_{(i,j)(t+\Delta t)}}{0.5(\Delta Y_{(i.j+1)}+\Delta Y_{(i,j)})\Delta Y_{(i,j)}} - \frac{TX1_{(i-1,j)(t+\Delta t)}}{0.5(\Delta X_{(i-1,j)}+\Delta X_{(i,j)})\Delta X_{(i,j)}} -$$

$$LCB_{(i,j)} - LCM_{(i,j)} - \frac{effe_{(i,j)}}{\Delta t}] * HO1_{(i,j)(t+\Delta t)} + \frac{TY1_{(i,j)(t+\Delta t)}}{0.5(\Delta Y_{(i.j+1)}+\Delta Y_{(i,j)})\Delta Y_{(i,j)}} * HO1_{(i,j+1)(t+\Delta t)} =$$

$$-\frac{Qnet}{\Delta X_{(i,j)}\Delta Y_{(i,j)}} - \frac{HO1_{(i,j)(t)} * effe_{(i,j)}}{\Delta t} - LCB_{(i,j)} * WL_{(i,j)} - LCM_{(i,j)} * HO3_{(i,j)(t+\Delta t)} -$$

$$\frac{TX1_{(i,j)(t+\Delta t)}}{0.5(\Delta X_{(i+1,j)}+\Delta X_{)i,j)})\Delta X_{(i,j)}} * HO1_{(i+1,j)(t+\Delta t)} - \frac{TX1_{(i-1,j)(t+\Delta t)}}{0.5(\Delta X_{(i-1,j)}+\Delta X_{)i,j)})\Delta X_{(i,j)}} * HO1_{(i-1,j)(t+\Delta t)} \text{..(4-25)}$$

equation (4-25) can be rewritten as:

$$A_{(j)} * HO1_{(i,j-1)(t+\Delta t)} + b_{(j)} * HO1_{(i,j)(t+\Delta t)} + Cc_{(j)} * HO1_{(i,j+1)(t+\Delta t)} = d_{(j)} \text{ .....(4-26)}$$

in which:

$$A_{(j)} = \frac{TY1_{(i,j-1)(t+\Delta t)}}{0.5(\Delta Y_{(i.j-1)}+\Delta Y_{(i,j)})\Delta Y_{(i,j)}}$$

$$b_{(j)} = [-\frac{TY1_{(i,j-1)(t+\Delta t)}}{0.5(\Delta Y_{(i.j-1)}+\Delta Y_{(i,j)})\Delta Y_{(i,j)}} -$$

$$-\frac{TX1_{(i,j)(t+\Delta t)}}{0.5(\Delta X_{(i+1,j)}+\Delta X_{(i,j)})\Delta X_{(i,j)}} - \frac{TY1_{(i,j)(t+\Delta t)}}{0.5(\Delta Y_{(i.j+1)}+\Delta Y_{(i,j)})\Delta Y_{(i,j)}} - \frac{TX1_{(i-1,j)(t+\Delta t)}}{0.5(\Delta X_{(i-1,j)}+\Delta X_{(i,j)})\Delta X_{(i,j)}} -$$

$$LCB_{(i,j)} - LCM_{(i,j)} - \frac{effe_{(i,j)}}{\Delta t}]$$

$$Cc_{(j)} = \frac{TY1_{(i,j)(t+\Delta t)}}{0.5(\Delta Y_{(i.j+1)}+\Delta Y_{(i,j)})\Delta Y_{(i,j)}}$$

and $d_{(j)}$ is the right side of equation (4-25)

Equation (4-26) is applied for R rows, substitute j from 1 to R to get :

$$b_{(1)} * HO1_{(i,1)(t+\Delta t)} + Cc_{(1)} * HO1_{(i,2)(t+\Delta t)} = d_{(1)}$$

$$A_{(2)} * HO1_{(i,1)(t+\Delta t)} + b_{(2)} * HO1_{(i,2)(t+\Delta t)} + Cc_{(2)} * HO1_{(i,3)(t+\Delta t)} = d_{(2)}$$

$$A_{(3)} * HO1_{(i,2)(t+\Delta t)} + b_{(3)} * HO1_{(i,3)(t+\Delta t)} + Cc_{(3)} * HO1_{(i,4)(t+\Delta t)} = d_{(3)}$$

$$A_{(R)} * HO1_{(i,R-1)(t+\Delta t)} + b_{(R)} * HO1_{(R,j)(t+\Delta t)} = d_{(R)}$$

Gauss elimination method (Gerald,1984 and Wang, 1982) is used here in to solve these equations:

$$HO1_{(i,1)(t+\Delta t)} + \frac{Cc_{(1)}}{b_{(1)}} HO1_{(i,2)(t+\Delta t)} = \frac{d_{(1)}}{b_{(1)}}$$

$$(b_{(2)} - A_{(2)} \frac{Cc_{(1)}}{b_{(1)}}) HO1_{(i,2)(t+\Delta t)} + Cc_{(2)} HO1_{(i,3)(t+\Delta t)} = d_{(2)} - A_{(2)} \frac{d_{(1)}}{b_{(1)}}$$

$$A_{(3)} HO1_{(i,2)(t+\Delta t)} + b_{(3)} HO1_{(i,3)(t+\Delta t)} + Cc_{(3)} HO1_{(i,4)(t+\Delta t)} = d_{(3)}$$

$$A_{(R)} * HO1_{(i,R-1)(t+\Delta t)} + b_{(R)} * HO1_{(R,j)(t+\Delta t)} = d_{(R)}$$

$$HO1_{(i,1)(t+\Delta t)} + \frac{Cc_{(1)}}{b_{(1)}} HO1_{(i,2)(t+\Delta t)} = \frac{d_{(1)}}{b_{(1)}}$$

$$HO1_{(i,2)(t+\Delta t)} + \frac{Cc_{(2)}}{(b_{(2)} - A_{(2)}\dfrac{Cc_{(1)}}{b_{(1)}})} HO1_{(i,3)(t+\Delta t)} = \frac{d_{(2)} - A_{(2)}\dfrac{d_{(1)}}{b_{(1)}}}{(b_{(2)} - A_{(2)}\dfrac{Cc_{(1)}}{b_{(1)}})}$$

$$b_{(3)} - A_{(3)}\frac{Cc_{(2)}}{b_{(2)} - A_{(2)}\dfrac{Cc_{(1)}}{b_{(1)}}} HO1_{(i,3)(t+\Delta t)} + Cc_{(3)} HO1_{(i,4)(t+\Delta t)} = d_{(3)} - A_{(3)}\frac{d_{(2)} - A_{(2)}\dfrac{d_{(1)}}{b_{(1)}}}{b_{(2)} - A_{(2)}\dfrac{Cc_{(1)}}{b_{(1)}}}$$

$$A_{(R)} * HO1_{(i,R-1)(t+\Delta t)} + b_{(R)} * HO1_{(R,j)(t+\Delta t)} = d_{(R)}$$

Hence it is found that :

$$\begin{bmatrix} 1 & F_{(1)} & 0 & 0 & & \cdots & C \\ 0 & 1 & F_{(2)} & 0 & 0 & \cdots & C \\ 0 & 0 & 1 & F_{(3)} & 0 & 0 \cdots & C \\ 0 & 0 & 0 & 1 & F_{(4)} & 0 \cdots & C \\ \vdots & & & & & & \vdots \\ & & & & & & F_{(R-1)} \\ R & 0 & 0 & 0 & 0 & 0 \; 0 \; 0 \; 0 & 1 \end{bmatrix} \begin{bmatrix} HO1_{(i,1)} \\ HO1_{(i,2)} \\ HO1_{(i,3)} \\ HO1_{(i,4)} \\ \vdots \\ HO1_{(i,R)} \end{bmatrix} = \begin{bmatrix} G_{(1)} \\ G_{(2)} \\ G_{(3)} \\ G_{(4)} \\ \vdots \\ G_{(R)} \end{bmatrix}$$

In which :

$$F_{(j)} = \frac{Cc_{(j)}}{b_{(j)} - A_{(j)}F_{ji-1)}} \quad \text{.....(4-27)}$$

$$G_{(j)} = \frac{d_{(j)} - A_{(j)}G_{(j-1)}}{b_{(j)} - A_{(j)}F_{(j-1)}} \quad \text{.....(4-28)}$$

equations (4-27) and (4-28) are used in the program that will be used in the solving of this system of column equations, this program will be explained in the section 4-2-4

4-2-2-2 Model Derivation for the Leaky (Lower) Layer.

Similar to the equations (4-23) and (4-24) which were derivative to the upper layer in the previous section, one finite difference equation can be formulated to the lower layer. By using the lower portion in Figure (4-3), there are four lateral flows ($QL1_{(i,j)}$, $QL2_{(i,j)}$, $QL3_{(i,j)}$, and $QL4_{(i,j)}$) in the horizontal plan between the $cell_{(i,j)}$ and the four neighboring cells, and there are two vertical flows, the first, ($Qleak_{(i,j)}$) between the lower and the upper layer, and the second ($Qqw_{(i,j)}$) between the lower layer and the out side of the system, $Qqw_{(i,j)}$ is the discharge of the wells that fully penetrate the lower layer. As in equations (4-4) to (4-7) it can be said:

$$QL1_{(i,j)} = TL1average\frac{HO3_{(i,j-1)} - HO3_{(i,j)}}{0.5(\Delta Y_{(i,j-1)} + \Delta Y_{(i,j)})}\Delta X_{(i,j)} \quad \text{.....(4-29)}$$

$$QL2_{(i,j)} = TL2average\frac{HO3_{(i+1.j)} - HO3_{(i,j)}}{0.5(\Delta X_{(i+1,j)} + \Delta X_{(i,j)})}\Delta Y_{(i,j)} \quad \text{.....(4-30)}$$

$$QL3_{(i,j)} = TL3average\frac{HO3_{(i,j+1)} - HO3_{(i,j)}}{0.5(\Delta Y_{(i,j+1)} + \Delta Y_{(i,j)})}\Delta X_{(i,j)} \quad \text{.....(4-31)}$$

$$QL4_{(i,j)} = TL4average\frac{HO3_{(i-1.j)} - HO3_{(i,j)}}{0.5(\Delta X_{(i-1,j)} + \Delta X_{(i,j)})}\Delta Y_{(i,j)} \quad \text{.....(4-32)}$$

TL1average, TL2average, TL3average, and TL4 average are the average values of lower layer local transmissivities between the node (i,j) and its four direct neighboring nodes (i,j-1), (i+1,j), (i,j+1), and (i-1,j) respectively. $HO3_{(i,j)}$ is the observed head at the lower layer at the nodal cell (i,j)

4-2-2-2-1 **Average Transmissivities (inter nodal transmissivities) for the Lower Layer**

As in the phreatic layer, harmonic average is used herein, to find the average transmissivities in the leaky aquifer as follows:

$$TL1average = \frac{2*(T3_{(i,j-1)} * T3_{(i,j)})}{T3_{(i,j-1)} + T3_{(i,j)}} \quad \text{.....(4-33)}$$

$$TL2average = \frac{2*(T3_{(i+1,j)} * T3_{(i,j)})}{T3_{(i+1,j)} + T3_{(i,j)}} \quad \text{.....(4-34)}$$

$$TL3average = \frac{2*(T3_{(i,j+1)} * T3_{(i,j)})}{T3_{(i,j+1)} + T3_{(i,j)}} \quad \text{.....(4-35)}$$

$$TL4average = \frac{2*(T3_{(i-1,j)} * T3_{(i,j)})}{T3_{(i-1,j)} + T3_{(i,j)}} \quad \text{.....(4-36)}$$

Where:

$T3_{(i,j)}$ is a local transmissivity for the nodal (i,j) in the lower layer, while $T_{(i-1,j)}$, $T_{(i,j+1)}$, $T_{(i+1,j)}$, and $T_{(i,j-1)}$ are local transmissivities in the nodes (i-1,j), (i,j+1), (i+1,j), and (i,j-1) respectively in the lower layer.

Transmissivity in a leaky aquifer is independent of its hydraulic head but its depends on the aquifer thickness when the aquifer is fully saturated, therefore, there is no need to compute the average permeability as in equations (4-14) to (4-15-a) in the phreatic layer. The inter nodal transmissivities that will be used in the leaky aquifer are that explained in equations (4-33) to (4-36) with the following directional simplified :

TL1average $\longrightarrow$ $TY3_{(i,j-1)}$

TL2average $\longrightarrow$ $TX3_{(i,j)}$

TL3average $\longrightarrow$ $TY3_{(i,j)}$

TL4average $\longrightarrow$ $TX3_{(i-1,j)}$

4-2-2-2-2 Nodal Ground Water Balance

Water storage change in the lower portion shown in Figure (4-2) over the time interval ($t+\Delta t$) should equal the summation of inflows and outflows, that's the definition of water balance that was previously defined, however, the four lateral flows ($QL1_{(i,j)}$, $QL2_{(i,j)}$, $QL3_{(i,j)}$, and $QL4_{(i,j)}$) and the vertical flow $Qleak_{(i,j)}$ are

assumed as inflows while $Qqw_{(i,j)}$ is assumed as outflows and that can be translated as equations as follows:

$$\Delta t(QL1_{(i,j)(t+\Delta t)} + QL2_{(i,j)(t+\Delta t)} + QL3_{(i,j)(t+\Delta t)} + QL4_{(i,j)(t+\Delta t)} + Qleak_{(i,j)(t+\Delta t)} - Qqw_{(i,j)}) = (HO3_{(i,j)(t+\Delta t)} - HO3_{(i,j)(t)}) * S_{(i,j)} * \Delta X_{(i,j)} * \Delta Y_{(i,j)} \quad \text{.....(4-37)}$$

Where:

$S_{(i,j)}$: Storage coefficient of the leaky aquifer at anodal cell (i,j), dimensionless

The signs of the flows $QL1_{(i,j)}$, $QL2_{(i,j)}$, $QL3_{(i,j)}$,$QL4_{(i,j)}$,and $Qleak_{(i,j)}$ in equation (4-37) are automatically corrected through the model application depending on the hydraulic heads in and around the cell under consideration. $Qqw_{(i,j)}$ is time independent and its one of the input data to the model, its assumed and resigned for a chosen cell, that cell represent a cell where the well (wells) are assumed, however, the rate of pumping or recharging $Qqw_{(i,j)}$ may be varied with the time or may be not, depending on the input data.

By substituting equations (4-29) to (4-32), equations (4-33) to (4-36), into equation (4-37),and divided the both sides on Δt and then on $\Delta X_{(i,j)} * \Delta Y_{(i,j)}$ one equation can be obtained :

$$TY3_{(i,j-1)(t+\Delta t)} \frac{HO3_{(i,j-1)(t+\Delta t)} - HO3_{(i,j)(t+\Delta t)}}{0.5(\Delta Y_{(i,j-1)} + \Delta Y_{(i,j)})\Delta Y_{(i,j)}} + TX3_{(i,j)(t+\Delta t)} \frac{HO3_{(i+1,j)(t+\Delta t)} - HO3_{(i,j)(t+\Delta t)}}{0.5(\Delta X_{(i+1,j)} + \Delta X_{(i,j)})\Delta X_{(i,j)}} +$$

$$TY3_{(i,j)(t+\Delta t)} \frac{HO3_{(i,j+1)(t+\Delta t)} - HO3_{(i,j)(t+\Delta t)}}{0.5(\Delta Y_{(i,j+1)} + \Delta Y_{(i,j)})\Delta Y_{(i,j)}} + TX3_{(i-1,j)(t+\Delta t)} \frac{HO3_{(i-1,j)(t+\Delta t)} - HO3_{(i,j)(t+\Delta t)}}{0.5(\Delta X_{(i-1,j)} + \Delta X_{(i,j)})\Delta X_{(i,j)}} +$$

$$LCM_{(i,j)}(HO1_{(i,j)(t+\Delta t)} - HO3_{(i,j)(t+\Delta t)}) - \frac{Qqw_{(i,j)}}{\Delta X_{(i,j)} * \Delta Y_{(i,j)}} =$$

$$\frac{HO3_{(i,j)(t+\Delta t)} - HO3_{(i,j)(t)}}{\Delta t} S_{(i,j)} \quad \text{.....(4-38)}$$

Rearranging equation (4-38) to get:

$$\frac{TY3_{(i,j-1)(t+\Delta t)}}{0.5(\Delta Y_{(i,j-1)}+\Delta Y_{(i,j)})\Delta Y_{(i,j)}} * HO3_{(i,j-1)(t+\Delta t)} + \frac{TX3_{(i,j)(t+\Delta t)}}{0.5(\Delta X_{(i+1,j)}+\Delta X_{(i,j)})\Delta X_{(i,j)}} * HO3_{(i+1,j)(t+\Delta t)} +$$

$$\frac{TY3_{(i,j)(t+\Delta t)}}{0.5(\Delta Y_{(i,j+1)}+\Delta Y_{(i,j)})\Delta Y_{(i,j)}} * HO3_{(i,j+1)(t+\Delta t)} + \frac{TX3_{(i-1,j)(t+\Delta t)}}{0.5(\Delta X_{(i-1,j)}+\Delta X_{(i,j)})\Delta X_{(i,j)}} * HO3_{(i-1,j)(t+\Delta t)} +$$

$$HO3_{(i,j)(t+\Delta t)}[-\frac{TY3_{(i,j-1)(t+\Delta t)}}{0.5(\Delta Y_{(i,j-1)}+\Delta Y_{(i,j)})\Delta Y_{(i,j)}} - \frac{TX3_{(i,j)(t+\Delta t)}}{0.5(\Delta X_{(i+1,j)}+\Delta X_{(i,j)})\Delta X_{(i,j)}}$$

$$-\frac{TY3_{(i,j)(t+\Delta t)}}{0.5(\Delta Y_{(i,j+1)}+\Delta Y_{(i,j)})\Delta Y_{(i,j)}} - \frac{TX3_{(i-1,j)(t+\Delta t)}}{0.5(\Delta X_{(i-1,j)}+\Delta X_{(i,j)})\Delta X_{(i,j)}} - LCM_{(i,j)} - \frac{S_{(i,j)}}{\Delta t}] =$$

$$-\frac{HO3_{(i,j)(t)} * S_{(i,j)}}{\Delta t} - \frac{Qqw_{(i,j)}}{\Delta X_{(i,j)} * \Delta Y_{(i,j)}} - LCM_{(i,j)} * HO1_{(i,j)(t+\Delta t)} \quad \text{.....(4-39)}$$

the system of raw equations for the lower layer can be arranged as:

$$\frac{TX3_{(i-1,j)(t+\Delta t)}}{0.5(\Delta X_{(i-1.j)}+\Delta X_{(i,j)})\Delta X_{(i,j)}} * HO3_{(i-1,j)(t+\Delta t)} + [-\frac{TY3_{(i,j-1)(t+\Delta t)}}{0.5(\Delta Y_{(i.j-1)}+\Delta Y_{(i,j)})\Delta Y_{(i,j)}} -$$

$$-\frac{TX3_{(i,j)(t+\Delta t)}}{0.5(\Delta X_{(i+1,j)}+\Delta X_{(i,j)})\Delta X_{(i,j)}} - \frac{TY3_{(i,j)(t+\Delta t)}}{0.5(\Delta Y_{(i.j+1)}+\Delta Y_{(i,j)})\Delta Y_{(i,j)}} - \frac{TX3_{(i-1,j)(t+\Delta t)}}{0.5(\Delta X_{(i-1,j)}+\Delta X_{(i,j)})\Delta X_{(i,j)}} -$$

$$LCM_{(i,j)} - \frac{S_{(i,j)}}{\Delta t}] * HO3_{(i,j)(t+\Delta t)} + \frac{TX3_{(i+1,j)(t+\Delta t)}}{0.5(\Delta X_{(i+1.j)}+\Delta X_{(i,j)})\Delta X_{(i,j)}} * HO1_{(i+1,j)(t+\Delta t)} =$$

$$\frac{Qqw_{(i,j)}}{\Delta X_{(i,j)}\Delta Y_{(i,j)}} - \frac{HO3_{(i,j)(t)} * S_{(i,j)}}{\Delta t} - LCM_{(i,j)} * HO1_{(i,j)(t+\Delta t)} -$$

$$\frac{TY3_{(i,j-1)(t+\Delta t)}}{0.5(\Delta Y_{(i,j-1)}+\Delta Y_{(i,j)})\Delta Y_{(i,j)}} * HO3_{(i,j-1)(t+\Delta t)} - \frac{TY3_{(i,j)(t+\Delta t)}}{0.5(\Delta Y_{(i,j+1)}+\Delta Y_{(i,j)})\Delta Y_{(i,j)}} * HO3_{(i,j+1)(t+\Delta t)} \text{..(4-40)}$$

equation (4-40) can be rewritten as:

$$A_{(i)} * HO3_{(i-1,j)(t+\Delta t)} + b_{(i)} * HO3_{(i,j)(t+\Delta t)} + Cc_{(i)} * HO1_{(i+1,j)(t+\Delta t)} = d_{(i)} \quad \text{.....(4-41)}$$

in which:

$$A_{(i)} = \frac{TX3_{(i-1,j)(t+\Delta t)}}{0.5(\Delta X_{(i-1.j)} + \Delta X_{(i,j)})\Delta X_{(i,j)}}$$

$$b_{(i)} = [-\frac{TY3_{(i,j-1)(t+\Delta t)}}{0.5(\Delta Y_{(i.j-1)} + \Delta Y_{(i,j)})\Delta Y_{(i,j)}} -$$

$$-\frac{TX3_{(i,j)(t+\Delta t)}}{0.5(\Delta X_{(i+1,j)} + \Delta X_{(i,j)})\Delta X_{(i,j)}} - \frac{TY3_{(i,j)(t+\Delta t)}}{0.5(\Delta Y_{(i.j+1)} + \Delta Y_{(i,j)})\Delta Y_{(i,j)}} - \frac{TX3_{(i-1,j)(t+\Delta t)}}{0.5(\Delta X_{(i-1,j)} + \Delta X_{(i,j)})\Delta X_{(i,j)}} -$$

$$LCM_{(i,j)} - \frac{S_{(i,j)}}{\Delta t}]$$

$$Cc_{(i)} = \frac{TX3_{(i+1,j)(t+\Delta t)}}{0.5(\Delta X_{(i+1.j)} + \Delta X_{(i,j)})\Delta X_{(i,j)}}$$

and $d_{(i)}$ is the right side of equation (4-40)

Equation (4-41) is applied for C columns, substitute i from 1 to C to get :

$$b_{(1)} * HO3_{(1,j)(t+\Delta t)} + Cc_{(1)} * HO3_{(2,j)(t+\Delta t)} = d_{(1)}$$

$$A_{(2)} * HO3_{(1,j)(t+\Delta t)} + b_{(2)} * HO3_{(2,j)(t+\Delta t)} + Cc_{(2)} * HO3_{(3,j)(t+\Delta t)} = d_{(2)}$$

$$A_{(3)} * HO3_{(2,j)(t+\Delta t)} + b_{(3)} * HO3_{(3,j)(t+\Delta t)} + Cc_{(3)} * HO3_{(4,j)(t+\Delta t)} = d_{(3)}$$

$$A_{(C)} * HO1_{(C-1,j)(t+\Delta t)} + b_{(C)} * HO1_{(C,j)(t+\Delta t)} = d_{(C)}$$

Gauss elimination method (Gerald,1984 and Wang, 1982) is used here in too, to solve these equations:

$$HO3_{(1,j)(t+\Delta t)} + \frac{Cc_{(1)}}{b_{(1)}} HO3_{(2,j)(t+\Delta t)} = \frac{d_{(1)}}{b_{(1)}}$$

$$(b_{(2)} - A_{(2)} \frac{Cc_{(1)}}{b_{(1)}}) HO3_{(2,j)(t+\Delta t)} + Cc_{(2)} HO3_{(3,j)(t+\Delta t)} = d_{(2)} - A_{(2)} \frac{d_{(1)}}{b_{(1)}}$$

$$A_{(3)} HO3_{(2,j)(t+\Delta t)} + b_{(3)} HO3_{(3,j)(t+\Delta t)} + Cc_{(3)} HO3_{(4,j)(t+\Delta t)} = d_{(3)}$$

$$A_{(C)} * HO3_{(C-1,j)(t+\Delta t)} + b_{(C)} * HO3_{(C,j)(t+\Delta t)} = d_{(C)}$$

$$HO3_{(1,j)(t+\Delta t)} + \frac{Cc_{(1)}}{b_{(1)}} HO3_{(2,j)(t+\Delta t)} = \frac{d_{(1)}}{b_{(1)}}$$

$$HO3_{(2,j)(t+\Delta t)} + \frac{Cc_{(2)}}{(b_{(2)} - A_{(2)} \frac{Cc_{(1)}}{b_{(1)}})} HO3_{(3,j)(t+\Delta t)} = \frac{d_{(2)} - A_{(2)} \frac{d_{(1)}}{b_{(1)}}}{(b_{(2)} - A_{(2)} \frac{Cc_{(1)}}{b_{(1)}})}$$

$$b_{(3)} - A_{(3)} \frac{Cc_{(2)}}{b_{(2)} - A_{(2)} \dfrac{Cc_{(1)}}{b_{(1)}}} HO3_{(3,j)(t+\Delta t)} + Cc_{(3)} HO3_{(4,j)(t+\Delta t)} = d_{(3)} - A_{(3)} \frac{d_{(2)} - A_{(2)} \dfrac{d_{(1)}}{b_{(1)}}}{b_{(2)} - A_{(2)} \dfrac{Cc_{(1)}}{b_{(1)}}}$$

$$A_{(C)} * HO3_{(C-1,j)(t+\Delta t)} + b_{(C)} * HO3_{(C,j)(t+\Delta t)} = d_{(C)}$$

Hence it is found that :

$$\begin{bmatrix} 1 & F_{(1)} & 0 & 0 & \cdots & R \\ 0 & 1 & F_{(2)} & 0 & 0 & \cdots & R \\ 0 & 0 & 1 & F_{(3)} & 0 & 0 & \cdots & R \\ 0 & 0 & 0 & 1 & F_{(4)} & 0 & \cdots & R \\ \vdots & & & & & & & \vdots \\ & & & & & & & F_{(C-1)} \\ R & 0 & 0 & 0 & 0 & 0 & 0 & 0 & 0 & 1 \end{bmatrix} \begin{bmatrix} HO3_{(1,j)} \\ HO3_{(2,j)} \\ HO3_{(3,j)} \\ HO3_{(4,j)} \\ \vdots \\ HO3_{(C,j)} \end{bmatrix} = \begin{bmatrix} G_{(1)} \\ G_{(2)} \\ G_{(3)} \\ G_{(4)} \\ \vdots \\ G_{(C)} \end{bmatrix}$$

In which :

$$F_{(i)} = \frac{Cc_{(i)}}{b_{(i)} - A_{(i)} F_{(i-1)}} \quad \text{.....(4-42)}$$

$$G_{(i)} = \frac{d_{(i)} - A_{(i)} G_{(i-1)}}{b_{(i)} - A_{(i)} F_{(i-1)}} \quad \text{.....(4-43)}$$

Similarly to equations (4-27) and (4-28) equation (4-42) and (4-43) are used in the program .

4-2-3 Boundary Conditions Simulation

There are three possible types of boundary conditions which may apply to any part of the boundary of the modeled domain (Kinzelbach, 1986).

1- Boundary condition of the first Kind, prescribed head boundary. In the modeled domain there should be at least one point that constitutes a first kind boundary. The heads of the nodal cells that lay on this kind of boundary are fixed and do not change during the time interval ($t+\Delta t$). Along prescribed potential boundaries, boundary cells are within the possibilities of the rectangular grid, positioned such that their center lies as closely as possible to the actual boundary of the modeled region. The treatment of the fixed potential node is possibly by assigning to it an extremely large effective porosity when the node in the upper layer or large storage coefficient when the node in the lower layer e.g. 10^{30} and then treating it like an ordinary internal node. A node which can store infinity much water will not change its head value in reaction to inflows or outflows appreciably.
2- Boundary conditions of the second kind, prescribed flux boundary. A special case of this type of boundary is the impervious boundary where the flux is zero. If stream lines form boundaries of the modeled domain they are treated a impervious boundaries. The boundary nodes are placed such that one or more edges of the nodal cell coincide (as closely as possible on a rectangular grid) with the impervious boundary of the modeled region.
3- Boundary conditions of the third kind, semi pervious boundary or mixed boundary conditions. This kind specifies a liner combination of head and flux at the boundary. They are used at semi pervious (leakage) boundaries such as river. The nodes are within the possibilities of the modeled region and positioned like the nodes of the first type of boundaries.

In general all the cells outside the model region are assigned as zero local transmissivities.

4-2-4 Brief description of the Quick Basic Program

This program is developed by this study through using the Quick Basic language. This program is intended to solve the equations of finite difference that were listed in the previous sections by Gauss elimination using the iterative alternating direction

implicit procedure. The program is listed in Appendix A, and the flow chart is shown in Figure (4-6). To explain the program, the following steps are listed:

1- The input data to the program may be classified into two kinds, first the data that is entered to the program directly this data is, the total time period of simulation (TP), number of time steps (NS), number of upper layer wells (NWU) number of lower layer wells (NWL),maximum number of pumping intervals (MNP), number of intervals for each well (NP), initial and final time of each pumping interval for each well (TI) and (TF), discharge for each pumping interval (Qqw),number of cells that contains the wells in X direction (Wx) and in Y direction (Wy), number of iterations (NI) are limited to a specified number to stop the program if there is no convergence between the iterations, maximum allowable nodal error for the upper and lower layers (ER1) and (ER3) respectively, and finally the number of rows and columns (R) and (C) respectively. Second the data that is performed using the Surfer and Excel programs and saved in a data files before running the program each file has three columns and (R*C) rows the first two columns are the XY coordinates while the third is the type of data, however, these data files are,

(HO1) : initial ground water head data file in the upper layer.

(HO3) : initial piezometer head data file in the lower layer.

(S) : storage coefficient data file for the lower layer.

(EFFE) : effective porosity data file for the upper layer.

(Qnet) : recharge data file for the upper layer.

(BL1) : bottom level data file of the upper layer.

(LCM) : leakage coefficient of the middle layer data file.

(perm) : permeability of the upper layer data file.

(trans): transmissivity of the lower layer data file.

(river) data file which contains the data of the Hussainiya river, this data is, the water level, the top elevation of the bed, the bottom elevation of the bed, the thickness of the bed , the leakage coefficient of the bed and area of the river.

2- The area in a horizontal plan of a surface water body $awb_{(i,j)}$ within a nodal cell may be smaller than the area of the nodal itself $\Delta X_{(i,j)}*\Delta Y_{(i,j)}$ this problem is treated in the program by making an adjustment to the leakage coefficient of the bed of surface water body as following:

$$LCB_{(i,j)} = LCB_{(i,j)} * \frac{awb_{(i,j)}}{\Delta X_{(i,j)} * \Delta Y_{(i,j)}} \quad \text{.....(4-44)}$$

in a case, where the $\Delta X_{(i,j)}$ and $\Delta Y_{(i,j)}$ are variable from cell to another, the dimensions of the cell are chosen to make the area of the cell equal as closely as possible to the area of the bed of surface water body.

3- Directional permeability for the upper layer and directional transmissivity for the lower layer are computed as explained in equations (4-14) to (4-15-a) and in equations (4-33) to (4-36).

4- The program proceeds to compute the simulated heads for the upper and lower layers using the input data and applying the iterative alternative direction implicit procedure. Column calculations are applied to the upper layer and then to the lower layer then raw calculations are applied to the upper layer and then to the lower layer to complete one iteration. The program continues in computing the iterations as well as computing the largest different CE1 and CE3 between the iterations for the upper layer and the lower layer respectively. At each iteration the program check CE1 and CE3 with ER1 and ER3, if they are less or equal, the program will be stopped after printing the results in a data files (HS1) and (HS3), if they are not, the program checks the number of iteration with the total number of iterations, if it is greater than the total number, the program will be stopped after printing the statement (No convergence).

5- If the program succeeds in calculating the simulated heads, it will compute the total recharge to the upper layer (sum1) the root mean square error (RMSE1) for the upper layer and (RMSE3) for the lower layer using equation (3-6).Computing the (RMSEk) is necessary to give an indication about how the simulated data are close to the observed data.

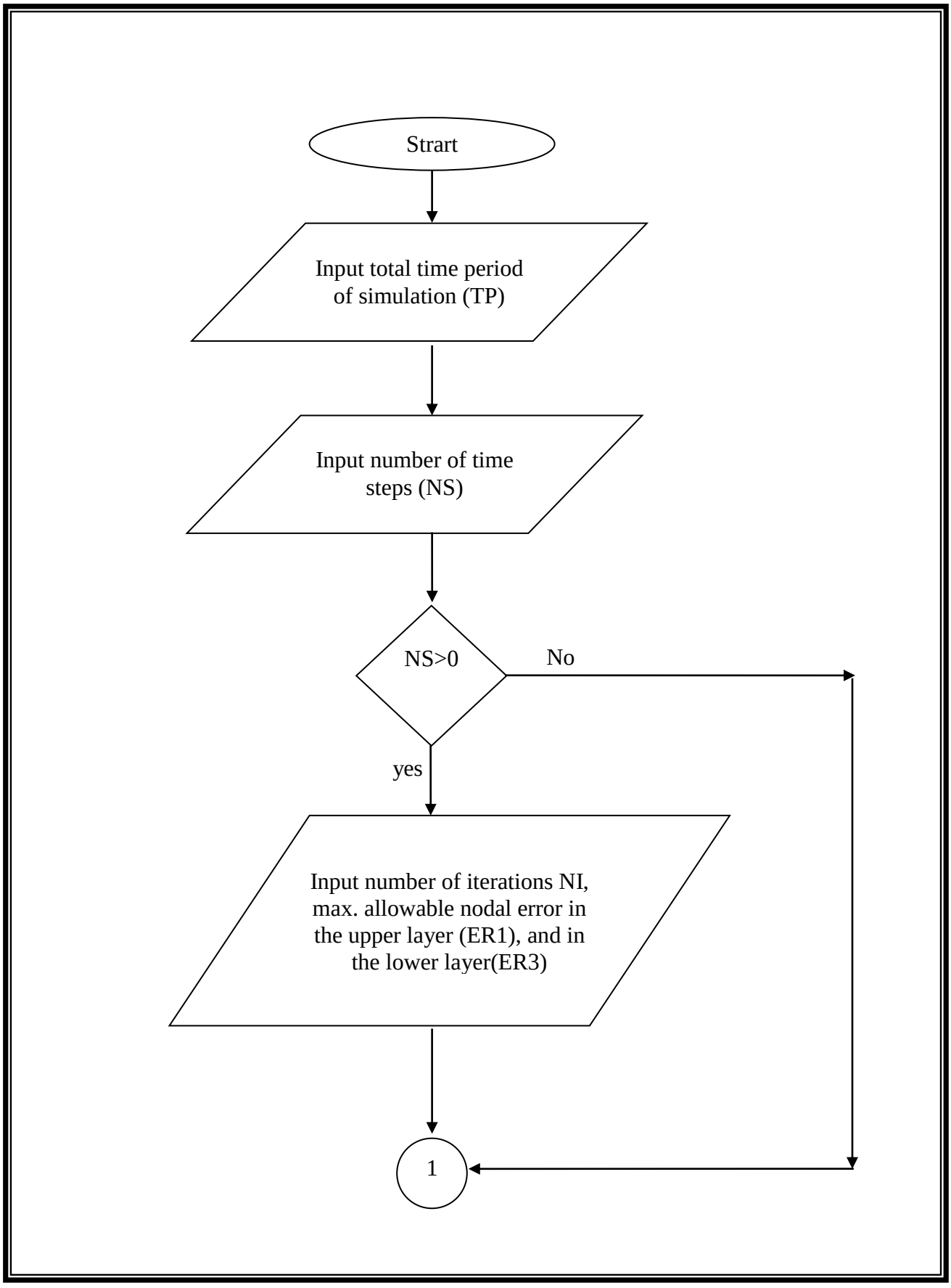

Figure : 4-6 Flow chart of the quick basic program

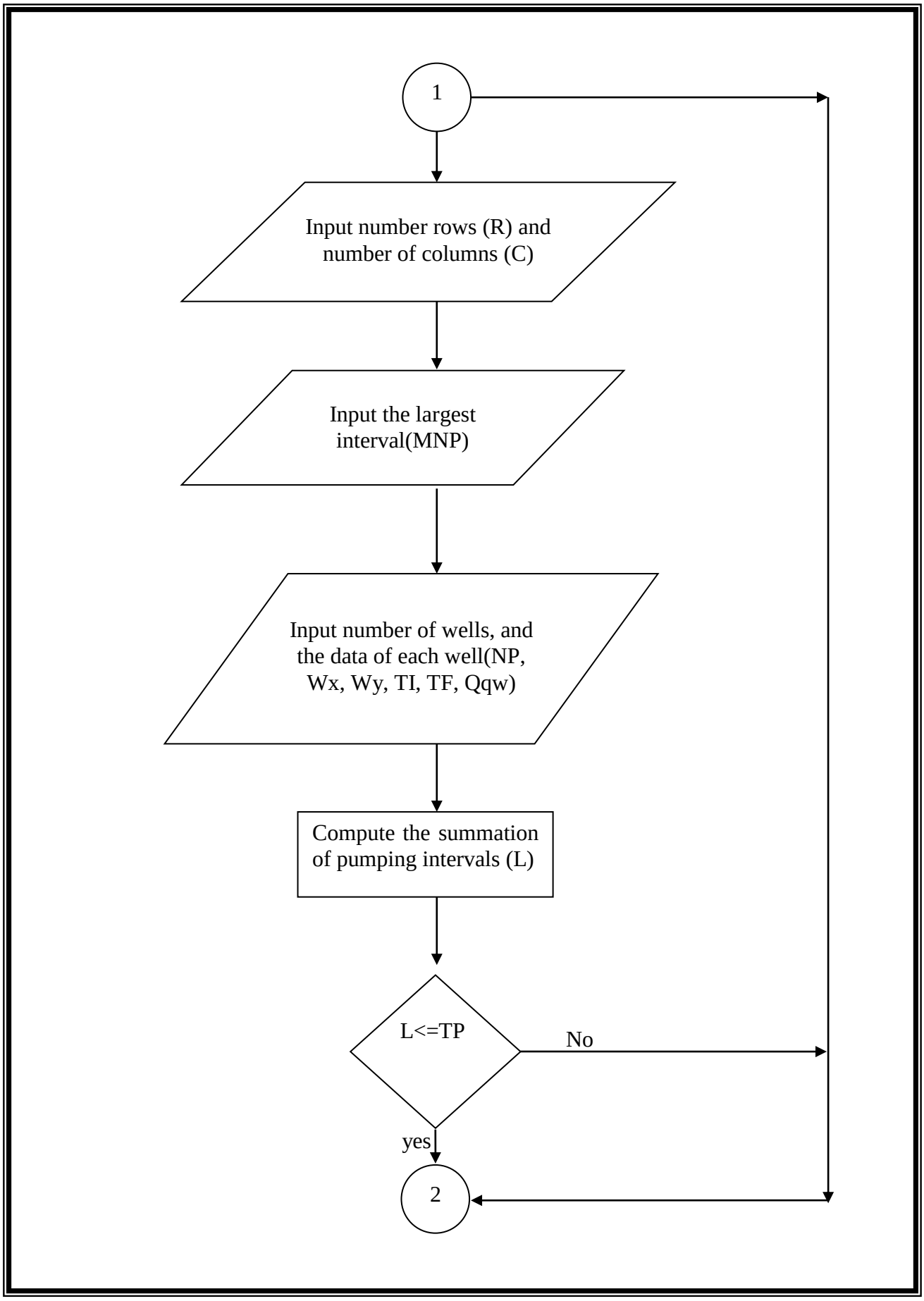

Figure : 4-6 Continue…..

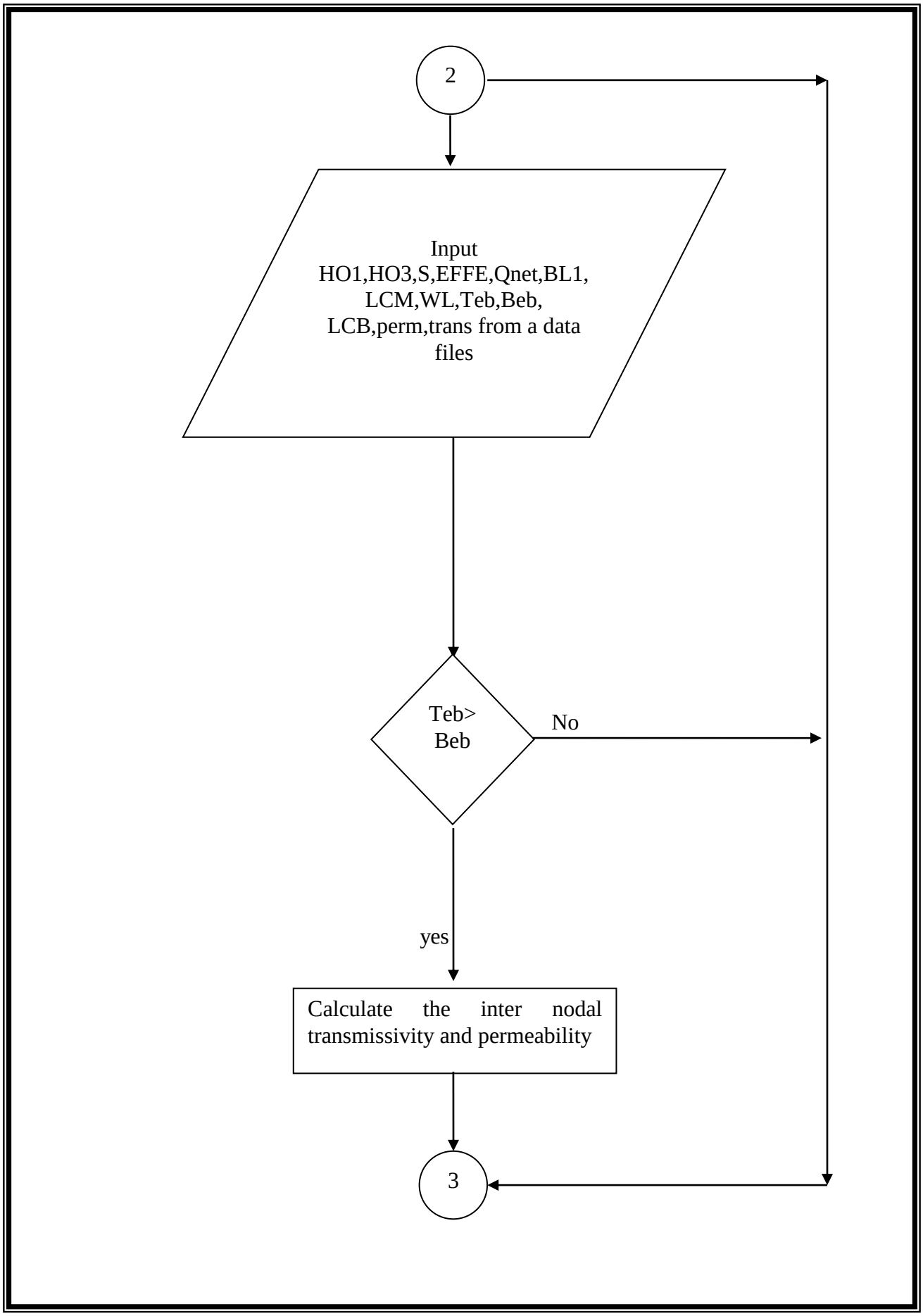

Figure : 4-6 Continue…..

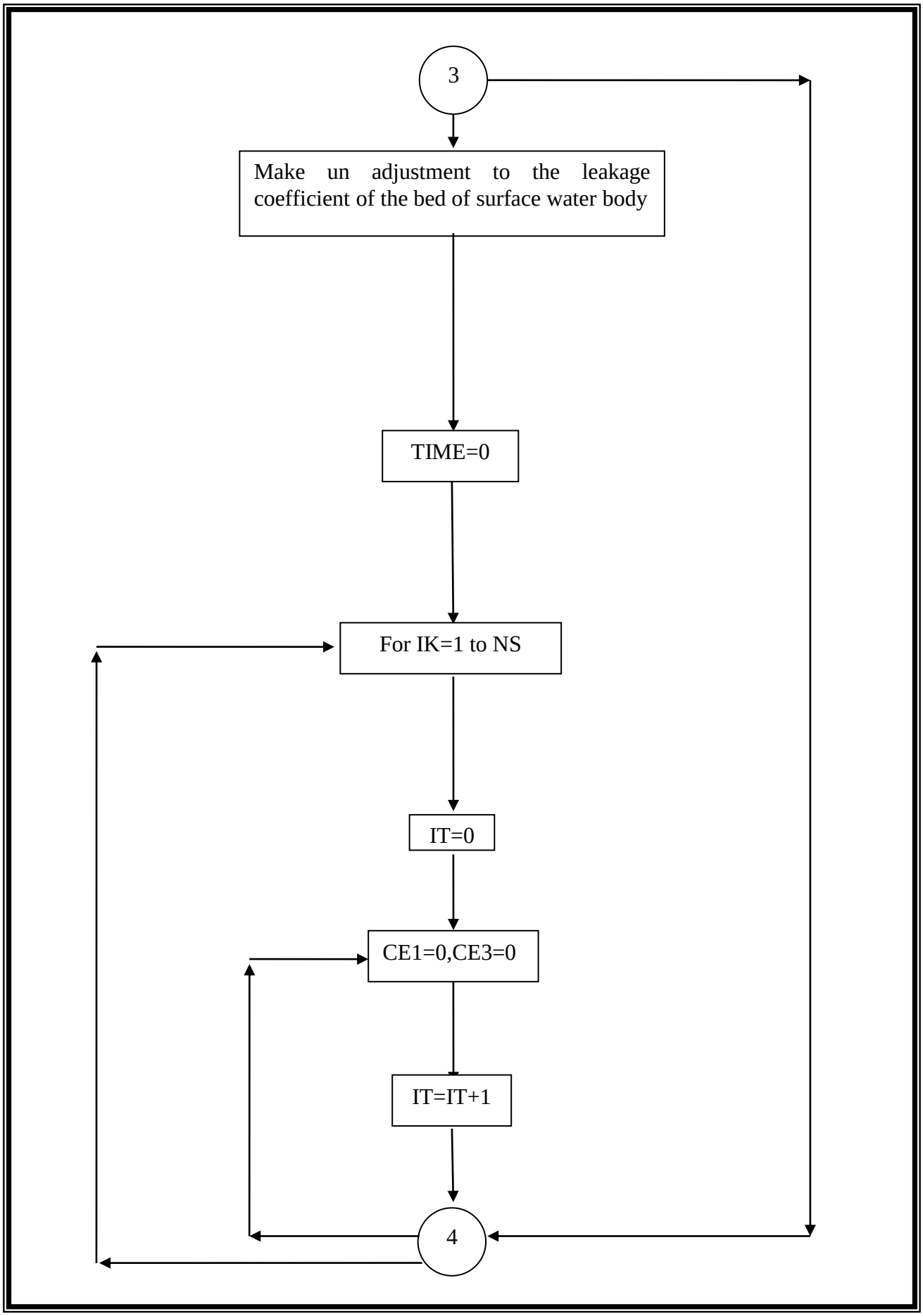

Figure : 4-6 Continue…..

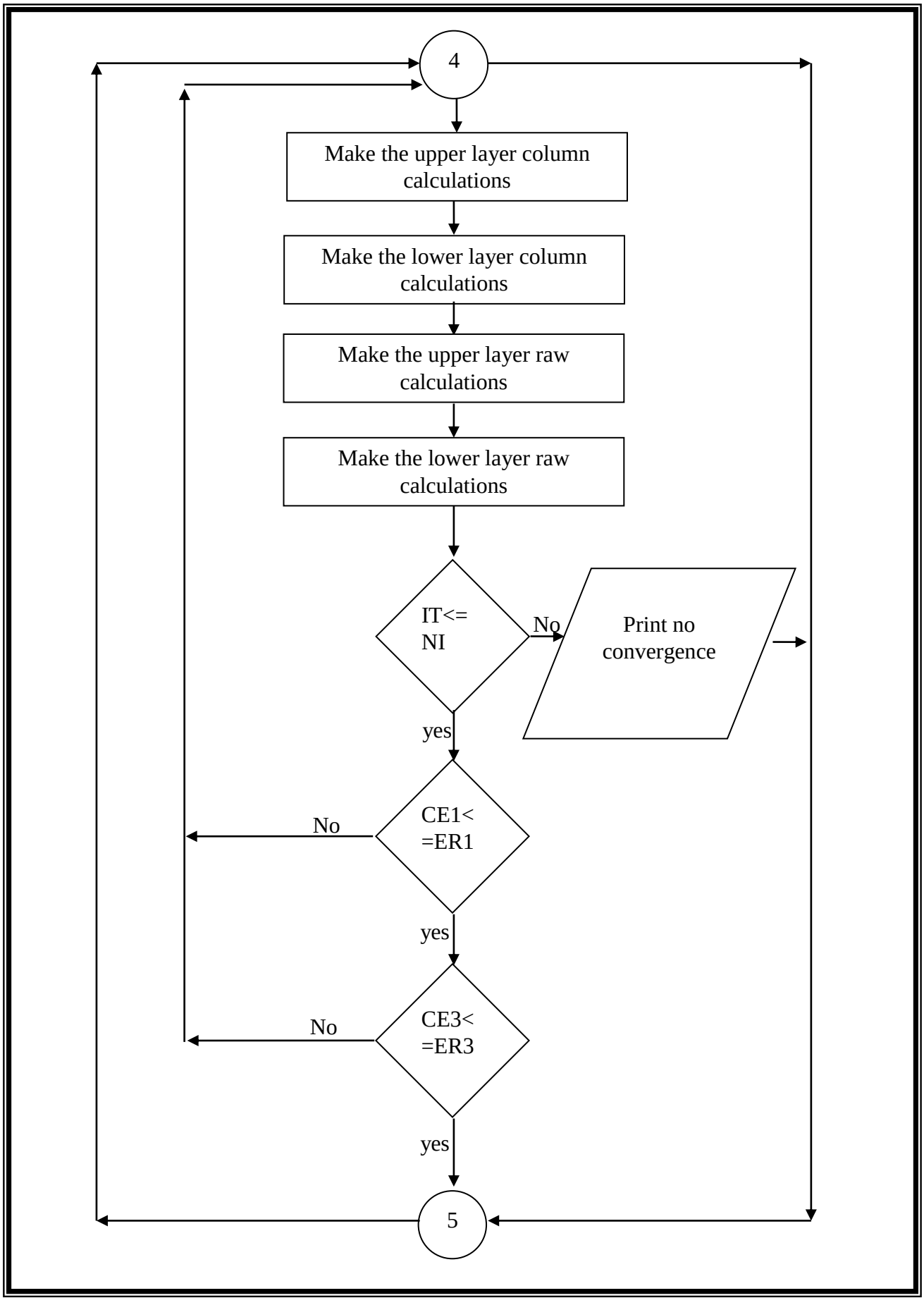

Figure : 4-6 Continue…..

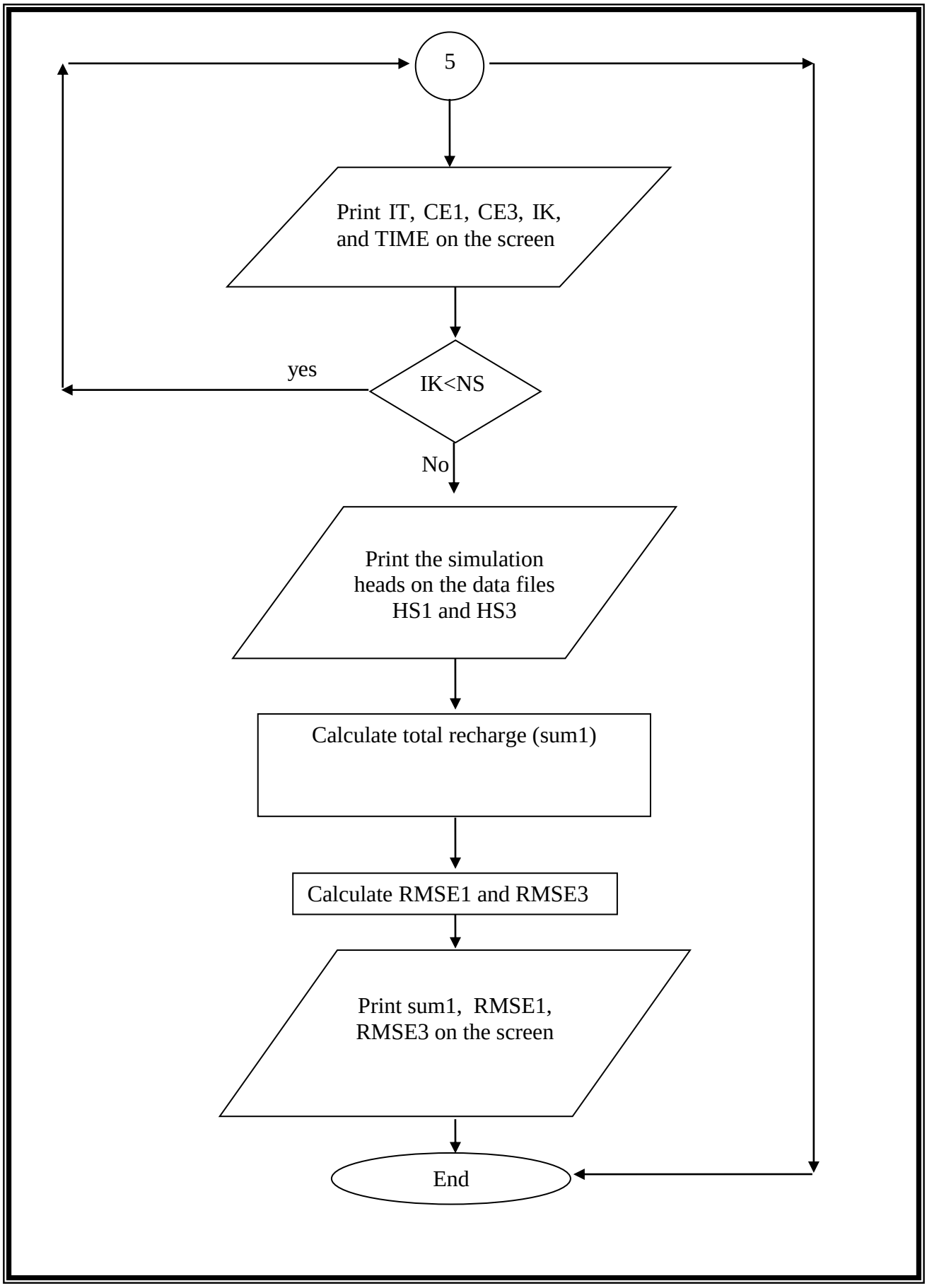

Figure : 4-6 Continue…..

4-2-5 Calibration of the mathematical model

The boundaries of the mathematical model are determined as explained in section (4-2-3), in the upper layer two kinds of the boundaries are considered, First, the first type boundary (constant head boundary) along Karbala covered drain, Eastern covered drain, and the portion of Hindyia canal between Hussainiya river and open Western drain, and Second, the third type boundary (semipervious boundary) that produces leakage from/to surface water body is considered along the Hussainiya river and the open Western drain. In the lower layer the first type boundary is considered around the model region.

Like the GMS model, trail and error method is adopted here to find the calibrated recharge, the same other parameters that are entered to the GMS model are entered to the mathematical model with the exception of transmissivity which increased to 140 m2/day. Steady state simulation can be done by evaluating zero values for both effective porosity of the upper layer and storage coefficient of the lower layer for all cells with the exception of constant head boundary cells**.**

As in the GMS model the best fit between simulated and observed contour lines is evaluated by calculating the Root Mean Square Error (RMSE) for the both layers, equation (4-45). Figures (4-7) and (4-8) show a comparison between the observed and simulated contour lines for both upper and lower layer respectively. RMSE for the upper layer is found as 0.725 cm and for the lower layer as 0.807 cm, The RMSE for both layers is less than 10% of the total observed hydraulic head difference across the modeled area (55cm). So, it can be said that the model successfully simulates steady state.

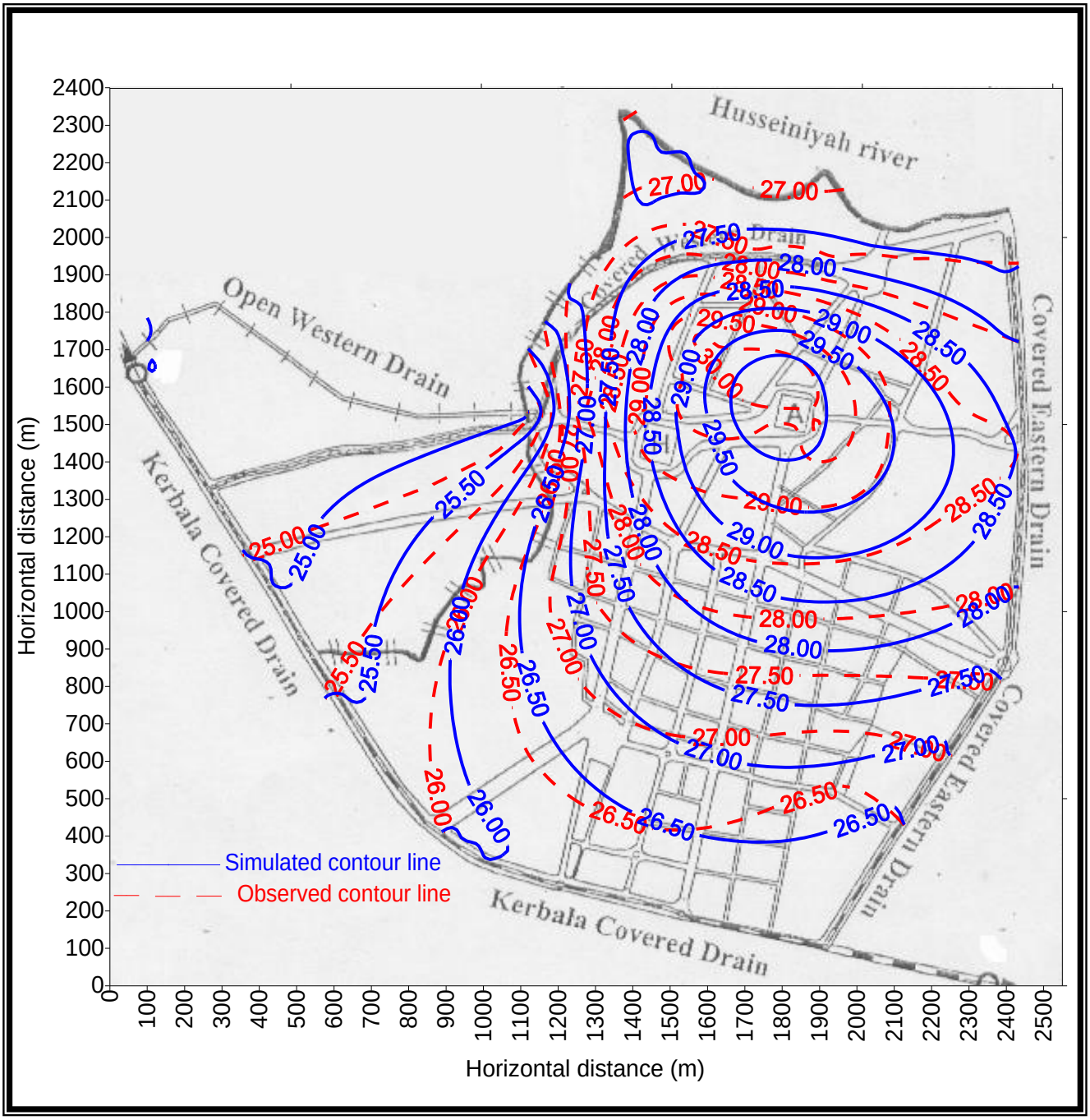

Figure (4-7) Simulated and observed water table level for the upper layer by the mathematical model (march 2000)

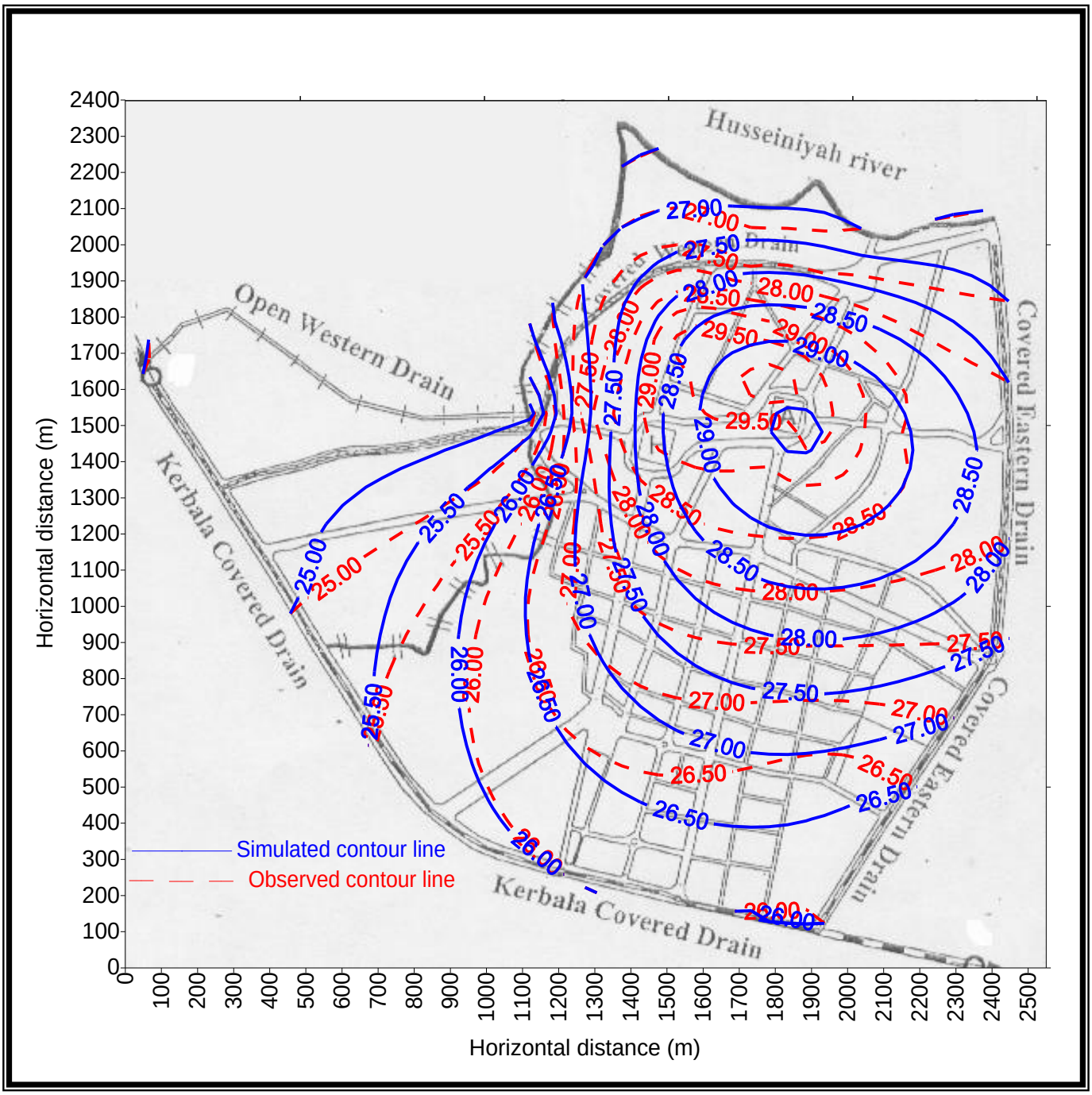

Figure (4-8) Simulated and observed peizometric head for the lower layer by the mathematical model (march2000)

The calibrated local recharges to the upper layer are shown in Figure (4-9), it ranges between (0-13) m3/day per nodal cell , and concentrates in the area of the two holy shrines with a slightly reduction to the ward of the boundary of the study area. Total recharge is found as 3256.758 m3/day.

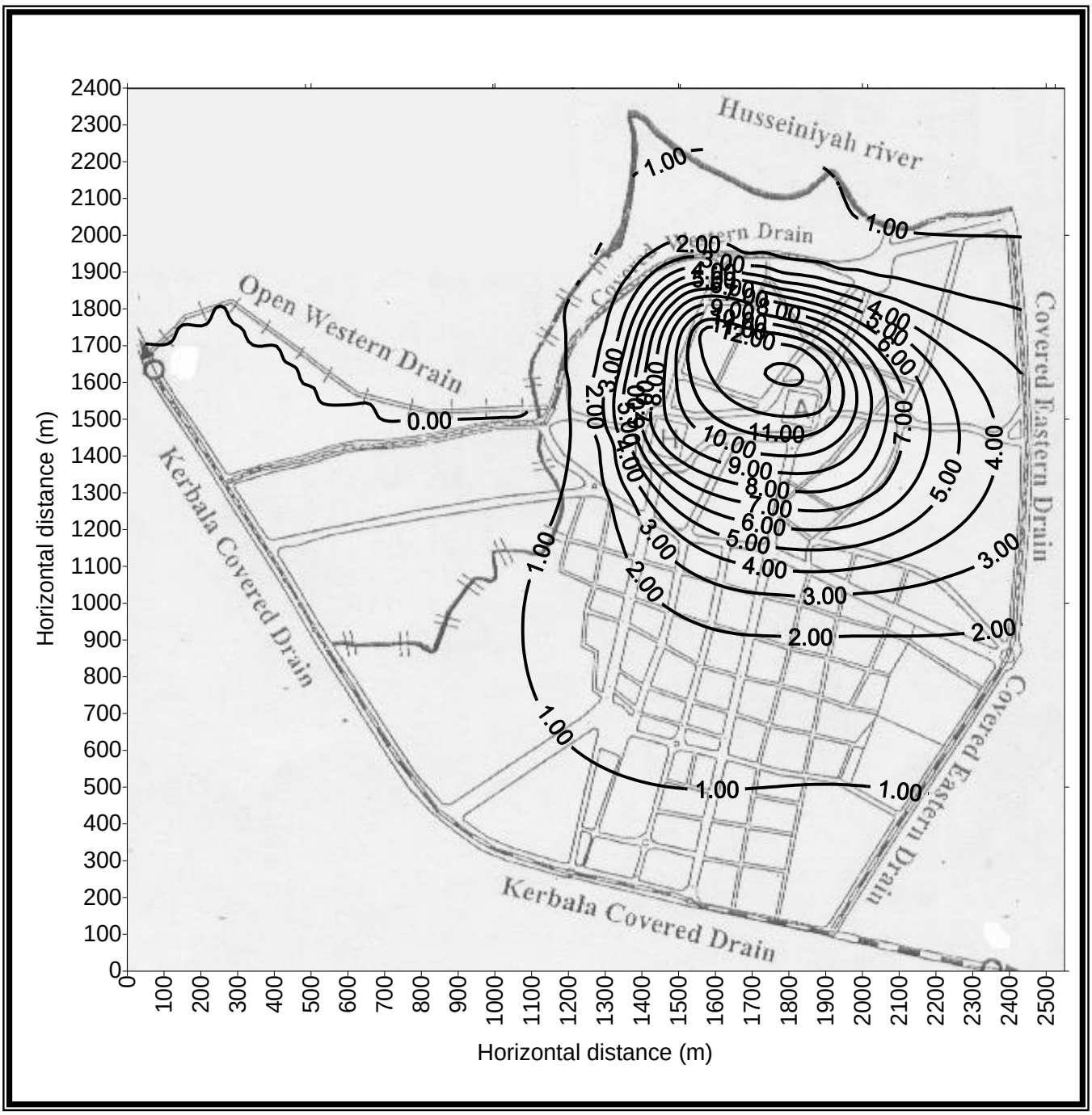

Figure (4-9) Calibrated (model) recharge (m3/day) per nodal cell

The mathematical model can also be used to examine some procedures of lowering ground water levels of the upper layer in the area of the two holy shrines regarding the city as a hole. Two procedures are adopted herein first, examining the effect of reducing local recharge to the upper layer and second, examining the effect of vertical drainage of the lower layer.

Figures (4-10) and (4-11) illustrate the simulated results of the water table level and the water table drawdown of 50% reduction in the local recharge respectively. The figures show that the drawdown ranges between (0-1.4)m, the maximum value is found in the area of the two holy shrines. The drawdown decreases towards the study area boundaries. Like the GMS model this drawdown is insufficient; therefore, a more reduction in the local recharge such as 75% is needed. Figures (4-12) and (4-13) illustrate the simulated results of the water table level and the water table drawdown of this case respectively. The figures show that the drawdown ranges between (0-2.1), the maximum value is observed in the area of the two holy shrines, and it is an acceptable value. Therefore; GMS model and the mathematical model proved that the treatment of the water supply network will not be enough to solve the problem of rising ground water level in the area of the two holy shrines. The problem needs an additional treatment for sewers network and septic tanks.

The procedure of the vertical drainage of lower layer can be carried out by using the same eight wells that are assumed in the mathematical model, Figure (3-12). Long term pumping schedules are also used but at a discharge of 200 m3/day for each well. Figures (4-14) and (4-15) illustrate the simulated results of the water table level and the water table drawdown of this case respectively. The figures show that the drawdown ranges between (0-2.82)m, the maximum value is observed at the holy shrine of AL-Abbas. Its clear from the figures that this procedure can also be adopted as a unique solution. The discharge of wells in this model is adopted because it’s the largest one. From that, it can be said that the lowering of the water table level at the area of the two holy shrines can be achieved by adopting one of the following procedures:-

1- Reducing the local recharge to the upper layer by about 75%.

2- Operating four lower layer wells surrounding each holy shrine at a discharge of 200 m3/day for a long pumping interval.

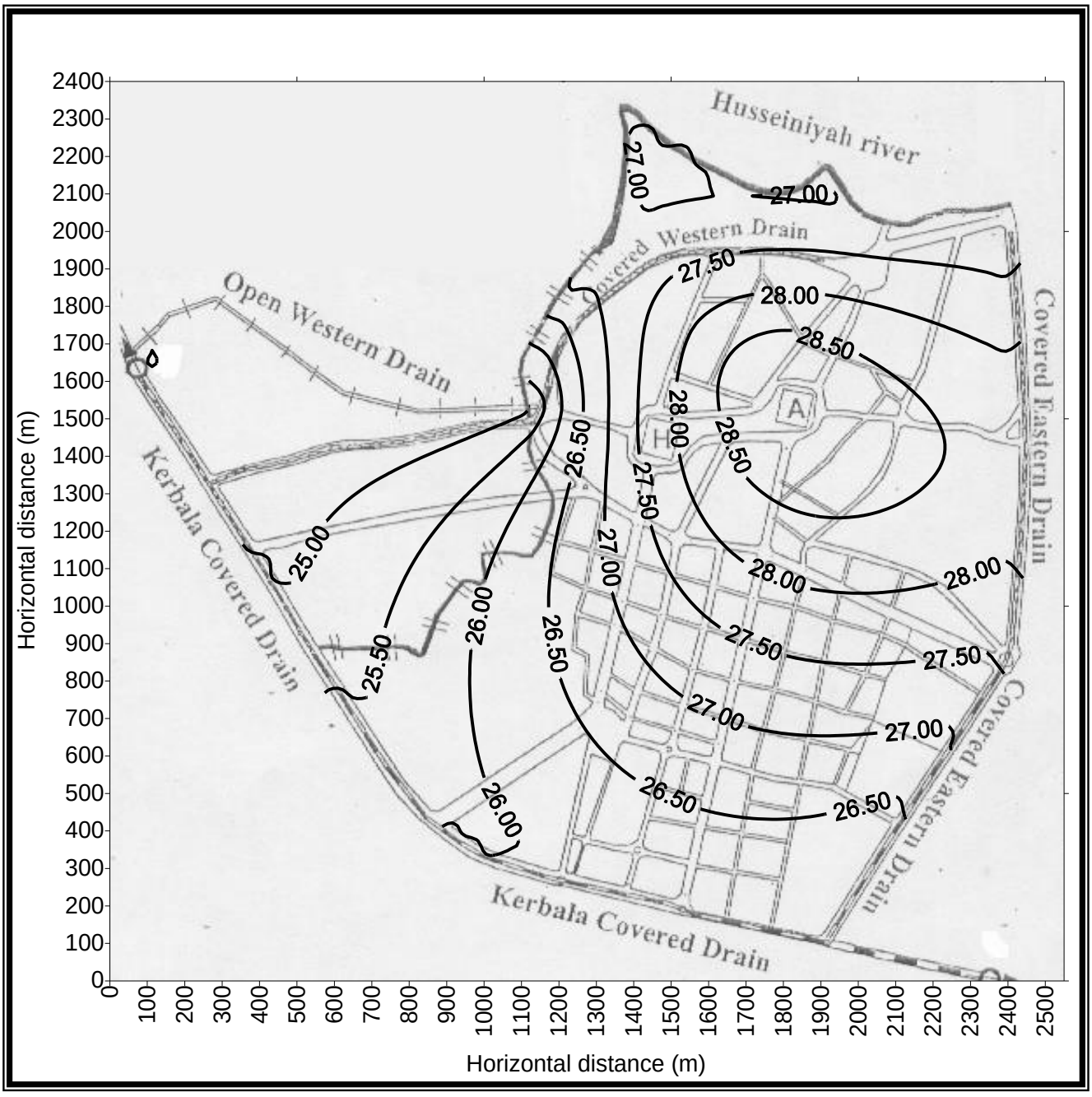

Figure (4-10) Simulation water table level of the upper layer by the mathematical model after reducing the local recharge about 50%

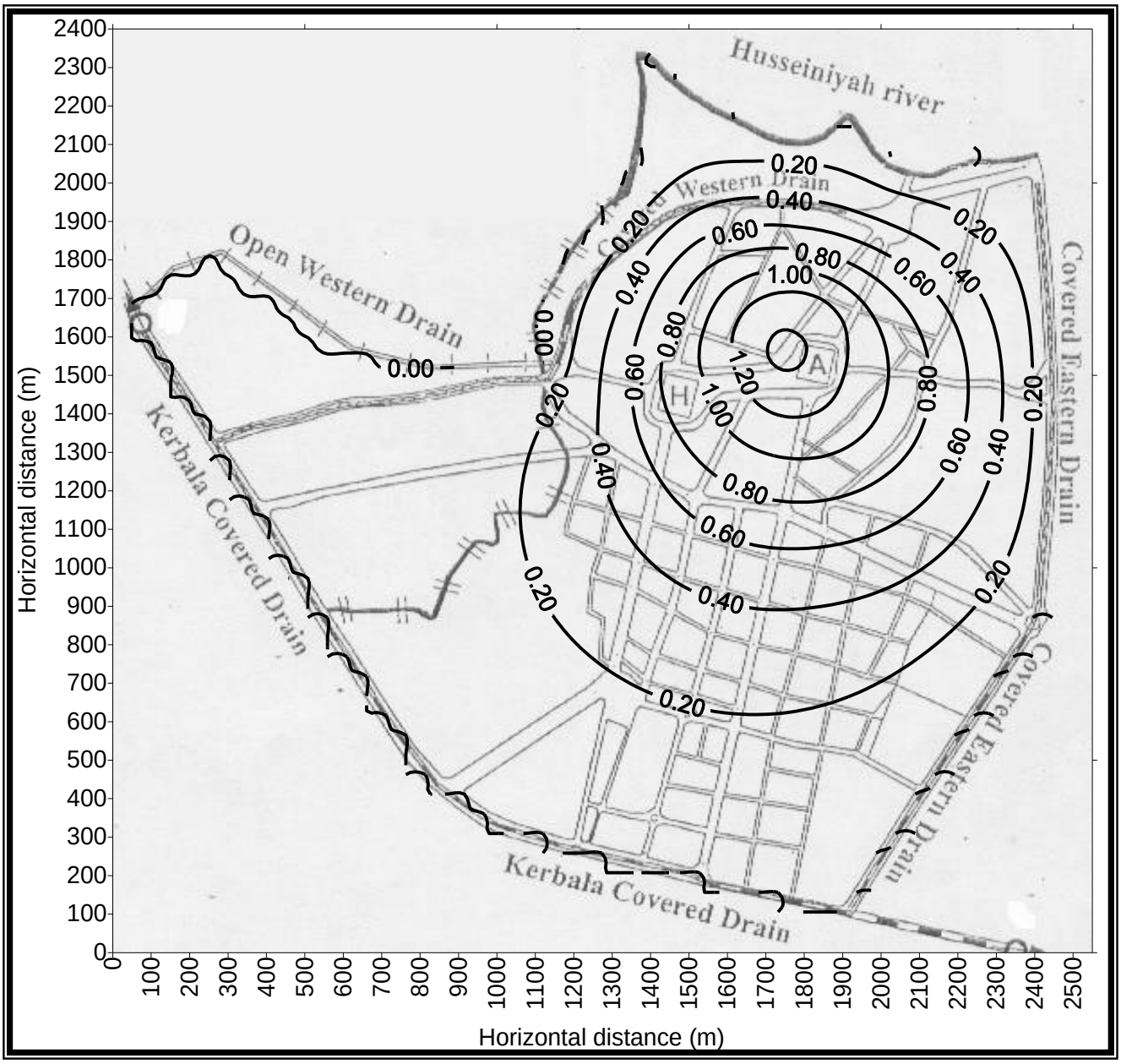

Figure (4-11) Simulation water table drawdown of the upper layer by the mathematical model after reducing the local recharge about 50%

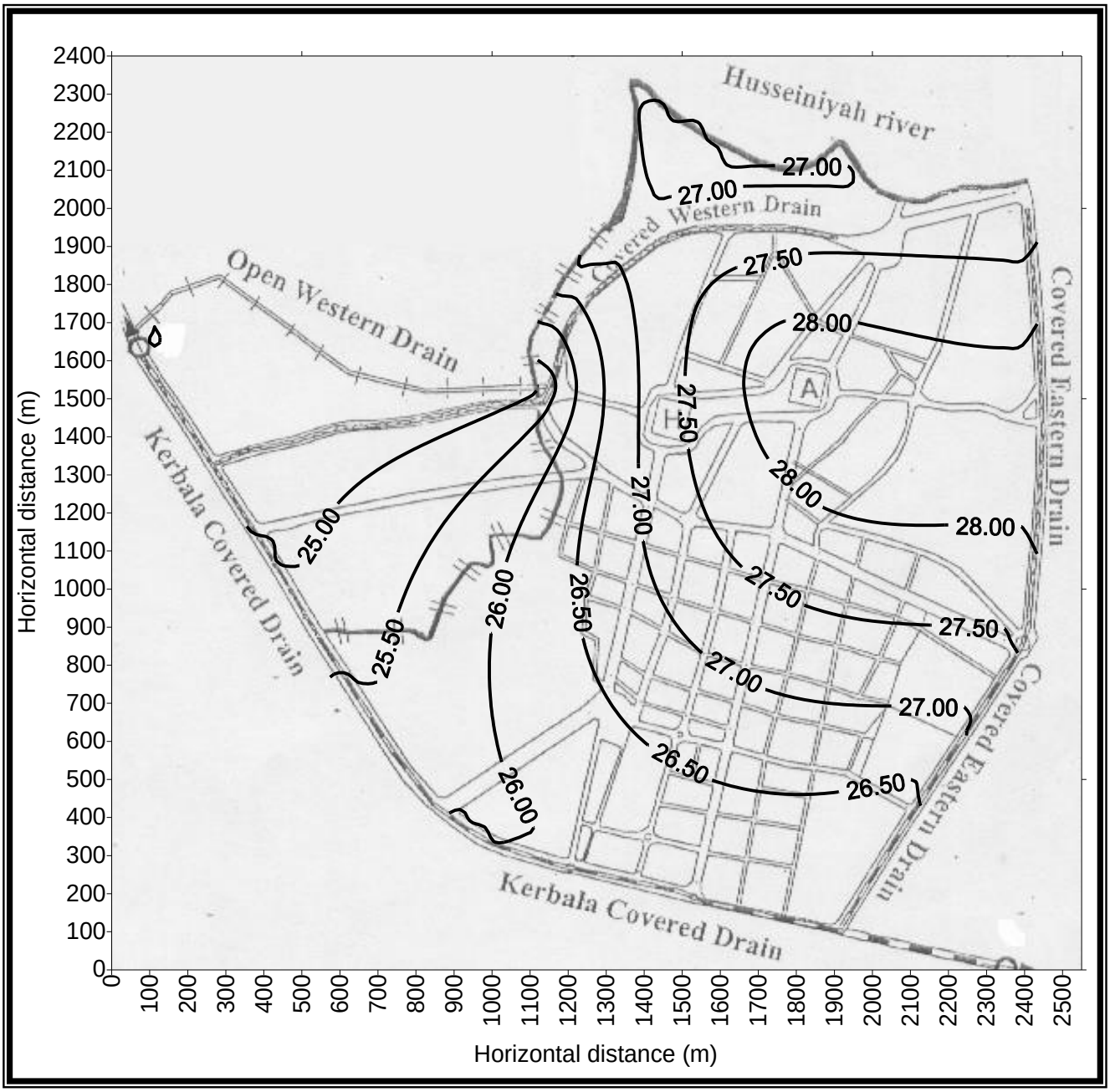

Figure (4-12) Simulation water table level of the upper layer by the mathematical model after reducing the local recharge about 75%

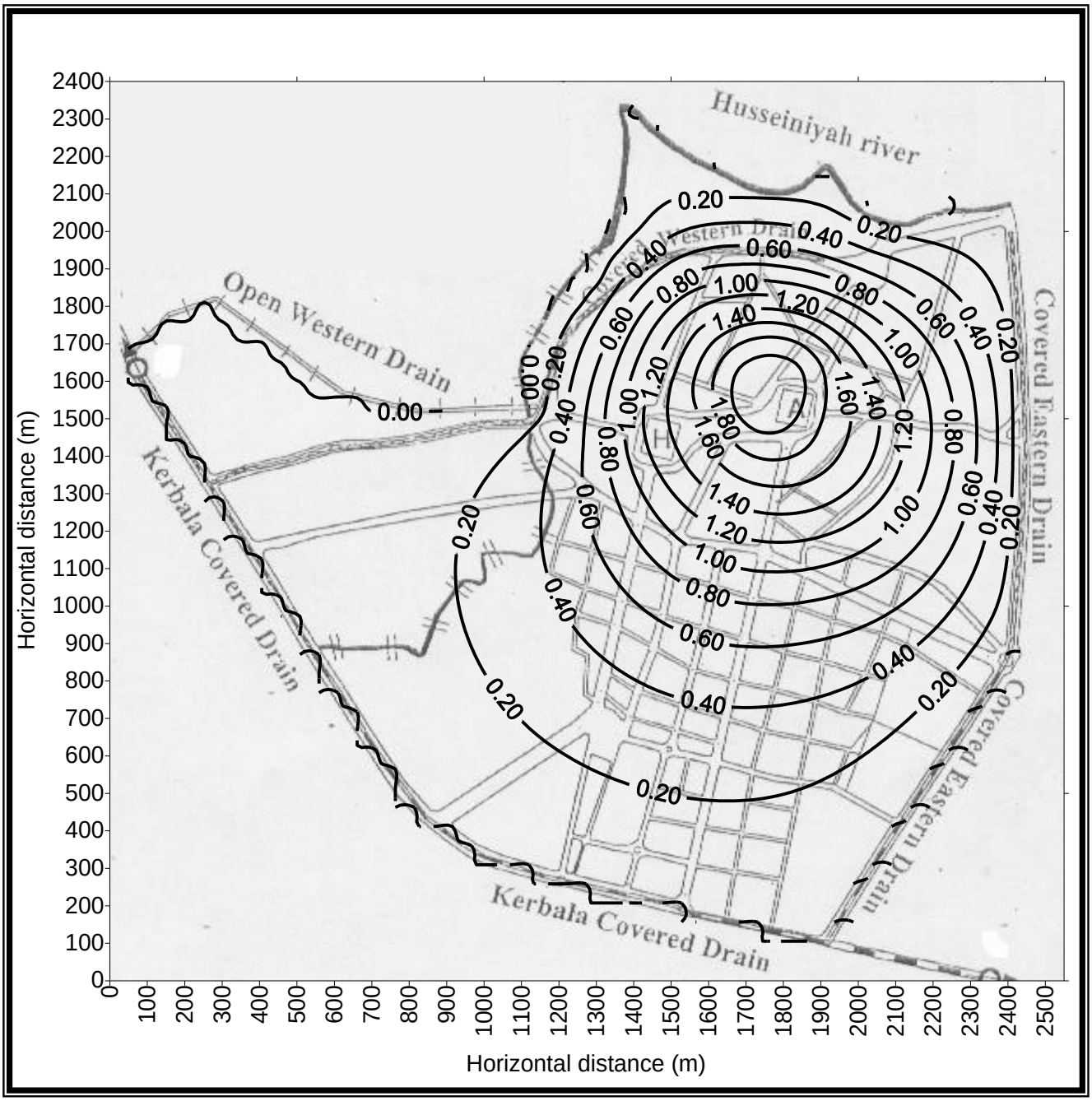

Figure (4-13) Simulation water table drawdown of the upper layer by the mathematical model after reducing the local recharge about 75%

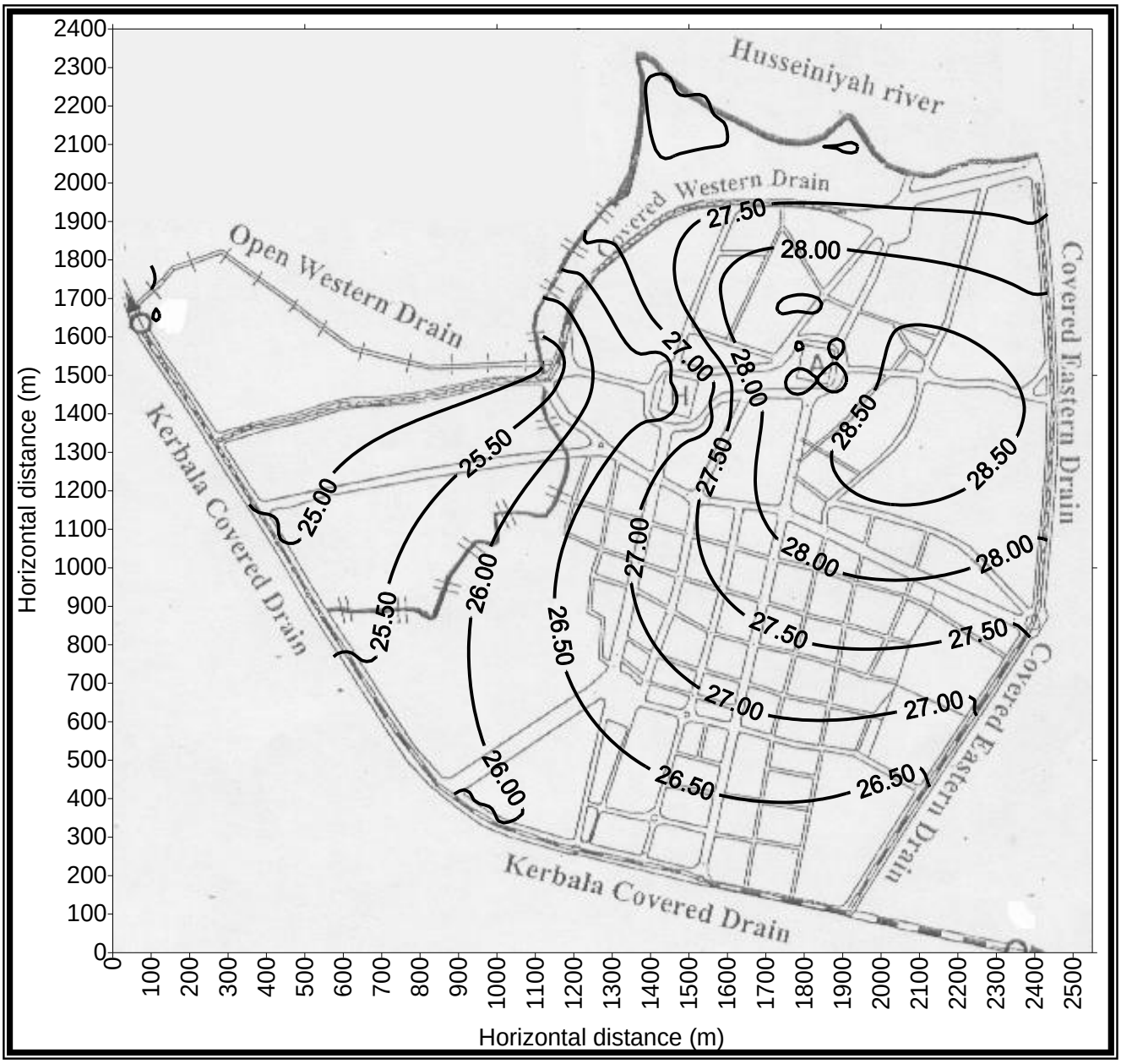

Figure (4-14) water table level of the upper layer after operating four wells surrounding each holy shrine

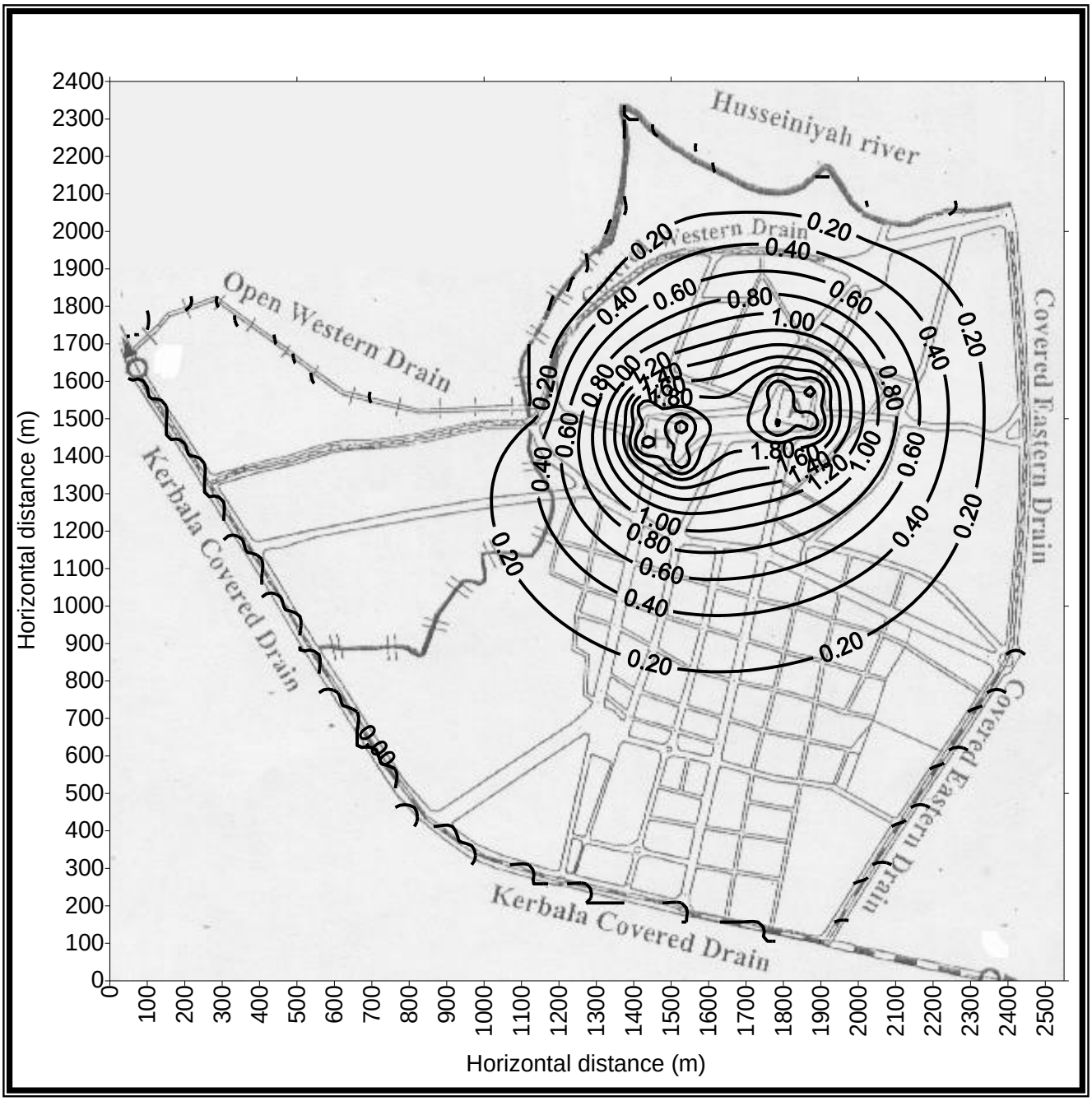

Figure (4-15) water table drawdown of the upper layer after operating four wells surrounding each holy shrine

CHAPTER FIVE

COMPARISON, CONCLUSIONS, AND RECOMMENDATIONS

5-1 Comparison Between the Results of the GMS Model and the Second Mathematical Model

The input data are the same in the two models except that the transmissivity of the lower layer and the local recharge of the upper layer are different due to calibration. Hence, transmissivity of the lower layer is assumed 100 m^2/day in the GMS model while it is assumed 140 m^2/day in the mathematical model. Local recharge that entered to the GMS model is different in amount and distribution from that entered to the mathematical model (see Figures (3-7) and (4-9)). Total local recharge estimated by the GMS model is 760.71 m^3/day while it is estimated as 3256.758 m^3/day by the mathematical model. Since the two models successfully simulate the steady state conditions the two values of recharge can be accepted, therefore the total local recharge produced to the upper layer can be between 760.71 m^3/day and 3256.758 m^3/day. However, these two different values of recharge are implied by calibration.

Output data are the simulated heads and the root means square error (RMSE) for both layers. From figures (3-5) and (3-6), it is seen that compatibility between the simulated heads and the observed heads in the GMS model is not as good as in the second mathematical model (see Figures (4-7) and (4-8)). In the GMS model RMSE for upper and lower layers are found as 1.45 cm and 1.96 cm respectively, while in the mathematical model they are found as 0.725 cm and 0.807 cm for both layers respectively. Although there is a difference in the RMSE and in the compatibility of contour lines between the two models, but the two models succeed in simulating the steady state condition of the model region.

RMSE of the mathematical model are less than RMSE of the GMS model, for both layers, therefore, mathematical model is introduced as the more accurate model.

The construction of the mathematical model needs many days with the help of Excel program and with possibility of using wrong data, while the construction of the GMS model needs only few hours with a high simplicity in changing the boundary condition or any other input data.

The two models agree in the proposed procedure of lowering water table level in the phreatic layer by reducing the local recharge. They show that the reduction by about 75% will be satisfactory, this reduction can be achieved by treating the leakage of water supply network and the disposed waste water system in the study area especially in area surrounding the two holy shrines.

The same places and same number of the lower layer wells are used in the two models (one well at each corner of the two holy shrines) but to achieve un acceptable drawdown, not same discharges of wells are assumed. The discharge of the wells in the mathematical model is used as 200 m^3/day for each well while its used as 70 m^3/day in the GMS model. The critical case is adopted which is 200 m^3/day. Table (5-1) summarizes the comparison between the results of the two models.

Table (5-1) Comparison the results between the mathematical model and the GMS model

Parameters		Mathematical model	GMS model
Input data	Starting heads	Data of Figure (2-12)	Data of Same figure
	Bottom elevation of the upper layer	Data of Figure (2- 18)	Data of Same figure
	Leakage coefficient	Permeability of the middle layer divided on the data of Figure (2- 19)	Data of Same figure
	Permeability	Data of Figure (2- 11)	Data of Same figure
	Transmissivity	140 m^2/day	100 m^2/day
	Local recharge	Data of Figure (4-9) with total recharge 3256.758 m^3/day	Data of Figure (3-7) with total recharge 760.71 m^3/day
Output data	Simulated heads	Data of Figures (4-7) and (4-8)	Data of Figures (3-5) and (3-6)
	RMSE	For the upper layer 0.725 cm For the lower layer 0.807 cm	For the upper layer 1.45 cm For the lower layer 1.96 cm
	Simplicity of use and time consuming	Very difficult and needs too many days in the construction	Very simple and needs only a few hours in the construction
Proposed procedure of lowering ground water level in the upper layer	Reducing local recharge	75%	75%
	Vertical drainage of the lower layer	1 wells at each corner of the two holy shrines with discharge 200 m^3/day	1 wells at each corner of the two holy shrines with discharge 70 m^3/day
	Opening all the drains in the study area	Not satisfy	———

5-2 Conclusions

From the results of the mathematical and the GMS models, the following conclusions can be adopted :-

1- The recharge of the upper layer of the study area ranges between (760.71-3256.758) m^3/day. This recharge comes from the leakage of the drinking pipes network, sewers, and septic tanks.

2- Maximum water level of the upper layer and maximum peizometric head of lower layer are observed in the area of the two holy shrines, especially near the holy shrine of AL-Abbas where the groundwater level is about 30.5m above see level

3- Because the recharge of the upper layer is concentrated in the area of the two holy shrines it has the major effect on the ground water level of this area. Reduction of the recharge all over the study area by about 75% will reduce the ground water level in the study area by (0-2.1)m and the maximum drawdown is observed in the area of the two holy shrines.

4- Vertical drainage of the lower layer can be used to solve the problem of rising ground water level under the two holy shrines. Four wells surrounding each holy shrines at their corners are considered. The discharge of each well is 200 m^3/day. Long time pumping interval is adopted to get and maintaining a draw down under the holy shrines more than 2m .

5- Opening of surrounding covered drains will reduce the ground water level in the study area by (0-2.85)m but the drawdown in the area of the two holy shrines will not exceed (1)m. However, drawdown in the area of the two holy shrines must not be less than (2)m; therefore, opening all the surrounding drains will not be enough to solve the problem.

6- According to the results of the RMSE, mathematical model is introduced as the more accurate model.

5-3 Recommendations

From the results of the models the following recommendations are suggested.

1- Simulating the groundwater flow in the study area using GMS V.5.

2- Replacing the drinking pipe networks by new networks and following a policy to minimize the excessive pressure in the networks to reduce the leakage.

3- Replacing the old sewer system and the existing septic tanks with a new efficient sewer system to collect and dispose the wastewater and the storm water of the study area.

4- Cleaning the existing covered drain or reconstructing the damaged parts to intercept the ground water flow.

5- Constructing one well outside each corner of the two holy shrines. These wells discharge groundwater from the lower layer and they are connected with a pipe network to deliver water to the Hindyia canal in case of rising ground water level below the two holy shrines in the future.

REFERENCES

1- AL-Furat Center for Studies and Designes of Irrigation Project (FCSDIP),1995, " Project of lowering groundwater levels in Kerbala City"

2- AL-Kutubi Engineering Laboratory, 1999, " Soil Investigation Report for the Site of a building under construction in Karbala City".

3- Auwayid, M.M., 2000," A brief study of subsurface water movement in the area surrounding the two holy shrines in Karbala City". Directorate of water supply and sewers of Karbala (DWSK).

4- Bear, J. & Verruijt,A., 1987, "Modeling groundwater flow and pollution", D.Reidal Publishing Company, Dordrecht, The Netherlands.

5- Boonstra, J. & de Ridder, N.A., 1981," Numerical modeling of ground water basins", International Institute for Land Reclamation and improvement, Wageningen, The Netherlands.

6- Bouwer, H.1978, " Groundwater hydrology", McGrou-Hill Inc., New York.

7- DeMarsily, G., Combes, P., and Goblet, P.,1992, "Comment on groundwater models cannot be validated", Advanced water resources.

8- Engineering Computer Graphics Laboratory (ECGL) of Brigham Young University, 1996, " GMS v2.0, Tutorials", 1996 Brigham Young University - Engineering Computer Graphics Laboratory.

9- Engineering Computer Graphics Laboratory (ECGL) of Brigham Young University, 1996, " GMS v2.0, Reference", 1996 Brigham Young University - Engineering Computer Graphics Laboratory.

10- GeoTrans, Inc., Roswell, GA, 2001. " Groundwater Modeling for the Southern Sector of A/M Area (U), Westinghouse Savannah River Company LLC.

11- Gerald, C.F.,1978, "Applied numerical analysis", second edition, Addison-Wesley Publishing Company, Inc.

12- Hassan AL-khateeb, 2001."Problem of shallow ground water level in the center of karbala city": evaluation and simulation, Ph.D thesis in the

environmental engineering submitted to AL-Mustansiria University, College of Engineering, Department of Civil Engineering.

13- Ibtisam R. Karim,2005. "Lowering groundwater levels in the ancient city of Babylon", Ph.D thesis in water resources engineering, University of Technology Department of Building and Construction.
14- Iraqi Scientific Society for Water Resources (ISSWR), 1999, "Study of lowering groundwater level at AL-Rawdhattain, AL-Husseiniyah and Al-Abasiyah in Kerbala"
15- Iraqi Meteorology Organization
16- Jacques W. Delleur.1999. "The hand book of ground water engineering". CRC Press LLC.
17- Kinzelbach, W.,1986, "groundwater modeling": an introduction with sample program in basic, EL-Sevier Science publishing Company, Inc., New York.
18- Konikow, L.F.,1988, "Application of models": in groundwater flow and quality modeling, D. Reidel Publishing Company, The Netherland.
19- Konikow, L. F, 1976, "Preliminary digital model of ground-water flow in the Madison group, Powder River basin and adjacent areas, Wyoming, Montana, South Dakota, North Dakota, and Nebraska." U.S. Geol. Survey Water-Resources Investigations.
20- Lerner, D.N., 1986, "Leaking pipes recharge groundwater", Groundwater Journal.
21- Lerner, D.N., 1989, "Groundwater recharge estimation", Heise, Hannoner, F.R.G.
22- Lucase, H.C. & Robinson, V.K., 1995, " Modeling of rising ground water levels in the chalk aquifer of the London basin", Quarterly Journal of Eng. Geology.
23- Mansour, A., 1993 " Fortran 77": with scientific & engineering applications, fifth addition, AL- Bshaar Library.(In Arabic)

24- McDonald MG and Harbaugh AW (1988), MODFLOW" A modular three-dimensional finite difference ground-water flow model". U. S. Geological Survey.

25- McWhoter, D.B. & Sunada, D.K.,1977, " Ground water hydrology and hydraulics", Water Resources Publication, Colorado.

26- Mercer, J.W. & Faust, C.R., 1981, "Groundwater modeling", Geo. Trans., Inc.,Reston, Virginia.

27- National Center for Construct Laboratories (NCCL), 1981,"Prelimiting report on sub soil investigation in the site of AL-Abbas shrine"

28- National Center for Construct Laboratories (NCCL), 1998," soil investigation report for AL-Hussein shrine"

29- P. Hulme, M. Grout, K. Seymour, K. Rushton, L. Brown, and R. Low, 2002,"Groundwater Resources Modelling": Guidance Notes and Template Project Brief,(Version 1), Environment Agency.

30- Prickett, T.A., 1975, "Modeling techniques for groundwater evaluation", Acadamic Press, new York.

31- Rasheeduddin, M, Yazicigil, H., & AL- Layla, R.I., 1989, " Numerical modeling of multi aquifer system in eastern of Saudi Arabia, Journal of Hydrology.

32- Rushton, K.R. & Redshow, S.C., " Seepage and ground water flow", John Wily and Sons.

33- Salah, R.H.,1998 " Programming with Quick basic", Baghdad University.(In Arabic).

34- U.S. Army Corps of Engineers ,1999, " Engineering and Design Groundwater Hydrology", Approved for public release; distribution is unlimited.

35- U.S. Department of the Interior,1985, "Groundwater manual", Government Printing Office, Denver.

36- Victoria Ljungberg & Sarah Qvist,2004. " Assessment of Groundwater Flow and Pollutant Transport through Modeling": a Pilot Study in the Sulur Watershed, Coimbatore District. Ms.c thesis submitted to the Department of

Land and Water Resources Engineering, Royal Institute of Technology, Stockholm, Sweden.

37- Wang, H.,1982, " Introduction to groundwater modeling": Finite difference and finite element methods, Freeman and Company.

38- Water science and technology board (1990)."Ground water models", Scientific and regulatory applications, National academy press. Washington D.C.

39- Wen- Hsing Chiang,2005, "3D-Groundwater Modeling with PMWIN", A simulation System for Modeling Groundwater Flow and Transport Processes. Springer-Verlag Berlin Heidelberg 2005.The Netherlands.

40- You-Kuan Zhang, Byong-min Seo, Nanh Lovanh, Pedro J.J. Alvarez, and Richard Heathcote,2001, " Evaluation of Computer Software Packages for RBCA Tier-3 Analysis", final report submitted to Scott Scheidel, Administrator: Iowa Comprehensive Petroleum Underground Storage Tank Fund Board.

Appendix (A)

```
REM Finite Difference Flow Model to Simulate the Ground Water Flow
REM in Karbala City
INPUT "Enter Time Period of Simulation in Days"; TP
PRINT "Enter Number of Time Steps through the Period of Simulation"
PRINT "This Number Should be Greater Than Zero"
INPUT ; NS
IF NS > 0 THEN 5
PRINT "NS should be greater than zero, the program will be stopped"
GOTO 170
5INPUT "Enter Number of lower layer Wells That Supposed to be "; NW
INPUT "Enter Number of upper layer Wells That Supposed to be "; NWU
INPUT "Enter maximum allowed Number of Iterations within one time step"; NI
PRINT " Enter Maximum allowed nodal head error in the phreatic layer"
INPUT ; ER1
PRINT " Enter Maximum allowed nodal head error in the lower layer"
INPUT ; ER3
INPUT " Enter Maximum Number of intervals for a well"; MNP
INPUT " Enter Number of Rows"; R
INPUT " Enter Number of Columns"; C
NB = C
IF R > C THEN NB = R
DIM HO1F(R, C), HO3F(R, C)
DIM HS1(R, C), HS3(R, C), HO1(R, C), HO3(R, C), DY(R), DX(C), TX1(R, C)
DIM TY1(R, C), TX3(R, C), TY3(R, C), GSL(R, C), X(R, C), Y(R, C), S(R, C)
DIM EFFE(R, C), Qnet(R, C), BL1(R, C), LCM(R, C), LCB(R, C), WL(R, C),
awb(R, C)
DIM perm(R, C), trans(R, C), Teb(R, C), Beb(R, C), Wx(NW), Wy(NW), leak(R,C)
DIM NP(NW), TI(NW, MNP), TF(NW, MNP), Qqw(NW, MNP), F(NB), G(NB), Qw(R, C)
DIM NPU(NWU), TIU(NWU, MNP), TFU(NWU, MNP), QqwU(NWU, MNP), QwU(R, C),
WxU(NWU), WyU(NWU)
OPEN "HO1.dat" FOR INPUT AS #1
OPEN "HO3.dat" FOR INPUT AS #2
OPEN "S.dat" FOR INPUT AS #4
OPEN "EFFE.dat" FOR INPUT AS #5
OPEN "Qnet.dat" FOR INPUT AS #6
OPEN "BL1.dat" FOR INPUT AS #7
OPEN "LCM.dat" FOR INPUT AS #8
OPEN "river1.dat" FOR INPUT AS #9
OPEN "perm.dat" FOR INPUT AS #12
OPEN "trans.dat" FOR INPUT AS #13
OPEN "HS1.dat" FOR OUTPUT AS #18
OPEN "HS3.dat" FOR OUTPUT AS #19
OPEN "leak.dat" FOR OUTPUT AS #20
FOR I = 1 TO R
DY(I) = 50
NEXT
FOR J = 1 TO C
DX(J) = 50
NEXT
FOR I = 1 TO R
FOR J = 1 TO C
INPUT #1, X(I, J), Y(I, J), HO1F(I, J)
INPUT #2, X(I, J), Y(I, J), HO3F(I, J)
INPUT #4, X(I, J), Y(I, J), S(I, J)
INPUT #5, X(I, J), Y(I, J), EFFE(I, J)
INPUT #6, X(I, J), Y(I, J), Qnet(I, J)
Qnet(I, J) = Qnet(I, J) / (DX(J) * DY(I))
INPUT #7, X(I, J), Y(I, J), BL1(I, J)
INPUT #8, X(I, J), Y(I, J), LCM(I, J)
INPUT #9, Teb(I, J), Beb(I, J), LCB(I, J), WL(I, J), awb(I, J)
```

```
  INPUT #12, X(I, J), Y(I, J), perm(I, J)
  INPUT #13, X(I, J), Y(I, J), trans(I, J)
  IF Teb(I, J) = 0 THEN 15
  IF Teb(I, J) > Beb(I, J) THEN 15
  PRINT " Top Elevation of the Bed of Surface Water Body"
  PRINT " is Less or Equal to the Bottom Elevation"
  PRINT " Check the Entered Data"
  PRINT " the Program Will Be Stopped"
  PRINT "I="; I, "J="; J
  GOTO 170
15NEXT
  NEXT
  IF NW = 0 THEN 21
  FOR I = 1 TO NW
  L = 0
  PRINT "Enter number of pumping intervals for the well in the lower layer";
  I
  INPUT ; NP(I)
  PRINT " Enter number of cell in X direction that the well in the lower
  layer"; I
  PRINT " is supposed to be"
  INPUT ; Wx(I)
  PRINT " Enter number of cell in y direction that the well in the lower
  layer"; I
  PRINT " is supposed to be"
  INPUT ; Wy(I)
  FOR J = 1 TO NP(I)
  PRINT "Enter Initial Time of Pumping Interval"; J
  PRINT " for the well of the lower layer"; I
  INPUT ; TI(I, J)
  PRINT "Enter Final Time of Pumping Interval"; J
  PRINT " for the well of the lower layer"; I
  INPUT ; TF(I, J)
  PRINT "Enter the Discharge of Well"; I
  PRINT "of the lower layer for the Interval"; J
  INPUT ; Qqw(I, J)
  Qqw(I, J) = Qqw(I, J) / (DY(Wy(I)) * DX(Wx(I)))
  TdL = TF(I, J) - TI(I, J)
  L = L + TdL
  NEXT
  IF L <= TP THEN 20
  PRINT " There is an Error in the pumping interval data of the lower layer"
  PRINT " the program will be stopped"
  GOTO 170
20NEXT
21IF NWU = 0 THEN 23
  FOR I = 1 TO NWU
  L = 0
  PRINT "Enter number of pumping intervals for the well in the upper layer"; I
  INPUT ; NPU(I)
  PRINT " Enter number of cell in X direction that the well in the upper
  layer"; I
  PRINT " is supposed to be"
  INPUT ; WxU(I)
  PRINT " Enter number of cell in y direction that the well in the upper
  layer"; I
  PRINT " is supposed to be"
  INPUT ; WyU(I)
  FOR J = 1 TO NPU(I)
  PRINT "Enter Initial Time of Pumping Interval"; J
  PRINT " for the well of the upper layer"; I
  INPUT ; TIU(I, J)
  PRINT "Enter Final Time of Pumping Interval"; J
  PRINT " for the well of the upper layer"; I
```

```
  INPUT ; TFU(I, J)
  PRINT "Enter the Discharge of Well"; I
  PRINT "of the upper layer for the Interval"; J
  INPUT ; QqwU(I, J)
  QqwU(I, J) = QqwU(I, J) / (DY(WyU(I)) * DX(WxU(I)))
  TdU = TFU(I, J) - TIU(I, J)
  L = L + TdU
  NEXT
  IF L <= TP THEN 22
  PRINT " There is an Error in the pumping interval data of the upper layer"
  PRINT " the program will be stopped"
  GOTO 170
22NEXT
  REM Calculations of Internodal Transmissivty and Permeability
  REM and Area Adjustment
23FOR I = 1 TO R
  FOR J = 1 TO C
  LCB(I, J) = LCB(I, J) * awb(I, J) / (DX(J) * DY(I))
  NEXT
  NEXT
  FOR I = 1 TO R - 1
  FOR J = 1 TO C - 1
  Z1 = perm(I, J) + perm(I, J + 1)
  Z2 = perm(I, J) + perm(I + 1, J)
  Z3 = trans(I, J) + trans(I, J + 1)
  Z4 = trans(I, J) + trans(I + 1, J)
  IF Z1 = 0 THEN TX1(I, J) = 0: GOTO 25
  TX1(I, J) = perm(I, J) * perm(I, J + 1) * 2 / (perm(I, J) + perm(I, J + 1))
25IF Z2 = 0 THEN TY1(I, J) = 0: GOTO 30
  TY1(I, J) = perm(I, J) * perm(I + 1, J) * 2 / (perm(I, J) + perm(I + 1, J))
30IF Z3 = 0 THEN TX3(I, J) = 0: GOTO 40
  TX3(I, J) = trans(I, J) * trans(I, J + 1) * 2 / (trans(I, J) + trans(I, J +
  1))
40IF Z4 = 0 THEN TY3(I, J) = 0: GOTO 50
  TY3(I, J) = trans(I, J) * trans(I + 1, J) * 2 / (trans(I, J) + trans(I + 1,
  J))
50NEXT
  NEXT
  FOR I = 1 TO R
  FOR J = 1 TO C
  HS1(I, J) = HO1F(I, J)
  HS3(I, J) = HO3F(I, J)
  NEXT
  NEXT
  FOR I = 1 TO R - 1
  FOR J = 1 TO C - 1
  TX1(I, J) = TX1(I, J) / (.5 * (DX(J) + DX(J + 1)))
  TY1(I, J) = TY1(I, J) / (.5 * (DY(I) + DY(I + 1)))
  TX3(I, J) = TX3(I, J) / (.5 * (DX(J) + DX(J + 1)))
  TY3(I, J) = TY3(I, J) / (.5 * (DY(I) + DY(I + 1)))
  NEXT
  NEXT
  DTIME = TP / NS
95TIME = 0
  FOR IK = 1 TO NS
  FOR I = 1 TO R
  FOR J = 1 TO C
  HO1(I, J) = HS1(I, J)
  HO3(I, J) = HS3(I, J)
  NEXT
  NEXT
  TIME = TIME + DTIME
  REM IADI method
  IT = 0
```

```
  96CE1 = 0
    CE3 = 0
    IT = IT + 1
    REM Phreatic layer Column Calculations
    FOR J = 2 TO C - 1
    m = (IT / 2)
    IF m = INT(m) THEN J = C - J + 1
    FOR I = 2 TO R - 1
    QwU(I, J) = 0
    IF NWU = 0 THEN 99
    FOR mm = 1 TO NWU
    IF WyU(mm) <> I THEN 98
    IF WxU(mm) <> J THEN 98
    FOR kk = 1 TO NPU(mm)
    IF TIU(mm, kk) > TIME THEN 97
    IF TFU(mm, kk) < TIME THEN 97
    QwU(I, J) = QwU(I, J) + QqwU(mm, kk)
  97NEXT
  98NEXT
  99IF HS1(I, J) = 0 THEN 100
    IF HS1(I, J) <= BL1(I, J) THEN
    AM1 = .01
    AM2 = .01
    AM3 = .01
    AM4 = .01
    ELSE
 100DH = HS1(I, J) - BL1(I, J)
    AM1 = SQR(ABS((HS1(I - 1, J) - BL1(I - 1, J)) * DH))
    AM2 = SQR(ABS((HS1(I, J + 1) - BL1(I, J + 1)) * DH))
    AM3 = SQR(ABS((HS1(I + 1, J) - BL1(I + 1, J)) * DH))
    AM4 = SQR(ABS((HS1(I, J - 1) - BL1(I, J - 1)) * DH))
    END IF
    A = -TY1(I - 1, J) * AM1 / DY(I)
    Cc = -TY1(I, J) * AM3 / DY(I)
    IF HS1(I, J) > Beb(I, J) THEN
    QR1 = LCB(I, J)
    QR2 = LCB(I, J) * WL(I, J)
    ELSE
    QR1 = 0
    QR2 = LCB(I, J) * WL(I, J) - LCB(I, J) * Teb(I, J)
    END IF
    b1 = TY1(I - 1, J) * AM1 / DY(I) + TX1(I, J) * AM2 / DX(J) + TY1(I, J) *
AM3     / DY(I)
    b2 = TX1(I, J - 1) * AM4 / DX(J) + EFFE(I, J) / DTIME + LCM(I, J) + QR1
    b = b1 + b2
    d1 = QwU(I, J) + HS1(I, J + 1) * TX1(I, J) * AM2 / DX(J) + HS1(I, J - 1) *
    TX1(I, J - 1) * AM4 / DX(J)
    d2 = Qnet(I, J) + HO1(I, J) * EFFE(I, J) / DTIME + LCM(I, J) * HS3(I, J) +
    QR2
    d = d1 + d2
    F(1) = 0
    F(R - 1) = 0
    G(1) = 0
    G(R - 1) = 0
    w = b - A * F(I - 1)
    IF w = 0 OR EFFE(I, J) > 1 THEN
    F(I) = 0
    G(I) = HS1(I, J)
    ELSE
    F(I) = Cc / w
    G(I) = (d - A * G(I - 1)) / w
    END IF
    NEXT
    HF = ABS(HS1(R - 1, J) - G(R - 1))
```

```
   IF HF > CE1 THEN CE1 = HF
   HS1(R - 1, J) = G(R - 1)
   FOR v = R - 2 TO 2 STEP -1
   HA = G(v) - F(v) * HS1(v + 1, J)
   HF = ABS(HA - HS1(v, J))
   IF HF > CE1 THEN CE1 = HF
   HS1(v, J) = HA
   NEXT
   NEXT
   REM Lower Layer Column Calculations
   FOR J = 2 TO C - 1
   m = (IT / 2)
   IF m = INT(m) THEN J = C - J + 1
   FOR I = 2 TO R - 1
   Qw(I, J) = 0
   IF NW = 0 THEN 120
   FOR mm = 1 TO NW
   IF Wy(mm) <> I THEN 110
   IF Wx(mm) <> J THEN 110
   FOR kk = 1 TO NP(mm)
   IF TI(mm, kk) > TIME THEN 105
   IF TF(mm, kk) < TIME THEN 105
   Qw(I, J) = Qw(I, J) + Qqw(mm, kk)
105NEXT
110NEXT
120A = -TY3(I - 1, J) / DY(I)
   Cc = -TY3(I, J) / DY(I)
   b1 = TX3(I, J) / DX(J) + TX3(I, J - 1) / DX(J) + TY3(I, J) / DY(I)
   b2 = TY3(I - 1, J) / DY(I) + LCM(I, J) + S(I, J) / DTIME
   b = b1 + b2
   d1 = Qw(I, J) + HO3(I, J) * S(I, J) / DTIME + LCM(I, J) * HS1(I, J)
   d2 = HS3(I, J - 1) * TX3(I, J - 1) / DX(J) + HS3(I, J + 1) * TX3(I, J) /
   DX(J)
   d = d1 + d2
   F(1) = 0
   F(R - 1) = 0
   G(1) = 0
   G(R - 1) = 0
   w = b - A * F(I - 1)
   IF w = 0 OR S(I, J) > 1 THEN
   F(I) = 0
   G(I) = HS3(I, J)
   ELSE
   F(I) = Cc / w
   G(I) = (d - A * G(I - 1)) / w
   END IF
   NEXT
   HF = ABS(HS3(R - 1, J) - G(R - 1))
   IF HF > CE3 THEN CE3 = HF
   HS3(R - 1, J) = G(R - 1)
   FOR v = R - 2 TO 2 STEP -1
   HA = G(v) - F(v) * HS3(v + 1, J)
   HF = ABS(HA - HS3(v, J))
   IF HF > CE3 THEN CE3 = HF
   HS3(v, J) = HA
   NEXT
   NEXT
   REM Pheratic Layer Raw Calculations
   FOR I = 2 TO R - 1
   m = (IT / 2)
   IF m = INT(m) THEN I = R - I + 1
   FOR J = 2 TO C - 1
   QwU(I, J) = 0
   IF NWU = 0 THEN 123
```

```
    FOR mm = 1 TO NWU
    IF WyU(mm) <> I THEN 122
    IF WxU(mm) <> J THEN 123
    FOR kk = 1 TO NPU(mm)
    IF TIU(mm, kk) > TIME THEN 121
    IF TFU(mm, kk) <= TIME THEN 121
    QwU(I, J) = QwU(I, J) + QqwU(mm, kk)
 121NEXT
 122NEXT
 123IF HS1(I, J) = 0 THEN 125
    IF HS1(I, J) <= BL1(I, J) THEN
    AM1 = .01
    AM2 = .01
    AM3 = .01
    AM4 = .01
    ELSE
 125DH = HS1(I, J) - BL1(I, J)
    AM1 = SQR(ABS((HS1(I - 1, J) - BL1(I - 1, J)) * DH))
    AM2 = SQR(ABS((HS1(I, J + 1) - BL1(I, J + 1)) * DH))
    AM3 = SQR(ABS((HS1(I + 1, J) - BL1(I + 1, J)) * DH))
    AM4 = SQR(ABS((HS1(I, J - 1) - BL1(I, J - 1)) * DH))
    END IF
    A = -TX1(I, J - 1) * AM4 / DX(J)
    Cc = -TX1(I, J) * AM2 / DX(J)
    IF HS1(I, J) > Beb(I, J) THEN
    QR1 = LCB(I, J)
    QR2 = LCB(I, J) * WL(I, J)
    ELSE
    QR1 = 0
    QR2 = LCB(I, J) * WL(I, J) - LCB(I, J) * Teb(I, J)
    END IF
    b1 = TY1(I - 1, J) * AM1 / DY(I) + TX1(I, J) * AM2 / DX(J) + TY1(I, J) *
AM3     / DY(I)
    b2 = TX1(I, J - 1) * AM4 / DX(J) + LCM(I, J) + EFFE(I, J) / DTIME + QR1
    b = b1 + b2
    d1 = QwU(I, J) + Qnet(I, J) + HO1(I, J) * EFFE(I, J) / DTIME + LCM(I, J) *
    HS3(I, J) + QR2
    d2 = HS1(I - 1, J) * TY1(I - 1, J) * AM1 / DY(I) + HS1(I + 1, J) * TY1(I,
J)     * AM3 / DY(I)
    d = d1 + d2
    F(1) = 0
    F(C - 1) = 0
    G(1) = 0
    G(C - 1) = 0
    w = b - A * F(J - 1)
    IF w = 0 OR EFFE(I, J) > 1 THEN
    F(J) = 0
    G(J) = HS1(I, J)
    ELSE
    F(J) = Cc / w
    G(J) = (d - A * G(J - 1)) / w
    END IF
    NEXT
    HF = ABS(HS1(I, C - 1) - G(C - 1))
    IF HF > CE1 THEN CE1 = HF
    HS1(I, C - 1) = G(C - 1)
    FOR v = C - 2 TO 2 STEP -1
    HA = G(v) - F(v) * HS1(I, v + 1)
    HF = ABS(HS1(I, v) - HA)
    IF HF > CE1 THEN CE1 = HF
    HS1(I, v) = HA
    NEXT
    NEXT
    REM Lower Layer Raw Calculations
```

```
   FOR I = 2 TO R - 1
   m = (IT / 2)
   IF m = INT(m) THEN I = R - I + 1
   FOR J = 2 TO C - 1
   Qw(I, J) = 0
   IF NW = 0 THEN 150
   FOR mm = 1 TO NW
   IF Wy(mm) <> I THEN 140
   IF Wx(mm) <> J THEN 140
   FOR kk = 1 TO NP(mm)
   IF TI(mm, kk) > TIME THEN 130
   IF TF(mm, kk) <= TIME THEN 130
   Qw(I, J) = Qw(I, J) + Qqw(mm, kk)
130NEXT
140NEXT
150A = -TX3(I, J - 1) / DX(J)
   Cc = -TX3(I, J) / DX(J)
   b1 = TY3(I - 1, J) / DY(I) + TX3(I, J) / DX(J) + TY3(I, J) / DY(I)
   b2 = TX3(I, J - 1) / DX(J) + LCM(I, J) + S(I, J) / DTIME
   b = b1 + b2
   d1 = Qw(I, J) + HO3(I, J) * S(I, J) / DTIME + LCM(I, J) * HS1(I, J)
   d2 = HS3(I - 1, J) * TY3(I - 1, J) / DY(I) + HS3(I + 1, J) * TY3(I, J) /
   DY(I)
   d = d1 + d2
   F(1) = 0
   F(C - 1) = 0
   G(1) = 0
   G(C - 1) = 0
   w = b - A * F(J - 1)
   IF w = 0 OR S(I, J) > 1 THEN
   F(J) = 0
   G(J) = HS3(I, J)
   ELSE
   F(J) = Cc / w
   G(J) = (d - A * G(J - 1)) / w
   END IF
   NEXT
   HF = ABS(HS3(I, C - 1) - G(C - 1))
   IF HF > CE3 THEN CE3 = HF
   HS3(I, C - 1) = G(C - 1)
   FOR v = C - 2 TO 2 STEP -1
   HA = G(v) - F(v) * HS3(I, v + 1)
   HF = ABS(HS3(I, v) - HA)
   IF HF > CE3 THEN CE3 = HF
   HS3(I, v) = HA
   NEXT
   NEXT
   REM end of iteration step
   PRINT " Number of Iterations ="; IT
   PRINT "In the Time Step "; IK
   PRINT "Maximum Difference Between the"
   PRINT "Heads in the Pheratic Layer="; CE1
   PRINT "Maximum Difference Between the"
   PRINT "Heads in the lower Layer="; CE3
   PRINT "Time in Days="; TIME
   IF IT <= NI THEN 160
   PRINT " No Convergence"
   GOTO 170
160IF CE1 > ER1 THEN 96
   IF CE3 > ER3 THEN 96
   NEXT
   FOR I = 1 TO R
   FOR J = 1 TO C
   PRINT #18, X(I, J), Y(I, J), HS1(I, J)
```

```
   PRINT #19, X(I, J), Y(I, J), HS3(I, J)
   NEXT
   NEXT
   sum1 = 0
   sum2 = 0
   sum3 = 0
   sum4 = 0
   FOR I = 1 TO R
   FOR J = 1 TO C
   sum1 = sum1 + Qnet(I, J) * DX(J) * DY(I)
   sum3 = sum3 + (HS1(I, J) - HO1F(I, J)) ^ 2
   sum4 = sum4 + (HS3(I, J) - HO3F(I, J)) ^ 2
   df = HS1(I, J) - HS3(I, J)
   leak(I, J) = (df * LCM(I, J) * DX(J) * DY(I))
   PRINT #20, X(I, J), Y(I, J), leak(I, J)
   IF EFFE(I, J) > 1 OR LCB(I, J) > 0 THEN 169
   sum2 = sum2 + (df * LCM(I, J) * DX(J) * DY(I))
169NEXT
   NEXT
   RMSE1 = (sum3) ^ .5 / (R * C)
   RMSE3 = (sum4) ^ .5 / (R * C)
   PRINT " Total Recharge="; sum1
   PRINT "Amount of Leakage to the Lower Layer="; sum2
   PRINT "Root Mean Square Error for the Upper Layer="; RMSE1
   PRINT "Root Mean Square Error for the Lower Layer="; RMSE3
170END
```

Appendix (B)

Logs of boreholes drilled by NCCL in 1981 around the holy shrine of AL-Abbas

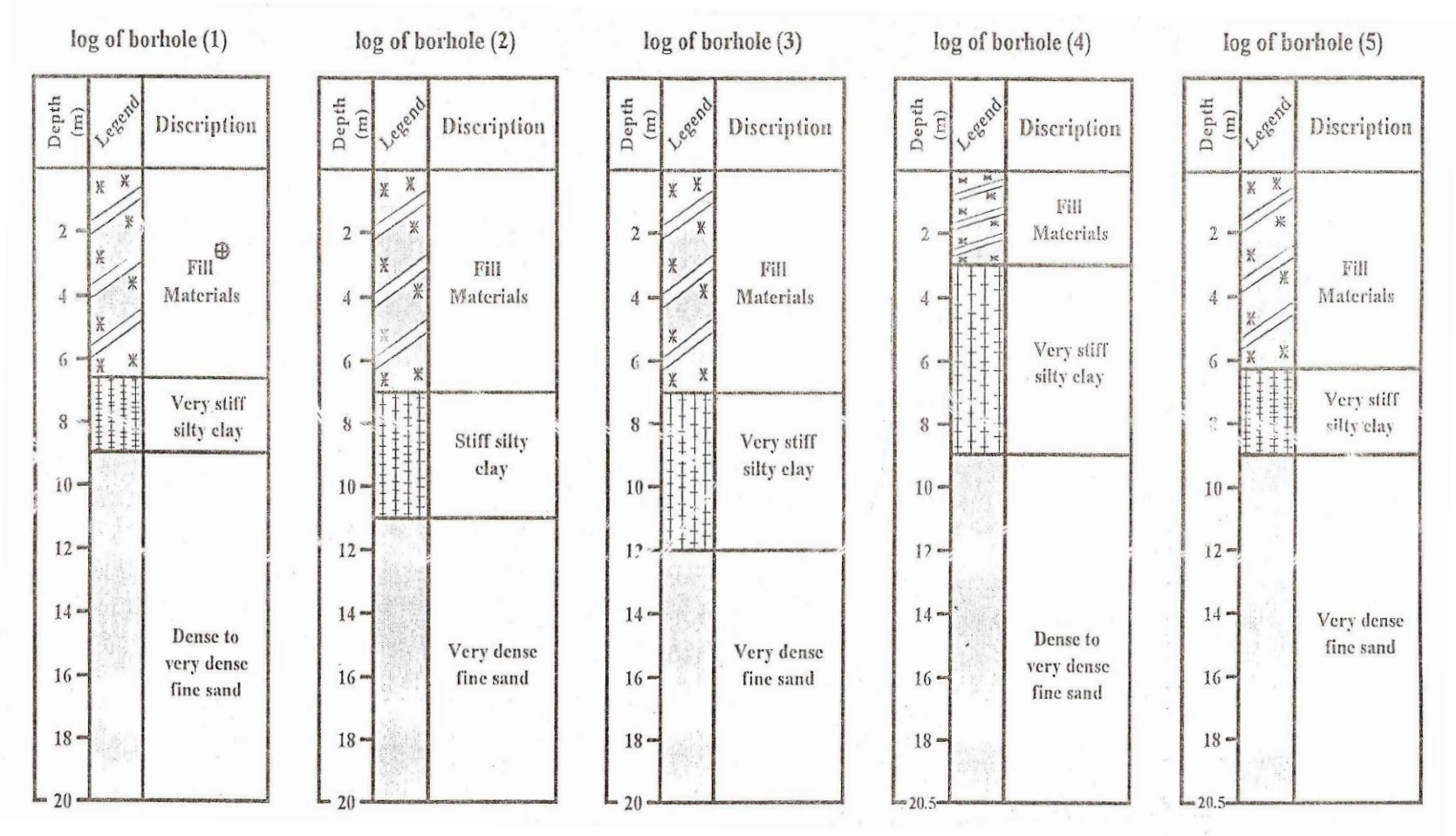

Logs of boreholes drilled by NCCL in 1992 around the holy shrine of AL-Abbas

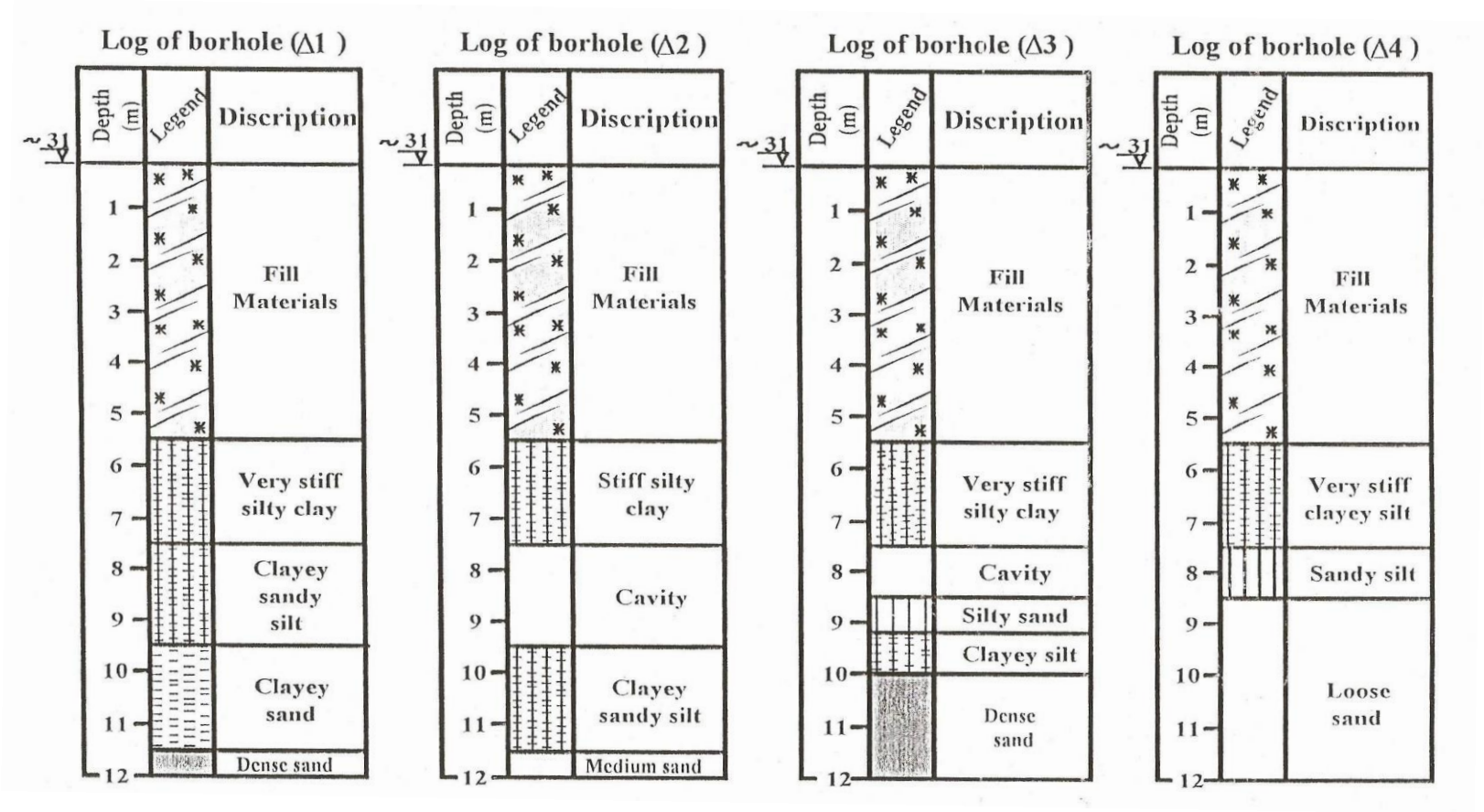

Logs of boreholes drilled by NCCL in 1998 around the holy shrine of AL-Hussain

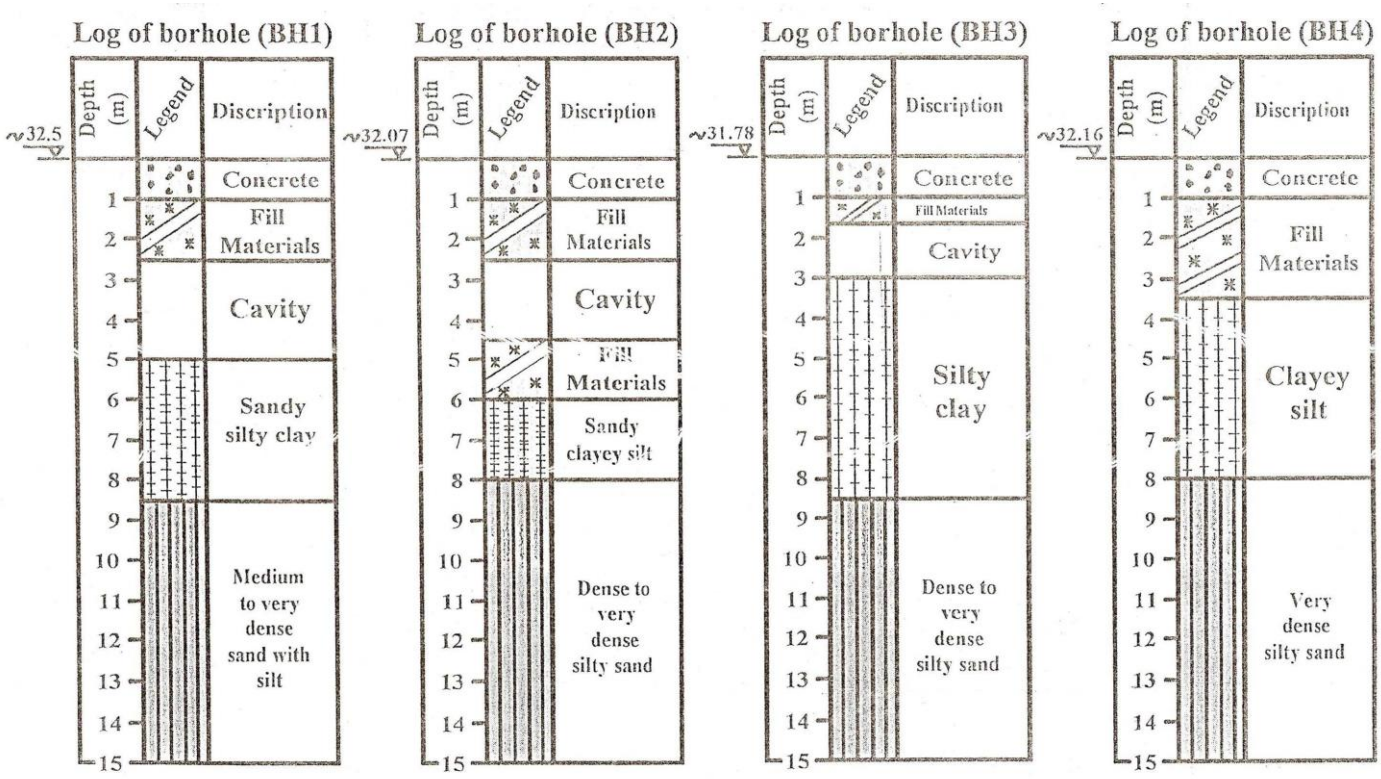

Logs of boreholes drilled by ISSWR in 1999 around the holy shrine of AL-Hussain

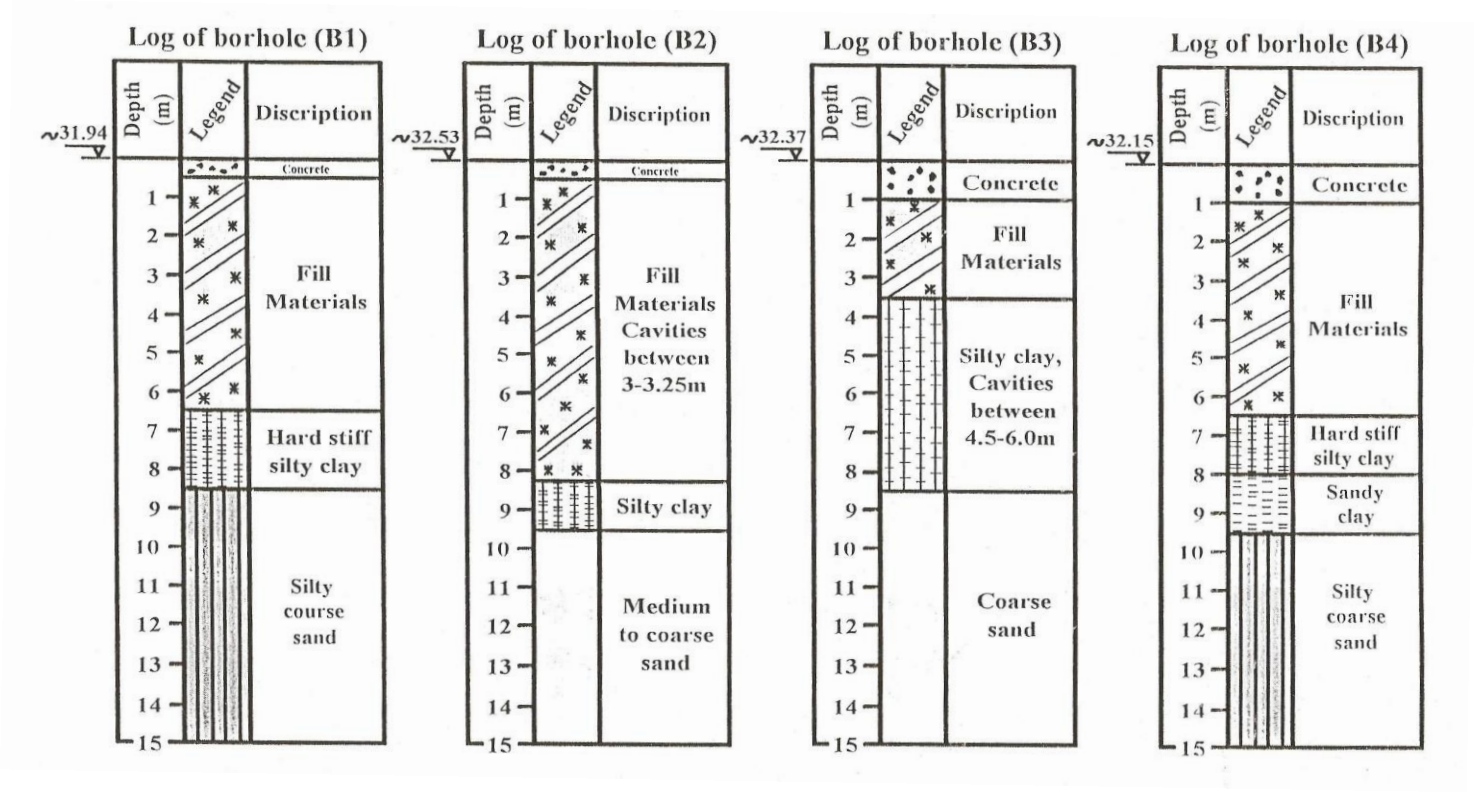

Logs of boreholes drilled by ISSWR in 1999 around the holy shrine of AL-Abbas

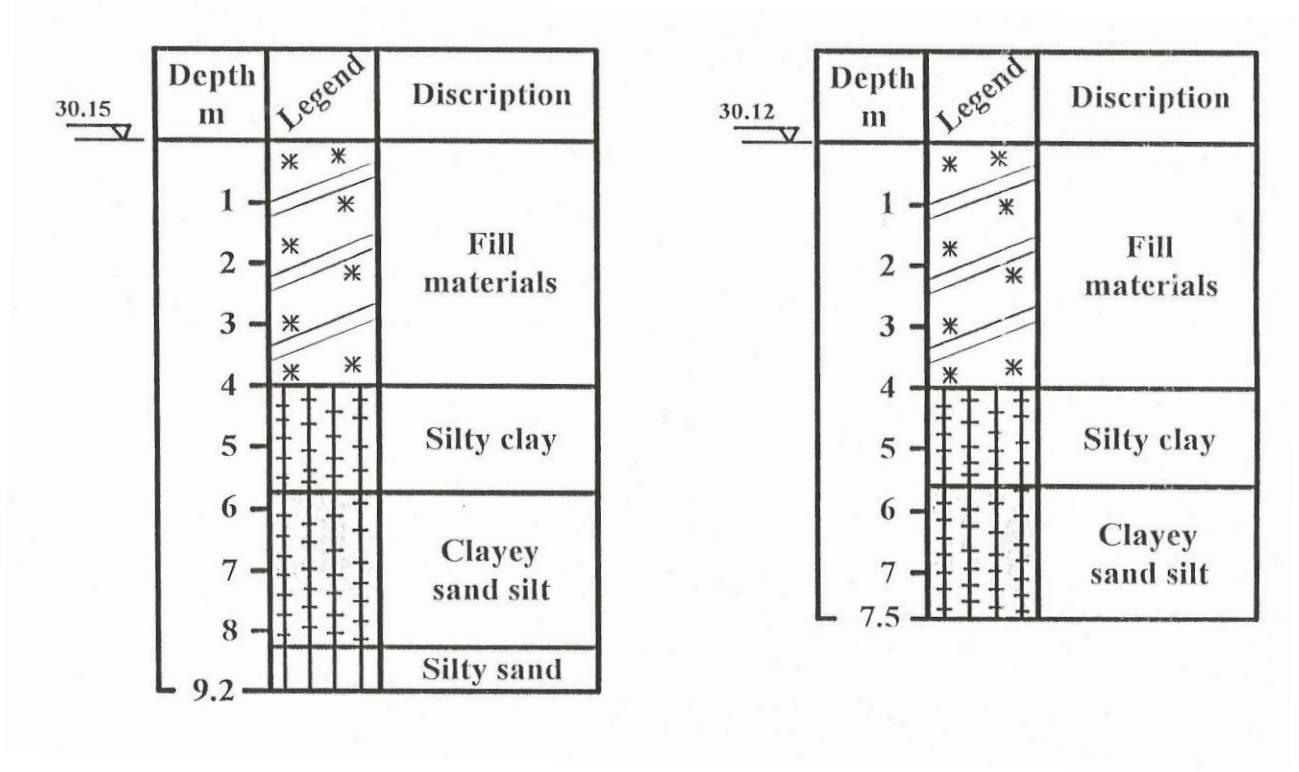

Logs of boreholes of soil investigation drilled by AL-Kutubi Eng. in 1999 near the holy shrine of AL-Abbas

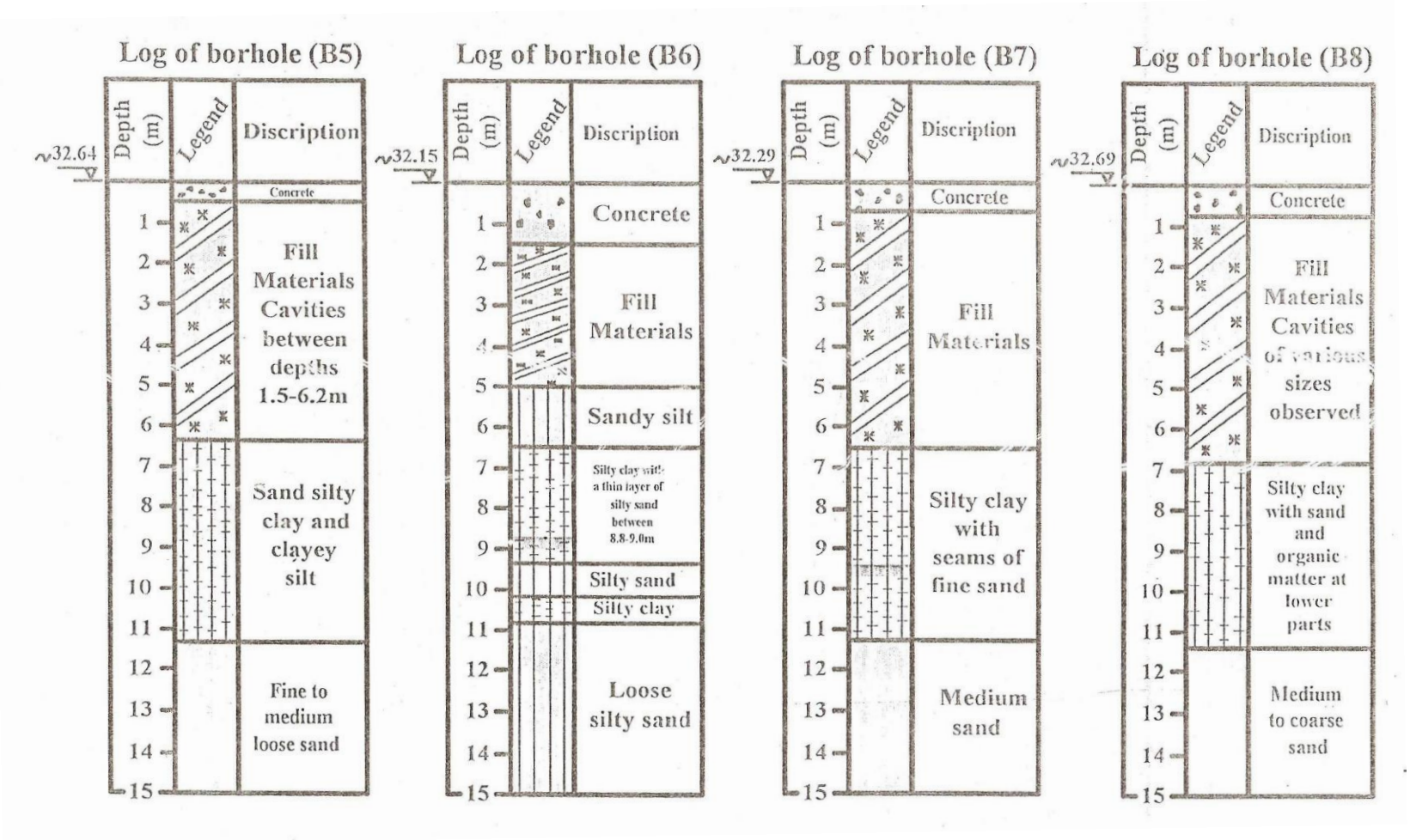

Logs of the boreholes of shallow piezometers drilled by ISSWR in 1999 in the area surrounding the two holy shrines

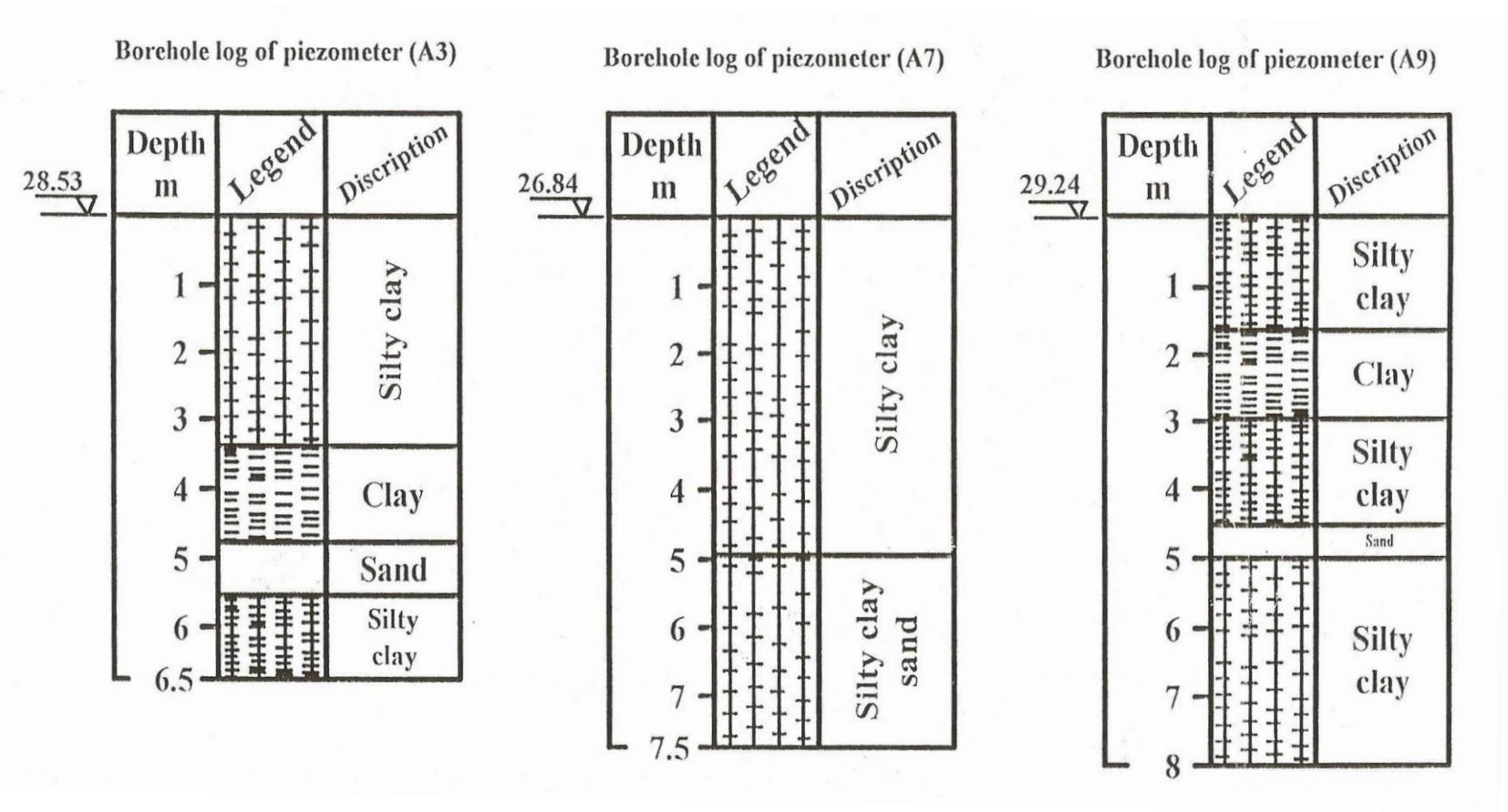

Logs of the boreholes of deep piezometers drilled by ISSWR in 1999 in the area surrounding the two holy shrines

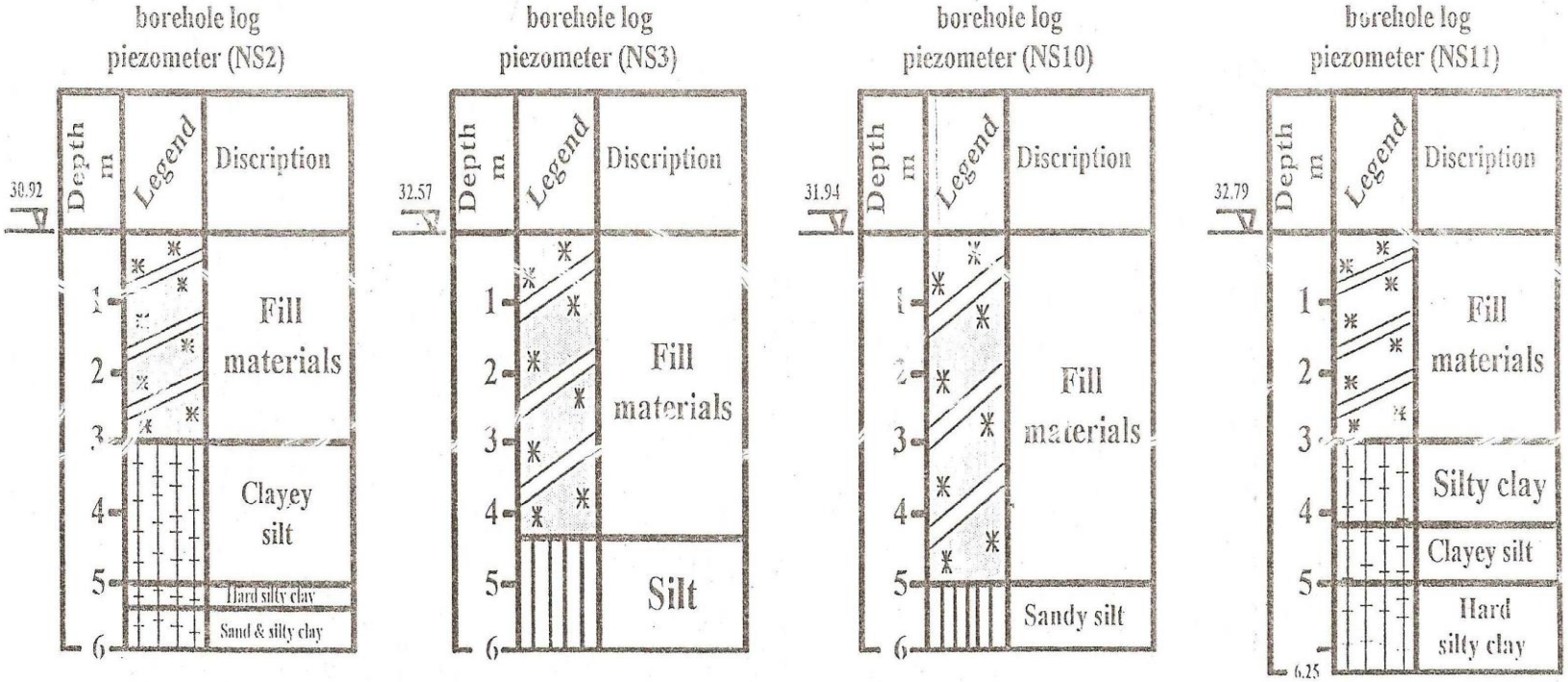

Logs of the boreholes of shallow pizometers drilled by FCSDIP in 1995 in Karbala city

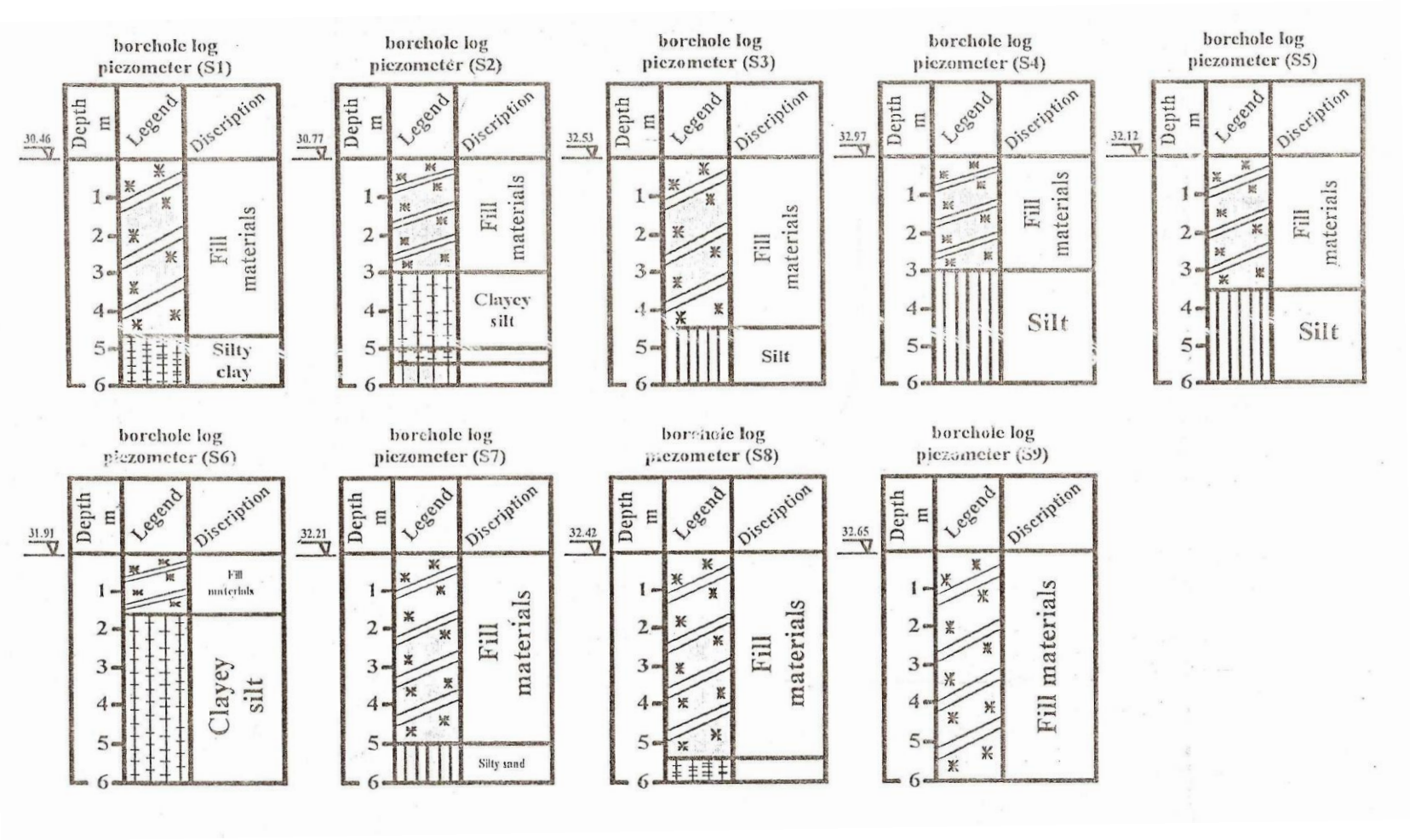

Logs of the boreholes of shallow piezometers drilled by DWSK in 2000 in the area surrounding the two holy shrines

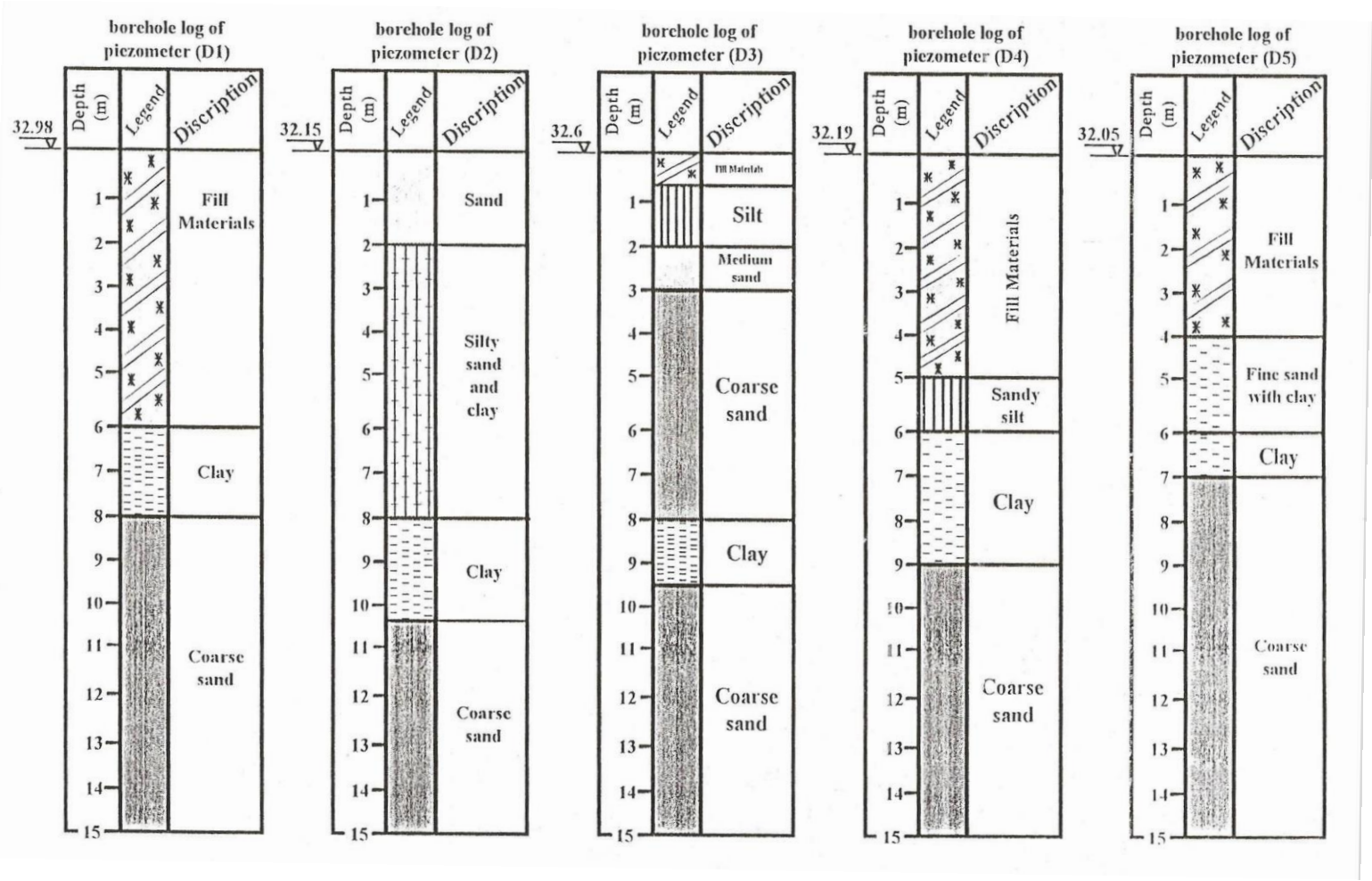

Logs of the boreholes of the sinks and pumping well drilled by ISSWR in 1999 in the area surrounding the two holy shrines

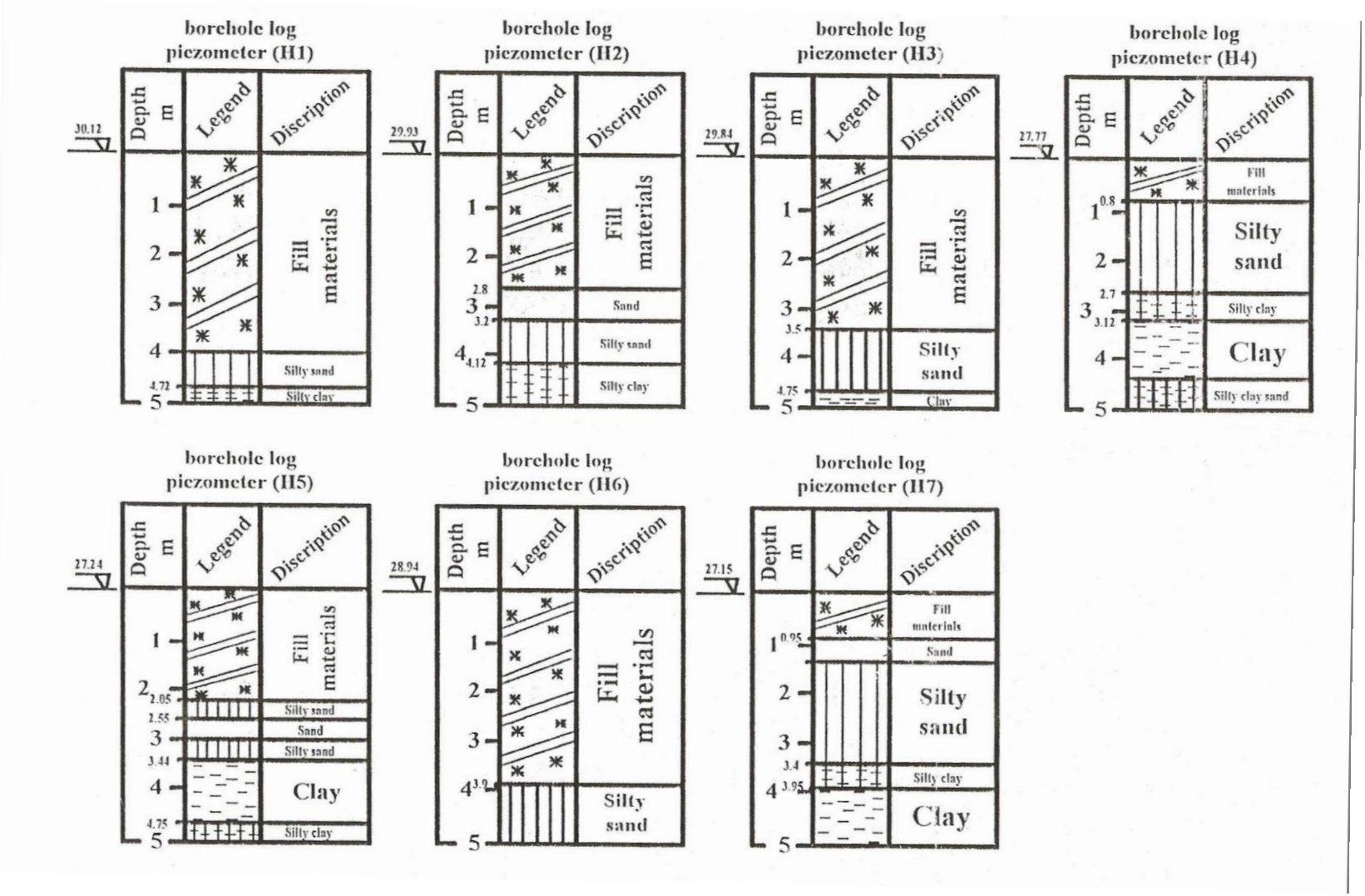

Logs of the boreholes of shallow piezometers drilled by Hassan AL-Khateeb in 2000 in Karbala city

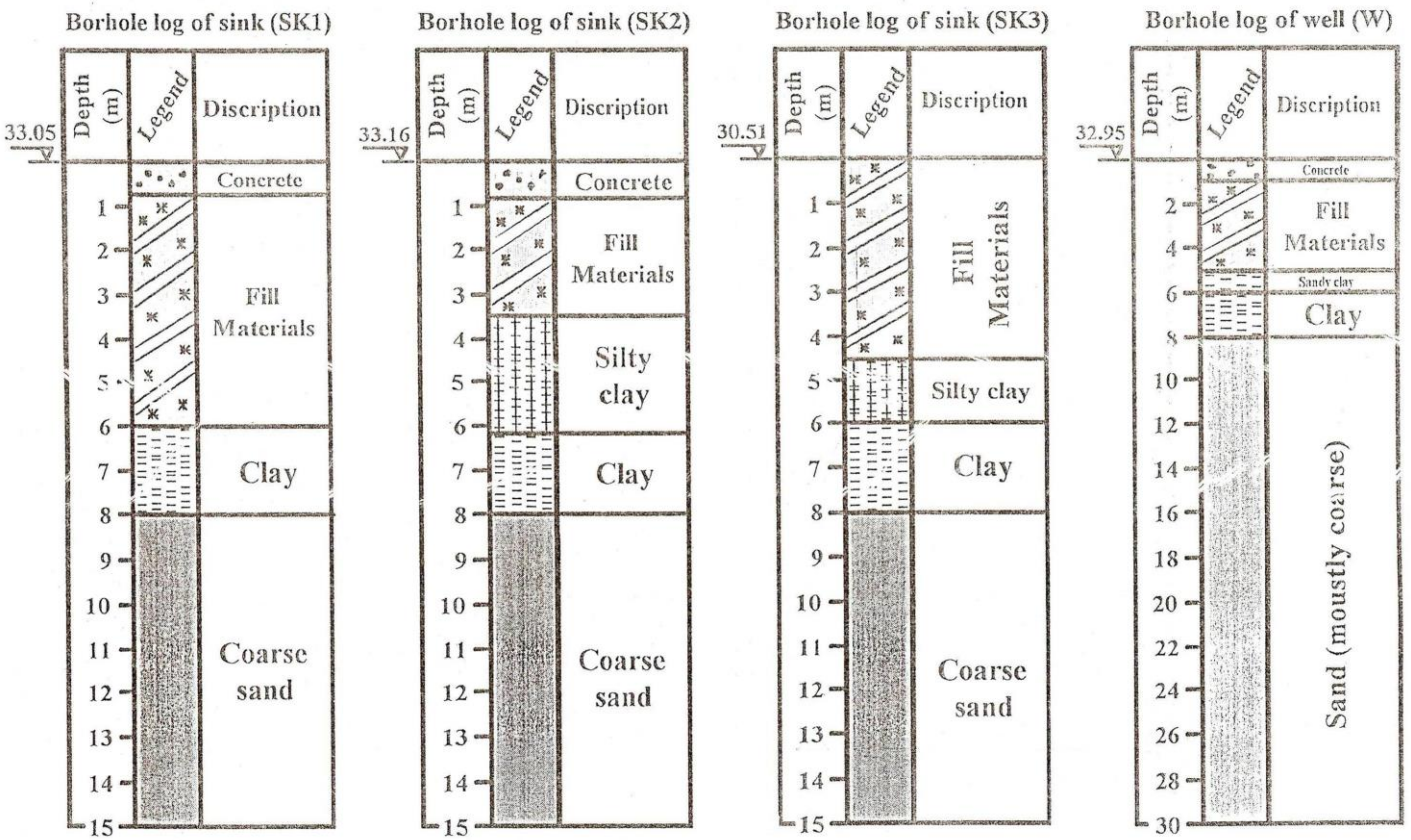

Appendix (C)

Groundwater levels data recorded by ISSWR,1999

Data	Piezometer name																	
	S1	S2	S3	S4	S5	S6	S7	S8	S9	D1	D2	D3	D4	D5	SK1	SK2	SK3	W
	Top elevation of the piezometer mal																	
	30.499	30.89	32.54	33.00	33.08	32.03	32.22	32.43	32.65	32.98	32.105	32.616	32.187	32.054	33.037	33.195	30.514	32.954
	Ground water level mal																	
14/12/1998	28.41	28.99	30.4		30.95	30.55	30.15	30.45	30.32	30.28	29.41	29.85	30.04	29.74		30.89		29.87
29/12/1998	29.5	29.16	30.31	30.04	30.37	30.33	30.12	30.41	30.21	30.21	29.44	29.8	29.88	29.05		30.32	28.47	29.87
2/1/1999		28.98	30.51	30.00		30.78	30.15	30.55	30.25	30.16	29.47	30.14	29.98	29.97			28.56	29.92
17/1/1999		28.99	30.48	30.03	30.28	30.7	30.11	30.44	30.21	29.96	29.45	30.17	30.01	29.97	30.06	30.34	28.56	29.92
1/2/1999		28.98	30.51	30.00		30.7	30.15	30.55	30.25	29.96	29.48	30.16	30.08	29.97	30.04		28.56	29.9
6/2/1999	28.57	29.01	30.47	30.02	30.32	30.82	30.18	30.59	30.31	29.96	29.45	30.14	30.05	30.02	30.04	30.31	28.59	29.91
3/3/1999	28.63	29.04	30.52	30.04	30.39	30.82	30.25	30.75	30.38	29.91	29.49	30.14	30.08	30.09	30.04	30.44	28.59	29.95
16/3/1999	28.54	28.89	30.16	29.99	30.32	30.69	30.15	30.71	30.24	29.78	29.38	29.96	29.99	30.00	30.05	30.33	28.56	29.83
31/3/1999	28.65	29.29	30.54	30.4	30.59	30.59	30.18	30.93	30.4	29.72	29.59	30.22	30.08	30.06	30.06	30.65	28.66	30.02
18/4/1999	28.62	29.19	30.54	30.05	30.18	30.68	30.19	30.78	30.3	29.78	29.45	30.17	30.07	30.04	30.06	30.5	28.69	29.95
5/5/1999	28.61	29.14		30.1	30.63		30.22	30.79	30.4	29.88	29.66	30.19	30.09	30.13	30.12	30.57	28.64	29.85
15/5/1999	28.6	29.21		30.1	30.65		30.21	30.83	30.4	29.9	29.65	30.2	30.09	30.14	30.11	30.6	28.64	29.85
1/6/1999	28.63	29.15		30.1	30.65		30.22	30.77	30.45	29.88	29.66	30.22	30.06	30.16	30.4	30.58	28.66	29.85
10/6/1999	28.64	29.17		30.15	30.56		30.28	30.81	30.55	30.00		30.27	30.17	30.19	30.13	30.59	28.66	29.9

Ground water levels data recorded by Hassan AL-Khateeb

Data	Piezometer name																					
	P2	P3	P4	P5	P6	P7	P8	NS2	NS3	S7	S8	S9	NS10	NS11	D1	D4	H1	H2	H3	H4	H5	H6	H7
	Top elevation of the piezometer mal																						
	32.84	32.44	32.25	32.25	32.36	32.44	32.44	30.92	32.57	32.21	32.42	32.65	31.94	31.79	32.98	32.19	30.12	29.93	29.83	27.77	27.24	28.94	27.15
	Ground water level mal																						
1/3/2000	29.27	28.99	28.95	28.96	29.12	29.14	29.27	28.22	29.52	30.02	30.65	29.9	29.86	30.14	29.6	29.8	28.63	28.57	28.94	27.37	26.57	27.96	26.33
4/3/2000	29.4	29.03	29.05	29.07	29.22	29.27	29.37	28.25	29.49	30.02	30.67	29.9	29.85	30.15	29.6	29.79	28.64	28.56	28.93	27.38	26.55	27.96	26.32
6/3/2000	29.45	29.05	29.05	29.1	29.22	29.32	29.4	28.27	29.5	30.03	30.69	29.91	29.84	30.13	29.61	29.79	28.63	28.58	28.94	27.38	26.57	27.95	26.31
8/3/2000	29.42	29.06	29.05	29.11	29.17	29.31	29.41	28.3	29.48	30.02	30.65	29.9	29.85	30.12	29.6	29.78	28.65	28.58	28.93	27.39	26.56	27.96	26.31
11/3/2000	29.37	29.06		29.09	29.15	29.2	29.37	28.29	29.47	30.05	30.7	29.92	29.86	30.14	29.61	29.79	28.65	28.59	28.93	27.37	26.54	27.97	26.3
13/3/2000	29.21			28.92	29.12	29.15	29.33	28.26	29.45	30.05	30.72	29.92	29.86	30.13	29.61	29.79	28.64	28.58	28.93	27.36	26.53	27.96	26.29
15/3/2000	29.17	29.04		28.91	29.12	29.13	29.3	28.24	29.42	30.03	30.69	29.91		30.11	29.6	29.78	28.65	28.56	28.91	27.34	26.52	27.97	26.31
20/3/2000	29.22		28.93	28.94	29.11	29.16	29.25	28.23	29.43	30.02	30.65	29.9	29.87	30.1	29.58	29.77	28.65	28.57	28.89	27.34	26.52	27.98	26.31
23/3/2000	29.21	29.02			29.15	29.15	29.24	28.21	29.41	30.03	30.68	29.91	29.88	30.1	29.59	29.77	28.67	28.58	28.9	27.35	26.51	28.00	26.29
27/3/2000	29.19	29.05	29.04	28.96	29.16	29.16	29.25	28.22	29.42	30.04	30.71	29.92	29.88	30.11	29.6	29.77	28.68	28.59	28.9	27.35	26.52	28.01	26.29
29/3/2000	29.17	29.05		28.88	29.1	29.11	29.24	28.2	29.41		30.69	29.92	29.87	30.12	29.6		28.68	28.6	28.91	27.34	26.5	27.98	26.28
3/4/2000	29.14	29.03	28.8	28.86	29.02	29.03	29.22	28.23	29.39	30.06	30.67	29.93	29.89	30.14	29.59	29.78	28.69	28.61	28.91	27.33	26.52	27.99	26.27
8/4/2000	29.09	29.07	28.78	28.79	29.01	29.03	29.27	28.24	29.41	30.07	30.64	29.95	29.91	30.13	29.59	29.79	28.69	28.63	28.92	27.32	26.51	28.02	26.28
13/4/2000	29.02	29.01	28.81		29.02	29.05	29.24	28.55	29.5	30.04	30.66	29.96	29.92	30.12	29.59	29.77	28.68	28.65	28.93	27.33	26.51	28.01	26.29
16/4/2000	29.03	29.02	28.8	28.85	29.01	29.03	29.23	28.43	29.46	30.04	30.62	29.94	29.92	30.09	29.59	29.77	28.66	28.64	28.92	27.34	26.52	27.99	26.28
19/4/2000	29.02	29.02	28.8	28.83	29.00	29.01	29.21	28.35	29.44	30.03	30.6	29.94	29.93	30.13	29.58	29.76	28.64	28.61	28.93	27.32	26.51	27.97	26.29
24/4/2000	29.05	28.95	28.79		28.97	29	29.23	28.33	29.44	30.03	30.61	29.93	29.91	30.16	29.59	29.76	28.62	28.56	28.91	27.32	26.5	27.98	26.31
28/4/2000	29.07	28.91	28.8	28.8	28.96	28.99	29.21	28.23	29.47	30.00	30.61	29.9	29.86	30.17	29.57	29.76	28.6	28.54	28.89	27.32	26.49	28.01	26.29
5/5/2000	29.04	28.85	28.73	28.76	28.93	28.98	29.12	28.18	29.34	29.96	30.43	29.86	29.79	30.15	29.54	29.75	28.53	28.52	28.88	27.31	26.47	27.97	26.26
8/5/2000	29.01	28.83	28.71	28.74	28.9	28.97	29.13	28.11	29.33	29.95	30.42	29.82	29.76	30.13	29.53	29.74	28.55	28.52	28.9	27.28	26.47	27.94	26.24
12/5/2000	28.95	28.84	28.7	28.74	28.89	28.92	29.14	27.98	29.34	29.97	30.51	29.79	29.74	30.12	29.51	29.75	28.56	28.52	28.92	27.24	26.46	27.91	26.21
15/5/2000	28.94	28.84			28.87	28.89	29.13	27.99	29.29	29.98	30.54	29.76	29.75	30.14	29.51	29.75	28.56	28.53	28.91			27.88	26.18

18/5/2000	28.93	28.84		28.72	28.86	28.88	29.12	27.97	29.2	30.01	30.57	29.77	29.74	30.17	29.52	29.75	28.57	28.51	28.91	27.23	26.44	27.92	26.15
21/5/2000	28.93	28.84	28.72	28.72	28.86	28.88	29.13	27.96	29.18	30.04	30.52	29.78	29.73	30.18	29.51	29.76	28.57	28.51	28.88	27.22	26.42	27.87	26.11
24/5/2000		28.85	28.72	28.73	28.86	28.89	29.14	27.94	29.17	30.03	30.53	29.76	29.72	30.16	29.51	29.76	28.57	28.53	28.9	27.2	26.41	27.85	26.09

Data	Piezometer name																						
	P2	P3	P4	P5	P6	P7	P8	NS2	NS3	S7	S8	S9	NS10	NS11	D1	D4	H1	H2	H3	H4	H5	H6	H7
	Top elevation of the piezometer mal																						
	32.84	32.44	32.25	32.25	32.36	32.44	32.44	30.92	32.57	32.21	32.42	32.65	31.94	31.79	32.98	32.19	30.12	29.93	29.83	27.77	27.24	28.94	27.15
	Ground water level mal																						
29/5/2000	28.97	28.87	28.73	28.75	28.88	28.92	29.15	27.99	29.2	30.01	30.54	29.77	29.73	30.19	29.51	29.76	28.56	28.53	28.92	27.19	26.41	27.89	26.08
3/6/2000	28.89	28.88	28.72	28.77	28.95	28.96	29.16	28.03	29.91	30.02	30.56	29.77	29.74	30.17	29.52	29.76	28.56	28.55	28.88	27.21	26.42	27.91	26.12
7/6/2000	29.03	28.92	28.76	28.8	29.04	29.07	29.18	28.06	29.24	30.02	30.59	29.78	29.76	30.15	29.52	29.76	28.56	28.53	28.91	27.23	26.42	27.92	26.14
10/6/2000	29.06	28.93	28.78	28.8	29.06	29.1	29.19	28.08	29.27	30.03	30.61	29.79	29.77	30.16	29.53	29.77	28.55	28.52	28.95	27.25	26.43	27.93	26.15
17/6/2000	29.11	28.97	28.77	28.78	29.09	29.11	29.21	28.1	29.31		30.64	29.82	29.78	30.2	29.53		28.57	28.51	28.99	27.26	26.44	27.93	26.17
21/6/2000	29.15	29.00	28.78	28.78	29.08	29.1	29.22	28.11	29.3		30.67	29.85	29.78	30.12	29.54		28.56	28.52	28.97	27.27	26.43	27.94	26.19
24/6/2000	29.17	29.01	28.78	28.78	29.07	29.09	29.2	28.13	29.33		30.66	29.84	29.79	30.2	29.54		28.57	28.5	29.02	27.29	26.45	27.92	26.2
28/6/2000	29.2	29.03	28.79	28.82	29.06	29.09	29.2	28.15	29.35		30.68	29.82	29.81	30.21	29.55		28.58	28.52	29.04	27.3	26.47	27.89	26.22
1/7/2000	29.23	29.04	28.81	28.86	29.08	29.11	29.22	28.19	29.34		30.68	29.83	29.82	30.21	29.55		28.57	28.51	29.02	27.31	26.47	27.88	26.23
5/7/2000	29.27	29.06	28.86	28.91	29.1	29.14	29.24	28.22	29.37		30.7	29.82	29.82	30.19	29.55		28.58	28.49	29.03	27.33	26.48	27.9	26.22
9/7/2000	29.23	29.05	28.85	28.86	29.12	29.15	29.26	28.25	29.38		30.68	29.83	29.83	30.12	29.56		28.59	28.5	29.05	27.33	26.47	27.89	
15/7/2000	29.21	29.04	28.86	28.87	29.13	29.16	29.28	28.28	29.39		30.7	29.85	29.83	30.22	29.55		28.58		29.04	27.31	26.45	27.87	
19/7/2000	29.22	29.05	28.87	28.89	29.13	29.17	29.28	28.29	29.41		30.72	29.84	29.83	30.21	29.55		28.57		29.03	27.3	26.45	27.88	
23/7/2000	29.22	29.06	28.86	28.87	29.14	29.17	29.29	28.27	29.41		30.74	29.86	29.81	30.22	29.55				29.04	27.29	26.46	27.87	
27/7/2000	29.24	29.07	28.82	28.84	29.15	29.16	29.28	28.3	29.4		30.76	29.86	29.83		29.56				29.02	27.28	26.47	27.87	
31/7/2000	29.24	29.08	28.83	28.86	29.16	29.16	29.28	28.28	29.42		30.77	29.87		30.19	29.56				29.04	27.29	26.46	27.86	

الخلاصة

تعتبر مدينة كربلاء واحدة من أهم المدن الإسلامية في العالم. اكتسبت هذه المدينة أهميتها من المراقد الطاهرة للإمام الحسين و أخيه العباس عليهما السلام.

مدينة كربلاء تعاني من مشكلة ارتفاع مناسيب المياه الجوفية خصوصا في منطقة الحضرتين حيث سجلت أعلى المناسيب. الدراسات السابقة أثبتت إن تسرب شبكات الإسالة وشبكات المجاري وأحواض التعفن المنزلية هو المغذي الرئيسي للمياه الجوفية في المدينة كما وأثبتت إن مقطع التربة مكون من ثلاث طبقات . طبقة عليا تمثل المكمن الغير محصور بمعدل سمك 5 م وطبقة سفلى تمثل المكمن شبه المحصور بمعدل سمك 30م بالإضافة إلى طبقة وسطى شبه نفاذة بمعدل سمك 2م.

في هذه الدراسة تم إنشاء نموذجيين عدديين يستخدمان طريقة الفروق المتناهية لتمثيل جريان المياه الجوفية في المدينة. الأول هو نموذج الـ GMS والثاني نموذج رياضي عددي يستخدم لغة الـ Quick Basic في حل المعادلات. تم استخدام النموذجيين لاختبار بعض اجرائات تخفيض مناسيب المياه الجوفية في الطبقة العليا.

نتائج النموذجيين بينت أن تخفيض التسرب بنسبة 75% سوف يقود إلى انخفاض في مناسيب المياه الجوفية تحت المرقدين أكثر من 2م كما وبينت إن البزل العمودي للطبقة السفلى باستخدام أربعة آبار حول كل مرقد شريف ممكن استخدامه للوصول إلى نفس الانخفاض.

نموذج الـ GMS بين إن البزل الأفقي للطبقة العليا من خلال إعادة تأهيل المبازل الموجودة في منطقة الدراسة سوف يقود إلى انخفاض جدير بالاعتبار في مناسيب المياه الجوفية يمتد على كل المنطقة ولكن ليس بالمقدار الكافي تحت الضريحين المقدسين حيث لا يتجاوز 1م. هذه الدراسة بينت أيضا إن النموذج الرياضي يحاكي جريان المياه الجوفية في المدينة أفضل من نموذج الـ GMS .

وزارة التعليم العالي والبحث العلي

جامعة بابل

كلية الهندسة

قسم الهندسة المدنية

محاكاة جريان المياه الجوفية في مدينة كربلاء

رسالة مقدمة إلى كلية الهندسة في جامعة بابل كجزء من متطلبات

نيل درجة الماجستير في علوم الهندسة المدنية/ الموارد المائية

من قبل

نبيل محمد حسين

دبلوم عالي هندسة مدنية

تموز

2008

إشراف

د .صلاح توفيق

د .عبد الحسن خضير شكر